A Study of *Fusarium graminearum* Virulence Factors

A DISSERTATION
SUBMITTED TO THE FACULTY OF THE GRADUATE SCHOOL
OF THE UNIVERSITY OF MINNESOTA
BY

Jon R. Menke

IN PARTIAL FULFILLMENT OF THE REQUIREMENTS
FOR THE DEGREE OF
DOCTOR OF PHILOSOPHY

H. Corby Kistler

May 2011

Acknowledgments

I thank my advisor, Dr. Corby Kistler, for supporting my research, being a mentor, and providing optimism and encouragement regarding my research and academic performance. I also thank the current and past members of the Kistler Lab for their patience, support, and feedback regarding my research goals, objectives, and results and for providing a solid foundation upon which to base my thesis project. In particular, Karen Hilburn provided excellent and expedient technical support and valuable advice regarding the behavior of *F. graminearum*.

I thank the other members of my thesis committee: Dr. Ben Lockhart, Dr. Gary Muehlbauer, and Dr. Nevin Young for their comments and suggestions regarding my research and thesis.

I thank the research groups that provided support and services that were vital to my research project. Dr. Yan Hong Dong and the members of her lab provided expertise in mycotoxin identification and mycotoxin and ergosterol measurement results for thousands of samples. Dr. Mark Sanders of the U of MN imaging center provided assistance with laser scanning confocal microscopy. Dr. Wayne Xu of the U of MN Supercomputing Institute provided assistance with microarray analysis software issues. The Cereal Disease Lab provided unlimited access to the technical resources and materials I needed to complete my thesis research.

I thank the faculty and staff that have been helpful throughout my graduate studies. I thank my fellow graduate students, past and present, for providing encouragement and discussing solutions to problems posed by my research.

Finally, I thank my family for their unconditional love and support. The love, patience, support, encouragement, and understanding of Wyatt, Lisa, Delores, Jan, Holli, Ethel Jerrine, Sharon, and David have been and continue to be integral to the completion of my research and academic studies.

Abstract

The plant pathogen *F. graminearum* (*Gibberella zeae*) presents a two-fold threat to farmers and consumers. Not only does this filamentous fungus cause the disease Fusarium head blight (FHB) that results in significant yield loss in infected grains, it also taints these grains with potent mycotoxins harmful to humans, animals, and plants alike. Equally alarming is the evidence that grain can appear to be physically sound while still being significantly contaminated with trichothecene mycotoxins. *Tri12* encodes a predicted major facilitator superfamily transporter protein suggested to play a role in the export of trichothecene mycotoxins produced by the Fusarium species. However, the role of Tri12p in toxin sensitivity and plant pathogenicity of *Fusarium graminearum* was previously unknown. In this study, the correct intron positions for *Tri12* in *F. graminearum* (*FgTri12*) were established using cDNA sequencing, EST data, and comparative genomics. Reverse genetics was used to establish that *FgTri12* plays a role in self-protection and influences toxin production and virulence of the fungus *in planta*. To identify the subcellular location of FgTri12p during toxin production in culture, FgTri12p was tagged with eGFP. FgTri12p::eGFP was localized in small motile vesicles, the plasma membrane, and the lumen of vacuoles within fungal cells. Treatment of cells with latrunculin A resulted in the absence of motile vesicles labeled with FgTri12p::eGFP, suggesting their formation relies upon actin polymerization. To determine if FgTri12p co-localizes with enzymes involved in trichothecene metabolism, its cellular fate was compared with FgTri1p::eGFP, a fluorescently tagged oxygenase catalyzing a key intermediate step in trichothecene biosynthesis. While FgTri1p::eGFP

initially localizes to small motile vesicles and later accumulates in the vacuole, during the period of initial trichothecene biosynthesis it is targeted to the periphery of intermediate sized vesicles, presumed to be the site of toxin synthesis. These results indicate *FgTri12* plays a role in self-protection and influences toxin production and virulence of the fungus *in planta.*

The interactions between *F. graminearum* and its hosts – wheat, rice, or barley – differ in disease severity and the levels of trichothecenes that accumulate in response to infection. The transcriptome of the fungus in rice and wheat was examined in order to identify genes expressed *in planta*. The hypothesis that fungal genes expressed *in planta,* but not during growth in culture, could include those that determine the plant infection phenotype was tested by reverse genetics: Four genes expressed exclusively *in planta* were deleted and two of these were determined to significantly alter disease phenotype. FGSG_03539, also called *Tri9,* is a previously uncharacterized gene in the major trichothecene biosynthetic gene cluster. A mutant with a *tri9* deletion has attenuated virulence and lower trichothecene levels in wheat compared to wild type or a mutant strain complemented with the intact *Tri9* gene. FGSG_11164 encodes a predicted trypsin protease and deletion of this gene also results in a small but significant reduction in pathogenicity toward wheat. The results demonstrate that a reverse genetic approach using *in planta* gene expression data may supplement forward genetic screens for identifying genes encoding virulence factors.

Table of Contents

Acknowledgements i
Abstract.....ii
Table of Contents.....iv
List of Tables.....v
List of Figures.....vi

Chapter 1
Literature
Review……..…...1
Introduction…….…..…....2
Pathogenesis…….....3
Resistance to FHB in wheat and barley.....26
Figure.....43
References.....44

Chapter 2
Cellular localization and functional characterization of FgTri12p in *Fusarium graminearum*…….57
Introduction.....58
Results..... 60
Discussion.....68
Methods.....79
Tables.....87
Figures.....93
Supplemental Videos.....118
References.....120

Chapter 3
Identification of *Fusarium graminearum* virulence factors by comparative gene expression analysis…….128
Introduction.....129
Results..... 131
Discussion.....141
Methods.....157
Tables.....166
Figures.....173
Supplemental Table.....185
References.....186

Bibliography.....192

List of Tables

Chapter 2

Table 1. Pathogenicity and trichothecene concentrations *in planta*……..87

Table 2. Trichothecene concentration in liquid TBI medium seven days after inoculation with PH-1, *fgtri12,* or *fgtri12/Fgtri12*……...……88

Table 3. Colony diameter of all strains grown on TBI medium……89

Table 4. Pathogenicity and trichothecene concentrations for *FgTri12*::*eGFP in planta*…….90

Table 5. Trichothecene concentration in liquid TBI medium seven days after inoculation with *FgTri12*::*eGFP*……..……91

Table 6. Oligonucleotides used in this study…….92

Chapter 3

Table 1. Microarray-based transcript profiles for *F. graminearum* obtained from PLEXdb (www.plexdb.org)…….……166

Table 2. Oligonucleotides used in this study……...167

Table 3. Trichothecene concentrations in samples of infected wheat and rice spikelets used for mRNA extraction.....168

Table 4. Ergosterol concentration in samples of infected wheat spikelets and rice panicles used for mRNA extraction……..……169

Table 5. Pathogenicity and trichothecene concentrations for PH-1, PH-1*tri9*, and PH-1*tri9/Tri9* on wheat.....170

Table 6. Concentrations of trichothecenes in liquid TBI medium after inoculation with PH-1, PH-1*tri9,* or PH-1*tri9/Tri9*.....171

Table 7. Pathogenicity of the PH-1*tpp1* mutant on wheat.....172

List of Figures

Chapter 1

Figure 1. The Tri cluster and three other genes – *Tri101*, *Tri1*, and *Tri16* –involved in trichothecene biosynthesis.....43

Chapter 2

Figure 1. Gene model for *FgTri12.* Locations of oligonucleotides used for sequencing are located above the gene model. Sizes of exons and total sequence coverage are listed below the model. Intron locations are denoted on the model itself, while intron sizes are listed in the lower box.....93

Figure 2. Needleman-Wunsch global alignment of predicted amino acid sequences of FgTri12p and FsTri12p. Amino acid number of (i) and outward (o) ends of predicted transmembrane domains are noted above boxes representing each of the 14 domains.....94

Figure 3. Split marker PCR method used for disruption of *FgTri12*. A) Left and right flanking regions of *Tri12* are amplified using LF1F + LF2R and RF3F + RF4R oligonucleotide combinations. Sequences specific to the 5' and 3' regions of *hph* have been added to the 5' ends of LF2R and RF3F. HY and YG regions of the *hph* are amplified using HYG/F + HY/R and HYG/R + YG/R oligonucleotide combinations. B) LF and HY amplicons and LF1F and HY/R oligonucleotides are used to produce LFHY fusion products via PCR. YG and RF amplicons and YG/F and RF4R oligonucleotides are used to produce YGRF fusion products via PCR. C) Transformation of protoplasts with LFHY and YGRF fusion products disrupt the *FgTri12* gene via a triple crossover event.....95

Figure 4. Southern blotting of genomic DNA. 1) Location of *PstI* restriction enzyme cut sites in PH-1 and *fgtri12* and the expected size of the fragment targeted by hybridization probes. 2) Hybridization of A) *FgTri12* B) *hph* C) *neo* specific probes to digested genomic DNA from I) PH-1 II) *fgtri12* III) *fgtri12/FgTri12.* These results demonstrate the presence of single copies of *FgTri12* in PH-1 and *fgtri12/FgTri12,* a single copy of *hph* in *fgtri12*, and a single copy of *neo* in *fgtri12/FgTri12.* The relative sizes of the fragments labeled with the *FgTri12* probe in PH-1 DNA and *hph* probe in *fgtri12* DNA are consistent with expected digestion patterns. The two bands that hybridize with the *hph* probe in the *fgtri12/FgTri12* complement strain demonstrate that a duplication event occurred during integration of the *FgTri12* complementation construct.....96

Figure 5. Radial growth and pigmentation of A) PH-1, B) *fgtri12,* C) *fgtri12/FgTri12*, and D) *FgTri12::eGFP* on TBI medium.....97

Figure 6. Radial growth and pigmentation of A) PH-1, B) *fgtri12,* C) *fgtri12/FgTri12*, and D) *FgTri12::eGFP* on minimal medium.....98

Figure 7. Synthesis of FgTri12p::eGFP fusion protein. A) T12eGFP1F + T12eGFP2R and Tri12eGFP3F + Tri12eGFP4R oligonucleotide combinations are used to amplify the 5' and 3' regions flanking the *Tri12* stop codon via PCR. The *eGFPhph* construct is amplified with eGFPwLFTri12seq and eGFPwRFTri12seq oligonucleotides. These oligonucleotides possess sequences specific to the regions directly 5' and 3' of the *FgTri12* stop codon. B) RF, LF, and e*GFhph* constructs and T12eGFP1F and T12eGFP4R oligonucleotides are used to generate a continuous LF::e*GFPhph*::RF fusion construct. C) Transformation of PH-1 protoplasts with LF::e*GFPhph*::RF fusion construct results in eGFP tagging of the carboxy terminus of FgTri12p.....99

Figure 8. Synthesis of FgTri1p::eGFP fusion protein. A) T1eGFP1F + T1eGFP2R and Tri1eGFP3F + Tri1eGFP4R oligonucleotide combinations are used to amplify the 5' and 3' regions flanking the *Tri12* stop codon via PCR. The *eGFPhph* construct is amplified with eGFPF and eGFPR oligonucleotides. Tri1eGFP2R and Tri1eGFP3F oligonucleotides possess sequences specific to the 5' and 3' ends of the e*GFPhph* construct. B) RF, LF, and e*GFPhph* constructs and T12eGFP1F and T12eGFP4R oligonucleotides are used to generate a LF::e*GFPhph*::RF fusion construct. C) Transformation of PH-1 protoplasts with LF::e*GFPhph*::RF fusion construct results in eGFP tagging of the carboxy terminus of FgTri1p.....100

Figure 9. Southern blotting of genomic DNA from PH-1 and *FgTri12::eGFP*. 1) Location of *BglII* restriction enzyme cut sites in PH-1 and *FgTri12::eGFP* and the expected size of the fragment targeted by hybridization probes. 2) Hybridization of A) *Tri12,* B) *hph,* and C) *eGFP* specific probes to digested genomic DNA from I) PH-1 and II) *FgTri12::eGFP*. These results demonstrate the presence of single copies of *FgTri12* in PH-1 and *FgTri12::eGFP* and a single copy of *hph* and eGFP in *FgTri12::eGFP*. The relative sizes of the fragments labeled with the *Tri12* probe in PH-1 and *FgTri12::eGFP* are consistent with expected digestion patterns.....101

Figure 10. Southern blotting of genomic DNA from PH-1 and *FgTri1::eGFP*. 1) Location of *XbaI* restriction enzyme cut sites in PH-1 and *FgTri1::eGFP* and the expected size of the fragment targeted by hybridization probes. 2) Hybridization of A) *Tri1,* B) *hph,* and C) *eGFP* specific probes to digested genomic DNA from I) PH-1 and II) *FgTri1::eGFP*. These results demonstrate the presence of single copies of *FgTri12* in PH-1 and *FgTri1::eGFP* and a single copy of *hph* and eGFP in *FgTri1::eGFP*. The relative sizes of the fragments labeled with the *Tri12* probe in PH-1 and *FgTri1::eGFP* are consistent with expected digestion patterns.....102

Figure 11. Morphology of *F. graminearum* mycelia grown in liquid minimal medium (top) or TBI medium (bottom). DIC images were taken at I) 12 hours, II) 18 hours, III) 24 hours, and IV) 36 hours after cultures were inoculated with fresh macroconidia. Shaken cultures (150 rpm) were incubated in total darkness at 25˚C. Scale bar = 10 µm.....103

Figure 12. Coralloid morphology of *F. graminearum* hyphae grown in TBI medium. DIC image of cells was taken 36 hours after culture was inoculated with fresh conidia. Shaken cultures (150 rpm) were incubated in total darkness at 25˚C. Scale bar = 10 µm.....104

Figure 13. CMAC stained vacuoles and late endosomes in *FgTri12::eGFP* cells from TBI cultures. I) DIC, II) GFP, III) CMAC, and IV) CMAC/GFP/DIC layered images taken after 42 hours of incubation at 28˚ C in total darkness. Scale bar = 10µm.....105

Figure 14. Cell morphology and localization of FgTri12p::eGFP to the subapical ovoid portion of an advancing hypha in TBI liquid culture after 18 hours of incubation at 28˚C in total darkness.. I) Bright field, II) DIC, III) GFP, and IV) DIC/GFP overlay images. Scale bar = 10µm.....106

Figure 15. Cell morphology and FgTri12p::eGFP localization in TBI liquid culture after 24 hours of incubation at 28˚C in total darkness. I) Bright field, II) DIC, III) GFP, and IV) GFP/DIC overlay images of A) a swollen ovoid region of a cell near an advancing hyphal strand and B) swollen ovoid region of a cell within a mature hyphal strand. FgTri12p::eGFP localizes to a) motile organelles and b) the plasma membrane, but not to c) vacuoles of single early and mature ovoid cells.....107

Figure 16. Cell morphology and FgTri12p::eGFP localization among contiguous cells in TBI liquid culture after 24 hours of incubation at 28˚C in total darkness. I) Bright field, II) DIC, III) GFP, and IV) GFP/DIC overlay images of four contiguous cells demonstrate sequential localization of FgTri12p::eGFP to the A) plasma membrane, B) motile organelles, and C) vacuoles. This suggests FgTri12::eGFP is transported from the plasma membrane to the vacuole. Scale bar = 10 µm.....108

Figure 17. Hyphal morphology and FgTri12p::eGFP localization in TBI liquid culture after 30 hours of incubation at 28˚C in total darkness. I) Bright field and II) GFP images of mature ovoid cells and adjacent cells demonstrate that FgTri12p::eGFP localizes to the A) plasma membrane, B) motile organelles, and C) vacuoles. Evidence of the motility of these organelles can be observed in supplemental video 4. Scale bar = 10µm.....109

Figure 18. Hyphal morphology and FgTri12p::eGFP localization in TBI liquid culture after 36 hours of incubation at 28˚C in total darkness. I) Bright field and II) GFP images of mature ovoid cells and adjacent cells demonstrate that FgTri12p::eGFP localizes to the A) plasma membrane, B) motile organelles, and C) vacuoles. Scale bar = 10µm.....110

Figure 19. Hyphal morphology and FgTri12p::eGFP localization in TBI liquid culture after 42 hours of incubation at 28˚C in total darkness. I) Bright field, II) DIC, III) GFP, and IV) GFP/DIC overlay images of mature ovoid cells and adjacent cells demonstrate that FgTri12p::eGFP localizes to vacuoles of various sizes. Scale bar = 10µm.....111

Figure 20. Cell morphology and localization of FgTri1p::eGFP to a swollen ovoid region of an advancing hyphal strand. I) Bright field, II) DIC, III) GFP, and IV) DIC/GFP overlay images of cells in TBI liquid culture were taken after 18 hours of incubation at 28˚C in total darkness. The white arrow denotes localization of FgTri1p::eGFP to one of several motile organelles. Scale bar = 10µm.....112

Figure 21. Cell morphology and localization of FgTri1p::eGFP to swollen ovoid region of a mature hyphal strand in TBI liquid culture. I) Bright field, II) DIC, III) GFP, and IV) DIC/GFP overlay images of cells in TBI liquid culture were taken after 25 hours of incubation at 28˚C in total darkness. The white arrow denotes localization of FgTri1p::eGFP to the periphery of stationary organelles.....113

Figure 22. Cell morphology and localization of FgTri1p::eGFP within a mature hyphal strand in TBI liquid culture after 30 hours of incubation at 28˚C in total darkness. I) Bright field and II) DIC demonstrate cell morphology, while III) GFP and IV) DIC/GFP overlay images demonstrate the localization of FgTri1p::eGFP to A) the periphery of stationary organelles and B) intracellular membranous structures. Scale bar = 10µm....114

Figure 23. Cell morphology and localization of FgTri1p::eGFP within a mature hyphal strand in TBI liquid culture after 36 hours of incubation at 28˚C in total darkness. I) Bright field and II) DIC images demonstrate cell morphology, while III) GFP and IV) DIC/GFP overlay images demonstrate the localization of FgTri1p::eGFP to A) the periphery of stationary organelles, B) intracellular membranous structures, and C) vacuoles. Scale bar = 10µm.....115

Figure 24. Cell morphology and localization of FgTri1p::eGFP within a mature hyphal strand in TBI liquid culture after 34 hours of incubation at 28˚C in total darkness.. I) Bright field and II) DIC images demonstrate cell morphology, while III) GFP and IV) DIC/GFP overlay images demonstrate the localization of FgTri1p::eGFP to A) the periphery of stationary organelles and B) vacuoles. Scale bar = 10µm.....116

Figure 25. Radial growth of *FgTri12::eGFP* on recovery medium plates after overnight incubation at 25˚C. Cells were A) and B) untreated; C) treated with latruculin A for 1 hour; D) treated with DMSO; E) and F) removed from treatment medium, washed with fresh TBI medium, and incubated for four hours before plating.....117

Chapter 3

Figure 1. Disease symptoms on rice cultivar M201 inoculated with *F. graminearum* conidia A) 48 hai, B) 96 hai, or C) 192 hai.....173

Figure 2. Disease symptoms on wheat cultivar Norm inoculated with *F. graminearum* conidia A) 48 hai, B) 96 hai, or C) 192 hai.....174

Figure 3. Global distribution of arithmetic means of probe set signal intensities. Each of the 100 bins displayed in each graph are derived from the average signal intensity of three microarray hybridizations for A) rice 48 hai, B) rice 96 hai, C) rice 192 hai, D) wheat 48 hai, E) wheat 96 hai, F) wheat 192 hai, G) barley 48 hai, H) barley 96 hai, and I) barley 144 hai with *F. graminearum* conidia.....175

Figure 4. Venn diagram showing *F. graminearum* genes expressed exclusively *in planta*. These genes are expressed in wheat, rice, and barley but not in CM, MM-N, MM-C or in CM spore germination cultures. The identities of the genes in this diagram are listed in supplementary table A.....176

Figure 5. Expression profiles of *F. graminearum* genes involved in trichothecene biosynthesis and efflux in rice, wheat, and barley at early (48 hai), intermediate (96 hai), and late stages of infection (192 hai in rice and wheat; 144 hai in barley).....177

Figure 6. Expression of *F. graminearum* genes in the putative butenolide cluster during the infection of rice, wheat, and barley; growth in CM, MM-C or MM-N; spore germination in CM, and growth in medium containing glutamine or agmatine as a nitrogen source. In the current study, FGSG_08079 – FGSG_08084 are expressed exclusively *in planta*.....178

Figure 7. Expression profiles of genes that encode predicted proteases expressed exclusively *in planta*.....179

Figure 8. Expression profiles of four genes expressed exclusively *in planta* that were chosen for reverse genetic analysis.....180

Figure 9. Split marker PCR method used for disruption of targeted genes. A) Left and right flanking (LF and RF) regions of target gene are amplified using LF1F + LF2R and RF3F + RF4R oligonucleotide combinations. Sequences specific to the 5' and 3' regions of *hph* have been added to the 5' ends of LF2R and RF3F. HY and YG regions of the *hph* are amplified using HYG/F + HY/R and HYG/R + YG/R oligonucleotide combinations. B) LF and HY amplicons and LF1F and HY/R oligonucleotides are used to produce LFHY fusion products via PCR. YG and RF amplicons and YG/F and RF4R oligo-nucleotides are used to produce YGRF fusion products via PCR. C) Transformation of protoplasts with LFHY and YGRF fusion products disrupt the target gene via a triple crossover event.....181

Figure 10. Southern blotting of PH-1*tri9*, PH-1*tri9/Tri9*, and PH-1 genomic DNA. 1) Location of *SpeI* restriction enzyme cut sites in the left and right flanking regions (LF and RF) of PH-1 and PH-1*tri9* and the expected sizes of fragments targeted by hybridization probes. 2) Hybridization of A) *Tri9* B) *hph* C) *neo* specific probes to digested genomic DNA from I) PH-1 II) PH-1*tri9* III) PH-1*tri9/Tri9.* These results demonstrate the presence of single copies of *Tri9* in PH-1 and PH-1*tri9/Tri9,* a single copy of *hph* in PH-1*tri9*, and a single copy of *neo* in PH-1*tri9/Tri9.* The relative sizes of the fragments

labeled with the *Tri9* probe in PH-1 DNA and *hp*h probe in PH-1*tri9* DNA are consistent with expected digestion patterns. Integration of the PH-1*Tri9* complementation construct resulted in the deletion of the *hph* construct that was present in the *tri9* strain prior to transformation.....182

Figure 11. Disease symptoms on infected wheat spikes. A) PH-1, B) PH-1*tri9*, and C) PH-1*tri9/Tri9* strains were used to inoculate a central spikelet of the wheat cultivar Norm. Symptoms of disease are more widespread on spikelets infected with PH-1 and PH-1*tri9/Tri9*.....183

Figure 12. Southern blotting of PH-1*tpp1* and PH-1 genomic DNA. 1) Location of *XmnI* restriction enzyme cut sites in the right and left flanking regions (LF and RF) of PH-1 and PH-1*tpp1* and the expected sizes of the fragments targeted by hybridization probes. 2) Hybridization of A) *Tpp1* or B) *hph* specific probes to digested genomic DNA from I) PH-1 or II) PH-1 *tpp1*. These results demonstrate the presence of a single copy of *Tpp1* in PH-1 and a single copy of *hph* in PH-1*tpp1*. The relative sizes of the fragments labeled with the *Tpp1* probe in PH-1 DNA and *hph* probe in PH-1*tpp1* DNA are consistent with expected digestion patterns.....184

Chapter 1

Literature Review

Introduction

The plant pathogen *Fusarium graminearum* presents a two-fold threat to farmers and consumers. Not only does the fungus cause symptoms that result in significant yield loss in infected grains, it also taints these grains with potent mycotoxins harmful to humans, animals, and plants alike. Equally alarming is the evidence that grain can appear to be physically sound while still being significantly contaminated with trichothecene mycotoxins (Hollingsworth, 2008). Trichothecene contamination reduces the market value of grain. During the 1993 epidemic of Fusarium head blight (FHB) experienced by farmers living in Manitoba, Minnesota, North Dakota, and South Dakota, the Minneapolis Grain Exchange discounted the price paid for high quality milling wheat by more than 17% for any trace of trichothecene contamination. Total losses incurred by wheat and barley farmers during this epidemic totaled at least $700 million (McMullen, 1997). Yield losses and price discounts incurred annually by farmers in the upper Midwest have resulted in farm foreclosure and bankruptcy (Windels, 2000). This dismal situation strongly underscores the importance of studying FHB from multiple perspectives. This review will touch upon the current states of research regarding fungal pathogenicity, trichothecene toxin production, and resistance in economically important grasses.

Pathogenesis

Infection

F. graminearum can initiate interaction with a perspective host via sexually produced ascospores or asexually produced conidia. Spores can travel long distances, driven by wind or rain. Upon contact with a host, spore germination occurs and the fungus begins the infection cycle (Gilbert and Fernando, 2004). Temporal gene expression patterns specific to *in vitro* conidial germination have been recently explored using an Affymetrix microarray (Seong et al., 2008).

Paths of infection used by the fungus are similar in wheat and barley. The fungus grows subcutaneously as well as through stomatal pores, among crevices within floral bracts, and directly through floral bracts (Bushnell, 2003). Similar growth patterns have been documented in barley (Boddu et al., 2006). A green fluorescent protein (GFP) tagged strain of *F. graminearum* was used to demonstrate barley can also be infected via colonization of ovary epithelial hairs found at the tip of a barley floret (Skadsen and Hohn, 2004). Detailed studies of the infection paths used in oat or rice have yet to be undertaken. In rice, symptoms spread outward from an initial point of infection. The fungus is able to colonize an entire flower, suggesting subcutaneous growth (Goswami and Kistler, 2005). Production of conidia in wheat has been observed as early as 72 hours post inoculation (Pritsch et al., 2000).

Signs, symptoms, and disease phenotypes associated with *F. graminearum* infection differ among host grasses. For corn flowers, the stigma, or silk, is the primary point of infection, resulting in maize ear rot. Subsequent to infection, the fungus often colonizes an entire ear with white, pink, and red mycelia. Symptoms of FHB on wheat include purple to black necrotic lesions, awn twisting and deformation, bleaching and tanning attributed to blight, and atrophy of the developing grain resulting in "tombstone" kernels (McMullen et al, 1997; Goswami and Kistler, 2004). Under prolonged warm and moist conditions, signs of the fungus can be seen as pink mycelial masses on the surface of infected spikes (Goswami and Kistler, 2004.) Occasionally, the rachis of a blighted head will be girdled, leading to the loss of the entire spike. Symptoms of FHB on barley include isolated areas of tan to dark brown discoloration as well as evidence of water-soaking restricted to the initially infected inflorescence (Bushnell et al., 2003; Goswami and Kistler, 2004). Signs of the fungus can also be present on barley under prolonged warm and moist conditions (Goswami and Kistler, 2004). On rice, symptoms of infection are limited to discrete brown to black necrotic lesions (Goswami and Kistler, 2005). Similarly, symptoms observed on oats are localized to the initially infected pedicel (Langevin et al., 2004).

The availability of a high-quality genome-wide DNA sequence assembly, comparative genomic and annotation resources, and an Affymetrix whole genome expression array specific to *F gramineraum*, as well as the amenable nature of *F. gramineaum* to genetic engineering, have greatly accelerated the identification of genes necessary for plant infection, pathogenicity, and completion of the fungal life cycle (Cuomo et al., 2007;

Güldener et al., 2006b; Seong et al., 2005). Community database resources for microarray gene expression data management (Munich Information Center for Protein Sequences (MIPS) *F. graminearum* Genome Database (FGDB); http://mips.helmholtz-muenchen.de/genre/proj/FGDB/) and distribution (PLEXdb; www.plexdb.org) are also available for this organism (Güldener et al., 2006a; Wise et al., 2007; Wong et al., 2011). Gene expression studies focused on identifying and characterizing *F. graminearum* genes involved in trichothecene production and pathogenesis have helped to identify the roles of several different proteins that influence the ability of the fungus to grow, reproduce, or cause disease (Goswami et al., 2006; Güldener et al., 2006b; Qi et al., 2006; Seong et al., 2008; Stephens et al., 2008; Gardiner et al., 2009). These genes play roles in basic metabolic processes, iron acquisition, structural integrity, signaling, transcriptional regulation, and the production of the trichothecene mycotoxins. One gene encoding a secreted virulence factor has also been identified.

Pathogenicity factors involved in trichothecene biosynthesis

Trichothecenes are implicated as virulence factors in host-*Fusarium* interactions (Proctor et al., 1995). In wheat and barley, trichothecene accumulation is associated with increased fungal virulence (Gardiner et al., 2010). Trichothecene production plays a significant role in the spread of FHB. Wheat spikes point-inoculated with non-trichothecene producing *tri5* mutant strains of *F. graminearum* do not exhibit symptoms beyond the initially infected spikelets (Bai et al., 2002).

Trichothecenes are a class of sequiterpenoid secondary metabolites produced by several fungi, including members of the genera *Fusarium*, *Myrothecium*, *Trichoderma*, and *Stachybotrys*. Four types (A-D) of trichothecenes have been recognized, each classified by unique attributes of their chemical structures (Ueno, 1984). Type A and Type B trichothecenes, both produced by *Fusarium* species, can be differentiated by the presence of a carbonyl group located on C-8 of the sequiterpenoid backbone of toxins produced by the latter. The type C species of trichothecenes possesses an additional 7,8 epoxide not present in any of the other classifications, while Type D species contains a macrocyclic ring bridging C-4 and C-15 of the sequiterpenoid backbone. Members of the *Fusarium* genus synthesize neither type C nor type D toxins (Kimura et al., 2007).

Strains of *F. graminearum* produce the Type B trichothecenes deoxynivalenol (DON) and its acetylated derivatives, 15-acetyldeoxynivalenol (15ADON) and 3-acetyldeoxynivalenol (3ADON) or nivalenol (NIV). All of these toxins have been detected in wheat and barley. DON, 3ADON, and nivalenol (NIV) have been detected in infected oats (Langseth et al, 1996). Conversely, trichothecenes were not detected in rice infected with *F. graminearum* (Goswami and Kistler, 2005). Further study revealed the presence of DON and 15ADON in infected rice, though at almost ten-fold lower levels than those observed in wheat or barley (Chapter 3).

Though DON is not the most toxic trichothecene, it is one of the most common contaminants in barley, wheat, and corn worldwide (Rotter et al., 1996.) DON is a relatively stable compound not significantly affected by milling or baking. It is detectable

in finished goods produced from contaminated grains. The United States Food and Drug Administration advises that human consumption of bran, flour or germ containing more than 1 ppm of DON should be avoided (Petska and Smolinski, 2005). Trichothecene toxicity is complex. Trichothecenes bind ribosomes, inhibiting protein synthesis (Ueno, 1984). A "ribotoxic stress response" model has been proposed. This model entails the activation of transcription factors via MAPK mediated signaling. These transcription factors are involved in the production of cytokines, cyclooxygenase 2 (Cox2), and induction of apoptosis. The transduction mechanisms that recognize ribosome binding by DON and activate downstream signaling are unknown (Petska and Smolinski, 2005).

A diverse group of proteins are involved in trichothecene biosynthesis, efflux, and gene regulation controlling toxin accumulation. Several of these proteins are encoded by genes within a trichothecene biosynthetic cluster (Tri cluster), which spans ~26 kb of genomic sequence on chromosome 2 (Kimura et al., 2003, Wong et al., 2011). Three other genes directly involved in trichothecence biosynthesis are located outside of the Tri cluster (Rep and Kistler, 2010). There may be other proteins involved in synthesis that have yet to be identified (Kimura et al., 2007). In *F. graminearum*, the Tri cluster encodes a total of 13 proteins implicated in toxin production and efflux (Figure 1). The exact role some of these proteins play in the production of trichothecenes is known, while the roles of others remain unknown.

Genes in the Tri cluster

Two transcription factors, Tri6p and Tri10p, encoded by genes bordering *Tri5,* regulate transcription of genes located within the cluster and influence the expression of other genes. Promoter analysis of genes positively regulated by Tri6p revealed the presence of a Tri6p specific binding site in 5' UTRs of these genes (Hohn et al., 1999). All genes in the Tri cluster, with the exception of *Tri10*, possess this binding site in their 5' UTR, as do a number of genes outside of the cluster (Seong et al., 2009). Evidence of gene regulation by *Tri10* was first revealed in *F. sporotrichiodes*, where a decrease in the expression of genes necessary for several trichothecene biosynthetic steps was observed in a Δ*tri10* mutant strain (Tag et al., 2001). In *F. graminearum*, Δ*tri10* strains are significantly less pathogenic than wild-type strains and produce very small amounts of trichothecenes. Microarray-based gene expression studies of Δ*tri6* and Δ*tri10* knock-out strains *in planta* identified more than 200 genes regulated by these regulatory proteins, including genes active in the isoprenoid biosynthetic pathway responsible for the synthesis of farnysyl pyrophosphate, the chemical which is the initial substrate of the trichothecene biosynthetic pathway (Seong et al., 2009).

Tri5, the gene that encodes trichodiene synthase, is a known pathogenicity factor in wheat. It is required for the production of DON, as it facilitates the production of trichodiene via the cyclization of farnesyl pyrophosphate (Proctor et al., 1995). Mutants lacking the *Tri5* gene do not produce DON. Wheat spikes inoculated with these mutants do not exhibit symptoms beyond the initially infected spikelets (Bai et al., 2002).

The Tri cluster also contains three genes encoding cytochrome P450 like enzymes: *Tri4*, *Tri11*, and *Tri13*. Tri4p is a multifunctional oxygenase that performs three oxygenase steps to convert trichodiene to isotrichotriol. Tri11p hydroxylates C-15 of isotrichodermin to produce 15-decalnectrin (Desjardins, 2009). Tri13p, an oxygenase necessary for the production of NIV via C-4 oxygenation of calnectrin, is non-functional in 15ADON or 3ADON producing strains (Kimura et al., 2007).

Genes for two acetyltransferases, *Tri3* and *Tri7*, also lie within the Tri cluster. Tri3p acetylates 15-decalnectrin, producing calnectrin, the penultimate step in the pathway, before it branches into processes specific for the production of either Type A (T-2 toxin) or Type B (DON and its derivatives or NIV) trichothecenes (Garvey et al., 2009; Kimura et al., 2007). Tri7p acetylates C-4 of the trichothecene backbone during Type A toxin synthesis by *F. sporotrichiodes* to produce T-2 toxin. In 15ADON or 3ADON producers, this gene is either a pseudogene or is absent, respectively. *Tri7* is intact in NIV producers (Rep and Kistler, 2011).

Tri8p, an esterase, hydrolyses the acetyl ester at position C-3 of the 3,15 diacetyldeoxynivalenol molecule, resulting in the production of 15ADON. This step has been hypothesized to be the end of the biosynthetic pathway in 15ADON producing strains of *F. graminearum*. (McCormick and Alexander, 2002)

Characterization of *Tri12* in the Type A trichothecene producing *F. sporotrichiodes* suggests the encoded protein could be involved in self-protection against trichothecenes. Expression of this gene in yeast provided an avenue for trichothecene efflux similar to that which was observed in strains expressing PDR5, a previously described ABC transporter. Thus, *Tri12* has been implicated in self-protection and trichothecene efflux (Alexander et al., 1999). Characterization of *Tri12* in *F. graminearum* is described in Chapter 2.

The true biochemical function of Tri14p is unknown, though Δ*tri14* mutant strains are significantly less pathogenic and do not produce measurable levels of DON on wheat. Curiously, toxin production occurs in cultures of cracked corn (Dyer et al., 2005). The function of Tri9p remains unknown. Characterization of this gene is described in Chapter 3.

Trichothecene biosynthetic enzyme residing outside of the Tri cluster

Three other genes directly involved in trichothecene biosynthesis – *Tri101*, *Tri1,* and *Tri16* – reside outside of the Tri cluster (Figure 1) (Rep and Kistler, 2010). *Tri101* is located on chromosome 4 and is genetically unlinked to other genes involved in trichothecene synthesis. *Tri1* and *Tri16* compose a two-gene cluster on chromosome 1, though *Tri16* is a pseudogene in *F. graminearum* (Brown et al., 2003; Meek et al., 2003; Kimura et al., 2007).

Tri101p, an acetyltransferase, performs the essential C-3 position acetylation of the trichothecene backbone, leading to the synthesis of isotrichodermol from isotrichodermin (McCormick et al., 1999; Kimura et al., 2007). This protein has been shown to provide protection against trichothecene mycotoxins. Expression of *F. sporotrichiodes Tri101* (*FsTri101*) in *Schizosaccharomyces pombe,* as well as tobacco and rice seedlings, provided protection against Type A trichothecenes (Kimura et al., 1998; Muhitch et al., 2000; Ohsato et al., 2007). Expression of *FsTri101* in wheat decreased the spread of symptoms of FHB on spikes infected with *F. graminearum* (Okubara et al., 2002) *FsTri101* expressed in barley significantly decreased DON levels *in planta* during greenhouse testing of T3 and T4 transgenic wheat lines, though field tests of T4 transgenic lines showed no reduction in DON accumulation (Manoharan et al., 2006).

Tri1 encodes a cytochrome P450 like enzyme in *F. graminearum*. It is responsible for the hydroxylation of C-7 and C-8 of isotrichodermin and calnectrin based on the accumulation of these secondary metabolites observed in cultures of mutant strains (McCormick et al., 2004).

Using global analysis of *F. graminearum* gene expression under DON-inducing conditions compared with non-inducing conditions, FGSG_00007 and FGSG_10397 were selected for analysis via reverse genetics. These two genes, among others, are significantly up-regulated under toxin induction conditions. FGSG_00007, a predicted cytochrome P450 monooxygenase, possesses amino acid sequence similarity with OrdA, which is involved in the production of aflatoxin B1 and B2 biosynthesis by *Aspergillus*

spp. FGSG_10397 has no known function. Independent deletion of either of the genes resulted in increased virulence on wheat and increased DON production under toxin inducing and non-inducing conditions. The roles these genes play in trichothecene biosynthesis are unclear (Gardiner et al., 2009).

Virulence factors not directly implicated in the trichothecene biosynthesis pathway

Genes involved in activation, regulation, and facilitation of signal transduction

Many of the genes identified as virulence factors of *F. graminearum* are involved in facilitating signal transduction. Proteins involved in cell surface organization, the direct act of signal transduction, and the activation and regulation of signal transduction pathways are among this collection. Interestingly, a majority of the identified virulence genes involved in these processes also influence sexual or asexual reproduction.

Enzymes active in membrane dynamics

Plasma membrane lipid microdomains can cluster proteins into complexes involved in protein sorting and signal transduction. *MesA* has been shown to contribute to sterol organization on the hyphal surface and maintenance of hyphal polarity in *Aspergillus nidulans*. *Mes1*, an ortholog of *MesA*, influences asexual and sexual reproduction, hyphal growth, and virulence of *F. graminearum* on wheat spikes. Conidia production and morphology are altered in Δ*mes1* mutants. Conidia possess few compartments and septa

and are shorter and wider than those produced by the wild-type strain. Germinating conidia are compromised in their ability to maintain a polarity axis and germ tubes are wider and morphologically distinct from those of wild-type strains. Self-crossing and out-crossing of Δ*mes1* mutants resulted in the production of fewer perithicia, though ascospore morphology appeared normal. Mutant ascospore germlings produced through selfing possessed the same aberrant phenotype observed in germ tubes that emerge from mutant conidia. Wheat heads inoculated with Δ*mes1* strains contained fewer symptomatic spikelets, though these strains retain the ability to produce DON on cracked corn (Rittenour and Harris, 2008).

Sphingolipids, ubiquitous membrane components of fungi, likely play important roles in signal transduction, cell-to-cell communication, programmed cell death, and fungal pathogenesis. A sphingolipid C-9 methyltransferase, encoded by *Fgmt2* in *F. graminearum*, plays a role in the synthesis of the glycosphingolipid glucosylceramide. Glucosylceramides have been implicated as pathogenicity factors for *F. graminearum* infecting wheat and the human pathogen *Cryptococcus neoformans*. Disruption of *Fgmt2* in *F. graminearum* resulted in severe growth defects and the production of abnormal conidia. Moreover, mutant strains were severely compromised in their ability to cause symptoms on inoculated wheat heads. Symptom formation in *Arabidopsis thaliana* is also severely delayed in mutant strains (Ramamoorthy, et al., 2009).

Enzymes acting as molecular switches

Ras GTPases are small GTP-binding proteins that cycle between active (GTP-bound) and inactive (GDP-bound) conformations to act as switches in molecular circuits. Interacting with effector molecules to regulate divergent signaling pathways, these proteins serve as points of convergence in signal transduction cascades. These proteins are known to interact with MAP kinase signal transduction networks in fungi. Deletion of *RAS2* in *F. graminearum* results in delayed spore germination and female sterility. Δ*ras2* mutants are unable to cause symptoms beyond the inoculated spikelet on wheat heads, though trichothecene production appeared to be unaffected. The ability to colonize corn silk was also compromised. Phosphorylation of Gpmk1p/Map1 was significantly reduced in the mutant, suggesting *RAS2* plays a role in regulating the Gpmk1/Map1 MAP kinase pathway (Bluhm et al., 2007).

Fungal G proteins play integral roles for cell growth and division, mating, cell-cell fusion, morphogenesis, chemotaxis, virulence, pathogenicity, and secondary metabolite production. G proteins are known to control signaling pathways that regulate various cellular and developmental responses in fungi. Heterotrimeric G protein-mediated signaling pathways are composed of G protein-coupled receptor, G proteins, and downstream effectors such as kinases and ion channels (Yu, 2006). Independent deletion of genes encoding Gα subunit GzGpa1 and Gβ subunit GzGpb1 in *F. graminearum* resulted in increased production of DON and zearalenone. Moreover, deletion of GzGpa1 resulted in female sterility, while ΔGzGpb1 exclusively exhibited reduced virulence on

barley. Deletion of a second Gα subunit, GzGpa2, also resulted in reduced virulence on barley and increased chitin in the cell walls of mutants. These findings demonstrate the involvement of a ubiquitous signaling pathway in sexual development, toxin production, and pathogenicity in *F. graminearum* (Yu et al., 2008).

Enzymes that support and maintain signal transduction pathways

Shim et al. (2006) hypothesize that Fsr1 regulates virulence by acting as a scaffold for protein components of a signal transduction pathway. Conceptual translation of the amino acid sequence of Fsr1 revealed four putative functional domains that might carry out unique cellular functions: a caveolin-binding domain, a coiled-coil structural motif, a calmodulin-binding domain, and a WD40-repeat domain. Members of the striatin protein family possess these four domains and are predicted to function as scaffolding proteins that facilitate signal transduction or interact with kinases, phosphotases, or transcription factors. Targeted disruption of *Fsr1* in *F. graminearum* resulted in the inability of mutants to produce perithecia on carrot agar and a significant loss of virulence on barley spikes (Shim et al., 2006).

Ubiquitin-mediated degradation of regulatory and signaling proteins is important in a variety of cellular functions. In eukaryotes, Skp1-Cul1-F-box-protein (SCF) ubiquitin ligase complexes facilitate this degradation. F-box proteins, such as Fbp1, are likely active members of these complexes in *F. graminearum*. Functional analysis of *Fbp1* via reverse genetics revealed this protein is necessary for wild-type virulence and sexual

development. Δ*fbp1* mutants were less virulent on barley spikes. Acting as females in self-crosses, these strains were unable to produce perithecia. Mating attempts between Δ*fbp1* mutants acting as out-crossing males and MAT1-2-deleted strains resulted in a limited number of small perithecia containing asci with incomplete octads (Han et al., 2007).

MAP and serine/threonine kinases

The MAP kinase Gpmk1/MAP1, a MAP kinase with homology to a known pathogenicity gene of *Magnaporthe grisea*, regulates mating, production of conidiation, and pathogenicity of *F. graminearum*. Abolition of its function results in sexual sterility, reduced production of conidia, and the inability to cause symptoms on inoculated plants (Jenczmionka et al., 2003). Δ*gpmk1/map1* mutants were non-pathogenic on wheat flowers or roots and did not infect wounded floral tissue of wheat or tomato fruit, though they retained the ability to produce DON *in planta* (Urban et al., 2003). Further investigation revealed that *Gpmk1* regulates the expression of cell wall degrading enzymes such as endo-1,4-b-glucanase and other proteolytic, xylanolytic, and lipolytic enzymes (Jenczmionka and Shäfer, 2005).

Site directed mutagenesis of Mgv1, a MAP kinase, resulted in sexual self-sterility and reduced toxin production in wheat. Mutant strains had weak cell walls hypersensitive to degradation by driselase. Virulence of Δ*mgv1* mutants on wheat is significantly reduced compared to the PH-1 wild-type strain (Hou et al., 2002).

Ochiai et al. (2006) demonstrated the involvement of a protein kinase cascade in the regulation of trichothecene biosynthesis. These osmotic stress-activated protein kinases are active in histidine kinase signal transduction. *FgOs4* encodes a mitogen-activated protein kinase kinase (MAPKKK), while *FgOs5* and *FgOs2* encode a MAPKK and MAPK, respectively. Disruption of these genes resulted in decreased expression of *Tri6* and *Tri4* and decreased toxin production of nivalenol in rice culture.

GzSNF1, a serine/threonine protein kinase, influences perithecia, ascospore, and conidia formation and spore germination. Northern analyses of putative gene transcripts encoding an endo-1,4-ß-xylanase 1 precursor (GzXYL1), an endo-1,4-ß-xylanase 2 precursor (GzXYL2), an extracellular ß-xylosidase (GzXLP), and a hypothetical protein similar to pectate lyase (GzPL1) in Δ *gzsnf1* mutants revealed a significant decrease in the expression of these genes in minimal medium supplemented with 2% xylan. Δ*gzsnf1* mutants also exhibited reduced virulence on barley (Lee et al., 2009b).

Enzymes regulating protein kinases

The essential role of the C-type cyclin-like gene *FCC1* in fumonisin synthesis and its influence on conidia production in *Fusarium verticillioides* (*F. verticilloides*) was elucidated via reverse genetic analysis. C-type cyclins are involved in transcriptional activation, the repression of genes associated with stress responses, and also act as cell cycle-regulatory proteins (Shim and Woloshuk, 2001). Furthermore, C-type cyclins

regulate the activity of specific cyclin-dependent kinases through physical association (Bluhm and Woloshuk, 2006). Deletion of *CID1*, the ortholog of *FCC1* in *F. graminearum*, resulted in reduced conidia production, vegetative growth, and DON production. Additionally, mutants exhibited decreased virulence on corn stalks and FHB symptoms did not spread on inoculated wheat heads. Mutants were female sterile, as selfing of these strains produced no perithecia. Expression of *F. graminearum CID1* in *F. verticillioides* Δ*fcc1* mutants rescued the wild-type phenotype, suggesting these two genes are functionally conserved (Zhou, et al., 2010).

Reduced virulence on wheat coleoptiles, decreased conidia production, and lithium sensitivity were observed in *F. graminearum* Δ*fgtep1* mutants. FgTEP1, a homolog of tensin-like phosphatase 1, is active in the phosphatidylinositol-3 kinase signaling pathway. Complementation of yeast Δ*sctep* deletion strains with a copy of *FgTep1* rescued sensitivity to wortmannin, an inhibitor of phosphatidylinositol-3 kinase. Deletion of *FgTep1* in *F. graminearum* resulted in an increase in conidia size and a decrease in the number of septa per conidia, as well as decreased mycelial growth in the presence of lithium. Conidia germination efficiency was decreased in mutants in the presence of wortmannin. The lesions produced by the mutant strain on wheat coleoptiles were significantly smaller than those produced by the wild-type strain (Zhang et al., 2010).

Similarly, mycelial sensitivity to lithium and attenuated virulence on wheat coleoptiles was observed in *F. graminearum* Δ*fgptc1* mutants. *FgPtc1* encodes a Type 2C protein phosphatase. These enzymes participate in the regulation of signal transduction through

specific dephosphorylation of serine/threonine residues and are dependent on the presence of Mn^{2+} or Mg^{2+} (Jiang et al., 2010).

A protein with possible signal capabilities

Forward genetic screening of insertional mutants of the maize pathogen *Cochliobolus heterostrophus* resulted in the discovery of *CPS1*. *CPS1* encodes a novel enzyme possessing two AMP binding domains, though its true biochemical function is unknown. It is conserved in *F. graminearum* as well as a broad range of other filamentous ascomycetes. *F. graminearum* Δ*cps1* mutants exhibit reduced virulence on wheat (Lu et al., 2003).

Enzymes involved in transcriptional regulation

ZIF1 encodes a b-ZIP transcription factor that is conserved in filamentous ascomycetes. Deletion of *FgZIF1* affects *F. graminearum* virulence and reproduction. Mutants were unable to spread from the point of inoculation in wheat and produced less DON *in planta* than the wild-type strain. Δ*zif1* mutants produced small, sterile, pigmented perithecia, suggesting a female-specific role for *ZIF1* during fertilization or ascus development. Male fertility was unaffected. Deletion of *MoZIF1* in *Magnaporthe oryzae* resulted in reduced virulence and invasive growth. Expression of *FgZIF1* in *mozif1 M. oryzae* mutants rescued the wild-type phenotype, demonstrating this transcription factor is functionally conserved in *F. graminearum* and *M. oryzae* (Wang et al., 2011).

Topoisomerase I, encoded by *TOP1*, influences conidia production and pathogenicity in wheat. In eukaryotes, it has been shown to be involved in uncoiling DNA during transcription and DNA replication. Deletion of *TOP1* in *F. graminearum* results in the limitation of symptoms to the initially infected spikelet. Mutants produce ~30% fewer conidia than the wild-type strain. Interestingly, deletion of an orthologous gene in *Fusarium culmorum* results in the complete abolition of spore production (Baldwin et al, 2010).

The transducin beta-like gene *FTL1* also influenced ascospore formation and sexual reproduction. Based on comparative genetic analysis, *FTL1* likely encodes a component of a regulatory histone deacetylase complex. Δ*flt1* mutants, generated via insertional mutagenesis and gene replacement, exhibit female sterility, though they can mate as males. They are unable to colonize vascular tissue in the rachis of infected wheat or spread from infected anthers to ovaries. They exhibit increased sensitivity to plant defensins, and significant up-regulation of genes involved the production of aurofusarin. Finally, they retain their ability to produce DON and express several identified virulence factors, though mircoarray studies on a gene replacement mutant revealed the down-regulation of several genes that likely encode virulence factors (Ding et al., 2009).

Transposon-mediated mutagenesis was used to generate a mutant strain of *F. graminearum* that exhibits reduced radial growth on test media and compromised virulence on wheat. FGSG_10057 encodes a $Zn(II)_2Cys_6$-type transcription factor

(Dufresne et al., 2008). The ortholog of this gene in *Magnaporthe grisea* (MGG_09263) influences appressorium formation and pathogenicity on rice seedlings (Jeon et al., 2007).

Enzymes involved in nutrient acquisition, metabolism, and structural integrity

Several research groups have screened random insertional mutant libraries for mutants with reduced virulence or the inability to colonize corn silk or wheat heads. These studies have identified several enzymes involved in the metabolism of amino acids and purines.

The creation of arginine and adenine auxotrophic mutants via restriction enzyme-mediated integration (REMI) mutagenesis resulted in identification of two metabolic entities that influence mycelial growth, virulence on barley, and sexual reproduction in *F. graminearum*. *ARG2* and *ADE5* encode acetylglutamate synthase and phosphoribosylamine-glycine ligase, necessary for the metabolism of arginine and adenine, respectively. Independent targeted deletion of each of these genes resulted in the inability of either mutant to produce perithecia or grow on minimal media. Conidia production was completely absent in Δ*arg2* mutants and rarely observed in Δ*ade5* mutants. Virulence of both mutants on barley was severely attenuated. Addition of arginine or adenine to cultures used to measure radial growth and sexual fertility and for the production of conidia for virulence tests rescued wild-type phenotypes in all respects for both mutants (Kim et al., 2007).

Reverse genetic analysis of *CBL1* and *MSY1* established that these genes encode cystathionine beta-lyase and methionine synthase, respectively. Δ*cbl1* and Δ*msy1* mutants are less virulent on wheat than the wild-type strain. Both mutants are methionine auxotrophs, suggesting auxotrophy may reduce fungal virulence. In this study, two other genes encoding a putative b-ZIP transcription factor and transducin beta-subunit-like protein were also identified as probable virulence factors (Seong et al., 2005).

A histidine auxotrophic REMI mutant exhibited a phenotype similar to that which is observed in arginine, adenine, and methionine auxotrophic mutants. Reverse genetic analysis of *GzHIS7* revealed this gene encodes a putative glutamine amidotransferase that is essential for histodine biosynthesis. Δ*gzhis7* mutants are reduced in radial growth, virulence, and sexual reproduction, but not conidia production (Seo et al., 2007).

GzICL1 and *GzMCL1* encode isocitrate lyase and methylisocitrate lyase, respectively. Each of these enzymes act as key enzymes in the glyoxylate and methylcitrate cycles, respectively, and are involved in the metabolism of two- or three-carbon compounds in fungi. Orthologs of each of these enzymes have been implicated as pathogenicity and virulence factors in other plant pathogens. The targeted disruption of genes encoding these enzymes resulted in significantly reduced virulence in *Leptosphaeria maculans*, *Magnaporthe grisea*, *Stagonospora nodorum*, and *Colletotrichum lagenarium*. Reverse genetic analysis of *GzICL1* revealed the involvement of the glyoxylate cycle in self-fertility. Δ*gzicl1* strains produced very few, if any, perithicia when selfed. Outcrossing these strains with a MAT1-1 self-sterile strain resulted in production of perithicia similar

to that observed with the wild-type strain, indicating that *GzICL1* does not affect male fertility. Δ*gzicl1* and Δ*gzmcl1* mutants exhibited the inability to metabolize certain two- or three-carbon compounds. Deletion of either of these genes in *F. graminearum* has no effect on fungus virulence on wheat or barley. Double deletion of these genes in a single strain results in significantly reduced virulence on both plants, suggesting overlapping or reciprocally redundant functions *in planta* (Lee et al., 2009a).

HMR1 was selected for further characterization based on reduced virulence observed during screening of REMI mutants for the inability to colonize corn silk or wheat heads. *HMR1* encodes hydroxymethyl-glutaryl CoA reductase, an enzyme essential for sterol and isoprenoid biosynthesis. Complete disruption of this gene appears to be lethal, though it is amenable to genetic manipulation. Deletion of the N-terminal 254 amino acids of HMR1 resulted in decreased mycelia growth on V-8 agar. These mutants were also significantly reduced in virulence on flowering wheat heads and failed to cause necrosis beyond the point of inoculation. Interestingly, a portion of the 5' coding region of this gene exhibits cryptic promoter activity, enabling transcription of the catalytic domain of the protein (Seong et al., 2006). *HMR1* is also under the regulatory control of Tri6, a transcription factor found in the Tri biosynthetic cluster, as are all other genes for enzymes in the isoprenoid biosynthetic pathway (Seong et al., 2009).

Hydroxamates are instrumental in fungal iron metabolism (Hass, 2003). *SID1* encodes an ornithine N^5–oxygenase that carries out the first step in the synthesis of a hydroxymate siderophore that facilitates the uptake of iron from outside of the cell. *F. graminearum*

Δ*sid1* mutants are able to colonize an infected spikelet but are unable to spread through the rachis. Mutants are also unable to produce siderophores or maintain wild-type growth rates in culture. Complementation of cultures with $FeSO_4$ restored wild-type growth in the mutant strain (Greenshields et al., 2007).

A similar phenotype was observed in *F. graminearum* Δ*nps6* mutants. Nonribosomal peptide synthetases (NRPSs) are multifunctional proteins that biosynthesize small peptides. This type of synthesis occurs in bacteria and fungi independent of ribosome mediated peptide synthesis. Products of NRPSs can play critical roles in plant–microbe interactions. NPS6, a nonribosomal peptide synthetase, is specifically involved in extracellular siderophore biosynthesis. Triacetyl fusarinine C, the major extracellular siderophore of *F. graminearum*, is not produced by Δ*nps6* mutants. Δ*nps6* mutants exhibit reduced virulence on wheat. Symptoms caused by mutants are slow to spread on infected wheat heads. Iron application rescues the wild-type virulence phenotype. NPS6 is conserved in several plant-fungal interactions and this effect has been observed in orthologous mutants generated in the maize pathogen *Cochliobolus heterostrophus*, the brassica pathogen *Alternaria brassicicola,* and the rice pathogen *Cochliobolus miyabeanus* (Oide et al. 2006).

Two genes encoding chitin synthases, *GzCHS5* and *GzCHS7*, were shown to be necessary for hyphal growth, perithecia formation, and pathogenicity. These genes were identified via REMI mutagenesis and further characterized via reverse genetic analysis. *GzCHS5* encodes a putative class V chitin synthase, while *GzCHS7* encodes a putative class VII

chitin synthase. Independent deletion of these genes resulted in reduced virulence on barley and reduced cell wall rigidity when measured by atomic force microscopy (Kim et al., 2009).

Transposon-mediated mutagenesis was used to generate a mutant strain of *F. graminearum* that is unable to form perithecia. Symptoms of FHB did not advance from spikelets inoculated with this strain. FGSG_01974 encodes a predicted glycolipid transfer protein with similarity to HET-C2. Research conducted on HET-C2 in *Podospora anserina* suggests it may play a role in cell-wall biosynthesis (Dufresne et al., 2008).

Proteins involved in vesicle trafficking

Vesicles are major intermediates for protein transport. Docking and fusion of secretory vesicles at intracellular and plasma membranes have important roles in vegetative or sexual growth in fungi. In this process, v-SNARE proteins are packaged together with cargo proteins into vesicles. Interaction between a v-SNARE and membrane-integrated t-SNARE protein catalyzes the fusion of the apposing membranes of the transport intermediate and the target compartment (Hong, 2005). *GzSYN1* and *GzSYN2* encode syntaxin like t-SNARE proteins in *F. graminearum*. Targeted deletion of *GzSYN1* and *GzSYN2* resulted in a 67% and 75% decrease in virulence on barley, respectively. While the ability to sexually reproduce was retained in Δ*gzsyn1* mutants, perithicia were unevenly distributed. This mutant also exhibited decreased radial hyphal growth in culture. Δ*gzsyn2* mutants are female sterile, though they can act as males in outcrosses

with Δ*mat*1-2 strains. Outcrosses result in the normal formation of perithecia. Asci are viable, though they exhibit abnormal morphology. Radial hyphal growth of Δ*gzsyn2* mutants is similar to that of wild-type strains, though the mycelia of both Δ*gzsyn1* and Δ*gzsyn2* mutants were generally thinner than those of wild-type strains (Hong et al., 2010).

A secreted virulence factor

In *F. graminearum*, *Fgl1* encodes a secreted lipase. Targeted disruption of *Fgl1* resulted in attenuation of virulence in wheat; symptoms did not to spread beyond the spikelets adjacent to inoculated spikelets. Maize infected with Δ*fgl1* mutants exhibited only minor symptoms, and estimates of disease severity were much lower in cobs infected with these strains (Voigt et al., 2005).

Resistance to FHB in wheat and barley

The complex nature of wheat resistance to FHB makes it difficult to select for via conventional breeding (Somers et al., 2005). Unfortunately, most resistant germplasm is of exotic origin and possesses poor agronomic traits; inheritance of resistance is oligogenic to polygenic; and screening for resistance is environmentally biased, tedious, and expensive (Buerstmayer et al., 2003). Therefore, significant effort has been directed at elucidating the molecular basis of resistance to FHB.

Five different types of resistance to FHB have been described in wheat. Type I and Type II resistances describe resistance to initial infection and resistance to the spread of infection from the point of inoculation, respectively. Genetic resources providing resistance to DON via toxin decomposition (Type V), kernel infection (Type III), and trichothecene tolerance (Type IV) are also desirable targets of wheat and barley breeders (Waldron et al., 1999). FHB symptoms in barley usually do not spread internally from initially infected spikelets to adjacent spikelets due to what is considered innate Type II resistance. Therefore, barley breeding efforts focus on Type I resistance. Certain varieties of wheat possess Type II resistance to infection, while others allow the infection to spread and colonize the entire spike (Bai and Shaner, 2004). Considering the isolated nature of symptoms observed on rice and oat, it is likely these plants also employ Type II-like resistance to combat the invading fungus.

QTL for FHB resistance in wheat and barley

Quantitative trait locus (QTL) mapping is commonly employed to identify genetic regions of wheat and barley conferring resistance to FHB. QTL mapping describes the use of molecular markers to identify genetic locations of alleles that confer resistance or other desirable traits. Restriction fragment length polymorphism (RFLP), simple sequence repeat (SSR), amplified fragment length polymorphism (AFLP), single nucleotide polymorphism (SNP), and diversity array technology (DArT) are the most commonly used markers used in QTL mapping (Buerstmayer et al., 2009). Molecular

markers that segregate with particular traits are useful for marker-assisted selection in practical breeding programs (Buerstmayer et al., 2002).

QTL for FHB resistance in wheat

QTL for FHB resistance have been identified on all wheat chromosomes with the exception of chromosome 7B (Buerstmayer et al., 2009). The wheat variety Sumai 3 exhibits Type II resistance, making it a desirable target for molecular analysis and a desirable source of FHB resistance in wheat breeding programs (Kolb et al., 2001). *Fhb1*, a major QTL encoding Type II resistance, has been mapped to chromosome 3BS (Bai et al., 1999, Waldron et al., 1999). Analysis of wheat varieties possessing *Fhb1* revealed the ability of these varieties to convert DON to DON-3-O-glucoside (Lemmens et al., 2005). Interestingly, studies conducted on *DOGT-1*, an *Arabadopsis thaliana* gene encoding a UDP-glycosyltransferase, revealed the ability of this enzyme to convert DON to DON-3-O-glucoside in transgenic yeast strains. Over-expression of this gene in transgenic *Arabadopsis thaliana* resulted in enhanced tolerance of DON (Poppenberger et al, 2003). Schweiger et al. (2010) demonstrated that heterologous expression of a full-length cDNA encoding a barley glocosyltransferase (HvUGT13248) in yeast could confer resistance to DON. Moreover, yeast strains expressing HvUGT13248 produced DON-3-O-glucoside, which is a product of DON detoxification. A Bowman-Birk type trypsin inhibitor also has been mapped to chromosome 3BS. The exact function of the *Fhb1* locus remains unknown (Jia et al., 2009). A second QTL contributing to type II resistance has been mapped to chromosome 6B of Sumai 3 and other Chinese wheat varieties. This QTL,

formally named *Fhb2*, mapped as a single Mendelian factor in a fine mapping population and is likely proximal to the centromere of chromosome 6B (Yang et al., 2003; Cuthbert et al., 2007). A QTL on chromosome 5A is often present in FHB resistant varieties of wheat. It has been suggested this locus may contribute more to Type I resistance than Type II resistance based on data obtained from single floret inoculation studies (Buerstmayer et al., 2009).

QTL for FHB resistance in barley

QTL for FHB resistance have been identified on all eight chromosomes of barley. FHB mapping studies published on populations derived from pairs of either six-rowed or two-rowed parents have indicated QTL for FHB are often coincidental with QTL for heading date, plant height, seeds per inflorescence, inflorescence density, lateral floret size, and kernel discoloration (de la Peña et al., 1999; Zhu et al., 1999; Ma et al., 2000; Kolb et al., 2001; Mesfin et at., 2003, Canci et al., 2003, Nduulu et al., 2007). Resistance to FHB also has been observed in a two-rowed by six-rowed population of barley. QTL associated with resistance to DON accumulation have been described in two-rowed, six-rowed, and two-rowed by six-rowed populations of barley. These QTL are also often coincidental with QTL for FHB resistance and other morphological traits (Mesfin et at., 2003; Smith et al., 2004). The *Vrs1* locus in barley is the primary determinant of the two-rowed/six-rowed spike type. Two-rowed cultivars are generally more resistant to FHB than six-rowed cultivars. A FHB resistance QTL is associated with the two-rowed spike type

locus *Vrs1*, though it is not clear if this locus is genetically linked to resistance (de la Peña et al., 1999; Zhu et al., 1999; Ma et al., 2000; Mesfin et at., 2003).

Plant response to infection by *F. graminearum*

The genes that underlie resistance mechanisms used by plants to defend themselves from *F. graminearum* are diverse. Direct and comparative gene expression and biochemical studies have revealed the involvement of several genes and proteins in FHB resistance in wheat and barley. Within select studies, researchers have attempted to differentiate between plant responses that are specifically induced in wheat or barley challenged with wild-type or mutant strains of the fungus or with DON. Components implicated in defense responses of wheat and barley fall into several categories, such as pathogenesis-related (PR) proteins, chitinases, putative trypsin and xylanase inhibitors, programmed cell death (PCD) related proteins, WRKY-like transcription factors and coiled-coil nucleotide-binding site leucine-rich repeat (CC-NBS-LRR) proteins, cytochrome P450-like enzymes, mechanisms implicated in trichothecene detoxification, proteins active in phenylpropanoid metabolism, and proteins involved in the generation of an oxidative burst. The *F. graminearum* defense responses in wheat are swift, with the induction of genes encoding peroxidase, PR-1, PR-2 (β-1,3-glucanase), chitinase, PR-4, and a thaumatin-like protein detected as early as six hours after spray inoculation (Pritch et al., 2000).

Defense responses recognized in wheat

Several studies have focused on analyzing defense responses that are induced or upregulated in wheat cultivars displaying type II resistance. Two-dimensional displays of proteins extracted from wheat spikelets of the resistant wheat cultivar 'Ning7840' infected with *F. graminearum* revealed the induction or upregulation of multiple defense related genes. LC-MS/MS analysis was used to identify superoxide dismutase, dehydroascorbate reductase, and glutathione S-transferases indicating an oxidative burst of H_2O_2 inside tissues infected by *F. graminearum*. PR-2 (β-1,3-glucanase) upregulation was also observed in infected spikelets (Zhou et al., 2005).

Microarray analysis, coupled with suppression subtractive hybridization, was used to monitor gene expression patterns of wheat spikes of FHB-resistant cultivar Ning 7840 and susceptible cultivar Clark during the first 72 hours after inoculation with *F. graminearum*. Genes differentially expressed between these cultivars identified six gene clusters, each possessing temporally unique expression patterns. Two clusters containing genes encoding two putative cytochrome P450s, a putative chitinase II precursor, a PR-1 type pathogenesis-related protein, and two putative proteinase inhibitor-like proteins exhibited similar expression patterns throughout the experiment. A third cluster, composed of genes with relatively high expression levels early in the infection process, but decreased levels later in the infection process, was enriched for genes implicated in defense response. These genes are predicted to encode additional cytochrome P450

enzymes, two PR proteins, NPR-1, and a PDR-like ABC transporter (Bernardo et al., 2007).

Sumai 3 exhibited accelerated expression of genes encoding class IV and VII chitinases and β-1,3-glucanases relative to a susceptible mutant (Li et at., 2001). Two genes identified via sequence analysis of a cDNA library generated from Sumai 3 24 hours after inoculation with *F. graminearum* were mapped to wheat chromosomes 3AS and 6BL, though the contribution of these genes to plant defense is unknown (Hill-Ambroz et al., 2006).

A microarray-based transcriptome study of a Sumai 3 derived near-isogenic line pair carrying *Fhb1* and a corresponding susceptible allele further explored temporal gene expression patterns present in wheat infected with *F. graminearum*. Moreover, a comparison between genes expressed in wheat or barley inoculated with the fungus revealed conserved patterns of gene expression in both hosts as well as differences among the genes expressed in each host. In this study (Jia et al., 2009), the authors identified wheat gene transcripts that exhibited accumulation differences between the resistant and susceptible wheat lines inoculated with spore suspensions or in water inoculated controls. Annotation of these transcripts revealed the expression of a cell wall related proline-rich protein and expansin protein precursor implicated in cell expansion and other processes that occur during cell-wall modification. A predicted Bowman-Birk trypsin inhibitor that might inhibit germination and growth of *F. graminearum* and a protein possessing a NB-ARC (nucleotide-binding adaptor shared by APAF-1, certain R

gene products, and CED-4) signaling motif often found in plant resistance genes and regulators of cell death in animals were also encoded by two of these transcripts (HarvEST : http://harvest.ucr.edu/; van der Biezen and Jones, 1998). Genes with conserved expression patterns between wheat and barley are predicted to encode xylanase inhibitors, WRKY transcription factors, UDP-glucosyltransferases, ABC transporters, NF-X1 transcription factors, programmed cell death related proteins, and ethylene- and jasmonic acid-related proteins. Genes expressed in barley but significantly repressed in wheat are predicted to encode histones, a histone deacetylase, ribosomal proteins, tubulin proteins, microtubule-associated proteins, proline-rich proteins, and proteins involved in photosynthetic activities. The authors posit the repression of genes encoding these proteins may be related to or underlie events associated with programmed cell death (Jia et al., 2009).

A cDNA-AFLP based comparative gene expression study explored temporal gene expression patterns of four different wheat varieties with contrasting phenotypes for FHB resistance. Differing transcript levels between resistant and susceptible varieties mapped to genes encoding a putative UDP-glucosyltransferase, a putative phenylalanine ammonia-lyase, a DNAJ-like protein, a PR-like protein, and a cytochrome P450-like protein (Steiner et al., 2009.)

Two studies used bi-directional suppressive subtractive hybridization (SSH) cDNA subtraction and GeneCalling^{TM} mRNA-profiling technology to identify wheat defense and stress-related genes induced in response to *F. graminearum* (Kong et al., 2005, Kong

et al., 2007). In the first study, the authors identified a gene encoding a putative Class I chitinase induced in infected wheat. Induction of multiple cytochrome P450-like enzymes was observed in both studies. Genes posited to underlie stress responses were also induced in the second study, as was a predicted multi-drug resistance gene.

Golkari and others (2007) used cDNA microarrays to identify organ specific gene expression patterns and genes differentially expressed in wheat infected with *F. graminearum*. Glume, lemma, palea, anther, ovary, and rachis derived cDNA samples were hybridized to a cDNA array derived from a suppression subtraction hybridization (SSH) library of wheat-*F. graminearum* interactions. Genes predicted to encode PR proteins and proteins involved in the production of active oxygen species, phenylpropanoid metabolism, and defense related signal transduction were induced in infected wheat heads. These proteins included β -1-3-glucanases (PR-2), chitinases (PR-3), and thaumatin-like proteins (PR-5); cinnamate-4-hydroxylase; and ascorbate peroxidase, monodehydroascorbate reductase, and metallothione. Interestingly, a WRKY-like transcription factor and CC–NBS–LRR class proteins were significantly upregulated in anthers of infected spikelets. Arabidopsis WRKY factors have been implicated as positive and negative regulators of plant defense mechanisms (Eulgem and Somssich, 2007), while CC-NBS-LRR proteins are proposed to directly or indirectly recognize the presence of pathogens (Meyers et al., 2003).

Desmond et al. (2008) reported that infiltration of wheat stems with DON elicits hydrogen defense responses, peroxide production, and programmed cell death in wheat.

PR1.1, PR2 (β 1–3 glucanase), PR3 (chitinase), PR4 (wheatwin), PR5 (thaumatin-like protein), PR10, peroxidase, and germin-like gene transcripts were observed within 24 hours of DON treatment. Moreover, H_2O_2 production, cell death, and DNA laddering were observed in DON treated tissues.

Defense responses recognized in barley

Microarray analysis of temporal gene expression patterns in barley during *F. graminearum* infection has provided a foundational dataset regarding genes that underlie barley defenses. Boddu et al. (2006) generated transcript accumulation profiles from barley spikes from 0 to 144 hours after infection with *F. graminearum*. These profiles were analyzed to identify barley gene transcripts that exhibit differential accumulation in *F. graminearum* infected plants compared with water-inoculated controls. Transcripts encoded by PR genes and oxidative burst and oxidative stress response associated genes are induced by *F. graminearum* infection. These genes are predicted to encode glutathione S-transferases, peroxidases, and oxalate oxidase. Transcripts predicted to encode WRKY-class transcription factors and components of the phenylpropanoid biosynthetic pathway were also induced. WRKY-class transcription factors are known to interact with PR proteins in other plant microbe interactions, while the metabolites produced by the phenylpropanoid biosynthetic pathway are utilized for biosynthesis of a variety of cellular compounds and structures, such as anthocyanins, lignin, and phytoalexins. Other transcripts exhibiting differential accumulation in infected plants are predicted to encode proteins implicated in trichothecene detoxification such as UDP-

glucosyltransferases, ABC transporters, and probable multidrug and toxic compound extrusion (MATE) factors (Boddu et al., 2006).

A *F. graminearum* Δ*tri5* strain was used to show barley exhibits a specific response to trichothecene accumulation that can be differentiated from a basal defense response to the pathogen. Transcript expression patterns in barley plants inoculated with wild-type or *Tri5* mutant strains were compared to identify genes underlying these responses. The results of this comparison indicate trichothecenes induce a variety of genes controlling diverse cellular processes. Among these are genes implicated in trichothecene detoxification and transport, secondary metabolism, ubiquitination, programmed cell death, and regulation of transcription. Genes that influence trichothecene detoxification and transport are predicted to encode putative UDP-glucosyltransferases, ABC transporters, a MATE efflux protein, and a MFS superfamily protein. Proteins implicated in ubiquination and PCD include an AAA family ATPase, a F-box domain containing protein, proteins containing F-box and U-box domains, NF-X1 type zinc finger family proteins, and a pirin-like protein. Several cytochrome P450 enzymes are implicated in secondary metabolism, while two Cys2/His2 zinc- finger proteins are implicated in transcriptional regulation. Based on this evidence, Boddu et al. (2007) propose that trichothecene accumulation results in at least two general host responses. One response induces a set of genes that attempts to detoxify and neutralize the impact of trichothecenes while another induces a set of host genes that result in cell death and increased susceptibility to *F. graminearum*. Transcripts encoding PR proteins, oxidative burst enzymes, glutathione-S-transferases, proteases, tryptophan biosynthetic genes,

shikimate pathway genes, and phenylpropanoid pathway genes were considered to be components of a basal defense response in barley.

Two-dimensional electophoresis profiles of acidic proteins expressed among barley spikelets from six genotypes were compared to identify differentially expressed proteins in infected and uninfected FHB-resistant and FHB-susceptible barley. Profiles were generated for samples harvested 24 and 72 hours after plants were inoculated with *F. graminearum* or dilute CMC media. Nineteen different proteins associated with mechanisms of resistance to FHB were identified. Oxidative stress defense response proteins such as peroxidase precursors, peroxidases, and malate dehydrogenases showed significant increases in abundance in the resistant barley genotype CI4196, the intermediate resistant genotype CDC Bold, and the susceptible genotype Stander. No protein precursors of jasmonic acid (JA), salicylic acid (SA), or phenylalanine-ammonia lyase pathways were among the differentially expressed proteins identified in this study. The authors propose the deferential expression of these precursors likely occurred within the initial 24-hour period after inoculation and therefore would not be observed using their sampling methods. PR-9 proteins, only activated by the JA pathway, were found in greater abundance in CDC Bold, CI4196, and Stander genotypes. Levels of chitinase 2b were significantly increased in CI4196. Three thaumatin-like proteins were expressed among four genotypes possessing different levels of resistance to FHB (Geddes et al., 2008).

Direct treatment of barley spikelets with DON induced defense responses similar to those induced by trichothecenes produced by *F. graminearum in planta* (Boddu et al., 2007. Gardiner et al., 2010). Gardiner et al. (2010) conducted a comparative study of transcript accumulation patterns induced by DON, accumulation patterns in barley during *F. graminearum* infection with a trichothecene producing strain, and accumulation patterns in barley infected with a trichothecene non-producing strain. Two classes of transcripts were revealed: transcripts with increased accumulation in the presence of deoxynivalenol (DON) and *in planta Fusarium graminearum*-derived trichothecenes; and transcripts expressed exclusively in the presence of DON. DON induced upregulation of gene transcripts predicted to encode proteins implicated in trichothecene detoxification, such as UDP-glucosyltransferases, ABC transporters, and cytochrome P450 enzymes. Glutathione-S-transferases and cysteine synthases were also upregulated, leading the authors to suggest glutathione could play a role in ameliorating the impact of DON accumulation. Several other classes of genes were induced by DON application, including transcription factors and signal transduction proteins.

Summary of defense responses recognized in wheat and barley

The results of these studies suggest conservation of certain defense responses to *F. graminearum* invasion in wheat and barley. These responses include the expression of genes that are predicted to encode mechanisms active in generation of an oxidative burst, phenylpropanoid pathway genes, and genes encoding PR proteins. Both plants express UDP-glucosyltransferases, cytochrome P450-like enzymes, and ABC transporters likely

involved in the detoxification and export of fungal toxins. Proposed indicators of PCD have been reported in both wheat and barley, though it appears the severity of tissue damage caused by this process is greater in wheat. Expression of WRKY transcriptional regulators in response to *F. graminearum* infection has been observed in both plants. These factors are known to play a role in regulating plant responses to biotic and abiotic stress. Genes that encode mechanisms involved with ethylene and JA biosynthesis are also induced in wheat and barley. Plant responses dependent on ethylene and JA are proposed to be generally associated with defense against invading necrotrophic pathogens (Glazebrook, 2005). Jai et al. (2009) provides an excellent detailed comparative summary of transcript accumulation data observed in wheat and barley subsequent to infection with *F. graminearum*.

Genetic engineering of resistance to FHB

Successful genetic engineering of transgenic wheat and barley provides an alternative method for developing cultivars with resistance as well as other desirable traits. Antifungal genes introduced into wheat encode proteins that degrade or disorganize fungal cell walls and membranes or enhance host defense response by interfering with fungal protein synthesis, pathogenesis, and accumulation of DON (Dahleen et al., 2001).

Tri101p, an acetylase, performs the essential C-3 position acetylation of isotrichodermin that is required for the subsequent synthesis of downstream trichothecenes. Furthermore, this protein has been shown to provide protection against trichothecene mycotoxins

(Kimura et al., 2007; Kimura et al., 1998). Conlon barley plants and Bobwhite wheat plants have each been genetically engineered to express *Tri101* from *F. sporotrichioides* (*FsTri101*) (Okubara et al., 2002; Manoharan et al., 2006). T_3 transgenic barley plants expressing *FsTri101* exhibited reduced incidence of FHB and reduced levels of DON in greenhouse tests relative to untransformed plants. Unfortunately, subsequent testing of T_4 plants in the field resulted in no effect on DON concentration in infected plants relative to untransformed plants. In greenhouse studies, wheat expressing *FsTri101* exhibited partial resistance to FHB. These plants exhibited decreased symptom severity relative to wild-type plants (Okubara et al., 2002).

cDNAs of transcripts for genes encoding PR proteins of Sumai 3 were transformed into the FHB susceptible cultivar ‘ Bobwhite’ via a biolistic transformation protocol. Eighty percent of plants with initial transgene expression were completely silenced in T_1 or T_2 generations. Also, two transgenic lines, expressing PR2 (β 1–3 glucanase) and PR3 (chitinase) or PR5 (thaumatin-like protein) from rice exhibited enhanced resistance to FHB in greenhouse experiments, but failed to provide improved resistance in the field (Chen et al., 1999; Anand et al., 2003;). Conversely, the expression of a barley class II chitinase in transgenic wheat resulted in a reduction in the number of scabby kernels and FHB severity observed in greenhouse and field experiments. One transgenic line from this study also exhibited reduced DON concentration relative to the wild-type control (Shin et al., 2008). Over-expression of the defense response genes endcoding α-1-purothionin, thaumatin-like protein 1 (tlp-1), or β-1,3-glucanase in transgenic wheat resulted in enhanced resistance to FHB in greenhouse tests and field tests. These plants

exhibited lower FHB severity, DON concentration, or fewer scabby kernels than wild-type controls. One transgenic line expressing β-1,3-glucanase exhibited all of these traits in field studies (Mackintosh et al., 2007).

Trichothecenes mycotoxins interact with the peptidyltransferase center of eukaryotic ribosomes, inhibiting protein synthesis (Fried et al., 1981). Efforts to map trichothecene resistance in *Saccharomyces cerevisiae* revealed that a mutation in the *RPL3* gene, which encodes the ribosomal protein L3, conferred resistance to trichodermin, an upstream precursor to the trichothecene DON. In germination tests, transgenic tobacco plants expressing a truncated form of the yeast L3 protein gene exhibited resistance to DON. Transgenic wheat expressing the N-terminal fragment of yeast ribosomal protein L3 exhibited reductions in disease severity and kernel DON levels in greenhouse and field experiments (Di et al., 2010).

Systemic acquired resistance (SAR) is an inducible plant defense mechanism that can confer resistance to a broad range of plant pathogens. SAR is associated with the accumulation of elevated levels of SA and expression of the pathogenesis-related (*PR*) group of genes. *Arabidopsis NPR1* (*AtNPR1*) is a known regulator of SAR; loss-of-function mutations in *AtNPR1* result in attenuated activation of SAR and enhanced susceptibility of *A. thaliana* to a variety of pathogens. Transgenic wheat expressing *AtNPR1* exhibited faster and stronger activation of PR1 expression in response to *F. graminearum* infection and had levels of resistance to FHB similar to Sumai 3 (Makandar et al., 2006).

Finally, transgenic wheat expressing a maize b-32 antifungal gene that encodes a ribosome inactivating protein exhibited enhanced type II (resistance to the spread of infection) and type III resistance (resistance to DON) to FHB in greenhouse studies (Balconi et al., 2007).

Transgenic wheat varieties with resistance to FHB have shown some promise in early stages of their development. One of the primary challenges faced by researchers using genetic engineering to develop wheat and barley with desirable resistance traits lies in the synthesis of transgenic lines that consistently express transgenes at useful levels in subsequent generations. Gene silencing caused by integration of multiple gene copies and the observation that not all wheat and barley varieties are equally amenable to transformation and transgenic manipulation continue to confound researchers in this field. Therefore, it appears that genetically engineering FHB resistance is not likely to replace traditional and modern breeding efforts in the near future. Instead, as technology in this area continues to advance, transgenic approaches will begin to complement the efforts of wheat and barley breeders.

Figure

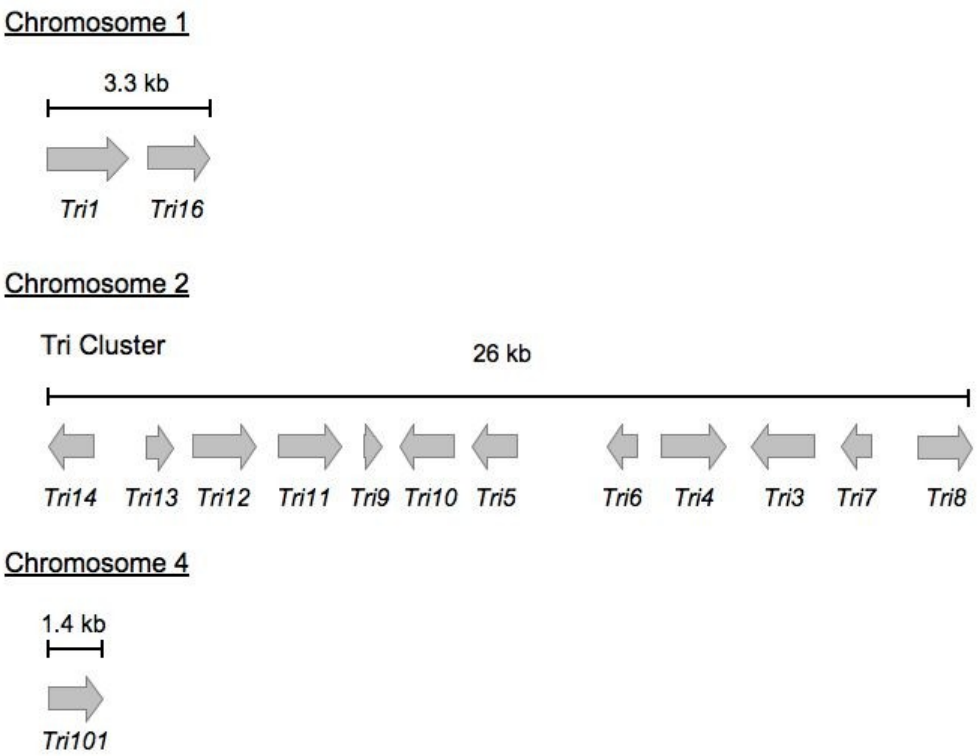

Figure 1. The Tri cluster and three other genes – *Tri101*, *Tri1*, and *Tri16* –involved in trichothecene biosynthesis.

References

Alexander, N. J., S. P. McCormick & T. M. Hohn, (1999) Tri12, a trichothecene efflux pump from *Fusarium sporotrichioides*: gene isolation and expression in yeast. *Molecular and General Genetics* **261**: 977-984.

Anand, A., T. Zhou, H. N. Trick, B. S. Gill, W. W. Bockus & S. Muthukrishnan, (2003) Greenhouse and field testing of transgenic wheat plants stably expressing genes for thaumatin-like protein, chitinase and glucanase against *Fusarium graminearum*. *Journal of Experimental Botany* **54**: 1101-1111.

Bai, G. H., A. E. Desjardins & R. D. Plattner, (2002) Deoxynivalenol-nonproducing *Fusarium graminearum* causes initial infection, but does not cause disease spread in wheat spikes. *Mycopathologia* **153**: 91-98.

Bai, G. H., F. L. Kolb, G. Shaner & L. L. Domier, (1999) Amplified fragment length polymorphism markers linked to a major quantitative trait locus controlling scab resistance in wheat. *Phytopathology* **89**: 343-348.

Bai, G. H. & G. Shaner, (2004) Management and resistance in wheat and barley to Fusarium head blight. *Annual Review of Phytopathology* **42**: 135-161.

Balconi, C., C. Lanzanova, E. Conti, T. Triulzi, F. Forlani, M. Cattaneo & E. Lupotto, (2007) Fusarium head blight evaluation in wheat transgenic plants expressing the maize b-32 antifungal gene. *European Journal of Plant Pathology* **117**: 129-140.

Baldwin, T. K., M. Urban, N. Brown & K. E. Hammond-Kosack, (2010) A role for topoisomerase in *Fusarium graminearum* and *F. culmorum* pathogenesis and sporulation. *Molecular Plant-Microbe Interactions* **23**: 566-577.

Bernardo, A., G. H. Bai, P. G. Guo, K. Xiao, A. C. Guenzi & P. Ayoubi, (2007) *Fusarium graminearum*-induced changes in gene expression between Fusarium head blight-resistant and susceptible wheat cultivars. *Functional & Integrative Genomics* **7**: 69-77.

Bluhm, B. H. & C. P. Woloshuk, (2006) Fck1, a C-type cyclin-dependent kinase, interacts with Fcc1 to regulate development and secondary metabolism in *Fusarium verticillioides*. *Fungal Genetics and Biology* **43**: 146-154.

Bluhm, B. H., X. Zhao, J. E. Flaherty, J. R. Xu & L. D. Dunkle, (2007) *RAS2* regulates growth and pathogenesis in *Fusarium graminearum*. *Molecular Plant-Microbe Interactions* **20**: 627-636.

Boddu, J., S. Cho, W. M. Kruger & G. J. Muehlbauer, (2006) Transcriptome analysis of the barley-*Fusarium graminearum* interaction. *Molecular Plant-Microbe Interactions* **19**: 407-417.

Boddu, J., S. H. Cho & G. J. Muehlbauer, (2007) Transcriptome analysis of trichothecene-induced gene expression in barley. *Molecular Plant-Microbe Interactions* **20**: 1364-1375.

Brown, D. W., R. H. Proctor, R. B. Dyer & R. D. Plattner, (2003) Characterization of a Fusarium 2-gene cluster involved in trichothecene C-8 modification. *Journal of Agricultural and Food Chemistry* **51**: 7936-7944.

Buerstmayr, H., T. Ban & J. A. Anderson, (2009) QTL mapping and marker-assisted selection for Fusarium head blight resistance in wheat: a review. *Plant Breeding* **128**: 1-26.

Buerstmayr, H., M. Lemmens, L. Hartl, L. Doldi, B. Steiner, M. Stierschneider & P. Ruckenbauer, (2002) Molecular mapping of QTLs for Fusarium head blight resistance in spring wheat. I. Resistance to fungal spread (type II resistance). *Theoretical and Applied Genetics* **104**: 84-91.

Buerstmayr, H., B. Steiner, L. Hartl, M. Griesser, N. Angerer, D. Lengauer, *et al*. (2003) Molecular mapping of QTLs for Fusarium head blight resistance in spring wheat. II. Resistance to fungal penetration and spread. *Theoretical and Applied Genetics* **107**: 503-508.

Bushnell, W.R., B. Hazen, and C Pritsch (2003) Histology and physiology of Fusarium head blight. In *Fusarium Head Blight of Wheat and Barley*. Leonard, K.J. and Bushnell, W.R. (eds). , St. Paul: American Phytopathology Society Press, pp. 44-83.

Canci, P. C., L. M. Nduulu, R. Dill-Macky, G. J. Muehlbauer, D. C. Rasmusson & K. P. Smith, (2003) Genetic relationship between kernel discoloration and grain protein concentration in barley. *Crop Science* **43**: 1671-1679.

Chen, W. P., P. D. Chen, D. J. Liu, R. Kynast, B. Friebe, R. Velazhahan, S. Muthukrishnan & B. S. Gill, (1999) Development of wheat scab symptoms is delayed in transgenic wheat plants that constitutively express a rice thaumatin-like protein gene. *Theoretical and Applied Genetics* **99**: 755-760.

Cuomo, C. A., U. Güldener, J. R. Xu, F. Trail, B. G. Turgeon, A. Di Pietro, *et al.* (2007) The *Fusarium graminearum* genome reveals a link between localized polymorphism and pathogen specialization. *Science* **317**: 1400-1402.

Cuthbert, P. A., D. J. Somers & A. Brule-Babel, (2007) Mapping of *Fhb2* on chromosome 6BS: a gene controlling Fusarium head blight field resistance in bread wheat (*Triticum aestivum* L.). *Theoretical and Applied Genetics* **114**: 429-437.

Dahleen, L. S., P. A. Okubara & A. E. Blechl, (2001) Transgenic approaches to combat Fusarium head blight in wheat and barley. *Crop Science* **41**: 628-637.

de la Pena, R. C., K. P. Smith, F. Capettini, G. J. Muehlbauer, M. Gallo-Meagher, R. Dill-Macky, D. A. Somers & D. C. Rasmusson, (1999) Quantitative trait loci associated with resistance to Fusarium head blight and kernel discoloration in barley. *Theoretical and Applied Genetics* **99**: 561-569.

Desjardins, A. E., (2009) From yellow rain to green wheat: 25 years of trichothecene biosynthesis research. *Journal of Agricultural and Food Chemistry* **57**: 4478-4484.

Desmond, O. J., J. M. Manners, A. E. Stephens, D. J. MaClean, P. M. Schenk, D. M. Gardiner, A. L. Munn & K. Kazan, (2008) The Fusarium mycotoxin deoxynivalenol elicits hydrogen peroxide production, programmed cell death and defence responses in wheat. *Molecular Plant Pathology* **9**: 435-445.

Di, R., A. Blechl, R. Dill-Macky, A. Tortora & N. E. Tumer, (2010) Expression of a truncated form of yeast ribosomal protein L3 in transgenic wheat improves resistance to Fusarium head blight. *Plant Science* **178**: 374-380.

Ding, S. L., R. Mehrabi, C. Koten, Z. S. Kang, Y. D. Wei, K. Y. Seong, H. C. Kistler & J. R. Xu, (2009) Transducin beta-like gene *FTL1* is essential for pathogenesis in *Fusarium graminearum*. *Eukaryotic Cell* **8**: 867-876.

Dufresne, M., T. van der Lee, S. Ben M'Barek, X. D. Xu, X. Zhang, T. G. Liu, C. *et al.* (2008) Transposon-tagging identifies novel pathogenicity genes in *Fusarium graminearum*. *Fungal Genetics and Biology* **45**: 1552-1561.

Dyer, R. B., R. D. Plattner, D. F. Kendra & D. W. Brown, (2005) *Fusarium graminearum TRI14* is required for high virulence and DON production on wheat but not for DON synthesis in vitro. *Journal of Agricultural and Food Chemistry* **53**: 9281-9287.

Eulgem, T. & I. E. Somssich, (2007) Networks of WRKY transcription factors in defense signaling. *Current Opinion in Plant Biology* **10**: 366-371.

Fried, H. M. & J. R. Warner, (1981) Cloning of yeast gene for trichodermin resistance and ribosomal protein-L3. *Proceedings of the National Academy of Sciences of the United States of America-Biological Sciences* **78**: 238-242.

Gardiner, D. M., K. Kazan & J. M. Manners, (2009) Novel genes of *Fusarium graminearum* that negatively regulate deoxynivalenol production and virulence. *Molecular Plant-Microbe Interactions* **22**: 1588-1600.

Gardiner, S. A., J. Boddu, F. Berthiller, C. Hametner, R. M. Stupar, G. Adam & G. J. Muehlbauer, (2010) Transcriptome analysis of the barley-deoxynivalenol interaction: evidence for a role of glutathione in deoxynivalenol detoxification. *Molecular Plant-Microbe Interactions* **23**: 962-976.

Garvey, G. S., S. P. McCormick, N. J. Alexander & I. Rayment, (2009) Structural and functional characterization of TRI3 trichothecene 15-O-acetyltransferase from *Fusarium sporotrichioides*. *Protein Science* **18**: 747-761.

Geddes, J., F. Eudes, A. Laroche & L. B. Selinger, (2008) Differential expression of proteins in response to the interaction between the pathogen *Fusarium graminearum* and its host, *Hordeum vulgare*. *Proteomics* **8**: 545-554.

Gilbert, J. & W. G. D. Fernando, (2004) Epidemiology and biological control of *Gibberella zeae Fusarium graminearum*. *Canadian Journal of Plant Pathology-Revue Canadienne De Phytopathologie* **26**: 464-472.

Glazebrook, J., (2005) Contrasting mechanisms of defense against biotrophic and necrotrophic pathogens. *Annual Review of Phytopathology* **43**: 205-227.

Golkari, S., J. Gilbert, S. Prashar & J. D. Procunier, (2007) Microarray analysis of *Fusarium graminearum*-induced wheat genes: identification of organ-specific and differentially expressed genes. *Plant Biotechnology Journal* **5**: 38-49.

Goswami, R. S. & H. C. Kistler, (2004) Heading for disaster: *Fusarium graminearum* on cereal crops. *Molecular Plant Pathology* **5**: 515-525.

Goswami, R. S. & H. C. Kistler, (2005) Pathogenicity and in planta mycotoxin accumulation among members of the *Fusarium graminearum* species complex on wheat and rice. *Phytopathology* **95**: 1397-1404.

Goswami, R. S., J. R. Xu, F. Trail, K. Hilburn & H. C. Kistler, (2006) Genomic analysis of host-pathogen interaction between *Fusarium graminearum* and wheat during early stages of disease development. *Microbiology* **152**: 1877-1890.

Greenshields, D. L., G. S. Liu, J. Feng, G. Selvaraj & Y. D. Wei, (2007) The siderophore biosynthetic gene *SID1*, but not the ferroxidase gene *FET3*, is required for full *Fusarium graminearum* virulence. *Molecular Plant Pathology* **8**: 411-421.

Güldener, U., G. Mannhaupt, M. Munsterkotter, D. Haase, M. Oesterheld, V. Stumpflen, H. W. Mewes & G. Adam, (2006a) FGDB: a comprehensive fungal genome resource on the plant pathogen *Fusarium graminearum*. *Nucleic Acids Research* **34**: D456-D458.

Güldener, U., K. Y. Seong, J. Boddu, S. H. Cho, F. Trail, J. R. Xu, *et al*. (2006b) Development of a *Fusarium graminearum* Affymetrix GeneChip for profiling fungal gene expression *in vitro* and *in planta*. *Fungal Genetics and Biology* **43**: 316-325.

Haas, H., (2003) Molecular genetics of fungal siderophore biosynthesis and uptake: the role of siderophores in iron uptake and storage. *Applied Microbiology and Biotechnology* **62**: 316-330.

Han, Y. K., M. D. Kim, S. H. Lee, S. H. Yun & Y. W. Lee, (2007) A novel F-box protein involved in sexual development and pathogenesis in *Gibberella zeae*. *Molecular Microbiology* **63**: 768-779.

Hill-Ambroz, K., C. A. Webb, A. R. Matthews, W. L. Li, B. S. Gill & J. P. Fellers, (2006) Expression analysis and physical mapping of a cDNA library of Fusarium head blight infected wheat spikes. *Crop Science* **46**: S15-S26.

Hohn, T. M., R. Krishna & R. H. Proctor, (1999) Characterization of a transcriptional activator controlling trichothecene toxin biosynthesis. *Fungal Genetics and Biology* **26**: 224-235.

Hollingsworth, C. R., C. D. Motteberg, J. V. Wiersma & L. M. Atkinson, (2008) Agronomic and economic responses of spring wheat to management of Fusarium head blight. *Plant Disease* **92**: 1339-1348.

Hong, S. Y., J. So, J. Lee, K. Min, H. Son, C. Park, S. H. Yun & Y. W. Lee, (2010) Functional analyses of two syntaxin-like SNARE genes, *GzSYN1* and *GzSYN2*, in the ascomycete *Gibberella zeae*. *Fungal Genetics and Biology* **47**: 364-372.

Hong, W. J., (2005) SNARES and traffic. *Biochimica et Biophysica Acta-Molecular Cell Research* **1744**: 120-144.

Hou, Z. M., C. Y. Xue, Y. L. Peng, T. Katan, H. C. Kistler & J. R. Xu, (2002) A mitogen-activated protein kinase gene (*MGV1*) in *Fusarium graminearum* is required for female fertility, heterokaryon formation, and plant infection. *Molecular Plant-Microbe Interactions* **15**: 1119-1127.

Jenczmionka, N. J., F. J. Maier, A. P. Losch & W. Schafer, (2003) Mating, conidiation and pathogenicity of *Fusarium graminearum*, the main causal agent of the head-

blight disease of wheat, are regulated by the MAP kinase Gpmk1. *Current Genetics* **43**: 87-95.

Jenczmionka, N. J. & W. Schafer, (2005) The Gpmk1 MAP kinase of *Fusarium graminearum* regulates the induction of specific secreted enzymes. *Current Genetics* **47**: 29-36.

Jeon, J., S. Y. Park, M. H. Chi, J. Choi, J. Park, H. S. Rho, *et al*. (2007) Genome-wide functional analysis of pathogenicity genes in the rice blast fungus. *Nature Genetics* **39**: 561-565.

Jia, H. Y., S. H. Cho & G. J. Muehlbauer, (2009) Transcriptome analysis of a wheat near-isogenic line pair carrying Fusarium head blight-resistant and -susceptible alleles. *Molecular Plant-Microbe Interactions* **22**: 1366-1378.

Jiang, L. H., J. R. Yang, F. Y. Fan, D. J. Zhang & X. L. Wang, (2010) The Type 2C protein phosphatase FgPtc1p of the plant fungal pathogen *Fusarium graminearum* is involved in lithium toxicity and virulence. *Molecular Plant Pathology* **11**: 277-282.

Kim, J. E., H. J. Lee, J. Lee, K. W. Kim, S. H. Yun, W. B. Shim & Y. W. Lee, (2009) *Gibberella zeae* chitin synthase genes, *GzCHS5* and *GzCHS7*, are required for hyphal growth, perithecia formation, and pathogenicity. *Current Genetics* **55**: 449-459.

Kim, J. E., K. Myong, W. B. Shim, S. H. Yun & Y. W. Lee, (2007) Functional characterization of acetylglutamate synthase and phosphoribosylamine-glycine ligase genes in *Gibberella zeae*. *Current Genetics* **51**: 99-108.

Kimura, M., I. Kaneko, M. Komiyama, A. Takatsuki, H. Koshino, K. Yoneyama & I. Yamaguchi, (1998) Trichothecene 3-O-acetyltransferase protects both the producing organism and transformed yeast from related mycotoxins - Cloning and characterization of *Tri101*. *Journal of Biological Chemistry* **273**: 1654-1661.

Kimura, M., T. Tokai, K. O'Donnell, T. J. Ward, M. Fujimura, H. Hamamoto, T. Shibata & I. Yamaguchi, (2003) The trichothecene biosynthesis gene cluster of *Fusarium graminearum* F15 contains a limited number of essential pathway genes and expressed non-essential genes. *FEBS Letters* **539**: 105-110.

Kimura, M., T. Tokai, N. Takahashi-Ando, S. Ohsato & M. Fujimura, (2007) Molecular and genetic studies of Fusarium trichothecene biosynthesis: pathways, genes, and evolution. *Bioscience Biotechnology and Biochemistry* **71**: 2105-2123.

Kolb, F. L., G. H. Bai, G. J. Muehlbauer, J. A. Anderson, K. P. Smith & G. Fedak, (2001) Host plant resistance genes for Fusarium head blight: mapping and manipulation with molecular markers. *Crop Science* **41**: 611-619.

Kong, L., J. M. Anderson & H. W. Ohm, (2005) Induction of wheat defense and stress-related genes in response to *Fusarium graminearum*. *Genome* **48**: 29-40.

Kong, L., H. W. Ohm & J. M. Anderson, (2007) Expression analysis of defense-related genes in wheat in response to infection by *Fusarium graminearum*. *Genome* **50**: 1038-1048.

Langevin, F., F. Eudes & A. Comeau, (2004) Effect of trichothecenes produced by *Fusarium graminearum* during Fusarium head blight development in six cereal species. *European Journal of Plant Pathology* **110**: 735-746.

Langseth, W. & O. Elen, (1996) Differences between barley, oats and wheat in the occurrence of deoxynivalenol and other trichothecenes in Norwegian grain. *Journal of Phytopathology-Phytopathologische Zeitschrift* **144**: 113-118.

Lee, S. H., Y. K. Han, S. H. Yun & Y. W. Lee, (2009a) Roles of the glyoxylate and methylcitrate cycles in sexual development and virulence in the cereal pathogen *Gibberella zeae*. *Eukaryotic Cell* **8**: 1155-1164.

Lee, S. H., J. Lee, S. Lee, E. H. Park, K. W. Kim, M. D. Kim, S. H. Yun & Y. W. Lee, (2009b) Gz*SNF1* is required for normal sexual and asexual development in the ascomycete *Gibberella zeae*. *Eukaryotic Cell* **8**: 116-127.

Lemmens, M., U. Scholz, F. Berthiller, C. Dall'Asta, A. Koutnik, R. Schuhmacher, *et al.* (2005) The ability to detoxify the mycotoxin deoxynivalenol colocalizes with a major quantitative trait locus for Fusarium head blight resistance in wheat. *Molecular Plant-Microbe Interactions* **18**: 1318-1324.

Li, W. L., J. D. Faris, S. Muthukrishnan, D. J. Liu, P. D. Chen & B. S. Gill, (2001) Isolation and characterization of novel cDNA clones of acidic chitinases and beta-1,3-glucanases from wheat spikes infected by *Fusarium graminearum*. *Theoretical and Applied Genetics* **102**: 353-362.

Lu, S. W., S. Kroken, B. N. Lee, B. Robbertse, A. C. L. Churchill, O. C. Yoder & B. G. Turgeon, (2003) A novel class of gene controlling virulence in plant pathogenic ascomycete fungi. *Proceedings of the National Academy of Sciences of the United States of America* **100**: 5980-5985.

Ma, Z. P., B. J. Steffenson, L. K. Prom & N. L. V. Lapitan, (2000) Mapping of quantitative trait loci for Fusarium head blight resistance in barley. *Phytopathology* **90**: 1079-1088.

Mackintosh, C. A., J. Lewis, L. E. Radmer, S. Shin, S. J. Heinen, L. A. Smith, *et al.* (2007) Overexpression of defense response genes in transgenic wheat enhances resistance to Fusarium head blight. *Plant Cell Reports* **26**: 479-488.

Makandar, R., J. S. Essig, M. A. Schapaugh, H. N. Trick & J. Shah, (2006) Genetically engineered resistance to Fusarium head blight in wheat by expression of Arabidopsis *NPR1*. *Molecular Plant-Microbe Interactions* **19**: 123-129.

Manoharan, M., L. S. Dahleen, T. M. Hohn, S. M. Neate, X. H. Yu, N. J. Alexander, *et al.* (2006) Expression of 3-OH trichothecene acetyltransferase in barley (*Hordeum vulgare* L.) and effects on deoxynivalenol. *Plant Science* **171**: 699-706.

McCormick, S. P. & N. J. Alexander, (2002) Fusarium *Tri8* encodes a trichothecene C-3 esterase. *Applied and Environmental Microbiology* **68**: 2959-2964.

McCormick, S. P., N. J. Alexander, S. E. Trapp & T. M. Hohn, (1999) Disruption of *TRI101*, the gene encoding trichothecene 3-O-acetyltransferase, from *Fusarium sporotrichioides*. *Applied and Environmental Microbiology* **65**: 5252-5256.

McCormick, S. P., L. J. Harris, N. J. Alexander, T. Ouellet, A. Saparno, S. Allard & A. E. Desjardins, (2004) *Tri1* in *Fusarium graminearum* encodes a P450 oxygenase. *Applied and Environmental Microbiology* **70**: 2044-2051.

McMullen, M., R. Jones & D. Gallenberg, (1997) Scab of wheat and barley: A re-emerging disease of devastating impact. *Plant Disease* **81**: 1340-1348.

Meek, I. B., A. W. Peplow, C. Ake, T. D. Phillips & M. N. Beremand, (2003) *Tri1* encodes the cytochrome P450 monooxygenase for C-8 hydroxylation during trichothecene biosynthesis in *Fusarium sporotrichioides* and resides upstream of another new Tri gene. *Applied and Environmental Microbiology* **69**: 1607-1613.

Mesfin, A., K. P. Smith, R. Dill-Macky, C. K. Evans, R. Waugh, C. D. Gustus & G. J. Muehlbauer, (2003) Quantitative trait loci for Fusarium head blight resistance in barley detected in a two-rowed by six-rowed population. *Crop Science* **43**: 307-318.

Meyers, B. C., A. Kozik, A. Griego, H. H. Kuang & R. W. Michelmore, (2003) Genome-wide analysis of NBS-LRR-encoding genes in Arabidopsis. *Plant Cell* **15**: 809-834.

Muhitch, M. J., S. P. McCormick, N. J. Alexander & T. M. Hohn, (2000) Transgenic expression of the *TRI101* or *PDR5* gene increases resistance of tobacco to the phytotoxic effects of the trichothecene 4,15-diacetoxyscirpenol. *Plant Science* **157**: 201-207.

Nduulu, L. M., A. Mesfin, G. J. Muehlbauer & K. P. Smith, (2007) Analysis of the chromosome 2(2H) region of barley associated with the correlated traits Fusarium head blight resistance and heading date. *Theoretical and Applied Genetics* **115**: 561-570.

Ochiai, N., T. Tokai, T. Nishiuchi, N. Takahashi-Ando, M. Fujimura & M. Kimura, (2007) Involvement of the osmosensor histidine kinase and osmotic stress-activated protein kinases in the regulation of secondary metabolism in *Fusarium graminearum*. *Biochemical and Biophysical Research Communications* **363**: 639-644.

Ohsato, S., T. Ochiai-Fukuda, T. Nishiuchi, N. Takahashi-Ando, S. Koizumi, H. Hamamoto, *et al*. (2007) Transgenic rice plants expressing trichothecene 3-O-acetyltransferase show resistance to the Fusarium phytotoxin deoxynivalenol. *Plant Cell Reports* **26**: 531-538.

Oide, S., W. Moeder, S. Krasnoff, D. Gibson, H. Haas, K. Yoshioka & B. G. Turgeon, (2006) *NPS6*, encoding a nonribosomal peptide synthetase involved in siderophore-mediated iron metabolism, is a conserved virulence determinant of plant pathogenic ascomycetes. *Plant Cell* **18**: 2836-2853.

Okubara, P. A., A. E. Blechl, S. P. McCormick, N. J. Alexander, R. Dill-Macky & T. M. Hohn, (2002) Engineering deoxynivalenol metabolism in wheat through the expression of a fungal trichothecene acetyltransferase gene. *Theoretical and Applied Genetics* **106**: 74-83.

Pestka, J. J. & A. T. Smolinski, (2005) Deoxynivalenol: toxicology and potential effects on humans. *Journal of Toxicology and Environmental Health-Part B-Critical Reviews* **8**: 39-69.

Poppenberger, B., F. Berthiller, D. Lucyshyn, T. Sieberer, R. Schuhmacher, R. Krska, *et al*. (2003) Detoxification of the Fusarium mycotoxin deoxynivalenol by a UDP-glucosyltransferase from *Arabidopsis thaliana*. *Journal of Biological Chemistry* **278**: 47905-47914.

Pritsch, C., G. J. Muehlbauer, W. R. Bushnell, D. A. Somers & C. P. Vance, (2000) Fungal development and induction of defense response genes during early infection of wheat spikes by *Fusarium graminearum*. *Molecular Plant-Microbe Interactions* **13**: 159-169.

Proctor, R. H., T. M. Hohn & S. P. McCormick, (1995) Reduced virulence of *Gibberella zeae* caused by disruption of a trichothecene toxin biosynthetic gene. *Molecular Plant-Microbe Interactions* **8**: 593-601.

Qi, W. H., K. Chil & F. Trail, (2006) Microarray analysis of transcript accumulation during perithecium development in the filamentous fungus *Gibberella zeae* (anamorph *Fusarium graminearum*). *Molecular Genetics and Genomics* **276**: 87-100.

Ramamoorthy, V., E. B. Cahoon, M. Thokala, J. Kaur, J. Li & D. M. Shah, (2009) Sphingolipid C-9 methyltransferases are important for growth and virulence but not for sensitivity to antifungal plant defensins in *Fusarium graminearum*. *Eukaryotic Cell* **8**: 217-229.

Rep, M. & H. C. Kistler, (2010) The genomic organization of plant pathogenicity in Fusarium species. *Current Opinion in Plant Biology* **13**: 420-426.

Rittenour, W. R. & S. D. Harris, (2008) Characterization of *Fusarium graminearum Mes1* reveals roles in cell-surface organization and virulence. *Fungal Genetics and Biology* **45**: 933-946.

Rotter, B. A., D. B. Prelusky & J. J. Pestka, (1996) Toxicology of deoxynivalenol (vomitoxin). *Journal of Toxicology and Environmental Health* **48**: 1-34.

Schweiger, W., J. Boddu, S. Shin, B. Poppenberger, F. Berthiller, M. Lemmens, G. J. Muehlbauer & G. Adam, (2010) Validation of a candidate deoxynivalenol-inactivating UDP-glucosyltransferase from barley by heterologous expression in yeast. *Molecular Plant-Microbe Interactions* **23**: 977-986.

Seo, B. W., H. K. Kim, Y. W. Lee & S. H. Yun, (2007) Functional analysis of a histidine auxotrophic mutation in *Gibberella zeae*. *Plant Pathology Journal* **23**: 51-56.

Seong, K., Z. M. Hou, M. Tracy, H. C. Kistler & J. R. Xu, (2005) Random insertional mutagenesis identifies genes associated with virulence in the wheat scab fungus *Fusarium graminearum*. *Phytopathology* **95**: 744-750.

Seong, K. Y., M. Pasquali, X. Y. Zhou, J. Song, K. Hilburn, S. McCormick, *et al*. (2009) Global gene regulation by Fusarium transcription factors *Tri6* and *Tri10* reveals adaptations for toxin biosynthesis. *Molecular Microbiology* **72**: 354-367.

Seong, K. Y., X. Zhao, J. R. Xu, U. Güldener & H. C. Kistler, (2008) Conidial germination in the filamentous fungus *Fusarium graminearum*. *Fungal Genetics and Biology* **45**: 389-399.

Shim, W. B., U. S. Sagaram, Y. E. Choi, J. So, H. H. Wilkinson & Y. W. Lee, (2006) *FSR1* is essential for virulence and female fertility in *Fusarium verticillioides* and *F. graminearum*. *Molecular Plant-Microbe Interactions* **19**: 725-733.

Shim, W. B. & C. P. Woloshuk, (2001) Regulation of fumonisin B-1 biosynthesis and conidiation in *Fusarium verticillioides* by a cyclin-like (C-type) gene, *FCC1*. *Applied and Environmental Microbiology* **67**: 1607-1612.

Shin, S. Y., C. A. Mackintosh, J. Lewis, S. J. Heinen, L. Radmer, R. Dill-Macky, *et al*. (2008) Transgenic wheat expressing a barley class II chitinase gene has enhanced resistance against *Fusarium graminearum*. *Journal of Experimental Botany* **59**: 2371-2378.

Skadsen, R. W. & T. A. Hohn, (2004) Use of *Fusarium graminearum* transformed with gfp to follow infection patterns in barley and Arabidopsis. *Physiological and Molecular Plant Pathology* **64**: 45-53.

Smith, K. P., C. K. Evans, R. Dill-Macky, C. Gustus, W. Xie & Y. Dong, (2004) Host genetic effect on deoxynivalenol accumulation in Fusarium head blight of barley. *Phytopathology* **94**: 766-771.

Somers, D. J., J. Thomas, R. DePauw, S. Fox, G. Humphreys & G. Fedak, (2005) Assembling complex genotypes to resist Fusarium in wheat (*Triticum aestivum* L.). *Theoretical and Applied Genetics* **111**: 1623-1631.

Steiner, B., H. Kurz, M. Lemmens & H. Buerstmayr, (2009) Differential gene expression of related wheat lines with contrasting levels of head blight resistance after *Fusarium graminearum* inoculation. *Theoretical and Applied Genetics* **118**: 753-764.

Stephens, A. E., D. M. Gardiner, R. G. White, A. L. Munn & J. M. Manners, (2008) Phases of Infection and Gene Expression of *Fusarium graminearum* During Crown Rot Disease of Wheat. *Molecular Plant-Microbe Interactions* **21**: 1571-1581.

Tag, A. G., G. F. Garifullina, A. W. Peplow, C. Ake, T. D. Phillips, T. M. Hohn & M. N. Beremand, (2001) A novel regulatory gene, *Tri10*, controls trichothecene toxin production and gene expression. *Applied and Environmental Microbiology* **67**: 5294-5302.

Ueno, Y., (1984) Toxicological features of T-2 toxin and related trichothecenes. *Fundamental and Applied Toxicology* **4**: S124-S132.

Urban, M., E. Mott, T. Farley & K. Hammond-Kosack, (2003) The *Fusarium graminearum MAP1* gene is essential for pathogenicity and development of perithecia. *Molecular Plant Pathology* **4**: 347-359.

Voigt, C. A., W. Schafer & S. Salomon, (2005) A secreted lipase of *Fusarium graminearum* is a virulence factor required for infection of cereals. *Plant Journal* **42**: 364-375.

van der Biezen, E.A. & D.G Jones, (1998) The NB-ARC domain: A novel signalling motif shared by plant resistance gene products and regulators of cell death in animals. *Current Biology* **8**: R226-R227.

Waldron, B. L., B. Moreno-Sevilla, J. A. Anderson, R. W. Stack & R. C. Frohberg, (1999) RFLP mapping of QTL for fusarium head blight resistance in wheat. *Crop Science* **39**: 805-811.

Wang, Y., W. D. Liu, Z. M. Hou, C. F. Wang, X. Y. Zhou, W. Jonkers, *et al.* (2011) A novel transcriptional factor important for pathogenesis and ascosporogenesis in *Fusarium graminearum*. *Molecular Plant-Microbe Interactions* **24**: 118-128.

Windels, C. E., (2000) Economic and social impacts of Fusarium head blight: Changing farms and rural communities in the Northern Great Plains. *Phytopathology* **90**: 17-21.

Wise, R.P., R.A. Caldo, L. Hong, L. Shen , E.K. Cannon, & J.A. Dickerson (2007) BarleyBase/PLEXdb: A unified expression profiling database for plants and plant pathogens. *In Plant Bioinformatics - Methods and Protocols*. Edwards D. (ed). Totowa, Humana Press, *Methods in Molecular Biology* **406**: 347-363.

Wong, P., M. Walter, W. Lee, G. Mannhaupt, M. Munsterkotter, H. W. Mewes, G. Adam & U. Güldener, (2011) FGDB: revisiting the genome annotation of the plant pathogen *Fusarium graminearum*. *Nucleic Acids Research* **39**: D637-D639.

Yang, Z. P., J. Gilbert, D. J. Somers, G. Fedak, J. D. Procunier & I. H. McKenzie, (2003) Marker assisted selection of Fusarium head blight resistance genes in two doubled haploid populations of wheat. *Molecular Breeding* **12**: 309-317.

Yu, H. Y., J. A. Seo, J. E. Kim, K. H. Han, W. B. Shim, S. H. Yun & Y. W. Lee, (2008) Functional analyses of heterotrimeric G protein G alpha and G beta subunits in *Gibberella zeae*. *Microbiology* **154**: 392-401.

Yu, J. H., (2006) Heterotrimeric G protein signaling and RGSs in *Aspergillus nidulans*. *Journal of Microbiology* **44**: 145-154.

Zhang, D. J., F. Y. Fan, J. R. Yang, X. L. Wang, D. W. Qiu & L. H. Jiang, (2010) FgTep1p is linked to the phosphatidylinositol-3 kinase signalling pathway and plays a role in the virulence of *Fusarium graminearum* on wheat. *Molecular Plant Pathology* **11**: 495-502.

Zhou, W. C., F. L. Kolb & D. E. Riechers, (2005) Identification of proteins induced or upregulated by Fusarium head blight infection in the spikes of hexaploid wheat (*Triticum aestivum*). *Genome* **48**: 770-780.

Zhou, X. Y., C. Heyer, Y. E. Choi, R. Mehrabi & J. R. Xu, (2010) The *CID1* cyclin C-like gene is important for plant infection in *Fusarium graminearum*. *Fungal Genetics and Biology* **47**: 143-151.

Zhu, H., L. Gilchrist, P. Hayes, A. Kleinhofs, D. Kudrna, Z. Liu, *et al*. (1999) Does function follow form? Principal QTLs for Fusarium head blight (FHB) resistance are coincident with QTLs for inflorescence traits and plant height in a doubled-haploid population of barley. *Theoretical and Applied Genetics* **99**: 1221-1232.

Chapter 2

Cellular localization and functional characterization of FgTri12p in *Fusarium graminearum*.

Introduction

The plant pathogen *F. graminearum* (*Gibberella zeae*) presents a two-fold threat to farmers and consumers. Not only does this filamentous fungus cause the disease Fusarium head blight (FHB) that results in significant yield loss in infected grains, it also taints these grains with potent mycotoxins harmful to humans, animals, and plants alike. Equally alarming is the evidence that grain can appear to be physically sound while still being significantly contaminated with trichothecene mycotoxins (Hollingsworth et al., 2008). Trichothecene contamination reduces the market value of grain. During the 1993 FHB epidemic experienced by farmers living in Manitoba, Minnesota, North Dakota, and South Dakota, the Minneapolis Grain Exchange discounted the price paid for high quality milling wheat by more than 17% for any trace of trichothecene contamination. Losses incurred by wheat and barley farmers during this epidemic totaled at least $700 million (McMullen et al. 1997). Yield losses and price discounts incurred annually by farmers in the upper Midwest have resulted in farm foreclosure and bankruptcy (Windels, 2000).

F. graminearum produces the Type B trichothecene mycotoxin deoxynivalenol (DON) and its acetylated derivatives, 15-acetyldeoxynivalenol (15ADON), 3-acetyldeoxynivalenol (3ADON), or nivalenol (NIV). Trichothecene mycotoxins are implicated as virulence factors in host-*Fusarium* interactions (Proctor et al., 1995). They are known to influence how the fungus interacts with some grasses. In wheat and barley, trichothecene accumulation is associated with increased fungal virulence (Gardiner et al., 2010b). Wheat spikes point-inoculated with non-trichothecene producing *tri5* mutant strains of *F. graminearum* do not exhibit symptoms beyond the initially infected spikelets (Bai et al., 2002).

Significant progress has been made in identifying genes involved in the biosynthesis of trichothecenes and the roles they play in this process. A diverse group of proteins are involved, including enzymes for trichothecene biosynthesis, an efflux protein, and transcription factors controlling gene regulation. Most of these proteins are encoded by

genes within the trichothecene biosynthetic cluster (Tri cluster) (Kimura et al., 2003). Two other genes directly involved in Type B trichothecene biosynthesis are located outside of the Tri cluster (Brown et al., 2003). The exact roles that some of these proteins play in the production of trichothecenes remains unknown. There also may be other proteins involved in synthesis that have yet to be identified (Kimura et al., 2007). The cellular location of trichothecene biosynthesis in fungal cells, how cells deal with the toxic effect of trichothecenes, and how trichothecenes exit cells are unknown.

Transmembrane transport proteins are important for fungi to colonize plants and cause disease. These transporters can act as virulence or pathogenicity factors by providing protection from the toxic secondary metabolites produced by plants or the fungus itself (Stergiopoulos et al., 2002). Multiple ATP-binding cassette (ABC) transporters or major facilitator superfamily (MFS) proteins implicated in self-protection, virulence, and/or pathogenicity have been described for the fungal plant pathogens *Botrytis cinerea*, *Cochliobolus carbonum*, *Cercospora kikuchii*, *F. culmorum*, *F. sambucinum*, *F. sporotrichiodes*, *Magnaporthe grisea*, *Mycosphaerella graminicola*, and *Penicillium digitatum* (Schoonbeek et al., 2003; Pitkin et al., 1996; Callahan et al., 1999; Skov et al., 2004; Fleissner et al., 2002; Alexander et al., 1999; Urban et al., 1999; Zwiers and De Waard, 2000; Stergiopoulos et al., 2002; Nakaune et al., 2002.). In plant pathogenic fungi, ABC transporters appear to be specifically involved in the transport of exogenous substances. ABC transporters that secrete endogenously produced virulence factors have not been identified. In contrast, MFS transporters are involved in the movement of endogenous toxins such as trichothecenes or exogenous substrates such as phytoalexins (Stergiopoulos et al., 2002, Alexander et al., 1999; Schoonbeek et al., 2001). MFS proteins have been shown to provide protection against the secondary metabolites HC-toxin, cercosporin, and diacetoxyscirpenol in *C. carbonum, C. kikuchii, and F. sporotrichiodes*, respectively (Pitkin et al., 1996; Callahan et al., 1999; Alexander et al., 1999).

Characterization of *Tri12* in *F. sporotrichiodes* (*FsTri12*) demonstrated that FsTri12p

plays a role in trichothecene efflux (Alexander et al., 1999). A mutant *fstri12* culture produced 97% less T-2 toxin than the wild type and exhibited reduced radial growth in the presence of the Type A trichothecene diacetoxyscripenol. FsTri12p also increased trichothecene flux in transgenic *Saccharomyces cerevisiae* strains expressing *FsTri12*. Based on the observation that *FsTri12* does not protect *Saccharomyces cerevisiae* from the toxic effects of diacetoxyscripenol, the authors posit *FsTri12* plays a minor role in self-protection against trichothecenes.

The exact function of *FgTri12* in *F. graminearum* is unknown. The objectives of this study were to establish an accurate gene model for *FgTri12*; to determine whether *FgTri12* promotes trichothecene efflux and self-protection in *F. graminearum* or contributes to fungal virulence and toxin production *in planta*; and to locate FgTri12p and FgTri1p over time within the cell during induction of trichothecene biosynthesis. This study is the first to report temporal and spatial localization patterns of FgTri1p and FgTri12p, proteins involved in the biosynthesis and efflux of trichothecenes.

Results

The two most commonly used sources of annotation for the *F. graminearum* genome are displayed at the Munich Information Center for Protein Sequences (MIPS) and Broad Institute databases (Güldener et al., 2006; Cuomo et al., 2007; Wong et al., 2011) and differ in their predictions for *FgTri12*. While both predictions agree upon the 5' start site and the position of the first two introns, the models differ considerably in the 3' region. To resolve these discrepancies, cDNA of *FgTri12* transcripts were synthesized via 3' RACE. A PCR amplicon spanning the entire 2229 bp 3' region of the *FgTri12* transcript was sequenced (Genebank Accession Number JF809795) (Figure 1). The sequenced cDNA matched perfectly with *FgTri12* gDNA for exon regions. The sequence also confirmed the presence and genetic location of the first two introns predicted by the gene models but disagreed with both the Broad and MIPS gene annotations at the 3' terminus. The cDNA showed that a third intron is present in the coding region of this gene; a

finding that was confirmed by an EST available in GenBank (CD456153). Two ESTs (BI950733 and gi|13621077) also support the presence and location of the first two predicted introns.

Pairwise alignment of *FgTri12* and *FsTri12* with a Smith-Waterman local alignment algorithm (Smith and Waterman, 1981; www.ebi.ac.uk/Tools/emboss/align) revealed 80.5% nucleotide identity between the coding sequences. The locations of the first and second introns of *FgTri12* are consistent with those predicted for *FsTri12*. The third intron of *FsTri12* lies entirely within the 3' UTR of the gene, whereas the final exon of *FgTri12* encodes a single base pair of the protein's final amino acid and the translational stop codon. Remarkably, the immediate 3' flanking region of both *FsTri12* and *FgTri12* are predicted to overlap the promoter region of the adjacent *Tri11* gene in both *F. graminearum* and *F. sporotrichioides*, with the polyadenylation sequence of the *FgTri12* transcript found only 70 bp upstream of the predicted translational start of *FgTri11*. *FgTri12* and *FsTri12* are predicted to encode 600 and 598 amino acid proteins, respectively. A comparison of the predicted amino acid sequences of FgTri12p and FsTri12p revealed a high degree of similarity. FgTri12p and FsTri12p have 78.1% amino acid identity and 89.4% similarity based on a Needleman-Wunsch global alignment (Needleman and Wunsch, 1970; http://emboss.bioinformatics.nl/). TMPred (Hofmann and Stoffel, 1993; www.ch.embnet.org) transmembrane domain predictions suggest that both FgTri12p and FsTri12p possess 14 membrane-spanning domains (Figure 2). The model preferred by TMPred places both the carboxy and amino termini on the cytoplasmic side of the plasma membrane. Amino acid sequence conservation in predicted transmembrane domains of FgTri12p and FsTri12p varies by domain. Several regions are highly conserved between FgTri12p and FsTri12p, including the 103 amino acid sequence that begins immediately after the first predicted transmembrane domain and ends before the fifth predicted transmembrane domain. A comparison among FgTri12p amino acid sequences from 15ADON, 3ADON, NIV producing strains of *F. graminearum*, PH-1, and *F. sporotrichioides* reveals 13 amino acid polymorphisms between these strains within this region, though eight of these polymorphisms are

conserved substitutions. The 14th predicted transmembrane domain of FgTri12p is completely conserved among 15ADON, 3ADON, NIV producing strains of *F. graminearum,* and *F. sporotrichioides*. The amino acid sequence that underlies the fifth predicted transmembrane domain displays a higher degree of variability between PH-1 and *F. sporotrichioides*; three insertion/deletion polymorphisms are present in this region. If these strains are compared to 3ADON and NIV producing strains, several chemotype specific polymorphisms are observed in this region.

Generation and characterization of *FgTri12* deletion mutant and complement strains

FgTri12 deletion mutants (*fgtri12*) were generated in the wild-type strain PH-1 by split-marker recombination mutagenesis (Catlett et al., 2003) with previously described modifications (Goswami et al., 2006) (Figure 3). The mutation in *FgTri12* was complemented by reintroducing a full-length copy of the *FgTri12* gene via genetic transformation, resulting in the complement strain *fgtri12/FgTri12*. Southern blotting was used to confirm the presence of the selectable markers (*hph*, *neo*) in tranformants, and the presence or absence of *FgTri12* in *fgtri12/FgTri12* or *fgtri12,* respectively (Figure 4).

The pathogenicity of the *fgtri12* deletion mutant was reduced compared to the wild-type strain or the *FgTri12* complement controls. PH-1, *fgtri12*, and *fgtri12/FgTri12* were assayed by point inoculation of wheat spikelets at anthesis. All strains were able to infect tissue and cause necrosis at the point of inoculation and were able to spread, causing disease symptoms beyond the inoculated spikelet. However, the mean number of symptomatic spikelets was reduced by 32% for plants inoculated with *fgtri12* compared to plants inoculated with PH-1 (Table 1). Likewise, the mean mass of spikes inoculated with *fgtri12* was 19% greater than those inoculated with PH-1. No significant differences in the number of symptomatic spikelets or mean mass of infected spikes were observed for plants inoculated with *fgtri12/FgTri12* or PH-1.

Infection of wheat with PH-1, *fgtri12*, or *fgtri12/FgTri12* resulted in the accumulation of

more DON than 15ADON (Table 1). The *fgtri12* deletion mutant accumulated significantly lower trichothecene concentrations than wild-type PH-1. The mean [DON] was 32% lower in spikelets inoculated with *fgtri12* compared to those inoculated with PH-1, while the mean [15ADON] was reduced by 58%. The *Tri12* complement *fgtri12/FgTri12* did not fully restore the wild-type trichothecene levels. The mean [15ADON] measured in spikelets inoculated with *fgtri12/FgTri12* was still significantly (38%) lower than the mean [15ADON] measured in plants inoculated with PH-1. Levels of DON were not significantly different in plants inoculated with *fgtri12* or *fgtri12/FgTri12.*

PH-1, *fgtri12*, and *fgtri12/FgTri12* grown in liquid toxin biosynthesis induction (TBI) medium resulted in higher levels of 15ADON than DON (Table 2). Unlike the situation *in planta*, the mean [15ADON] observed in cultures inoculated with *fgtri12* was actually significantly (39%) higher than in cultures inoculated with PH-1. Genetic complementation of the mutant reduced the level of trichothecenes in culture to a level significantly lower than that of wild type. The mean [15ADON] present in liquid TBI medium inoculated with *fgtri12/FgTri12* was 57% of that observed in cultures inoculated with PH-1.

Decreased levels of trichothecenes were observed in *fgtri12/FgTri12* inoculated plants and TBI cultures relative to the wild type. A similar situation was described in the complementation of *Tri6* and *Tri10* in *F. graminearum* (Seong et al., 2009). In these cases, wild-type [DON] and [15ADON] *in planta* were not completely restored by genetic complementation. Lower levels of trichothecenes could be the result of duplicate copies of the *hph* marker present in the complement strain. Southern blotting revealed two bands that hybridize with the *hph* specific probe in the complement strain (Figure 4). This suggests the *FgTri12* complementation construct likely integrated in the *hph* marker that is present as a single copy in the *tri12* strain. This integration resulted in a duplication event that generated a second copy of the *hph* marker. The hybridization of the *neo* and *hph* probes to the same DNA fragment supports this conclusion. Integration

of the complement construct into the *hph* marker would introduce a *PstI* site into this region. As predicted, digestion of *fgtri12/FgTri12* gDNA with this enzyme results in two fragments with sequence complementary to the *hph* probe. The duplication of targeted genes during the integration of exogenous DNA constructs in *F. graminearum* has been previously documented (Watson et al., 2008).

Growth of *fgtri12* was significantly reduced compared to wild-type and complement strains on toxin inducing medium but not on medium where toxin does not accumulate. Radial growth of PH-1, *fgtri12*, and *fgtri12/FgTri12* was compared over a 96-hour period on TBI medium agar (Figure 5, Table 3). Radial growth of *fgtri12* was reduced by 14% at 96 hours when compared to PH-1. Complementation restored wild-type radial growth in the *fgtri12/FgTri12* strain. Radial growth of all strains was similar under conditions where trichothecenes do not accumulate on MM (Figure 6). These results suggest that *Tri12* is involved in overcoming self-inhibition by trichothecenes.

Pigmentation of *fgtri12* was altered in liquid TBI medium (data not shown) and on agar based TBI and minimal media compared to PH-1 (Figures 5, 6). Complementation restored wild-type pigment in the *fgtri12/FgTri12* strain. These results indicate *FgTri12* could also play a role in the regulation of other secondary metabolites.

Cytology and expression of *Tri1* and *Tri12* during toxin synthesis

To determine their sub-cellular location during *in vitro* toxin biosynthesis, *Tri1* (*FgTri1::eGFP*) and *Tri12* (*FgTri12::eGFP*) were tagged with *eGFP* in the wild-type strain PH-1. Both tagging constructs were engineered to enable tagged strains to produce the targeted protein with its carboxyl terminus fused to eGFP (Figures 7, 8). Tagging of *FgTri12* and *FgTri1* strains was confirmed via Southern blot (Figures 9, 10). Pathogenicity tests, radial growth assays, and *in vitro* and *in planta* trichothecene production assays were conducted on *FgTri12::eGFP*. No significant difference was observed with respect to mean number of symptomatic spikelets; mean mass of infected

spikes; trichothecene accumulation *in planta* or in culture; or pigmentation between PH-1 and *FgTri12::eGFP* (Table 4, 5 ; Figures 5, 6). *FgTri12::eGFP* exhibited a slight, but significant, increase in radial growth on agar based TBI medium (Table 3), but no significant difference in radial growth on MM agar was observed (Figure 6).

Growth of *FgTri1::eGFP*, *FgTri12::eGFP*, and PH-1 in shaken liquid TBI cultures was observed via bright field, DIC, and fluorescence microscopy. To observe differences in cell morphology, PH-1 was grown from conidia at 25˚C in liquid TBI medium and minimal medium cultures (Figure 11). During the initial 18 hours of growth, cell morphology was similar in TBI and MM. After 18 hours, large circular organelles are evident only in cells grown in liquid TBI medium. After 36 hours in culture, certain cells growing in TBI medium exhibit swelling resulting in bulbous ovoid cells that form behind the advancing tip of a growing hyphal strand. These formations can result in the bifurcation of hyphae. Other hyphae within the cultures begin to exhibit coralloid morphology (Figure 12). Single or clusters of distinct circular organelles also are observed within these ovoid cells. The circular organelles stain blue with CMAC dye, indicating they are likely late endosomes or vacuoles (Figure13). 15ADON and DON were present in *FgTri12::eGFP*, *FgTri1::eGFP,* and PH-1 TBI cultures 40 hours after inoculation.

Fluorescence of eGFP in the *FgTri12::eGFP* strain was first observed in ovoid cells at 18 hours after suspension of spores in liquid TBI medium incubated at 28˚C (Figure 14). At this stage of expression, eGFP localizes to intracellular vesicular structures < 1μm in diameter (Supplemental slow-motion video 1). Slow-motion imaging of cells expressing *FgTri12::eGFP* revealed a saltatory movement of these motile structures. After 25 hours in TBI medium, FgTri12p::eGFP continues to localize to motile structures and is also observed in the plasma membrane and within the lumen of vacuoles (Supplemental time-lapse video 2). At this growth stage, cells expressing *FgTri12::eGFP* are few in number. Usually, expression is restricted to single swollen ovoid cells (Figure 15), though the presence of FgTri12p::eGFP in contiguous cells sometimes can be observed (Figure 16).

Cell contact with cover slip or slide surfaces appears to influence *FgTri12::eGFP* expression, as cells in contact with these surfaces are more likely to fluoresce. Over the next 17 hours, increasing numbers of cells exhibit FgTri12p::eGFP localization patterns observed in early time points. Vivid fluorescence from FgTri12p::eGFP was observed in vesicles within cells after 28, 30, 36, and 44 hours of incubation in liquid TBI medium (Figures 17-18; Supplemental time-lapse videos 3-6). After 42 hours, select cells exhibit localization of FgTri12p::eGFP to large stationary vacuoles and clusters of multiple smaller stationary structures, but not the plasma membrane (Figure 19). These clusters of smaller stationary organelles also stain blue with CMAC dye, so they are presumed to be either late endosomes or smaller vacuoles.

To correlate localization of FgTri12p with the site of trichothecene biosynthesis, expression of FgTri1p::eGFP was also monitored in TBI cultures. After 18 hours in 28˚C liquid TBI medium, fluorescence of eGFP in the *FgTri1::eGFP* strain, like that of *FgTri12::eGFP,* was also first observed in swollen ovoid regions of mycelia (Figure 20). Time-lapse imaging of cells revealed FgTri1p::eGFP localizes to motile vesicular structures, < 1µm in diameter, within these regions. The small fluorescent structures also exhibited saltatory patterns of movement (Supplemental time-lapse video 7). At this growth stage, cells exhibiting FgTri1p::eGFP expression are few in number and expression is restricted to single ovoid cells. Unlike FgTri12p::eGFP, after 25 hours in culture, FgTri1p::eGFP appears to localize in the periphery of small stationary circular structures (> 1µm) (Figure 21) as well as motile structures; expression of FgTri1p::eGFP is evident in cells adjacent to the swollen ovoid structures. While continuing to localize to motile organelles, FgTri1p::eGFP also localizes to the periphery of small stationary circular structures and is also present in a membranous network within the cytoplasm of cells (Figure 22, Supplemental time-lapse video 8). Similar localization patterns are observed after 36 hours in culture (Figure 23). After 40 hours in culture, FgTri1p::eGFP largely localizes to the vacuoles of cells, but remains present in motile organelles (Supplemental time-lapse video 9) while, to a lesser degree, other cells still exhibit fluorescence to the periphery of small stationary circular structures (Figure 22), motile

organelles, and in membranous structures in the cytoplasm (Figure 24). Laser scanning confocal microscopy and spectral unmixing were used to confirm that the spectrum of fluorescence emitted from fungal cells matched the emission spectrum of eGFP (Data not shown).

The fusion of a FgTri12p::eGFP tagged motile organelle with the plasma membrane was observed via time-lapse imaging (Supplemental time-lapse video 10). Following the fusion event, eGFP fluorescence appeared to diffuse within the area of the membrane where fusion occurred. A fusion event was also observed in the *FgTri1::eGFP* strain (Supplemental time-lapse video 11). In this strain, a small eGFP-tagged organelle appeared to fuse with a non-eGFP labeled stationary circular structure. Following this fusion event, eGPF fluorescence appeared to diffuse to the periphery of the stationary structure.

Latrunculin A abolished motility of organelles labeled with FgTri12p::eGFP

FgTri12p::eGFP labeled motile organelles were not observed in fungal cells treated with latrunculin A, while these organelles were present in cells treated with the solvent carrier DMSO alone. Cells removed from latrunculin A showed evidence of FgTri12p::eGFP labeled motile organelles after latrunculin A wash-out and four hours of incubation in recovery medium containing putrescine (Supplemental videos 12-14). Tissue samples plated on solid recovery medium demonstrated the effect latrunculin A had on cell growth and viability. Cells plated before and after latrunculin A treatment, and after latrunculin A wash-out, retained the ability to grow, though radial growth of latrunculin A treated and washed cells was considerably slower (Figure 25). Nevertheless this test demonstrated that latrunculin A-treated cells remained viable and that loss of eGFP-motile organelles was not caused by cell death or reduced growth.

Discussion

Tri12 cDNA sequence

The results of cDNA sequencing of *FgTri12* underscore the importance of using a combination of genetic comparative analysis and physical transcript data to validate *in silico* gene models. The structure of *FgTri12* determined by the cDNA sequence data, while at odds with gene models found currently in the MIPS and Broad Institute databases, directly supports the description of the *FgTri12* coding region predicted by a comparative genomics approach (Ward et al., 2002). Comparative analysis of FgTri12p and FsTri12p revealed a high degree of amino acid sequence conservation in some predicted transmembrane domains, while others are relatively polymorphic. It is not clear if these variations influence the varied self-protective roles of FgTri12p and FsTri12p. In *F. sporotrichioides*, the deletion of *FsTri12* results in severe attenuation of trichothecene accumulation in culture, while the deletion of *FgTri12* in *F. graminearum* actually results in an increase in trichothecene accumulation.

Functional analysis of *FgTri12*

MFS proteins play diverse roles in fungal self-protection against secondary metabolites and exogenous substances. FgTri12p plays a role in self-protection that is somewhat similar to that which has been proposed for FsTri12p (Alexander et al., 1999). Disruption of *FgTri12* in *F. graminearum* and *FsTri12* in *F. sporotrichioides* resulted in compromised radial growth in the prescence of trichothecenes. The *FgTri12* mutant produced reduced quantities of trichothecenes *in planta* and is less pathogenic on wheat than wild-type PH-1. These observations are consistent with the proposed role of self-protection. A reduction in the ability of the fungus to protect itself from the effects of trichothecenes likely results in reduced growth under toxin-inducing conditions *in planta*. The decrease in virulence associated with the absence of FgTri12p suggests it role is not trivial, though it is apparently not the only mechanism *F. graminearum* employs to

facilitate toxin efflux. In their investigation of global gene regulation by Fusarium transcription factors *Tri6* and *Tri10*, Seong et al. (2009) identified four predicted ABC transport proteins and at least one major facilitator superfamily (MFS) transporter that are regulated by *Tri6*. However, the closest amino acid sequence paralog of the current *FgTri12* gene model possesses less than 27% sequence identity (MIPS; mips.helmholtzmuenchen.de/genre/proj/FGDB).

Interestingly, more 15ADON than DON is present in culture supernatants of TBI cultures, while more DON that 15ADON is present in inoculated spikelets of wheat. These results suggest wheat may possess a mechanism that can convert 15ADON produced by the fungus *in planta* into DON, or *in planta* growth causes *F. graminearum* to produce more DON. Surprisingly, the *fgtri12* mutant produced significantly more 15ADON and DON in liquid TBI cultures than PH-1. This result is in contrast with results obtained from the study of *FsTri12* where a significant reduction of T-2 (~ 97%) and no diacetoxyscirpenol was observed in *FsTri12* mutant GYEP liquid cultures. Increased levels of trichothecene production in genetically modified strains of *F. graminearum* have been observed previously. Deletion of two *F. graminearum* genes, FGSG_00007 or FGSG_10397, encoding a cytochrome P450 monooxygenase and an unknown protein, respectively resulted in increased virulence on wheat and increased DON production under toxin inducing and non-inducing conditions., The roles these genes play in trichothecene biosynthesis are unclear (Gardiner et al., 2009a).

Expression of *FsTri12* in yeast demonstrated its ability to influence trichothecene flux in a living system (Alexander et al., 1999). In this organism, expression of *FsTri12* increased flux of 15-decalnectrin and calnectrin, indicating FsTri12p likely resided in the plasma membrane. The current study provides direct evidence that places FgTri12p in the plasma membrane. The actual passage of trichothecenes other than 15-decalnectrin and calnectrin through FsTri12p has not been experimentally proven, though trichothecenes are presumed to accumulate almost exclusively in culture medium (Alexander et al., 1999). FgTri12p appears have a regulatory function in trichothecene biosynthesis that is

probably manifested by the effect this protein has on internal concentrations of 15ADON or trichothecene pathway intermediates.

Cell morphology in TBI cultures

Several studies indicate cell morphology of *F. graminearum* noticeably changes *in planta* (Pritsch et al., 2000; Jansen et al., 2005; Boddu et al., 2006; Illgen et al., 2009; Rittenour and Harris, 2010; Brown et al., 2010). In the current study, the first notable *in vitro* changes in cell morphology under trichothecene induction conditions occurred 18 hours after suspension of conidia in TBI medium. The ovoid structures observed in TBI cultures are similar in shape to the bulbous coral-like hyphae described by Rittenour and Harris (2010) during the colonization of wheat cells 24 hours after inoculation of wheat glumes with *F. graminearum* conidia. Boddu et al. (2006) reported similar structures in the lemma of Morex barley florets 96 hours after inoculation. Thickened hyphae featuring ramified and coralloid growth were described by Pritsch et al. (2000) in wheat glumes 48 hours after inoculation. Similar features were also observed in TBI cultures 24 hours after inoculation. Based on the size (~10 μm) and morphology of vesicles in fungal cells growing in the metaxylem of wheat spikelets observed by Brown et al. (2010), it is proposed that these structures are analogous to the enlarged vacuoles observed inside ovoid cells present in TBI cultures.

None of the morphological changes described above are observed under conditions that do not induce trichothecenes in MM cultures. TBI and MM media are identical in chemical composition for all components except nitrogen source. Thus, the polyamine putrescine is capable of inducing *in vitro* morphological changes in the fungus and the biosynthesis of trichothecenes. Polyamines have been implicated in multiple biological processes in plants, including stress response and senescence. They are also known to be essential for cell proliferation and differentiation (Urano et al., 2005; Kusano et al., 2008). These biological processes are likely to be up-regulated in developing wheat spikes infected with *F. graminearum*. The stimulation of *Tri5* promoter driven GFP

expression observed in colonized spikes noted by Illgen et al. (2009) could be induced by polyamines that may be present in elevated concentrations in the developing kernel and rachis. Gardiner et al. (2010a) demonstrated the induction of wheat genes implicated in polyamine biosynthesis 24 hours after inoculation of wheat with *F. graminearum* and also demonstrated that putrescine accumulates in wheat spikes prior to toxin production by the pathogen., It is not clear what role polyamines may play in colonization of wheat by *F. graminearum*.

Subcellular localization of GFP tagged proteins

While the roles of many trichothecene biosynthetic enzymes have been established, the cellular mechanisms involved in transport, sub-cellular localization, and regulation of these enzymes are still unknown. In the present study, the transgenic strain F*gTri12::eGFP* was used to track the temporal and spatial expression patterns of FgTri12p in real time in living cells. In an effort to compare temporal and spatial expression analysis between FgTri12p and a second protein associated with trichothecene biosynthesis, FgTri1p was tagged with eGFP in an independent strain. FgTri1p, a cytochrome P450-like calnectrin C-7/8 hydroxylase (McCormick et al., 2004), is required for the production of 15ADON and functions at an intermediate step of Type B trichothecene biosynthesis. Calnectrin, a substrate used by FgTri1p to produce the pathway intermediate 7,8 dihydroxycalnectrin, marks the point of divergence between the Type A and Type B trichothecene biosynthesis pathways. At least one area of subcellular colocalization between FgTri12p::eGFP and FgTri1p::eGFP was identified. FgTri12p::eGFP was localized sequentially in small motile organelles, the plasma membrane, and within the lumen of late endosomes and vacuoles. FgTri1p::eGFP was localized sequentially in small motile organelles, the periphery of larger round organelles, and within the lumen of late endosomes and vacuoles. Additionally, these results provide evidence of the fusion of a small motile organelle with the plasma membrane in the *FgTri12p::eGFP* strain that resulted in the diffusion of fluorescence in the membrane. The fusion of a small organelle with a non-vacuolar small round organelle in the

FgTri1::eGFP strain resulted in the diffusion of fluorescence in the periphery of the structure. It is not certain if the organelles that initiated these fusion events are the same in both strains.

Possible identity of eGFP labeled motile structures

The motile structures observed in both strains exhibit similar patterns of movement within cells, though identity and genesis of these structures is unknown. Based on the results of this study, it is proposed these structures may be involved in the final stages of post-translational modification of these proteins and transport to their functional locations. In *A. nidulans,* similar organelles have been called Golgi equivalents (Lee et al., 2008). The fusion of GFP labeled structures with the plasma membrane and an unidentified intracellular organelle suggests that the transport and delivery of FgTri1p and FgTri12p to their functional locations has been observed. It is not certain if Golgi equivalents are involved in the transport and delivery of these proteins or if transport vesicles that exhibit similar patterns of motility mediate this process. The delivery of FgTri12p to the plasma membrane and FgTri1p to an intracellular organelle suggests two modes of transport may be involved in their movement within the cell. While FgTri12p likely reaches the plasma membrane via exocytosis, the movement of FgTri1p may rely on other mechanisms involved in intracellular trafficking.

Golgi equivalents are main components of the eukaryotic secretory system and function to modify nascent proteins sent from the endoplasmic reticulum. Adenosinediphospho-ribosylation factors (ADP-ribosylation factors) are GTP-binding proteins of the Ras superfamily involved in vesicle assembly and trafficking. ArfA is a homolog of ScArf1p and ScArf2p, two *S. cerevisiae* ADP-ribosylation factors that localize to the Golgi network and function in polarized budding. Treatment of *A. nidulans* cells expressing ArfA::GFP with Brefeldin A, an inhibitor of Arf GTP exchange factors that causes disruption of endoplasmic reticulum to Golgi transport, results in ArfA::GFP diffusion through the cytosol and accumulation into subcellular compartments. Moreover, it was

also shown that the deletion of an N-myristoylation motif resulted in the diffusion of the fusion protein throughout the cytosol. Based on these results and observed temporal FM4-64 staining patterns, Lee et al. (2008) concluded ArfA::GFP likely localizes to Golgi equivalents that are active in the process of exocytosis. These experiments also demonstrated a significant degree of motility in putative Golgi equivalents labeled with ArfA::GFP. The spatial and temporal localization patterns of ArfF::GFP fusion proteins observed in *A. nidulans* are very similar to those observed in *F. graminearum* during initial expression of FgTri12p::eGFP and FgTri1p::eGFP.

Pantazopoulou and Peñalva (2009) explored the organization and dynamics of Golgi equivalents in *A. nidulans*. The authors used a trans-Golgi-specific reporter to demonstrate the motility of Golgi equivalents during apical extension of the fungus. The motility patterns exhibited by Golgi equivalents are also very similar to those observed in *F. graminearum* during initial expression of FgTri12p::eGFP and FgTri1p::eGFP.

Trafficking and motility of eGFP labeled organelles

In two recent papers, Chanda et al. (2009, 2010) proposed models for the compartmentalization of a portion of the aflatoxin biosynthetic pathway and proposed a role for exocytosis in aflaxtoxin efflux from *A. parasiticus*. In the first paper, vesicles referred to as aflatoxisomes are described. These vesicles are so named due to the localization of OmtA and Ver-1, two aflatoxin biosynthetic enzymes, within them. In the second paper, Chanda et al. (2010) proposed exocytosis could play a role in aflaxtoxin efflux from *A. parasiticus* based on the observation that deletion of *aflT*, a gene in the aflatoxin biosynthetic cluster predicted to encode an MFS transporter with 14 transmembrane domains, does not have a significant effect on aflatoxin efflux from *A. parasiticus* (Chang et al., 2004). In their investigation of the possible role of exocytosis in aflatoxin efflux, Chanda et al. (2010) observed the movement of vesicles from the cytoplasm to the inner surface of the cytoplasmic membrane during peak levels of aflatoxin synthesis in culture. These vesicles appear to fuse with the plasma membrane,

likely releasing their contents into growth medium. The authors also provide evidence of aflatoxin in discrete patches on the cell surface via fluorescent antibody staining with aflatoxin specific antisera (anti-AFB_1) after the peak period of aflatoxin production. Based on these observations, Chanda et al. (2010) proposed three possible scenarios: 1) Aflatoxisomes are transported to the plasma membrane, where they either fuse with the membrane and release aflatoxin and aflatoxin biosynthetic enzymes into the extracellular space, 2) Aflatoxisomes act as shuttles that transport alflatoxins and biosynthetic enzymes across the plasma membrane, or 3) Aflatoxisomes interact with transmembrane transporter proteins that mediate the release of secondary metabolites from vesicles that adhere to the inner surface of the cytoplasmic membrane. The results of the current study of trichothecene biosynthesis in *F. graminearum* suggest exocytosis plays a role in delivering FgTri12p to the plasma membrane. It is unclear if it also plays an expanded role in facilitating the transport of trichothecenes across the plasma membrane.

Recent research efforts on the mechanisms of polar growth in fungi have focused on the regulation and facilitation of vesicle trafficking. Small GTPases and a protein complex aptly known as the exocyst have been implicated in regulating and facilitating exocytosis in yeast. The exocyst – an octameric protein complex composed of the hydrophilic proteins Sec3p, Sec5p, Sec6p, Sec8p, Sec10p, Sec15p, Exo70p, and Exo84p – is required for exocytosis. It is hypothesized to be involved in directing vesicles to sites of fusion on the cytoplasmic face of the plasma membrane (TerBush et al., 1996; Lipschutz and Mostov, 2002). This complex has also been shown to interact with members of the Rab and Rho families of small GTPases in yeast. Sec4p, a small Rab GTPase, resides on secretory vesicles and the plasma membrane and has been shown to interact with exocyst component protein Sec15p. Sec15p also interacts with Sro7p, a binding partner for the plasma membrane t-SNARE Sec9p. Exo84p, another component of the exocyst, and the type-V myosin, Myo2p, have also been shown to interact with Sro7. Three Rho GTPases – Rho1p, Rho3p, and Cdc42p – have been implicated in the regulation of the exocyst. Rho1p is involved in regulating the localization of the Sec3p component of the exocyst, while Rho3p appears to interact with Exo70p. Cell division cycle 42 (Cdc42) has been

proposed to have functional redundancy with Rho3 (Wu et al., 2008). Interestingly, Rho1p, Rho3p, and Cdc42p have been shown to have indirect control on actin organization. Conditional loss of function mutations in these proteins resulted in the loss of actin filaments in yeast (Yakir-Tmang and Gerst, 2009). Collectively, these GTPases and the proteins with which they interact appear to regulate the tethering, docking, and eventual fusion of the exocyst with the plasma membrane.

The transport of OmtA and Ver-1, two aflatoxin biosynthetic enzymes, to aflatoxisomes has been hypothesized to occur via cytoplasm to vacuole targeting **(**Cvt). Vbs, an enzyme implicated in the synthesis of the extremely toxic end products of aflatoxin biosynthesis, is predicted to move to aflatoxisomes from the ER-Golgi complex via the classical secretory pathway. The transport of Vbs through this alternate pathway is based on the observed N-glycosylation of this protein (Roze et al., 2011; Hong and Lindz, 2008; Baba et al., 1997). Analysis of the predicted amino acid sequence of the trichothecene biosynthetic enzyme FgTri1p with SignalP (Nielsen and Krogh; 1998*,* Emanuelsson et al., 2007) suggests this enzyme possesses a signal anchor (uncleaved signal peptide). It is not known if FgTri1P is N-glycosylated.

Vesicle trafficking Soluble (N-ethylmaleimide sensitive factor) NSF Attachment Protein Receptors (SNAREs) are involved in the docking of vesicles with organelles. The interaction of multiple t-SNAREs on the surface of the target organelle with a vSNARE on the surface of the vesicle forms a trans-SNARE complex that irreversibly binds the two membranes. Fusion follows, resulting in the union of the vesicle with the target organelle. A comprehensive study of SNARE localization in *Aspergillus oryzae* revealed the association of specific SNAREs with endoplasmic reticulum, plasma membrane, Golgi apparatus, endosomes, pre-vacuolar compartments, and vacuoles (Kuratsu et al., 2007).

Two SNAREs have been characterized in *F. graminearum*. GzSYN1 and *GzSYN2* encode syntaxin like t-SNARE proteins. Targeted deletion of *GzSYN1* and *GzSYN2* resulted in a

67% and 75% decrease in virulence on barley, respectively (Hong et al., 2010). It is not known if these SNAREs influence trichothecene biosynthesis, as no data regarding toxin production were included in this report. GFP::SYN1 fusion proteins were observed in vesicles, vacuoles, plasma membranes, and septa. GFP::GzSYN2 fusion proteins were observed in plasma membranes and septa. The influence these proteins have on trichothecene efflux or trafficking of trichothecene biosynthetic enzymes is unknown. *GzSYN1* and *GzSYN2* knock-out strains should be assayed on wheat to determine their capacity for producing trichothecenes. Considering the likely involvement of SNAREs in the trafficking of vesicles involved in the transport of components of the trichothecene biosynthetic pathway, further investigation of the predicted SNARE-like proteins listed in the MIPS database may be warranted.

The motility of secretory vesicles, vacuoles, Golgi elements, endoplasmic reticulum, and mitochondria in yeast is dependent on the interaction between actin and myosin (Seabra and Coudrier, 2004). This interaction also permits motility of mitochondria in *A. nidulans* and influences endocytosis in *A. nidulans* and *F. graminearum* (Suelmann and Fischer, 2000; Upadhyay and Shaw, 2008; Kim et al., 2009). Kinesin and dynein interaction with microtubules has been implicated in facilitating early endosome motility in *A. nidulans* and the plant pathogen *Ustilago maydis* (Abenza et al., 2009; Steinberg, 2007). Microtubules are also necessary for the motility of the endoplasmic reticulum in *Ustilago maydi***,** vesicles and mitochondria in *Allomyces macrogynus,* and vesicle motility in *Neurospora crassa* (Wedlich-Soldner et al., 2002; McDaniel and Roberson, 2000; Seiler et al., 1999). The motility of Golgi equivalents appears to rely on a complex association with actin, microtubules, and associated molecular motors in *A. nidulans* (Breakspear et al., 2007; Hubbard et al., 2008). To test for the involvement of actin in the motility of eGFP labeled small motile vesicles in *F. graminearum*, TBI cultures of *FgTri12::eGFP* were treated with latrunculin A. After one hour of exposure to latruculin A, FgTri12p::eGFP labeled small motile vesicles were completely absent in cells that exhibited eGFP fluorescence in plasma membranes and vacuoles. When latruculin A treated cells were washed to remove the toxin and returned to fresh TBI culture medium,

small motile FgTri12p::eGFP labeled vesicles were evident after four hours of incubation. Moreover, cells treated with latruculin A were viable when plated on recovery medium. These results demonstrate actin likely plays a role in the movement of FgTri12p.

A possible role for compartmentalization in trichothecene biosynthesis

The temporal and spatial expression patterns of FgTri12p and FgTri1p in cells during trichothecene synthesis were observed during this study. The presence of FgTri12p in the plasma membrane is easily reconciled with its recognized role in trichothecene tolerance and flux. Though this study provided no biochemical data establishing the cellular location of FgTri1p activity, the localization patterns of FgTri1p::eGFP suggest it is part of the trichothecene biosynthesis pathway is compartmentalized. Localization of FgTri1p::eGFP in the periphery of small organelles suggests the protein is likely anchored in membranes surrounding these spherical organelles. This observation is consistent with fact that FgTri1p is a cytochrome P-450 oxygenase (McCormick et al., 2004) and, as such, likely functions as a terminal oxidase of a short membrane associated electron transfer chain. TMPred predicts that the amino acid sequence of FgTri1p contains a 19 amino acid transmembrane domain at the N-terminus of the protein. Thus, it is likely that FgTri1p is inactive when localized to the lumen of the vacuole.

Aflatoxins, or polyketide-derived furanocoumarins, are produce via a biosynthetic process that involves at least 17 enzyme activities encoded by 25 or more genes that are clustered in a 75-kb region of a single chromosome. Several enzymes and metabolic intermediates that are part of the biosynthetic process have been reported to localize to peroxisomes, vesicles, and vacuoles within *A. parasiticus* during aflatoxin production. Peroxisomes have been demonstrated to supply part of the acetyl-CoA used for aflatoxin biosynthesis (Maggio-Hall et al., 2005). GFP tagging of the biosynthetic enzyme Nor-1, implicated in an early step in aflatoxin biosynthesis by *A. parasiticus*, has placed this enzyme in the cytoplasm of toxigenic cells during the early stage of aflatoxin production.

Localization of Nor-1::GFP fusion proteins to the vacuole coincide with high rates of aflatoxin biosynthesis (Hong and Lindz, 2009). Similar localization patterns were observed in the study of aflatoxin biosynthetic enzymes OmtA and Ver-1 (Lee et al., 2004. Hong and Lindz, 2008). A vesicle-vacuole fraction obtained from *A. parasiticus* during aflatoxin biosynthesis was able to convert sterigmatocystin, a late intermediate in aflatoxin biosynthesis, to aflatoxin B1. Inhibition of vesicle-vacuole fusion via the disruption of a Class C Vps tethering complex or chemical treatment with Sortin-3 resulted in an increase in aflatoxin efflux, suggesting that the metabolic pathway flows from peroxisomes to aflatoxisomes which serve to export the toxin out of the cell. The vacuole itself has been proposed to play a minor role in aflatoxin biosynthesis (Chanda et al, 2009).

The study of ß-lactam synthesis by *Acremonium chrysogenum* and *Aspergillus nidulans* has revealed the sub-cellular location of several enzymes involved in the biosynthesis of cephalosporin and penicillin. Enzymes and pathway precursors and intermediates have been placed in Golgi-derived vesicles, vacuoles, peroxisomes, and the cytoplasm, though the functional roles of these organelles or regions in penicillin biosynthesis, storage, or export have not been demonstrated directly (Müller et al., 1992; Lendenfeld et al., 1993; Spröte et al. 2009; Chanda et al., 2009; Meijer et al., 2010). The amino acid precursors used in ß-lactam synthesis are derived from the vacuole, while the two final enzymes involved in penicillin biosynthesis localize to peroxisomes (Lendenfeld et al., 1993; Meijer et al., 2010). The transporter CefM has been implicated in the translocation of biosynthetic intermediates necessary for the production of cephalosporin by *A. chrysogenum*. *CefM* disruption mutants are unable to produce cephalosporin and accumulate the upstream precursor penicillin N. CefM::GFP fusion proteins are targeted to intracellular peroxisomes during a phase of high cephalosporin production in culture. This protein is predicted to possess 12 transmembrane domains and hypothesized to facilitate the movement of penicillin N from the peroxisome to cytoplasm for further modification by downstream biosynthetic enzymes (Teijeira et al., 2009).

In the case of trichothecene biosynthesis in *F. graminearum,* both GFP-tagged FgTri12p and FgTri1p ultimately localize to the vacuole as determined by co-localization with the vacuole targeted dye CMAC. Because each protein moves to the vacuole relatively late in the biosynthetic process, it is proposed their fate in this organelle is protein turnover. Indeed, while cytochrome P-450 FgTri1p and MFS transporter FgTri12p are membrane-associated at earlier time points (with vesicles or the plasma membrane, respectively) according to their function, later they reside in the vacuolar lumen, suggesting that they are no longer in a functional state. Movement of these proteins from their functional milieu to vacuoles is likely dependent on components of the endocytotic pathway. How these proteins are directed and transported to the vacuole is unknown.

Future Research

A combination of biochemical and genetic approaches should be undertaken to determine sub-cellular mechanisms that influence and facilitate trichothecene biosynthesis. Additional fluorescent protein tagging studies are needed to establish co-localization or segregation between FgTri1p and other enzymes that act upstream (FgTri3p) or downstream (FgTri8p) of FgTri1p in the trichothecene biosynthetic pathway. Intracellular, exocytotic, and endocytotic vesicle trafficking involved in trichothecene biosynthesis are likely reliant on multiple mechanisms involved in transport, tethering, docking, and organelle fusion. Future experiments should focus on determining the identity and roles of components of these mechanisms that are integral to trichothecene biosynthesis.

Methods

Strains and Culture Conditions

Conidia of *F. graminearum* wild-type strain PH-1 (NRRL 31084) and all mutants were cultured at 25°C in liquid carboxymethylcellulose (CMC) medium (Per liter: low

viscosity carboxmethylcellulose (Sigma), 15.0 g; NH_4NO_3 1.0 g; KH_2PO_4, 1.0 g; $MgSO_4$-$7H_2O$, 0.5 g; yeast extract (Difco)) for five days. Spores were harvested by centrifugation at 3000 rpm for 10 min and washed twice with sterile distilled H_2O. Spore concentrations were determined using a hemacytometer.

Liquid trichothecene biosynthesis induction (TBI) cultures contained medium adapted from Gardiner et al. (2009b). Per liter, 1X TBI medium contained: 30 g sucrose, 1g KH_2PO_4, 0.5 g $MgSO_4 \cdot 7H_2O$, 0.5 g KCl, 10 mg $FeSO_4 \cdot 7H_2O$, 800 mg putrescine, 200 µL of trace element solution (per 100 mL, 5 g citric acid, 5 g $ZnSO_4 \cdot 7H_2O$, 0.25 g $CuSO_45H_2O$, 50 mg $MnSO_4 \cdot H_2O$, 50 mg H_3BO_3, 50 mg $NaMoO_4 \cdot 2H_2O$). In all cases, TBI stock medium was filtered through 0.45 µM bottle top filter sets (Corning).

Culture plates for radial growth assays contained TBI +1% bactoagar or minimal medium (MM) (Correll et al. 1987). TBI plates were made using 2X TBI supplemented 1:1 with sterile 2% H_2O agar. 2X TBI solution was adjusted to pH 4.5 with NaOH before dilution.

Protoplasting and Transformation

One ml of 10^8 ml^{-1} washed conidia harvested from a five-day-old CMC culture was used to inoculate a 100 ml YEPD (yeast extract, 3.0 g; Bactopeptone (Difco), 10.0g; glucose, 20.0 g; and distilled water to 1 l) culture that was incubated for 16-18 h at room temperature with shaking at 150 rpm. Tissue present after incubation was used to prepare protoplasts. Protoplast preparation and fungal transformation were performed as described previously (Hou et al., 2002).

Targeted Gene Replacement and Gene Complementation

Tri12 deletion mutants (*fgtri12*) were generated in the wild-type strain PH-1 by split-marker recombination mutagenesis (Catlett et al., 2003) with previously described modifications (Goswami et al., 2006). DNA oligonucleotides (IDT Inc., Coralville, Iowa)

listed in Table 6 were used to PCR amplify 5' and 3' flanking regions beginning 934 bp and ending 23 bp 5' of the *Tri12* start codon (911 bp) and the region 510 bp 5' and 455 bp 3' of the TAA stop codon (968 bp) using PH-1 genomic DNA as a template. The right and left flanks of *hph* were amplified using oligonucleotides also listed in Table 6 and the plasmid pCX62, which contains the *hph* gene, as a template.

The full genomic sequence of *FgTri12* and the 913 bp upstream and 513 bp downstream regions of the flanking genomic sequence were PCR amplified using the phosphorylated DNA oligonucleotides listed in Table 6. Genomic DNA from PH-1 was used as a template. The resulting amplicon was purified through a Qiagen PCR purification column and blunt end cloned into pSM334, which contains a copy of *neo* that was utilized for selection of transformed complementation strains. Prior to ligation, pSM334 was digested with *EcoR*V, treated with shrimp alkaline phosphatase (Fermentas, Glen Burnie, MD), and purified through a PCR purification column (Qiagen, Valencia, CA).

Hygromycin and/or geneticin resistant transformants were isolated and gene replacement mutations were confirmed by restriction enzyme digestion of PCR amplicons and Southern hybridization. V8 juice agar (200 ml V-8 juice (Campbell Soup Company, Camden NJ), 2 g $CaCO_3$, 15 g agar, water to 1 l) supplemented with 250 mg ml^{-1} hygromycin B (Calbiochem, La Jolla, CA) or 250 mg ml^{-1} geneticin was used for selection of transformants.

eGFP tagging

A fusion PCR based method described by Szewczyk et al. (2006) for constructing *C*-terminal GFP fusion proteins was used with modification to synthesize the constructs used to generate *FgTri12::eGFP* and *FgTri1::eGFP*. The *Neurospora* knock-in vector pGFP::hph::loxP (GenBank: FJ457011.1; Honda and Selker, 2009) was used as a template for the synthesis of the *eGFP::hph* portion of the fusion constructs. The *eGFP::hph* DNA sequence contained in this plasmid is supplemented with a 5' sequence

encoding a 10 Gly linkage amino acid sequence. Fusion products contain the 10 amino acid linkage region between the final amino acid of FgTri12p or FgTri1p and the eGFP start codon. Oligonucleotides used to amplify *FgTri12* and *FgTri1* regions flanking their stop codons and the *eGFPhph* portion of the construct are listed in Table 6. Hygromycin resistant transformants were isolated and gene tagging was confirmed by PCR and Southern hybridization. V8 juice agar supplemented with 250 mg ml $^{-1}$ hygromycin B was used for isolation of transformants.

Genomic DNA extraction, Southern blotting and cDNA sequencing

Tissue for DNA extraction was cultured in complete medium (CM) (Trail et al., 2003) for seven days at 25°C. Cultures were washed twice with ddH_2O and freeze-dried. Genomic DNA was extracted from dried cultures using G Biosciences Omniprep DNA kits. Genomic DNA used for Southern blotting was treated with RNAse A at room temperature for 15 minutes before digestion. For Southern blotting analysis, 20 µg of genomic DNA were digested. Three groups of DNA samples were analyzed to characterize *fstri12*, *fgtri12/FgTri12*, *FgTri12::eGFP*, and *FgTri1::eGFP* strains. For the characterization of *fstri12* and *fgtri12/FgTri12*, DNA samples from these strains and PH-1 were digested with *PstI*. *FgTri12::eGFP* and PH-1 were digested with *BglII*. *FgTri1::eGFP* and PH-1 were digested with *KpnI*. DNA probes were used to detect the presence of *hph*, *neo*, *eGFP*, *FgTri1,* and *FgTri12* in the appropriate fungal strains via hybridization. DNA oligonucleotides listed in Table 6 were used to synthesize these probes. Southern hybridization was performed as described by Rosewich et al. (1998), except probe hybridization and primary wash temperatures were increased to 65˚ C. The Amersham AlkPhos Direct Labeling and Detection System with CDP-Star (GE Healthcare) was used to label and detect the DNA probes.

3’ RACE-PCR was used to generate template DNA molecules for gene specific PCR. mRNA extracted from inoculated plants was used for cDNA synthesis. A universal cDNA cloning oligonucleotide (Table 6) was used to prime cDNA synthesis reactions. A

3' RACE-PCR oligonucleotide designed to anneal to the 5' end of synthesized cDNA and the gene specific oligonucleotide 1Fwd were use to generate PCR products used as templates for sequencing. These products were sequenced with the oligonucleotides shown above the proposed gene model for *FgTri12* (Figure 1) and listed in Table 6. PCR products were sequenced using a BigDye® Terminator v3.1 Cycle Sequencing Kit. (Life Technologies, Inc., Carlsbad, California). FinchTV (Geospiza, Inc., Seattle, WA) was used to edit sequencing traces. Sequence trace alignments were generated using Sequencher 4.7 (Gene Codes Corp, Ann Arbor, MI). Reference genomic DNA sequence for *FgTri12* was obtained from the Munich Information Center for Protein Sequences (MIPS) (mips.helmholtz-muenchen.de/genre/proj/FGDB).

RNA Extraction

Biomass from toxin biosynthesis induction cultures was harvested by filtration with Miracloth and washed twice with sterile distilled water. Tissue was flash-frozen in liquid nitrogen and lyophilized for 24 hours. Dried tissue was ground in liquid nitrogen before RNA extraction. RNA was isolated from fungal tissue using TRIzol™ reagent (Life Technologies, Carlsbad, CA) and RNeasy Mini Total RNA extraction kit (Qiagen, Valencia, CA) according to the manufacturers' protocol.

Pathogenicity and *in planta* mycotoxin assays

Wheat plants (*Triticum aestivum*), cultivar Norm, were grown as previously described (Goswami and Kistler, 2005). The fifth spikelet up from the first fully developed basal spikelet was inoculated with 10µl of a conidia suspension of 10^5 conidia ml^{-1} + 0.1% Triton X100 after the awns were removed. After inoculation, wheat plants were placed in a humidity chamber for 48 h. Plants were then transferred to a lighted growth chamber and grown for an additional eight days. Plants were exposed to a repeating 16/8 hour day/night diurnal cycle with daytime and nighttime temperatures maintained at 18° and 16°C, respectively. For pathogenicity determination, mycotoxin measurement, and

average mass of infected spike measurements, single-point inoculated spikes were scored for disease at 10 days after inoculation and then collected, weighed, and stored at -20°C. The five upper and four lower spikelets adjacent to the inoculated spikelet, as well as the inoculated spikelet itself, were scored for disease symptoms. Quantification of DON and 15ADON in inoculated spikelets was conducted as previously described (Goswami and Kistler, 2005). Results of pathogenicity and trichothecene production *in planta* assays of PH-1, *fgtri12*, and *fgtri12/FgTri12* are based on data from four biological replicates, while results from assays performed for PH-1 and *FgTri12::eGFP* are based on data from three biological replicates.

Trichothecene biosynthesis in liquid culture

Two ml stationary liquid TBI cultures inoculated with 10^4 ml^{-1} conidia were used to assay trichothecene production *in vitro*. Cultures were grown at 25°C in total darkness for seven days. Culture medium was filtered through cheesecloth to remove fungal tissue and freeze-dried. Dried samples were analyzed for the presence of DON and 15ADON as previously described (Goswami and Kistler, 2005).

Radial growth on TBI and minimal medium agar

Cultures for radial growth assays were grown in 60 x 15mm Petri dishes containing 10 ml aliquots of TBI agar at 25°C with a 12-hour light/dark diurnal cycle. Test cultures were independently inoculated at the center of the plate with 5 mm plugs of each strain. Circular plugs were cut from the leading edge of growth on MM agar source plates and placed tissue-side down on test plates. The average diameter of each colony was determined using four independent diameter measurements fixed to the culture plate. The results of three biological replicates were used to determine the average colony diameter for each strain at 24, 48, 72, and 96 hours after inoculation.

As a non-toxin control, additional cultures used for the observation of radial growth were

grown in 100 x 15mm Petri dishes containing 20 ml of minimal medium agar. Plates were imaged after 72 hours incubation at 25°C with a 12-hour light/dark diurnal cycle.

Bright-field, DIC, fluorescence, and laser scanning fluorescence confocal microscopy

To observe changes in cell morphology, PH-1 was grown in 50 ml liquid minimal medium or TBI medium at 25°C on an orbital shaker rotating at 150 rpm in total darkness. Cultures were sampled at 12, 16, 18, and 24 hours following inoculation with 5 x 10^5 conidia.

To observe FgTri12p::eGFP and FgTri1p::eGFP *in vivo*, 50 ml TBI cultures were grown at 28°C on an orbital shaker rotating at 150 rpm in total darkness. Cultures were sampled over a 44-hour period following inoculation with 5 x 10^5 conidia. Wet mounts of tissue were viewed using a Nikon Eclipse 90i upright microscope and a Nikon C1si laser scanning confocal microscope. Spectral unmixing of autofluorescence and GFP signals was done using known spectra for GFP (Clontech, Mountain View, CA). Regions of autofluorescence were selected in the untagged PH-1 strain using the Nikon EZ-C1 Viewer.

Mycelia from 42-hour cultures of *FgTri12::eGFP* strains were stained with CellTracker™ Blue CMAC (7-amino-4-chloromethylcoumarin) (Life Technologies, Carlsbad, CA) to identify late endosomes and vacuoles. CMAC dye was disolved in DMSO immediately before use. Addition of the dye solution to culture samples resulted in a final concentration of 100 μM CMAC and 1% DMSO. Stained cells were viewed 30 minutes after exposure to the dye.

Treatment of cells with latrunculin A

Latrunculin A was used to establish the involvement of actin in the cellular fate of FgTri12p::eGFP. PH-1 conidia were suspended in 20 ml TBI cultures at final

concentration of 10^4 conidia ml^{-1} and incubated at 28°C on an orbital shaker rotating at 150 rpm in total darkness. After 36 hours of incubation, samples from pretreated culture samples were plated on recovery medium (per liter: sucrose, 30 g; KH_2PO4, 1 g; $MgSO_4 \cdot 7H_2O$, 0.5 g; KCl, 0.5 g; $FeSO_4 \cdot 7H_2O$, 10 mg; $NaNO_3$, 850 mg; 200 µL of trace element solution (per 100 mL; citric acid, 5 g; $ZnSO_4 \cdot 7H_2O$, 5 g; $CuSO_45H_2O$, 0.25 g; $MnSO_4 \cdot H_2O$, 50 mg; H_3BO_3, 50 mg; $NaMoO_4 \cdot 2H_2O$, 50 mg)). Cultures were then treated with latrunculin A (Enzo Life Sciences, Plymouth Meeting, PA) in DMSO (Sigma-Aldrich Corp., Sigma-Aldrich Corp. St. Louis, MO) or DMSO alone and incubated under the same conditions for one hour. After treatment, cultures contained a final concentration of 5 ug ml^{-1} latrunculin A and 0.1% DMSO or 0.1% DMSO only. After incubation, samples were removed for microscopy and plated on recovery medium. Tissue was then filtered from the test cultures and washed with 4 volumes of 20 ml TBI medium. Tissue was resuspended in 25 ml TBI medium and incubated for an additional four hours. Samples were then obtained for microscopy and plated on recovery medium. Recovery plates were incubated overnight at 25°C.

Tables

Table 1. Pathogenicity and trichothecene concentrations *in planta*.

	Pathogenicity[a,b]		Trichothecene Concentration[c] (ppm)	
Strain	Symptomatic Spikelets	Mass of Spike	DON	15ADON
PH-1	7.8 ± 0.38	1.49 ± 0.07	542.9 ± 23.2	64.6 ± 4.6
fgtri12	5.3 ± 0.45[d]	1.78 ± 0.09[e]	369.1 ± 26.0[f]	27.3 ± 3.1[f]
fgtri12/*FgTri12*	7.2 ± 0.56	1.50 ± 0.09	383.8 ± 20.3[f]	40.0 ± 3.2[fg]

a. Mean ± SEM number of wheat spikelets per inflorescence exhibiting necrotic symptoms 10 days after inoculation of a single central spikelet.

b. Mean ± SEM mass of symptomatic spikes 10 days after inoculation of a single central spikelet.

c. Mean ± SEM of the concentration (mg g-1 dried infected tissue) of deoxynivalenol (DON) and 15-acetyldeoxynivalenol (15ADON) in the inoculated spikelet 10 days after inoculation.

d. Mean significantly less than value for PH-1, Mann-Whitney U test ($P < 0.001$).

e. Mean significantly greater than value for PH-1, Student's Unpaired t-test ($P < 0.01$).

f. Mean significantly less than value for PH-1, Student's Unpaired t-test ($P < 0.001$).

g. Mean significantly greater than value for *fgtri12*, Student's Unpaired t-test ($P < 0.01$).

Table 2. Trichothecene concentration in liquid TBI medium seven days after inoculation with PH-1, *fgtri12* or *fgtri12/Fgtri12*.

	Trichothecene Concentration (ppm)	
Strain	15ADON[a]	DON[b]
PH-1	22.3 ± 1.4	1.2 ± 0.1
fgtri12	31.1 ± 2.8[c]	2.8 ± 0.2[c]
fgtri12/FgTri12	12.7 ± 1.2[d]	0.9 ± 0.2[d]

a. Mean ± SEM concentration 15-acetyldeoxynivalenol (15ADON) in clarified culture medium 7 days after inoculation.

b. Mean ± SEM concentration deoxynivalenol (DON) in clarified culture medium 7 days after inoculation.

c. Mean significantly greater than value for PH-1, Student's Unpaired t-test ($P < 0.005$).

d. Mean significantly less than value for *fgtri12*, Student's Unpaired t-test ($P < 0.001$).

Table 3. Colony diameter of all strains on grown on TBI medium.

	Colony Diameter[a]			
Time[d]	PH-1	*Fgtri12*	*fgtri12/FgTri12*	*FgTri12*::*eGFP*
24	1.6 ± 0.03	1.5 ± 0.02[b]	1.6 ± 0.04	1.7 ± 0.05[c]
48	2.5 ± 0.04	2.2 ± 0.03[b]	2.6 ± 0.07	2.6 ± 0.02[c]
72	2.8 ± 0.04	2.5 ± 0.03[b]	2.9 ± 0.07	3.0 ± 0.03[c]
96	2.9 ± 0.04	2.5 ± 0.03[b]	3.0 ± 0.07	3.1 ± 0.04[c]

a) Mean ± SEM diameter of colonies grown on TBI agar.

b) Mean significantly less than value for PH-1, Student's Unpaired t-test ($P < 0.005$).

c) Mean significantly greater than value for PH-1, Student's Unpaired t-test ($P < 0.05$).

d) Time of measurement (hours) after colony plating.

Table 4. Pathogenicity and trichothecene concentrations for *FgTri12*::*eGFP in planta*.

	Pathogenicity[a,b]		Trichothecene Concentration[c] (ppm)	
Strain	Symptomatic Spikelets	Mass of Spike	DON	15ADON
PH-1	7.6 ± 0.4	1.50 ± 0.1	531.8 ± 27.2	68.0 ± 5.8
FgTri12::*eGFP*	6.9 ± 0.5	1.60 ± 0.1	525.8 ± 29.7	53.5 ± 4.8

a. Mean ± SEM number of wheat spikelets per inflorescence exhibiting necrotic symptoms 10 days after inoculation of a single central spikelet.

b. Mean ± SEM mass of symptomatic spikes 10 days after inoculation of a single central spikelet.

c. Mean ± SEM of the concentration (mg g-1 dried infected tissue) of deoxynivalenol (DON) and 15-acetyldeoxynivalenol (15ADON) 10 days after inoculation.

Table 5. Trichothecene concentration in liquid TBI medium seven days after inoculation with *FgTri12*::*eGFP*.

	Trichothecene Concentration (ppm)	
Strain	15ADON[a]	DON[b]
PH-1	25.1 ± 1.0	1.7 ± 0.1
FgTri12::eGFP	21.6 ± 1.0[c]	1.7 ± 0.1

a. Mean ± SEM concentration 15-acetyldeoxynivalenol (15ADON) in clarified culture medium 7 days after inoculation.
b. Mean ± SEM concentration deoxynivalenol (DON) in clarified culture medium 7 days after inoculation.
c. Mean significantly less than value for PH-1, Student's Unpaired t-test ($P < 0.05$).

Table 6. Oligonucleotides used in this study.

Method	Name	Sequence (5' to 3')
cDNA synthesis, 3'RACE-PCR, and FgTri12 sequencing	cDNA cloning primer	GGCCACGCGTCGACTAGTACTTTTTTTTTTTTTTTTV
	3' RACE PCR primer	GGCCACGCGTCGACTAGTAC
	1Fwd	ATGACTGCTACAGTTCACGAAAAAGG
	926Fwd	GGTCTTTGGCAAGCCCGAGCG
	2125Rev	ACGTCCGTCCAGTTTCTAGTTTCGA
	2132Fwd	GACGGACGTGGTGTTGTCAGTAAAA
	2307Rev	TCATGCAATCCTAAATCAGGCCCTC
Disruption of FgTri12	LF1F	CTGGGCTGTCAACAACTGAA
	LF2R	TTGACCTCCACTAGCTCCAGCGGCGCGTAGGGCGGTCTTGAAAATGA
	RF3F	ATAGAGTAGATGCCGACCGGGCCGGCTTTTTGGCTCCATTTTCACC
	RF4R	AGTGACGCCCTCAAGAGATG
	HYG/R	GCCGGCCCGGTCGGCATCTACTCTAT
	HY/R	GTATTGACCGATTCCTTGCGGTCCGAA
	YG/F	GATGTAGGAGGGCGTGGATATGTCCT
	HYG/F	CGCGCCGCTGGAGCTAGTGGAGGTCAA
Gene complementation	Tri12Full5PPhos	5Phos-AGACATCCATATCCATCTTGATATTG
	TRI12Full3PPHos	5Phos-GGTTCAACGCAGTATTAGGT
Synthesis of Tri12::eGFP fusion protein	T12eGFP1F	TTCCTACTTGTATTGTTGAGATGTTTCTA
	T12eGFP2R	GCTGTATCATCTGTTAGTGCTGTCTT
	T12eGFP3F	AATATCATAACTGTCCGGCATGCAGCTCG
	T12eGFP4R	AGGTAGGATGTTGGTAAGTTTATAGGTC
	eGFPFwLFTri12Seq	AAGACAGCACTAACAGATGATACAGCGGCGGAGGCGGCGGAGGCGGAGGCGGAGGC
	eGFPRwRFTri12Seq	CGAGCTGCATGCCGGACAGTTATGATATTGACCATGATTACGCCAAGCTATTTAGGTGA
Synthesis of Tri1::eGFP fusion protein	Tri1eGFP1F	GAAGAAGGGTGGAACACGAA
	Tri1eGFP2R	GCCTCCGCCTCCGCCTCCGCCGCCTCCGCCGTCATCCTGTACCAATTCCAATC
	Tri1eGFP3F	TCACCTAAATAGCTTGGCGTAATCATGGTCGTAGGAGGACGTCACAGTCTTGG
	Tri1eGFP4R	TCAGATTTGAGGCTCATAAGGTT
	eGFPF	GGCGGAGGCGGCGGAGGCGGAGGCGGAGGC
	eGFPR	GACCATGATTACGCCAAGCTATTTAGGTGA
Synthesis of Southern probes for *Tri12::eGFP* and *Tri1::eGFP*	Tri1South5P	GCTCGCGAACTAATCACTCC
	Tri1South3P	AATTCCAATCGCAGACAAGG
	eGFPSouth5P	CACATGAAGCAGCACGACTT
	eGFPSouth3P	GCACCAAGCAGCAGATGATA

Figures

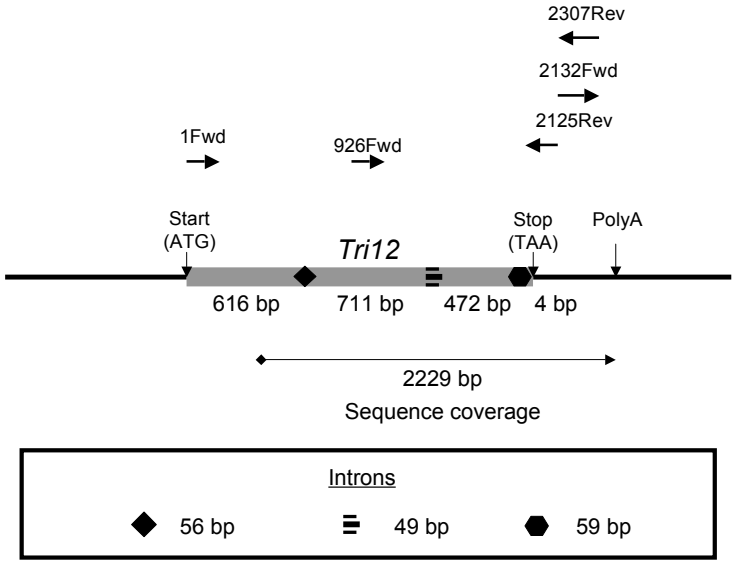

Figure 1. Gene model for *FgTri12.* Locations of oligonucleotides used for sequencing are located above the gene model. Sizes of exons and total sequence coverage are listed below the model. Intron locations are denoted on the model itself, while intron sizes are listed in the lower box.

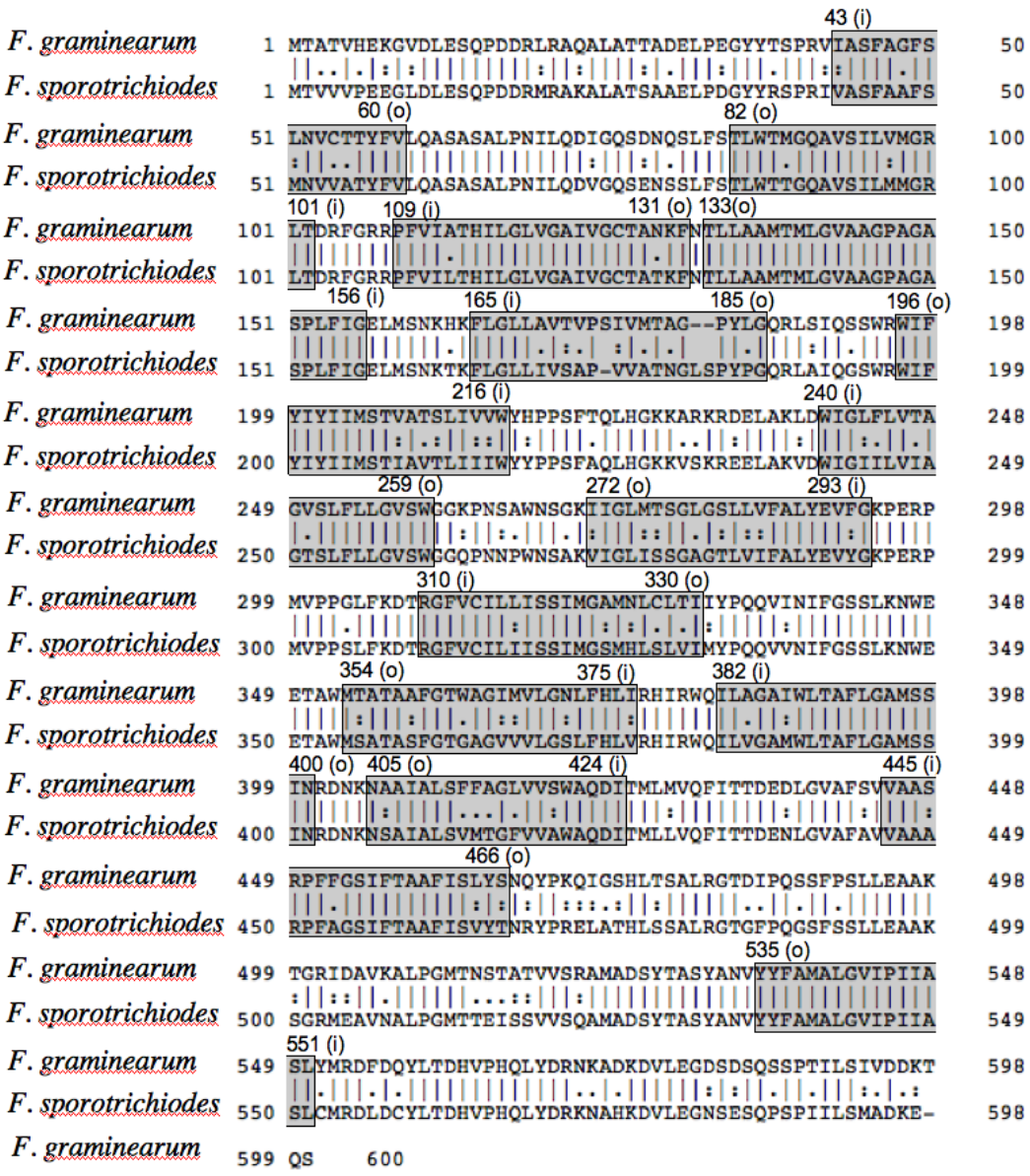

Figure 2. Needleman-Wunsch global alignment of predicted amino acid sequences of FgTri12p and FsTri12p. Amino acid number of (i) and outward (o) ends of predicted transmembrane domains are noted above boxes representing each of the 14 domains.

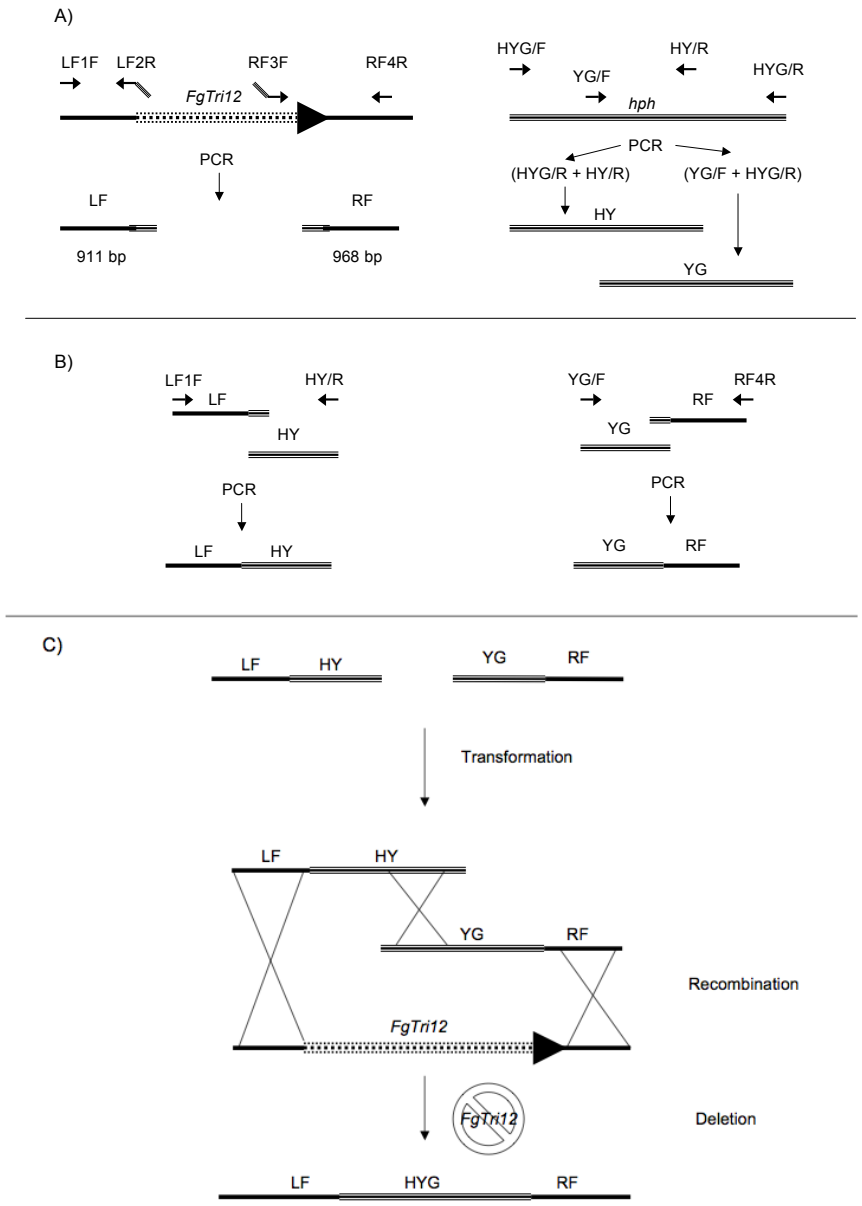

Figure 3. Split marker PCR method used for disruption of *FgTri12*. A) Left and right flanking regions of *FgTri12* are amplified using LF1F + LF2R and RF3F + RF4R oligonucleotide combinations. Sequences specific to the 5' and 3' regions of *hph* have been added to the 5' ends of LF2R and RF3F. HY and YG regions of the *hph* are amplified using HYG/F + HY/R and HYG/R + YG/R oligonucleotide combinations. B) LF and HY amplicons and LF1F and HY/R oligonucleotides are used to produce LFHY fusion products via PCR. YG and RF amplicons and YG/F and RF4R oligonucleotides are used to produce YGRF fusion products via PCR. C) Transformation of protoplasts with LFHY and YGRF fusion products disrupt the *FgTri12* gene via a triple crossover event.

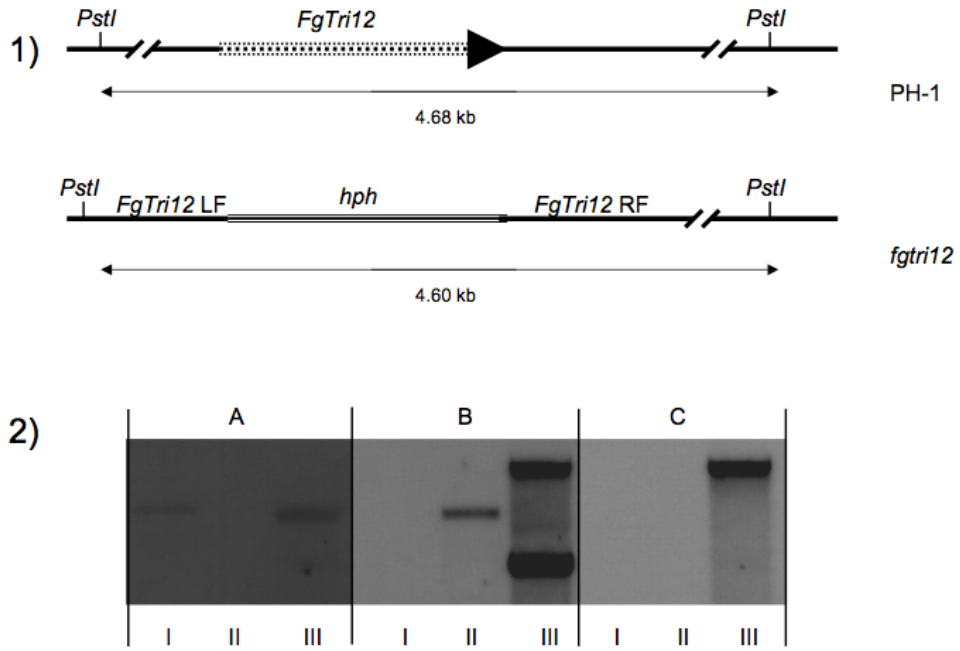

Figure 4. Southern blotting of genomic DNA. 1) Location of *PstI* restriction enzyme cut sites in PH-1 and *fgtri12* and the expected size of the fragment targeted by hybridization probes. 2) Hybridization of A) *FgTri12* B) *hph* C) *neo* specific probes to digested genomic DNA from I) PH-1 II) *fgtri12* III) *fgtri12/FgTri12.* These results demonstrate the presence of single copies of *FgTri12* in PH-1 and *fgtri12/FgTri12,* a single copy of *hph* in *fgtri12*, and a single copy of *neo* in *fgtri12/FgTri12.* The relative sizes of the fragments labeled with the *Tri12* probe in PH-1 DNA and *hph* probe in *fgtri12* DNA are consistent with expected digestion patterns. The two bands that hybridize with the *hph* probe in the *fgtri12/FgTri12* complement strain demonstrate that a duplication event occurred during integration of the *FgTri12* complementation construct.

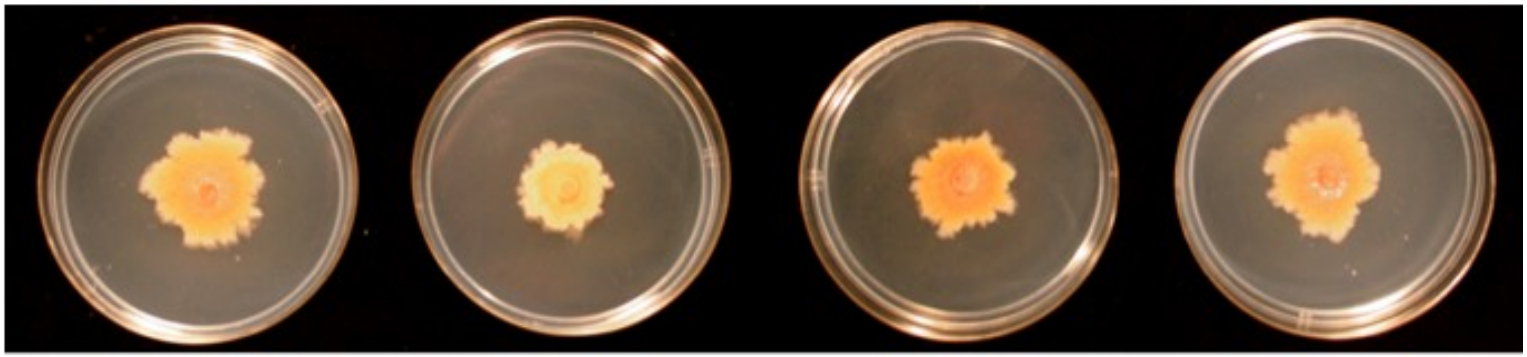

Figure 5. Radial growth and pigmentation of A) PH-1, B) *fgtri12,* C) *fgtri12/FgTri12*, and D) *FgTri12::eGFP* on TBI medium.

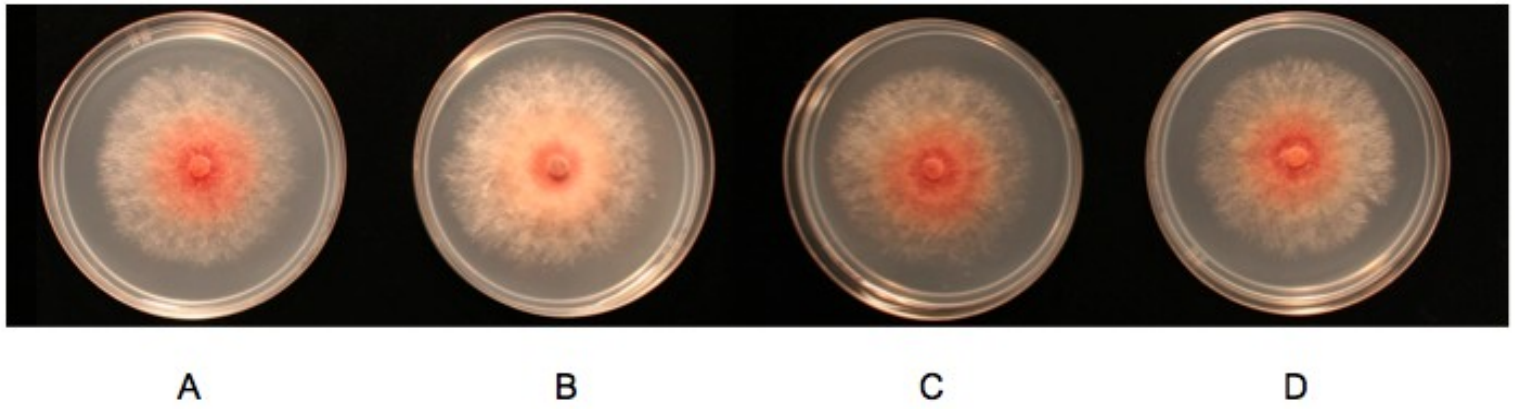

Figure 6. Radial growth and pigmentation of A) PH-1, B) *fgtri12,* C) *fgtri12/FgTri12*, and D) *FgTri12::eGFP* on minimal medium.

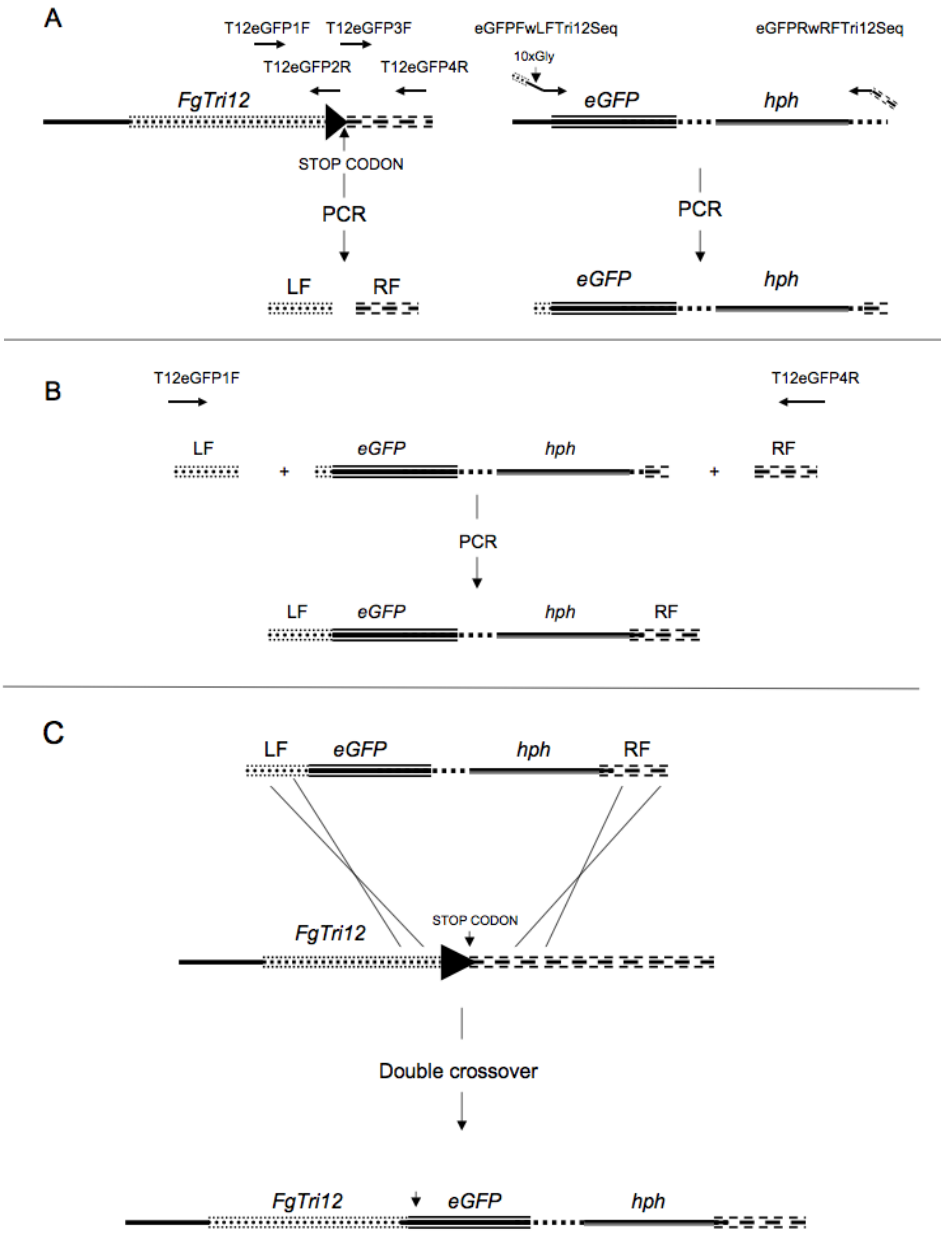

Figure 7. Synthesis of FgTri12p::eGFP fusion protein. A) T12eGFP1F + T12eGFP2R and Tri12eGFP3F + Tri12eGFP4R oligonucleotide combinations are used to amplify the 5' and 3' regions flanking the *Tri12* stop codon via PCR. The *eGFPhph* construct is amplified with eGFPwLFTri12seq and eGFPwRFTri12seq oligonucleotides. These oligonucleotides possess sequences specific to the regions directly 5' and 3' of the *Tri12* stop codon. B) RF, LF, and e*GFhph* constructs and T12eGFP1F and T12eGFP4R oligonucleotides are used to generate a continuous LF::e*GFPhph*::RF fusion construct. C) Transformation of PH-1 protoplasts with LF::e*GFPhph*::RF fusion construct results in eGFP tagging of the carboxy terminus of FgTri12p.

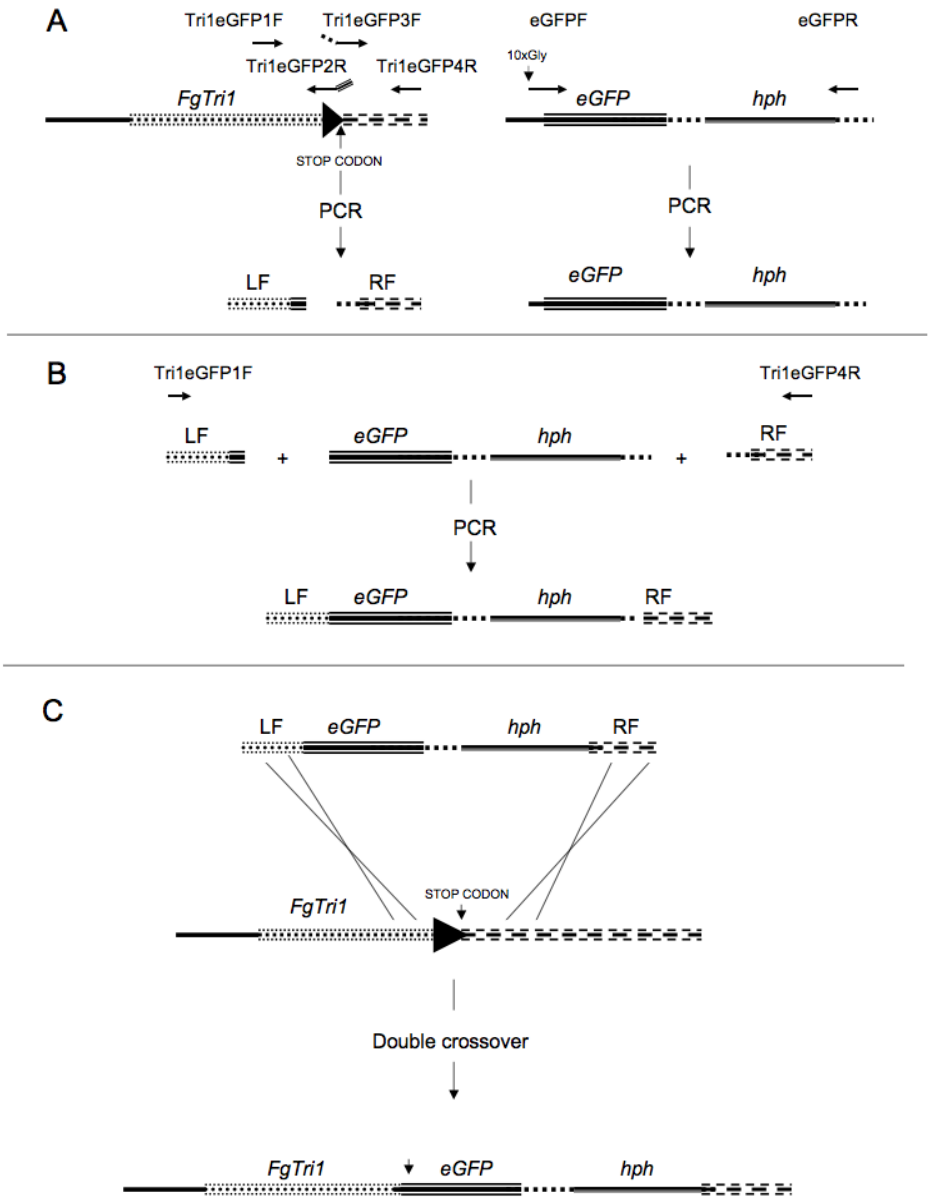

Figure 8. Synthesis of FgTri1p::eGFP fusion protein. A) T1eGFP1F + T1eGFP2R and Tri1eGFP3F + Tri1eGFP4R oligonucleotide combinations are used to amplify the 5' and 3' regions flanking the *Tri12* stop codon via PCR. The *eGFPhph* construct is amplified with eGFPF and eGFPR oligonucleotides. Tri1eGFP2R and Tri1eGFP3F oligonucleotides possess sequences specific to the 5' and 3' ends of the e*GFPhph* construct. B) RF, LF, and e*GFPhph* constructs and T12eGFP1F and T12eGFP4R oligonucleotides are used to generate a LF::e*GFPhph*::RF fusion construct. C) Transformation of PH-1 protoplasts with LF::e*GFPhph*::RF fusion construct results in eGFP tagging of the carboxy terminus of FgTri1p .

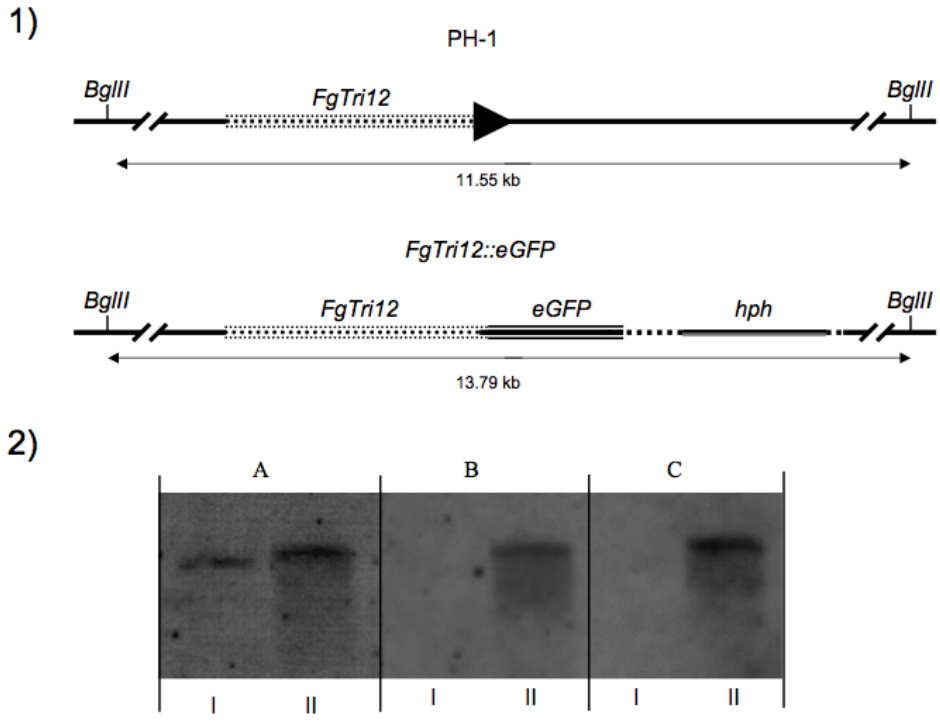

Figure 9. Southern blotting of genomic DNA from PH-1 and *FgTri12::eGFP*. 1) Location of *BglII* restriction enzyme cut sites in PH-1 and *FgTri12::eGFP* and the expected size of the fragment targeted by hybridization probes. 2) Hybridization of A) *Tri12,* B) *hph,* and C) *eGFP* specific probes to digested genomic DNA from I) PH-1 and II) *FgTri12::eGFP*. These results demonstrate the presence of single copies of *FgTri12* in PH-1 and *FgTri12::eGFP* and a single copy of *hph* and eGFP in *FgTri12::eGFP.* The relative sizes of the fragments labeled with the *Tri12* probe in PH-1 and *FgTri12::eGFP* are consistent with expected digestion patterns.

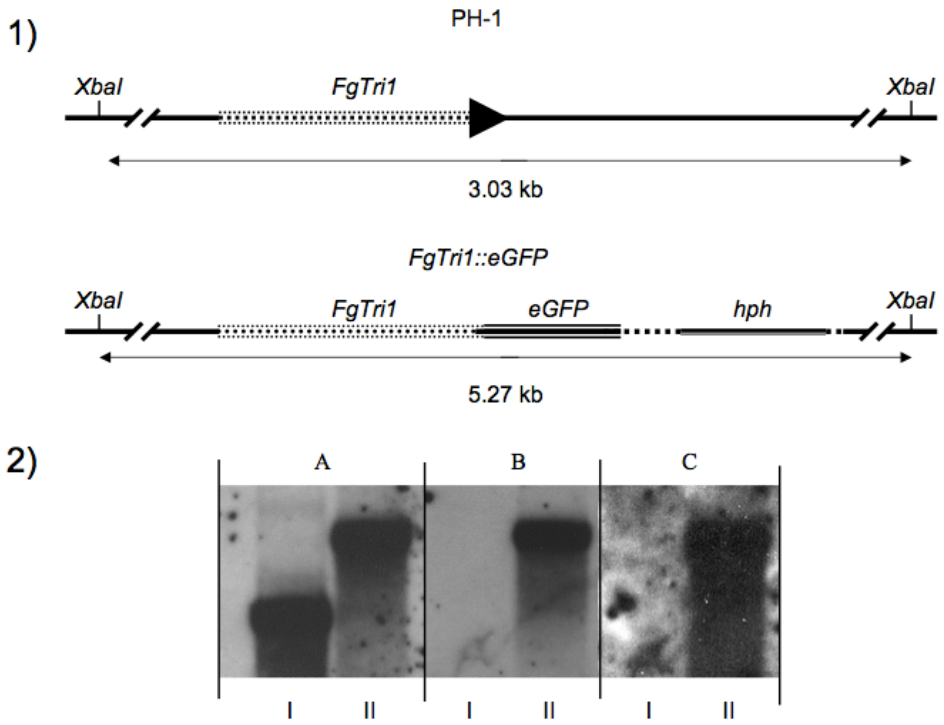

Figure 10. Southern blotting of genomic DNA from PH-1 and *FgTri1::eGFP*. 1) Location of *XbaI* restriction enzyme cut sites in PH-1 and *FgTri1::eGFP* and the expected size of the fragment targeted by hybridization probes. 2) Hybridization of A) *Tri1,* B) *hph,* and C) *eGFP* specific probes to digested genomic DNA from I) PH-1 and II) *FgTri1::eGFP*. These results demonstrate the presence of single copies of *FgTri12* in PH-1 and *FgTri1::eGFP* and a single copy of *hph* and eGFP in *FgTri1::eGFP.* The relative sizes of the fragments labeled with the *Tri12* probe in PH-1 and *FgTri1::eGFP* are consistent with expected digestion patterns.

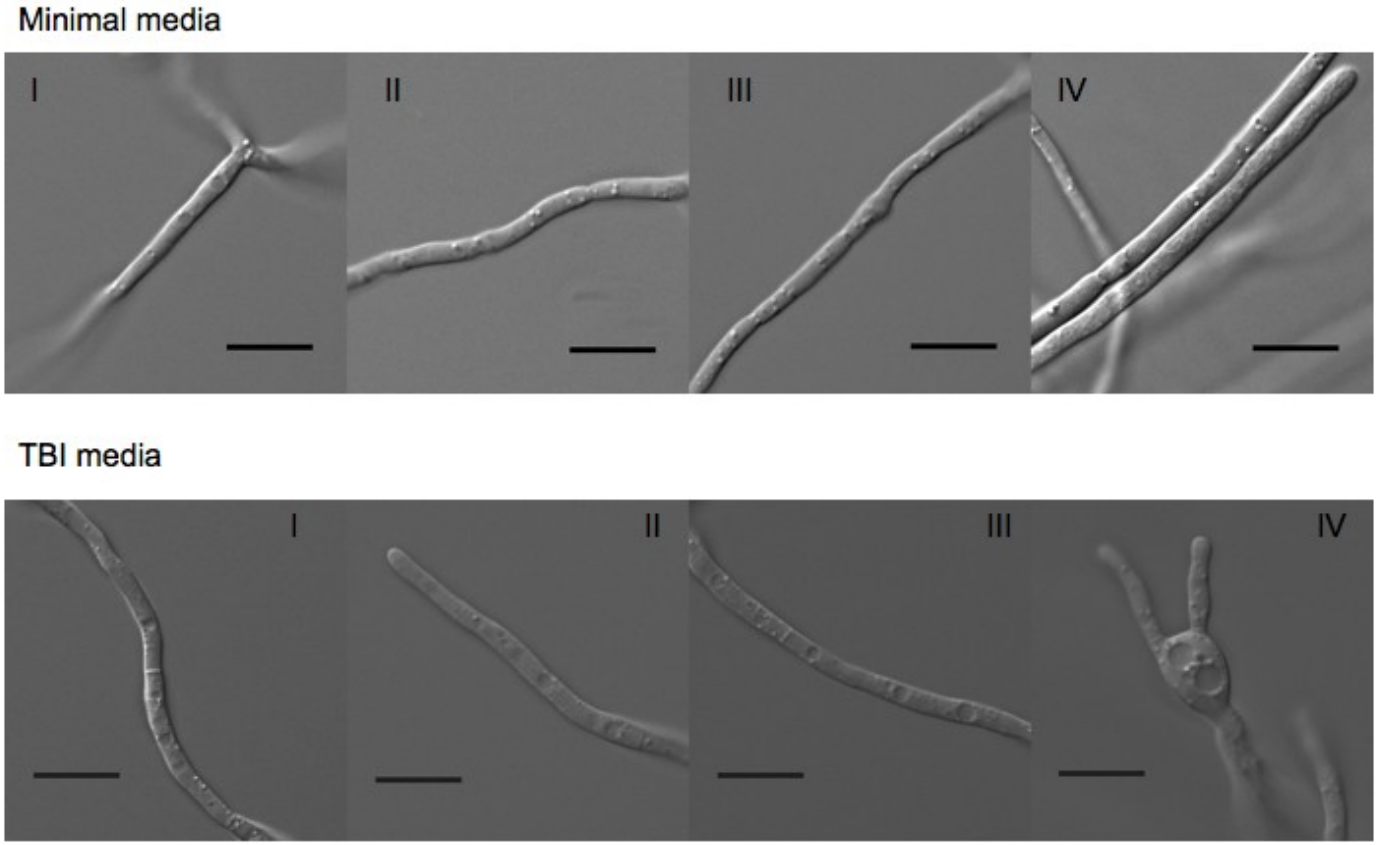

Figure 11. Morphology of *F. graminearum* mycelia grown in liquid minimal medium (top) or TBI medium (bottom). DIC images were taken at I) 12 hours, II) 18 hours, III) 24 hours, and IV) 36 hours after cultures were inoculated with fresh macroconidia. Shaken cultures (150 rpm) were incubated in total darkness at 25˚C. Scale bar = 10 µm.

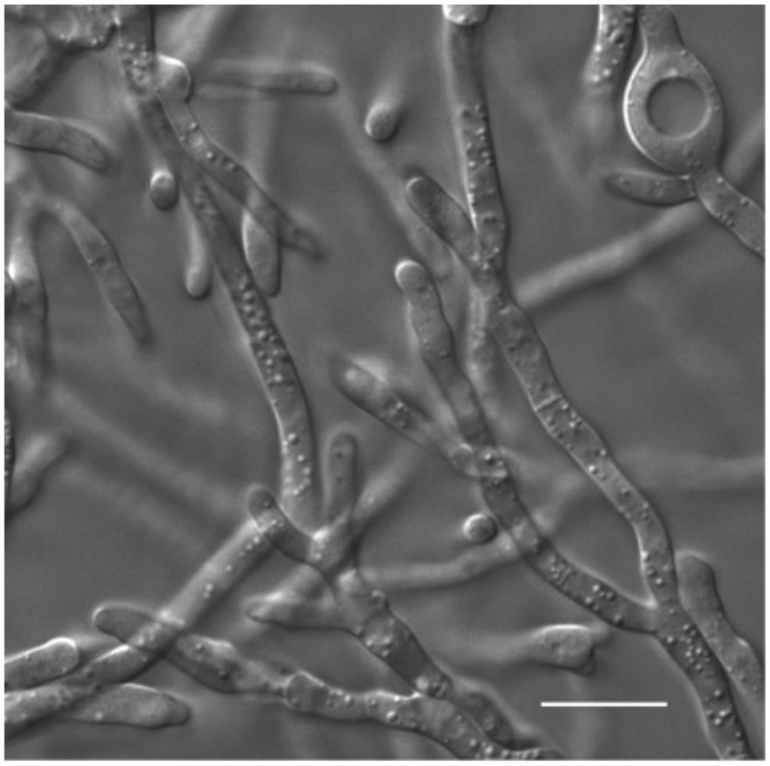

Figure 12. Coralloid morphology of *F. graminearum* hyphae grown in TBI medium. DIC image of cells was taken 36 hours after culture was inoculated with fresh conidia. Shaken cultures (150 rpm) were incubated in total darkness at 25˚C. Scale bar = 10 μm.

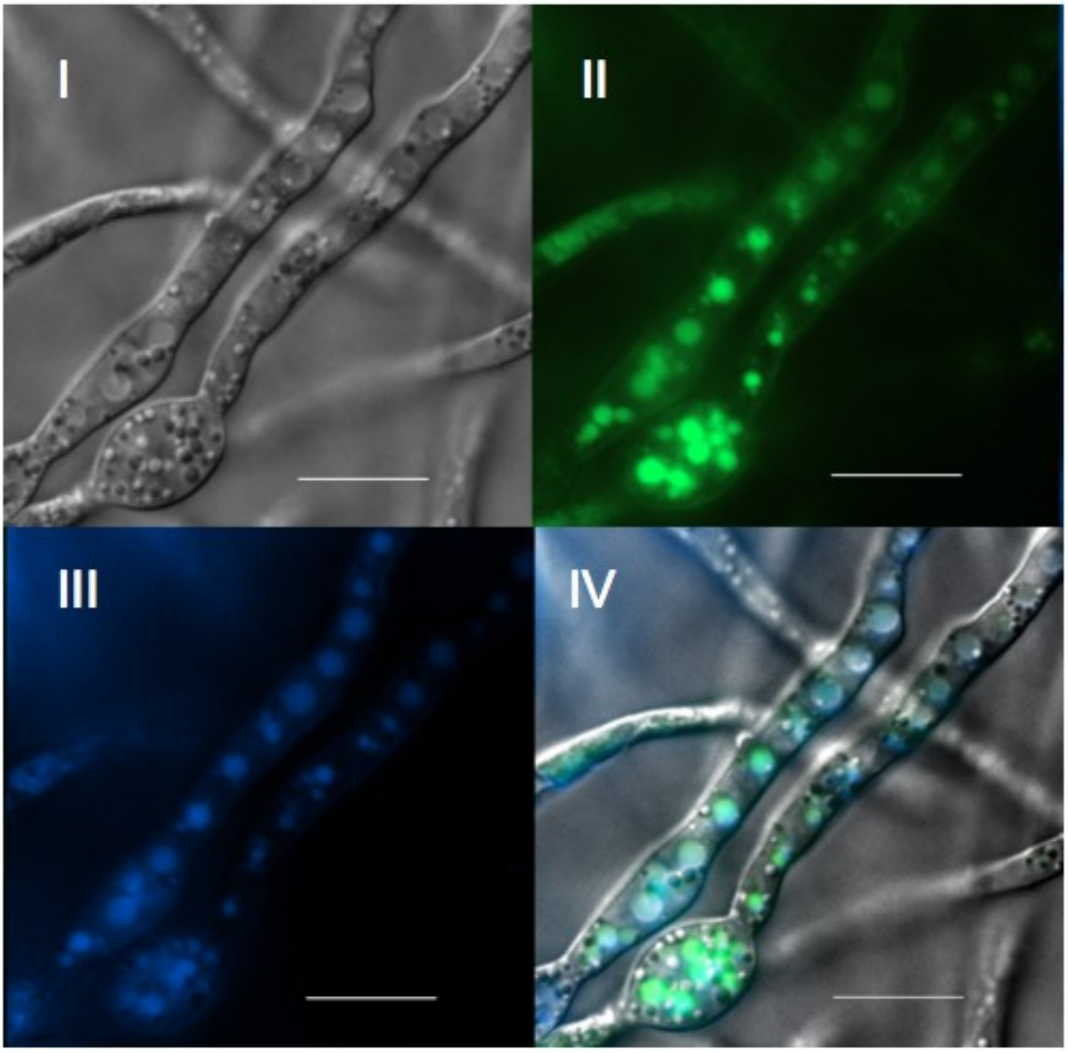

Figure 13. CMAC stained vacuoles and late endosomes in *FgTri12::eGFP* cells from TBI cultures. I) DIC, II) GFP, III) CMAC, and IV) CMAC/GFP/DIC layered images taken after 42 hours of incubation at 28˚ C in total darkness. Scale bar = 10µm.

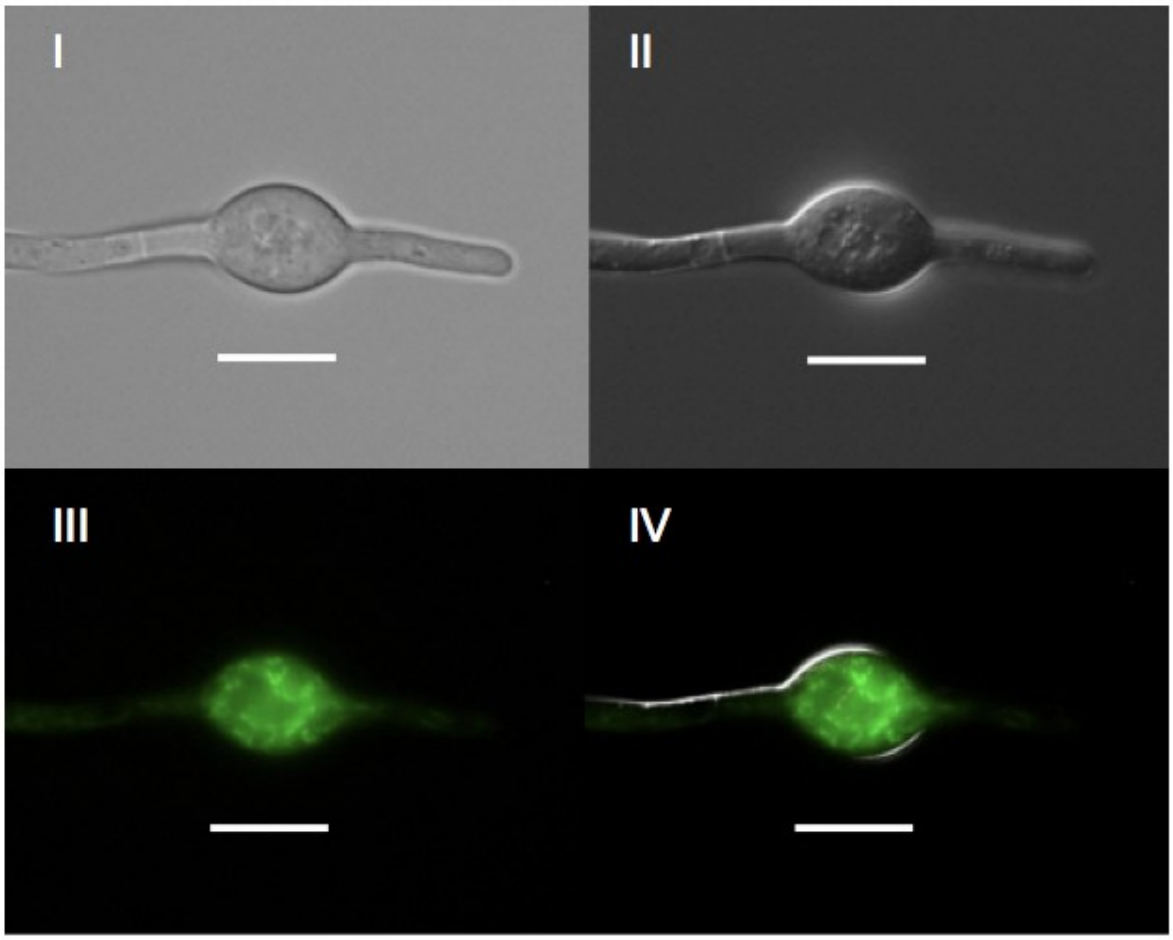

Figure 14. Cell morphology and localization of FgTri12p::eGFP to the subapical ovoid portion of an advancing hypha in TBI liquid culture after 18 hours of incubation at 28˚C in total darkness.. I) Bright field, II) DIC, III) GFP, and IV) DIC/GFP overlay images. Scale bar = 10µm.

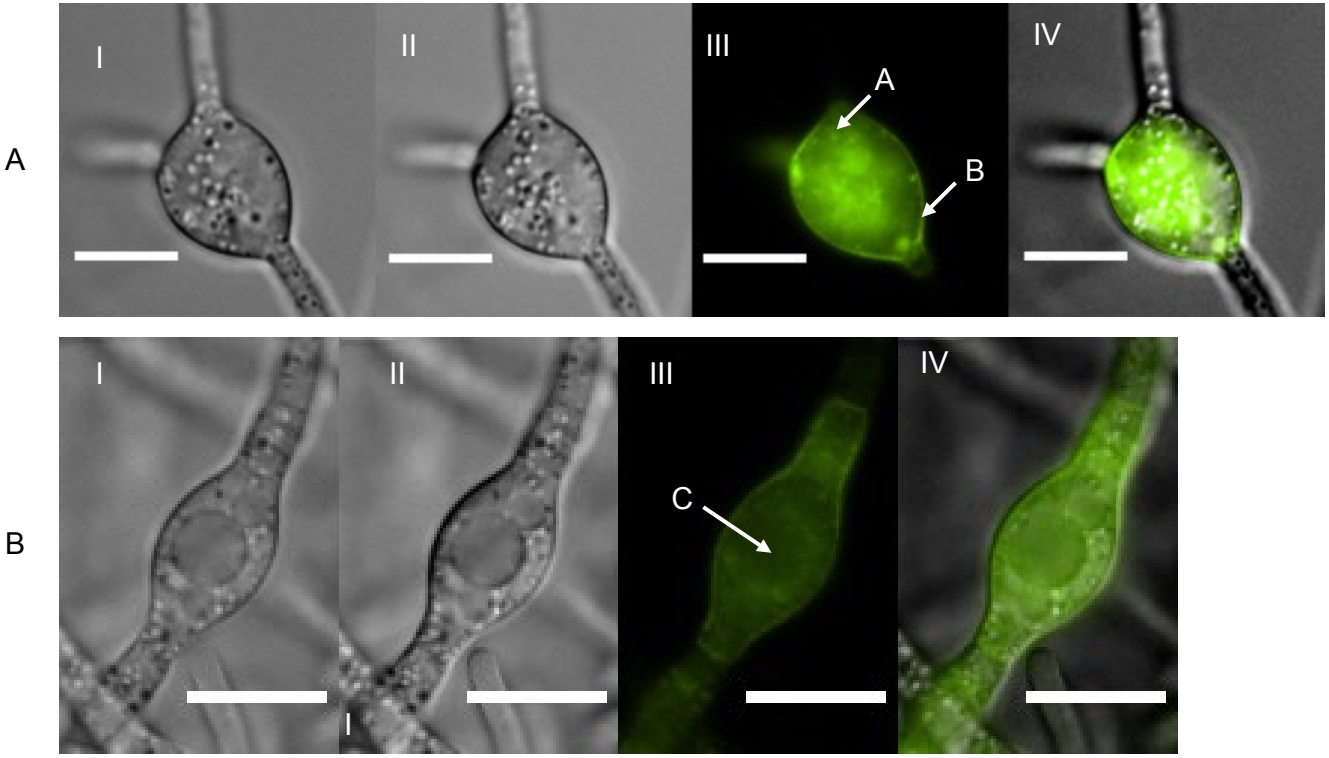

Figure 15. Cell morphology and FgTri12p::eGFP localization in TBI liquid culture after 24 hours of incubation at 28˚C in total darkness. I) Bright field, II) DIC, III) GFP, and IV) GFP/DIC overlay images of A) a swollen ovoid region of a cell near an advancing hyphal strand and B) swollen ovoid region of a cell within a mature hyphal strand. FgTri12p::eGFP localizes to a) motile organelles and b) the plasma membrane, but not to c) vacuoles of single early and mature ovoid cells.

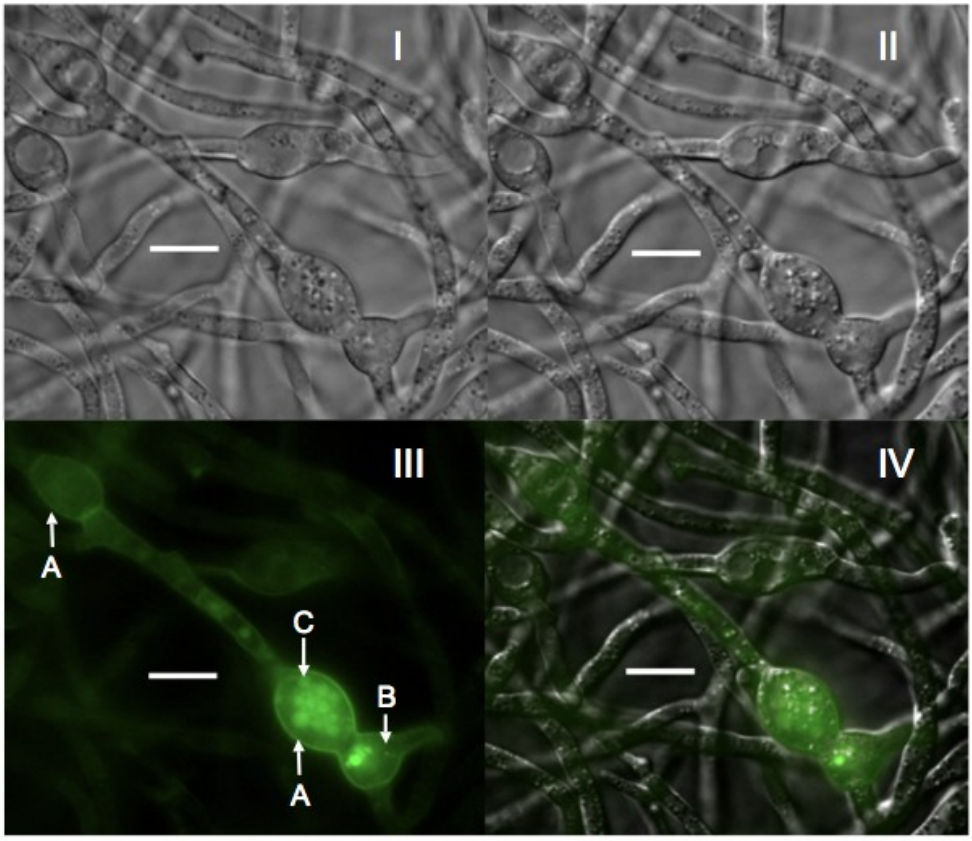

Figure 16. Cell morphology and FgTri12p::eGFP localization among contiguous cells in TBI liquid culture after 24 hours of incubation at 28˚C in total darkness. I) Bright field, II) DIC, III) GFP, and IV) GFP/DIC overlay images of four contiguous cells demonstrate sequential localization of FgTri12p::eGFP to the A) plasma membrane, B) motile organelles, and C) vacuoles. This suggests FgTri12::eGFP is transported from the plasma membrane to the vacuole. Scale bar = 10 μm.

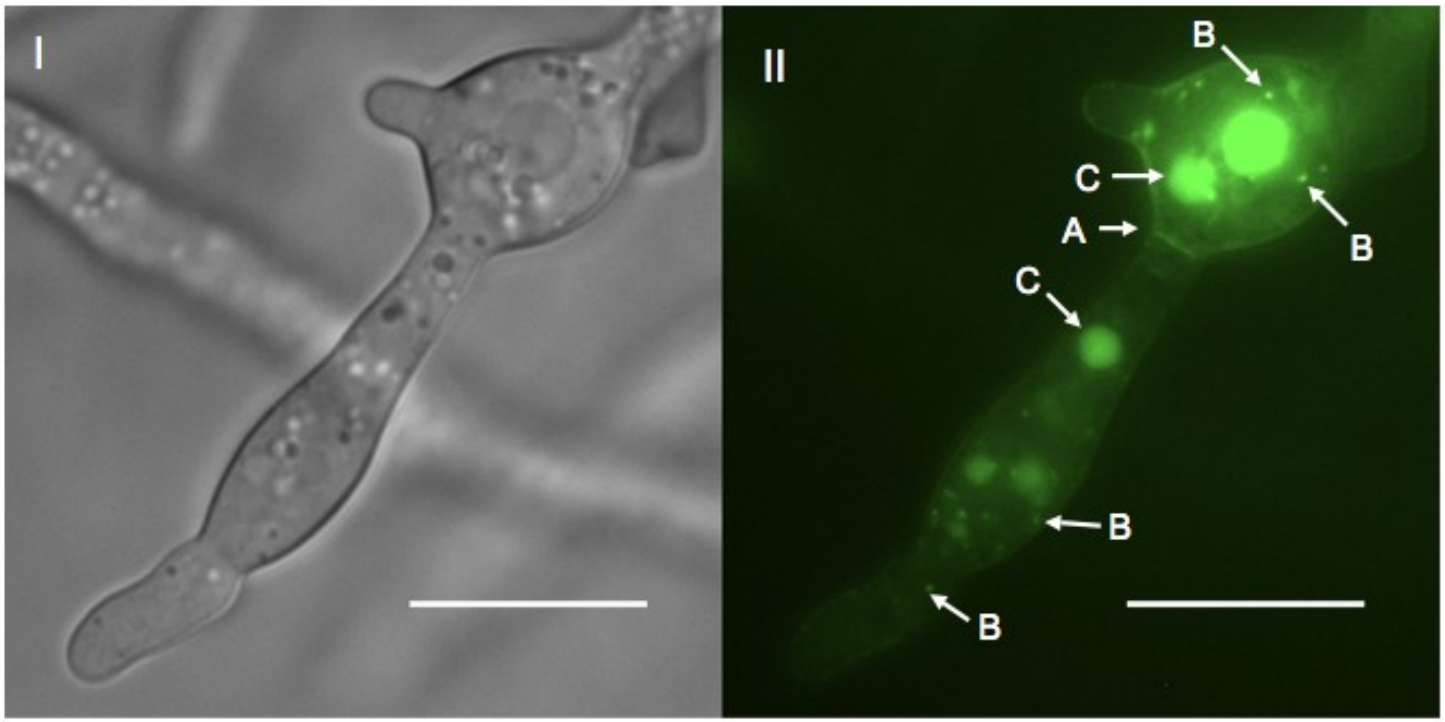

Figure 17. Hyphal morphology and FgTri12p::eGFP localization in TBI liquid culture after 30 hours of incubation at 28˚C in total darkness. I) Bright field and II) GFP images of mature ovoid cells and adjacent cells demonstrate that FgTri12p::eGFP localizes to the A) plasma membrane, B) motile organelles, and C) vacuoles. Evidence of the motility of these organelles can be observed in supplemental video 4. Scale bar = 10µm.

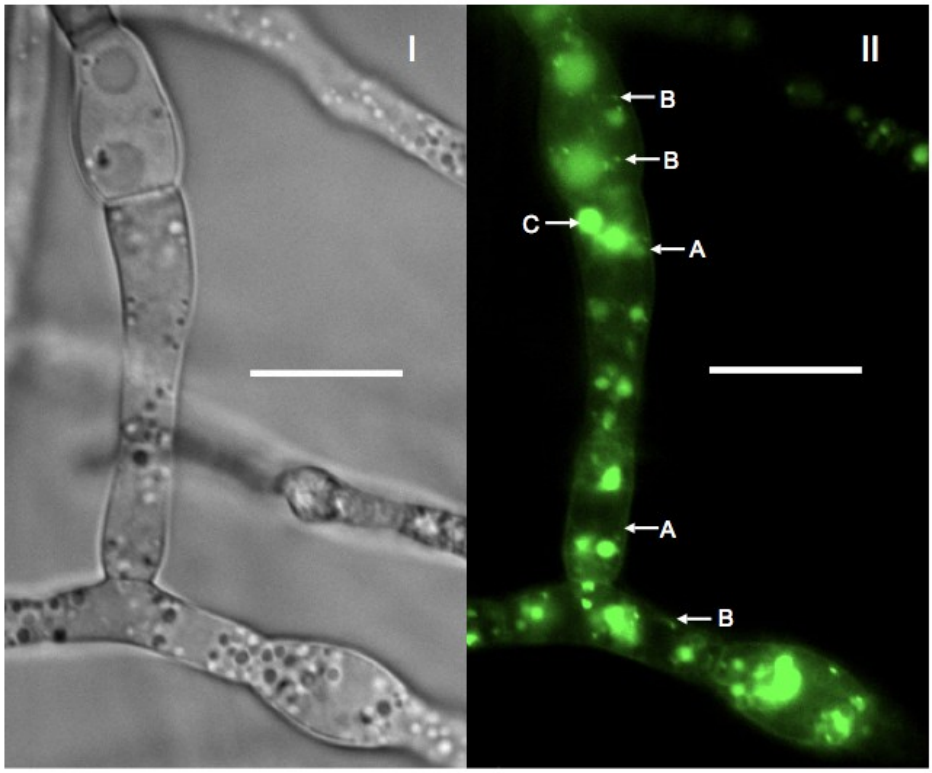

Figure 18. Hyphal morphology and FgTri12p::eGFP localization in TBI liquid culture after 36 hours of incubation at 28˚C in total darkness. I) Bright field and II) GFP images of mature ovoid cells and adjacent cells demonstrate that FgTri12p::eGFP localizes to the A) plasma membrane, B) motile organelles, and C) vacuoles. Scale bar = 10µm.

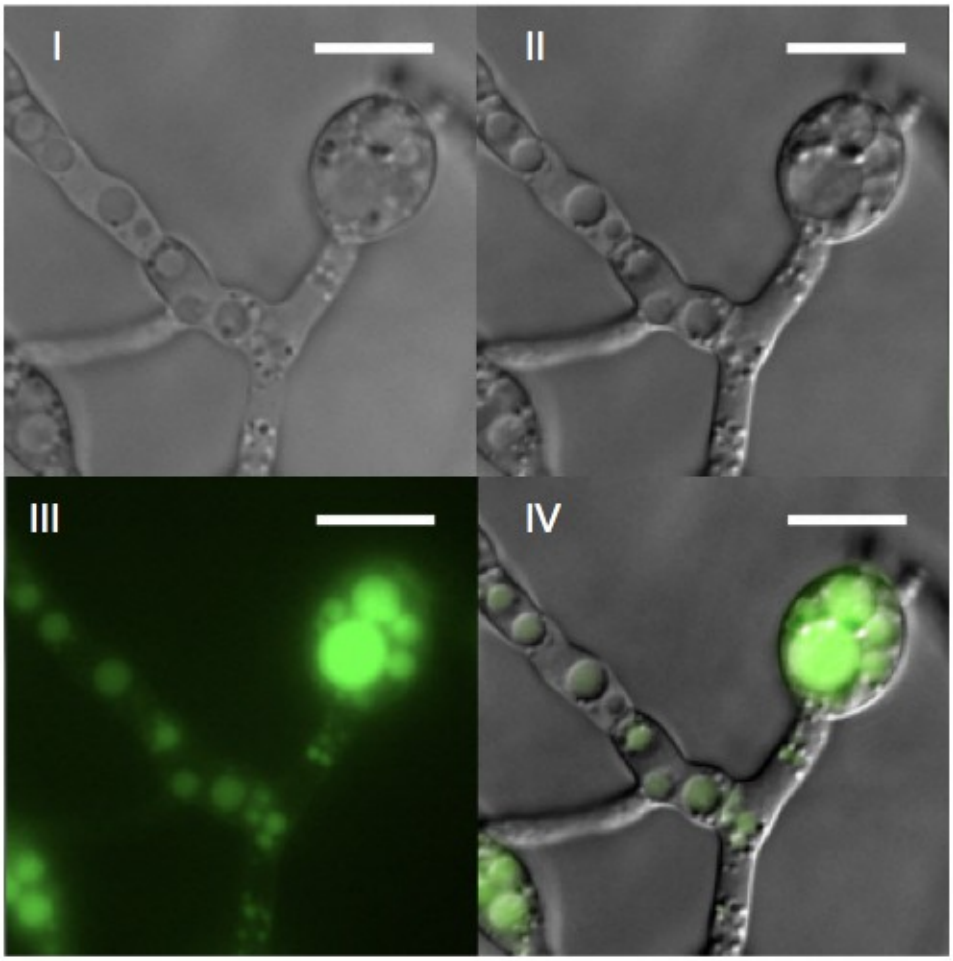

Figure 19. Hyphal morphology and FgTri12p::eGFP localization in TBI liquid culture after 42 hours of incubation at 28˚C in total darkness. I) Bright field, II) DIC, III) GFP, and IV) GFP/DIC overlay images of mature ovoid cells and adjacent cells demonstrate that FgTri12p::eGFP localizes to vacuoles of various sizes. Scale bar = 10µm.

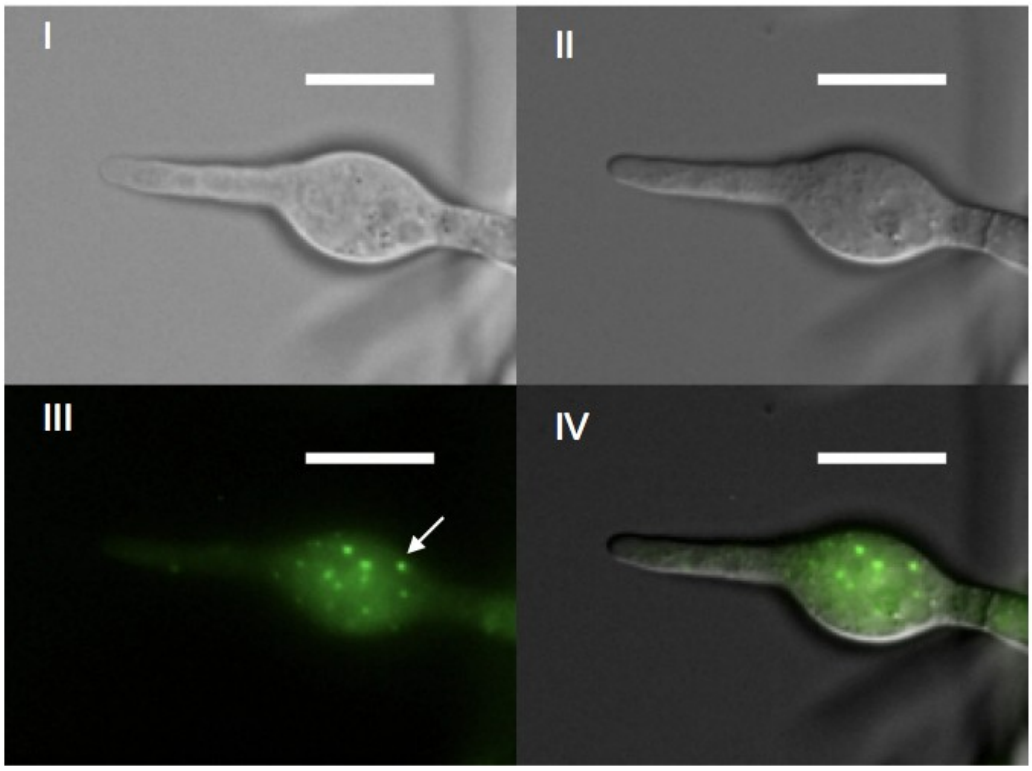

Figure 20. Cell morphology and localization of FgTri1p::eGFP to a swollen ovoid region of an advancing hyphal strand. I) Bright field, II) DIC, III) GFP, and IV) DIC/GFP overlay images of cells in TBI liquid culture were taken after 18 hours of incubation at 28˚C in total darkness. The white arrow denotes localization of FgTri1p::eGFP to one of several motile organelles. Scale bar = 10µm.

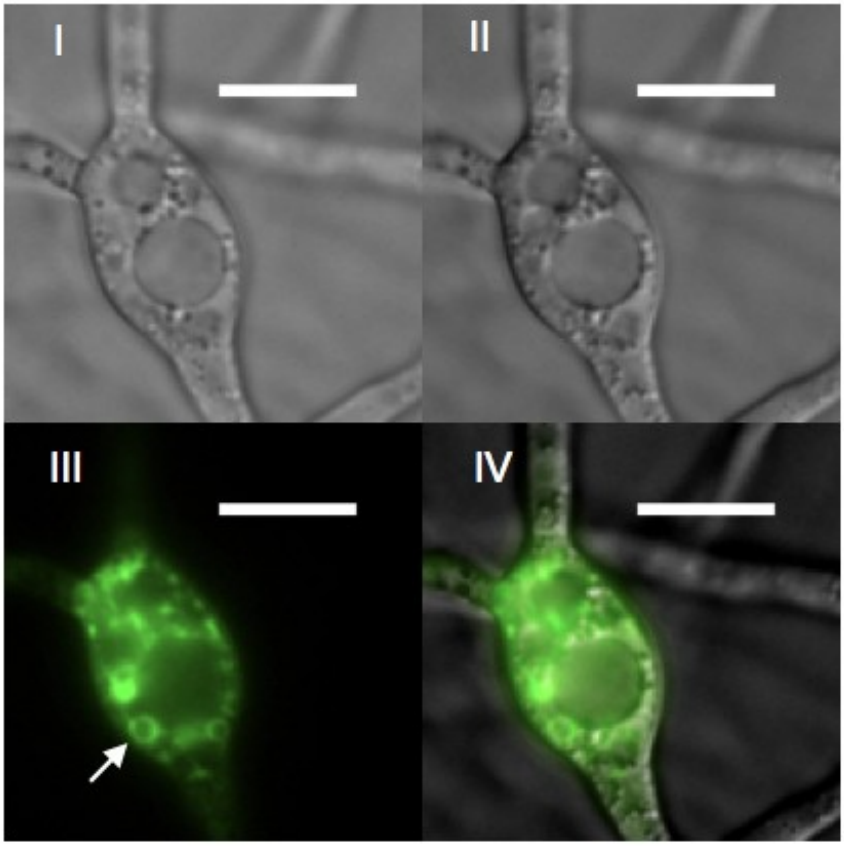

Figure 21. Cell morphology and localization of FgTri1p::eGFP to swollen ovoid region of a mature hyphal strand in TBI liquid culture. I) Bright field, II) DIC, III) GFP, and IV) DIC/GFP overlay images of cells in TBI liquid culture were taken after 25 hours of incubation at 28˚C in total darkness. The white arrow denotes localization of FgTri1p::eGFP to the periphery of stationary organelles.

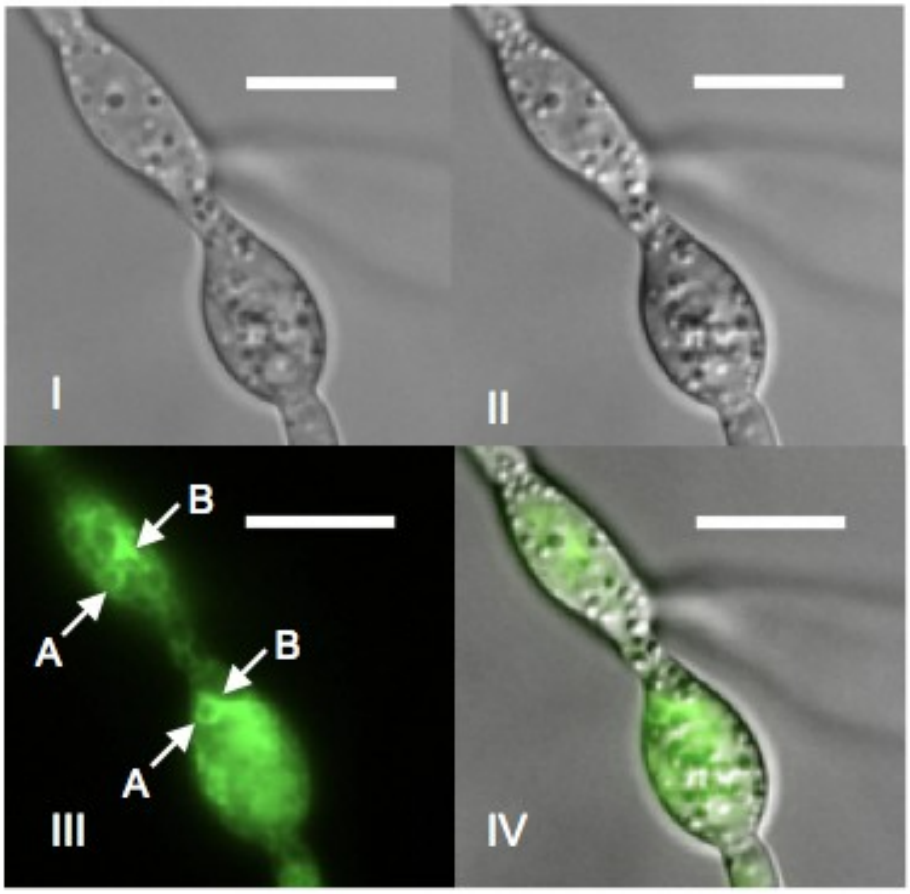

Figure 22. Cell morphology and localization of FgTri1p::eGFP within a mature hyphal strand in TBI liquid culture after 30 hours of incubation at 28˚C in total darkness. I) Bright field and II) DIC demonstrate cell morphology, while III) GFP and IV) DIC/GFP overlay images demonstrate the localization of FgTri1p::eGFP to A) the periphery of stationary organelles and B) intracellular membranous structures. Scale bar = 10μm.

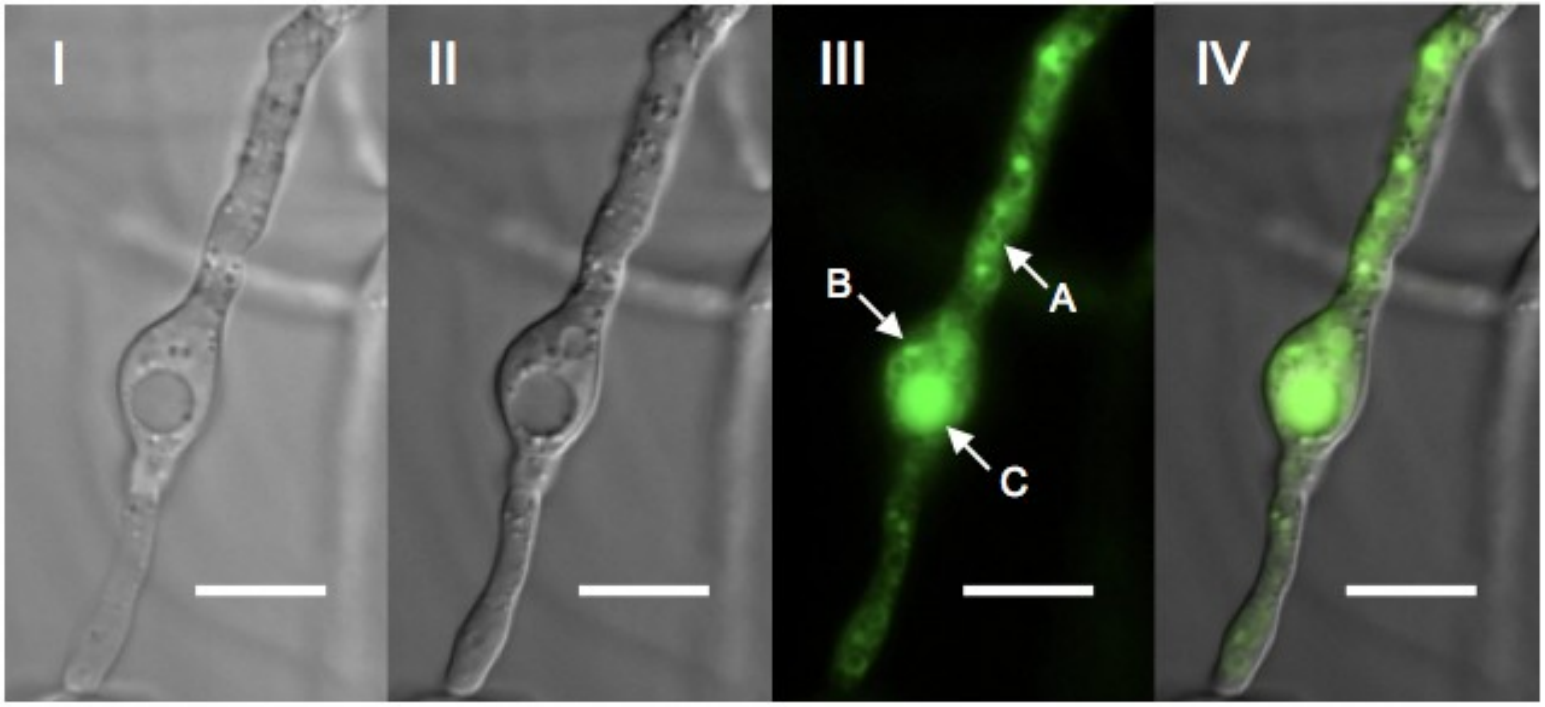

Figure 23. Cell morphology and localization of FgTri1p::eGFP within a mature hyphal strand in TBI liquid culture after 36 hours of incubation at 28˚C in total darkness. I) Bright field and II) DIC images demonstrate cell morphology, while III) GFP and IV) DIC/GFP overlay images demonstrate the localization of FgTri1p::eGFP to A) the periphery of stationary organelles, B) intracellular membranous structures, and C) vacuoles. Scale bar = 10µm.

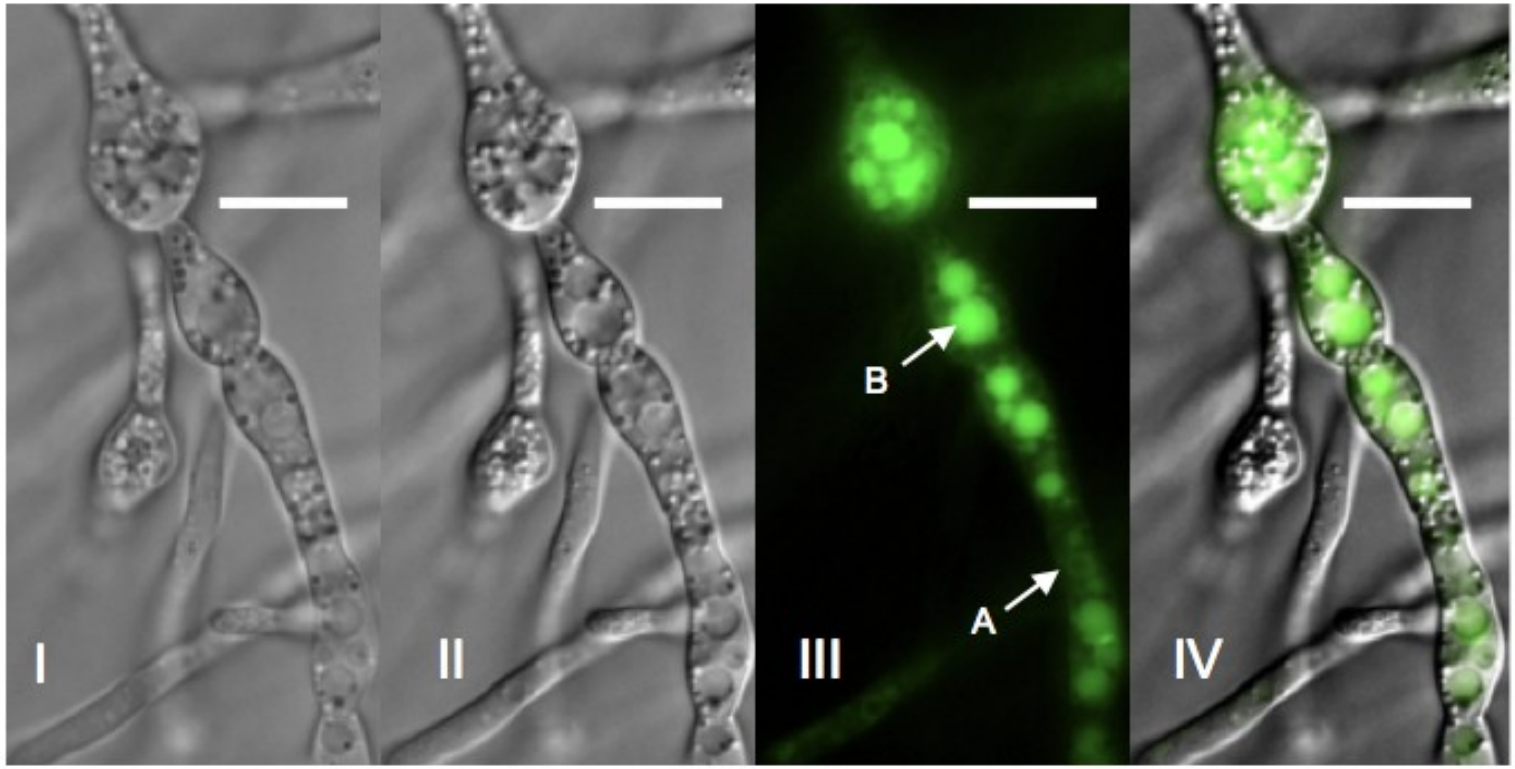

Figure 24. Cell morphology and localization of FgTri1p::eGFP within a mature hyphal strand in TBI liquid culture after 34 hours of incubation at 28˚C in total darkness.. I) Bright field and II) DIC images demonstrate cell morphology, while III) GFP and IV) DIC/GFP overlay images demonstrate the localization of FgTri1p::eGFP to A) the periphery of stationary organelles and B) vacuoles. Scale bar = 10µm.

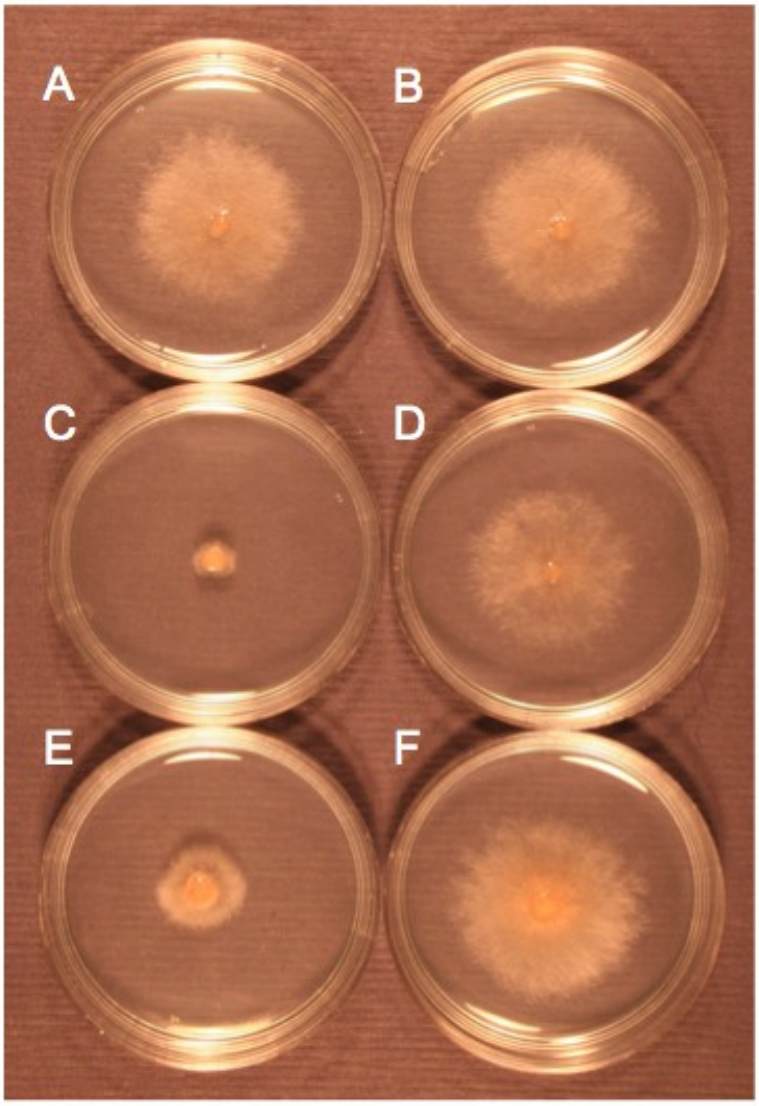

Figure 25. Radial growth of *FgTri12::eGFP* on recovery medium plates after overnight incubation at 25˚C. Cells were A) and B) untreated; C) treated with latruculin A for 1 hour; D) treated with DMSO; E and F) removed from treatment medium, washed with fresh TBI medium, and incubated for four hours before plating.

Supplemental Videos

Supplemental slow-motion video 1. FgTri12p::eGFP localizes to motile organelles in liquid TBI culture after 18 hours of incubation at 28˚C in total darkness (2 seconds:1 second).

Supplemental time-lapse video 2. FgTri12p::eGFP localizes to the plasma membrane and motile organelles, but not vacuoles of single early and mature ovoid cells after 25 hours of incubation at 28˚C in total darkness (1 second:42 seconds).

Supplemental time-lapse video 3. FgTri12p::eGFP localizes to the plasma membrane and multiple motile organelles, but not vacuoles of contiguous cells after 28 hours of incubation at 28˚C in total darkness (1 second:8.6 seconds).

Supplemental time-lapse video 4. FgTri12p::eGFP localizes to the plasma membrane, motile organelles, and vacuoles in shaking TBI liquid culture after 30 hours of incubation at 28˚C in total darkness (1 second:33.5 seconds).

Supplemental time-lapse video 5. FgTri12p::eGFP localizes to the plasma membrane, motile organelles, and vacuoles in TBI liquid culture after 36 hours of incubation at 28˚C in total darkness (1 second:33.2 seconds).

Supplemental time-lapse video 6. FgTri12p::eGFP localizes to the plasma membrane, motile organelles, and vacuoles in TBI liquid culture after 44 hours of incubation at 28˚C in total darkness (1 second:24.9 seconds).

Supplemental time-lapse video 7. FgTri1p::eGFP localizes to motile organelles in liquid TBI culture after 18 hours of incubation at 28˚C in total darkness (1 second:40.5 seconds).

Supplemental time-lapse video 8. FgTri1p::eGFP appears to localize in the periphery of small stationary circular structures (> 1μm), smaller motile structures, and the vacuole after 25 hours of incubation at 28˚C in total darkness (1 second:25.7 seconds).

Supplemental time-lapse video 9. FgTri1p::eGFP localizes in the periphery of small stationary circular structures (> 1μm), smaller motile structures, and the vacuole after 30 hours of incubation at 28˚C in total darkness (1 second:19.7 seconds).

Supplemental time-lapse video 10. The fusion of a FgTri12p::eGFP labeled small motile organelle with the plasma membrane.(1 second:22.1 seconds).

Supplemental time-lapse video 11. The fusion of a FgTri1p::eGFP labeled organelle with a larger stationary organelle (1 second:17.3 seconds).

Supplemental time-lapse video 12. FgTri12p::eGFP labeled motile organelles in cells after 36 hours of incubation at 28˚C in total darkness and before treatment with latrunculin A (1 second:23 seconds).

Supplemental time-lapse video 13. Absence of FgTri12p::eGFP labeled motile organelles in cells after treatment with latrunculin A for one hour (1 sec:10 seconds).

Supplemental time-lapse video 14. FgTri12p::eGFP labeled motile organelles in cells that were removed from latrunculin A medium, washed with TBI medium, and incubated in TBI medium for four hours (1 second::8.6 seconds).

References

Abenza, J. F., A. Pantazopoulou, J. M. Rodriguez, A. Galindo & M. A. Penalva, (2009) Long-distance movement of *Aspergillus nidulans* early endosomes on microtubule tracks. *Traffic* **10**: 57-75.

Alexander, N. J., S. P. McCormick & T. M. Hohn, (1999) Tri12, a trichothecene efflux pump from *Fusarium sporotrichioides*: gene isolation and expression in yeast. *Molecular and General Genetics* **261**: 977-984.

Baba, M., M. Osumi, S. V. Scott, D. J. Klionsky & Y. Ohsumi, (1997) Two distinct pathways for targeting proteins from the cytoplasm to the vacuole/lysosome. *Journal of Cell Biology* **139**: 1687-1695.

Bai, G. H., A. E. Desjardins & R. D. Plattner, (2002) Deoxynivalenol-nonproducing *Fusarium graminearum* causes initial infection, but does not cause disease spread in wheat spikes. *Mycopathologia* **153**: 91-98.

Boddu, J., S. Cho, W. M. Kruger & G. J. Muehlbauer, (2006) Transcriptome analysis of the barley-*Fusarium graminearum* interaction. *Molecular Plant-Microbe Interactions* **19**: 407-417.

Breakspear, A., K. J. Langford, M. Momany & S. J. Assinder, (2007) CopA : GFP localizes to putative Golgi equivalents in *Aspergillus nidulans*. *Fems Microbiology Letters* **277**: 90-97.

Brown, D. W., R. H. Proctor, R. B. Dyer & R. D. Plattner, (2003) Characterization of a Fusarium 2-gene cluster involved in trichothecene C-8 modification. *Journal of Agricultural and Food Chemistry* **51**: 7936-7944.

Brown, N. A., M. Urban, A. M. L. Van De Meene & K. E. Hammond-Kosack, (2010) The infection biology of *Fusarium graminearum*: Defining the pathways of spikelet to spikelet colonisation in wheat ears. *Fungal Biology* **114**: 555-571.

Callahan, T. M., M. S. Rose, M. J. Meade, M. Ehrenshaft & R. G. Upchurch, (1999) CFP, the putative cercosporin transporter of *Cercospora kikuchii*, is required for wild-type cercosporin production, resistance, and virulence on soybean. *Molecular Plant-Microbe Interactions* **12**: 901-910.

Catlett, N.L., B.N. Lee, O.C.Yoder, & B.G. Turgeon, (2003) Split-marker recombination for efficient targeted deletion of fungal genes. *Fungal Genetics News* 50, 9–11.

Chanda, A., L. V. Roze, S. Kang, K. A. Artymovich, G. R. Hicks, N. V. Raikhel, A. M. Calvo & J. E. Linz, (2009) A key role for vesicles in fungal secondary

metabolism. *Proceedings of the National Academy of Sciences of the United States of America* **106**: 19533-19538.

Chanda, A., L. V. Roze & J. E. Linz, (2010) A possible role for exocytosis in aflatoxin export in *Aspergillus parasiticus*. *Eukaryotic Cell* **9**: 1724-1727.

Chang, P. K., J. J. Yu & J. H. Yu, (2004) *aflT*, a MFS transporter-encoding gene located in the aflatoxin gene cluster, does not have a significant role in aflatoxin secretion. *Fungal Genetics and Biology* **41**: 911-920.

Correll, J.C., C.J.R Klittich & J.F. Leslie, (1987) Nitrate non-utilizing mutants of *Fusarium oxysporum* and their use in vegetative compatibility tests. *Phytopathology* **77**: 1640-1646.

Cuomo, C. A., U. Güldener, J. R. Xu, F. Trail, B. G. Turgeon, A. Di Pietro, J. D. Walton, *et al.* (2007) The *Fusarium graminearum* genome reveals a link between localized polymorphism and pathogen specialization. *Science* **317**: 1400-1402.

Emanuelsson, O., S. Brunak, G. von Heijne & H. Nielsen, (2007) Locating proteins in the cell using TargetP, SignalP and related tools. *Nature Protocols* **2**: 953-971.

Fleissner, A., C. Sopalla & K. M. Weltring, (2002) An ATP-binding cassette multidrug-resistance transporter is necessary for tolerance of *Gibberella pulicaris* to phytoalexins and virulence on potato tubers. *Molecular Plant-Microbe Interactions* **15**: 102-108.

Gardiner, D. M., K. Kazan & J. M. Manners, (2009a) Novel genes of *Fusarium graminearum* that negatively regulate deoxynivalenol production and virulence. *Molecular Plant-Microbe Interactions* **22**: 1588-1600.

Gardiner, D. M., K. Kazan & J. M. Manners, (2009b) Nutrient profiling reveals potent inducers of trichothecene biosynthesis in *Fusarium graminearum*. *Fungal Genetics and Biology* **46**: 604-613.

Gardiner, D. M., K. Kazan, S. Praud, F. J. Torney, A. Rusu & J. M. Manners, (2010a) Early activation of wheat polyamine biosynthesis during Fusarium head blight implicates putrescine as an inducer of trichothecene mycotoxin production. *Bmc Plant Biology* **10**: 13.

Gardiner, S. A., J. Boddu, F. Berthiller, C. Hametner, R. M. Stupar, G. Adam & G. J. Muehlbauer, (2010b) Transcriptome analysis of the barley-deoxynivalenol interaction: evidence for a role of glutathione in deoxynivalenol detoxification. *Molecular Plant-Microbe Interactions* **23**: 962-976.

Goswami, R. S. & H. C. Kistler, (2005) Pathogenicity and *in planta* mycotoxin accumulation among members of the *Fusarium graminearum* species complex on wheat and rice. *Phytopathology* **95**: 1397-1404.

Goswami, R. S., J. R. Xu, F. Trail, K. Hilburn & H. C. Kistler, (2006) Genomic analysis of host-pathogen interaction between *Fusarium graminearum* and wheat during early stages of disease development. *Microbiology* **152**: 1877-1890.

Güldener, U., G. Mannhaupt, M. Munsterkotter, D. Haase, M. Oesterheld, V. Stumpflen, H. W. Mewes & G. Adam, (2006) FGDB: a comprehensive fungal genome resource on the plant pathogen *Fusarium graminearum*. *Nucleic Acids Research* **34**: D456-D458.

Hollingsworth, C. R., C. D. Motteberg, J. V. Wiersma & L. M. Atkinson, (2008) Agronomic and economic responses of spring wheat to management of Fusarium head blight. *Plant Disease* **92**: 1339-1348.

Honda, S. & E. U. Selker, (2009) Tools for fungal proteomics: multifunctional neurospora vectors for gene replacement, protein expression and protein purification. *Genetics* **182**: 11-23.

Hong, S. Y. & J. E. Linz, (2008) Functional expression and subcellular localization of the aflatoxin pathway enzyme Ver-1 fused to enhanced green fluorescent protein. *Applied and Environmental Microbiology* **74**: 6385-6396.

Hong, S. Y. & J. E. Linz, (2009) Functional expression and sub-cellular localization of the early aflatoxin pathway enzyme Nor-1 in *Aspergillus parasiticus*. *Mycological Research* **113**: 591-601.

Hong, S. Y., J. So, J. Lee, K. Min, H. Son, C. Park, S. H. Yun & Y. W. Lee, (2010) Functional analyses of two syntaxin-like SNARE genes, *GzSYN1* and *GzSYN2*, in the ascomycete *Gibberella zeae*. *Fungal Genetics and Biology* **47**: 364-372.

Hou, Z. M., C. Y. Xue, Y. L. Peng, T. Katan, H. C. Kistler & J. R. Xu, (2002) A mitogen-activated protein kinase gene (MGV1) in *Fusarium graminearum* is required for female fertility, heterokaryon formation, and plant infection. *Molecular Plant-Microbe Interactions* **15**: 1119-1127.

Hubbard, M. A. & S. G. W. Kaminskyj, (2008) Rapid tip-directed movement of Golgi equivalents in growing *Aspergillus nidulans* hyphae suggests a mechanism for delivery of growth-related materials. *Microbiology* **154**: 1544-1553.

Ilgen, P., B. Hadeler, F. J. Maier & W. Schafer, (2009) Developing kernel and rachis node induce the trichothecene pathway of *Fusarium graminearum* during wheat head infection. *Molecular Plant-Microbe Interactions* **22**: 899-908.

Jansen, C., D. von Wettstein, W. Schafer, K. H. Kogel, A. Felk & F. J. Maier, (2005) Infection patterns in barley and wheat spikes inoculated with wild-type and trichodiene synthase gene disrupted *Fusarium graminearum*. *Proceedings of the National Academy of Sciences of the United States of America* **102**: 16892-16897.

Kim, J. E., H. J. Lee, J. Lee, K. W. Kim, S. H. Yun, W. B. Shim & Y. W. Lee, (2009) *Gibberella zeae* chitin synthase genes, *GzCHS5* and *GzCHS7*, are required for hyphal growth, perithecia formation, and pathogenicity. *Current Genetics* **55**: 449-459.

Kimura, M., T. Tokai, K. O'Donnell, T. J. Ward, M. Fujimura, H. Hamamoto, T. Shibata & I. Yamaguchi, (2003) The trichothecene biosynthesis gene cluster of *Fusarium graminearum* F15 contains a limited number of essential pathway genes and expressed non-essential genes. *FEBS Letters* **539**: 105-110.

Kimura, M., T. Tokai, N. Takahashi-Ando, S. Ohsato & M. Fujimura, (2007) Molecular and genetic studies of Fusarium trichothecene biosynthesis: Pathways, genes, and evolution. *Bioscience Biotechnology and Biochemistry* **71**: 2105-2123.

Kuratsu, M., A. Taura, J. Shoji, S. Kikuchi, M. Arioka & K. Kitamoto, (2007) Systematic analysis of SNARE localization in the filamentous fungus *Aspergillus oryzae*. *Fungal Genetics and Biology* **44**: 1310-1323.

Kusano, T., T. Berberich, C. Tateda & Y. Takahashi, (2008) Polyamines: essential factors for growth and survival. *Planta* **228**: 367-381.

Lee, L. W., C. H. Chiou, K. L. Klomparens, J. W. Cary & J. E. Linz, (2004) Subcellular localization of aflatoxin biosynthetic enzymes Nor-1, Ver-1, and OmtA in time-dependent fractionated colonies of *Aspergillus parasiticus*. *Archives of Microbiology* **181**: 204-214.

Lee, S. C. & B. D. Shaw, (2008) Localization and function of ADP ribosylation factor ArfA in *Aspergillus nidulans*. *Fems Microbiology Letters* **283**: 216-222.

Lendenfeld, T., D. Ghali, M. Wolschek, E. M. Kubicekpranz & C. P. Kubicek, (1993) Subcellular compartmentation of penicillin biosynthesis in *Penicillium chrysogenum* - the amino-acid precursors are derived from the vacuole. *Journal of Biological Chemistry* **268**: 665-671.

Lipschutz, J. H. & K. E. Mostov, (2002) Exocytosis: The many masters of the Exocyst. *Current Biology* **12**: R212-R214.

Maggio-Hall, L. A., R. A. Wilson & N. P. Keller, (2005) Fundamental contribution of beta-oxidation to polyketide mycotoxin production *in planta*. *Molecular Plant-Microbe Interactions* **18**: 783-793.

McCormick, S. P., L. J. Harris, N. J. Alexander, T. Ouellet, A. Saparno, S. Allard & A. E. Desjardins, (2004) *Tri1* in *Fusarium graminearum* encodes a P450 oxygenase. *Applied and Environmental Microbiology* **70**: 2044-2051.

McDaniel, D. P. & R. W. Robertson, (2000) Microtubules are required for motility and positioning of vesicles and mitochondria in hyphal tip cells of *Allomyces macrogynus*. *Fungal Genetics and Biology* **31**: 233-244.

McMullen, M., R. Jones & D. Gallenberg, (1997) Scab of wheat and barley: A re-emerging disease of devastating impact. *Plant Disease* **81**: 1340-1348.

Meijer, W. H., L. Gidijala, S. Fekken, J. Kiel, M. A. van den Berg, R. Lascaris, R. A. L. Bovenberg & I. J. van der Klei, (2010) Peroxisomes are required for efficient penicillin biosynthesis in *Penicillium chrysogenum*. *Applied and Environmental Microbiology* **76**: 5702-5709.

Müller, W. H., R. A. L. Bovenberg, M. H. Groothuis, F. Kattevilder, E. B. Smaal, L. H. M. Vandervoort & A. J. Verkleij, (1992) Involvement of microbodies in penicillin biosynthesis. *Biochimica et Biophysica Acta* **1116**: 210-213.

Nakaune, R., H. Hamamoto, J. Imada, K. Akutsu & T. Hibi, (2002) A novel ABC transporter gene, *PMR5*, is involved in multidrug resistance in the phytopathogenic fungus *Penicillium digitatum*. *Molecular Genetics and Genomics* **267**: 179-185.

Needleman S. B. & C. D.Wunsch, (1970) A general method applicable to the search for similarities in the amino acid sequences of two proteins. *Journal of Molecular Biology* 48: 443-453.

Nielsen, H., and A Krogh, (1998) Prediction of signal peptides and signal anchors by a hidden Markov model. In *Proceedings of the Sixth International Conference on Intelligent Systems for Molecular Biology (ISMB 6)*. Menlo Park, CA: AAAI Press, pp. 122–130.

Pantazopoulou, A. & M. A. Penalva, (2009) Organization and dynamics of the *Aspergillus nidulans* Golgi during apical extension and mitosis. *Molecular Biology of the Cell* **20**: 4335-4347.

Pitkin, J. W., D. G. Panaccione & J. D. Walton, (1996) A putative cyclic peptide efflux pump encoded by the *ToxA* gene of the plant-pathogenic fungus *Cochliobolus carbonum*. *Microbiology-Uk* **142**: 1557-1565.

Pritsch, C., G. J. Muehlbauer, W. R. Bushnell, D. A. Somers & C. P. Vance, (2000) Fungal development and induction of defense response genes during early

infection of wheat spikes by *Fusarium graminearum*. *Molecular Plant-Microbe Interactions* **13**: 159-169.

Proctor, R. H., T. M. Hohn, S. P. McCormick & A. E. Desjardins, (1995) *Tri6* encodes an unusual zinc-finger protein involved in regulation of trichothecene biosynthesis in *Fusarium sporotrichioides*. *Applied and Environmental Microbiology* **61**: 1923-1930.

Rittenour, W. R. & S. D. Harris, (2010) An *in vitro* method for the analysis of infection-related morphogenesis in *Fusarium graminearum*. *Molecular Plant Pathology* **11**: 361-369.

Rosewich, U. L., R. E. Pettway, B. A. McDonald, R. R. Duncan & R. A. Frederiksen, (1998) Genetic structure and temporal dynamics of a *Colletotrichum graminicola* population in a sorghum disease nursery. *Phytopathology* **88**: 1087-1093.

Roze, L., A. Chanda & J. Linz, (2011) Compartmentalization and molecular traffic in secondary metabolism: A new understanding of established cellular processes. *Fungal Genetics and Biology* **48**: 35-48.

Schoonbeek, H., G. Del Sorbo & M. A. De Waard, (2001) The ABC transporter BcatrB affects the sensitivity of *Botrytis cinerea* to the phytoalexin resveratrol and the fungicide fenpiclonil. *Molecular Plant-Microbe Interactions* **14**: 562-571.

Schoonbeek, H. J., J. G. M. van Nistelrooy & M. A. de Waard, (2003) Functional analysis of ABC transporter genes from *Botrytis cinerea* identifies BcatrB as a transporter of eugenol. *European Journal of Plant Pathology* **109**: 1003-1011.

Seabra, M. C. & E. Coudrier, (2004) Rab GTPases and myosin motors in organelle motility. *Traffic* **5**: 393-399.

Seiler, S., M. Plamann & M. Schliwa, (1999) Kinesin and dynein mutants provide novel insights into the roles of vesicle traffic during cell morphogenesis in Neurospora. *Current Biology* **9**: 779-785.

Seong, K. Y., M. Pasquali, X. Y. Zhou, J. Song, K. Hilburn, S. McCormick, *et al.* (2009) Global gene regulation by Fusarium transcription factors *Tri6* and *Tri10* reveals adaptations for toxin biosynthesis. *Molecular Microbiology* **72**: 354-367.

Skov, J., M. Lemmens & H. Giese, (2004) Role of a *Fusarium culmorum* ABC transporter (FcABC1) during infection of wheat and barley. *Physiological and Molecular Plant Pathology* **64**: 245-254.

Smith T. F. & M.S. Waterman, (1981) Identification of common molecular subsequences. J. *Molecular Biology* **147**: 195-197.

Spröte, P., A. A. Brakhage & M. J. Hynes, (2009) Contribution of peroxisomes to penicillin biosynthesis in *Aspergillus nidulans*. *Eukaryotic Cell* **8**: 421-423.

Steinberg, G., (2007) On the move: endosomes in fungal growth and pathogenicity. *Nature Reviews Microbiology* **5**: 309-316.

Stergiopoulos, I., L. H. Zwiers & M. A. De Waard, (2002) Secretion of natural and synthetic toxic compounds from filamentous fungi by membrane transporters of the ATP-binding cassette and major facilitator superfamily. *European Journal of Plant Pathology* **108**: 719-734.

Suelmann, R. & R. Fischer, (2000) Mitochondrial movement and morphology depend on an intact actin cytoskeleton in *Aspergillus nidulans*. *Cell Motility and the Cytoskeleton* **45**: 42-50.

Szewczyk, E., T. Nayak, C. E. Oakley, H. Edgerton, Y. Xiong, N. Taheri-Talesh, S. A. Osmani & B. R. Oakley, (2006) Fusion PCR and gene targeting in *Aspergillus nidulans*. *Nature Protocols* **1**: 3111-3120.

Teijeira, F., R. V. Ullan, S. M. Guerra, C. Garcia-Estrada, I. Vaca & J. F. Martin, (2009) The transporter CefM involved in translocation of biosynthetic intermediates is essential for cephalosporin production. *Biochemical Journal* **418**: 113-124.

TerBush, D. R., T. Maurice, D. Roth & P. Novick, (1996) The Exocyst is a multiprotein complex required for exocytosis in *Saccharomyces cerevisiae*. *Embo Journal* **15**: 6483-6494.

Trail, F., J. R. Xu, P. San Miguel, R. G. Halgren & H. C. Kistler, (2003) Analysis of expressed sequence tags from *Gibberella zeae* (anamorph *Fusarium graminearum*). *Fungal Genetics and Biology* **38**: 187-197.

Upadhyay, S. & B. D. Shaw, (2008) The role of actin, fimbrin and endocytosis in growth of hyphae in *Aspergillus nidulans*. *Molecular Microbiology* **68**: 690-705.

Urano, K., T. Hobo & K. Shinozaki, (2005) Arabidopsis ADC genes involved in polyamine biosynthesis areb essential for seed development. *FEBS Letters* **579**: 1557-1564.

Urban, M., T. Bhargava & J. E. Hamer, (1999) An ATP-driven efflux pump is a novel pathogenicity factor in rice blast disease. *EMBO Journal* **18**: 512-521.

Ward, T. J., J. P. Bielawski, H. C. Kistler, E. Sullivan & K. O'Donnell, (2002) Ancestral polymorphism and adaptive evolution in the trichothecene mycotoxin gene cluster of phytopathogenic Fusarium. *Proceedings of the National Academy of Sciences of the United States of America* **99**: 9278-9283.

Watson, R. J., S. Burchat & J. Bosley, (2008) A model for integration of DNA into the genome during transformation of *Fusarium graminearum*. *Fungal Genetics and Biology* **45**: 1348-1363.

Wedlich-Soldner, R., I. Schulz, A. Straube & G. Steinberg, (2002) Dynein supports motility of endoplasmic reticulum in the fungus *Ustilago maydis*. *Molecular Biology of the Cell* **13**: 965-977.

Windels, C. E., (2000) Economic and social impacts of Fusarium head blight: Changing farms and rural communities in the Northern Great Plains. *Phytopathology* **90**: 17-21.

Wong, P., M. Walter, W. Lee, G. Mannhaupt, M. Munsterkotter, H. W. Mewes, G. Adam & U. Güldener, (2011) FGDB: revisiting the genome annotation of the plant pathogen *Fusarium graminearum*. *Nucleic Acids Research* **39**: D637-D639.

Wu, H., G. Rossi & P. Brennwald, (2008) The ghost in the machine: small GTPases as spatial regulators of exocytosis. *Trends in Cell Biology* **18**: 397-404.

Yakir-Tamang, L. & J. E. Gerst, (2009) Phosphoinositides, exocytosis and polarity in yeast: all about actin? *Trends in Cell Biology* **19**: 677-684.

Zwiers, L. H. & M. A. De Waard, (2000) Characterization of the ABC transporter genes *MgAtr1* and *MgAtr2* from the wheat pathogen *Mycosphaerella graminicola*. *Fungal Genetics and Biology* **30**: 115-125.

Chapter 3

Identification of *Fusarium graminearum* virulence factors by comparative gene expression analysis

Introduction

Fusarium graminearum, one of the causal organisms of Fusarium head blight (FHB), has historically had a significant negative impact on agricultural economics and food safety. This plant pathogen not only causes significant yield loss in infected grains, it also taints these grains with potent trichothecene mycotoxins harmful to humans, animals, and plants alike. From 1998 to 2000, production loss and price impacts from FHB were estimated at $871 million, with secondary economic losses of $1.8 billion. More than half of these losses occurred in Minnesota and North Dakota (Nganje et al., 2004). Humans and animals that consume grains tainted with trichothecene mycotoxins produced by *F. graminearum* can display multiple symptoms, including hemorrhage and emesis. Feed refusal is observed among cattle, pigs, and poultry. Trichothecenes are teratogenic and immunosuppressive compounds (Desjardins et al., 1993). Based on the risk associated with trichothecene ingestion, the United States Food and Drug Administration advises that human consumption of bran, flour or germ containing more than 1 ppm of DON should be avoided (Petska and Smolinski, 2005).

Symptoms of FHB on wheat include purple to black necrotic lesions, awn twisting and deformation, bleaching and tanning attributed to blight, and atrophy of the developing grain (McMullen et al, 1997; Goswami and Kistler, 2004). Under prolonged warm and moist conditions, signs of the fungus are sometimes present in the form of pink mycelial masses on the surface of infected spikes (Goswami and Kistler, 2004.) Occasionally, the rachis of a blighted head will be girdled, leading to the loss of the entire spike. Diseased

barley exhibits isolated areas of tan to dark brown discoloration as well as evidence of water-soaking restricted to the initially infected inflorescence (Bushnell et al., 2003; Goswami and Kistler, 2004.). Signs of the fungus can also be present on barley under prolonged warm and moist conditions (Goswami and Kistler, 2004). On rice, symptoms of infection are limited to discrete brown to black necrotic lesions (Goswami and Kistler, 2005).

Levels of trichothecenes present *in planta* vary, depending on the host. Strains of *F. graminearum* produce the Type B trichothecenes nivalenol (NIV) or deoxynivalenol (DON) and its acetylated derivatives, 15-acetyldeoxynivalenol (15ADON) and 3-acetyldeoxynivalenol (3ADON). These toxins are readily detected in wheat and barley but previously have not been detected in rice infected with *F. graminearum* (Goswami and Kistler, 2005).

The goal of this study was to identify *F. graminearum* genes expressed *in planta*, as these genes may be enriched among those determining the outcome of the fungus-plant interaction. The transcriptomes of *F. graminearum* on wheat and rice were examined because of their different disease phenotypes. Community resources for microarray gene expression data are available for *F. graminearum* (PLEXdb; www.plexdb.org; Wise et al., 2007), making it possible to compare expression profiles in wheat and rice with those from the fungus grown in culture or during infection of barley. Using these resources, genes expressed exclusively in all plants or in particular plant species were identified. A

small number of genes from this group were selected for mutagenesis to determine their potential effect on infection.

Results

Disease symptoms and detection of type B trichothecenes and ergosterol *in planta*

Discrete brown necrotic lesions were observed on rice florets and wheat spikelets 48 hours after spray inoculation (hai) with conidia (Figures 1 and 2). Lesions darkened and increased in size on rice florets at 96 and 192 hai. Symptoms were often observed throughout an entire spikelet, though symptoms did not advance beyond the delimited lesions of an infected spikelet. Necrosis of the rachis of wheat heads was observed 96 hai, demonstrating symptoms had advanced beyond initially infected wheat spikelets. At this stage of infection, awn deformation and twisting, as well as bleaching of wheat spikelets, were also observed. Symptoms continued to spread in wheat at 192 hai. Confluence of symptoms was observed between adjacent spikelets and the rachis spanning these spikelets. Awn deformation intensified, as did the bleaching and tanning of infected wheat spikelets.

The Type B trichothecenes DON (1.5 ppm) and 15ADON (~1.0 ppm) were detected at low levels in wheat 48 hai and increased at each subsequent stage of infection (Table 3). Ergosterol concentration in infected tissue was used as a measure of fungal biomass *in planta*. Ergosterol was detected in wheat 48 hai and ergosterol concentration was higher

at 192 hai (Table 4). Neither DON nor 15ADON were detected in rice 48 hai. Ergosterol was present in rice at the earliest stage of infection. No significant increase in ergosterol levels was observed in rice at 96 or 192 hai compared to the 48 hai time point. Low levels of DON and 15ADON (≤1 ppm) were detected in rice at 96 hai. At 192 hai, DON and 15ADON concentrations in rice reached 3 ppm and ~1 ppm, respectively. These levels are roughly 50-fold less than levels measured in wheat at this time point. These results demonstrate that during infection of wheat, *F. graminearum* produces increasing amounts of biomass and trichothecenes over time. Conversely, during infection of rice, from 48 hai onward, *F. graminearum* does not increase its biomass and trichothecene levels appear to increase only slightly over time.

Genes expressed exclusively *in planta*

F. graminearum GeneChips were used to obtain transcript expression profiles of the fungus during its interaction with wheat and rice. Profiles of the fungus were obtained at early (48 hai), intermediate (96 hai), and late (192 hai) stages of infection for both hosts. Figure 3 illustrates global distribution patterns of probe set signal intensities in rice and wheat at the early, intermediate, and late stages of infection as well as similar time points for barley. Collectively, signal intensities observed for rice and barley are consistently lower than in wheat. In rice, signal levels and global distribution patterns remained relatively constant over time. In wheat and barley, signal level intensities increased and global distribution patterns changed at each successive time point.

To address the goal of identifying genes important for infection of plants, comparative transcriptome analysis was conducted using profiles of the fungus *in planta*, including previous data obtained from barley (Güldener et al., 2006); during spore germination or vegetative growth in liquid CM; or during vegetative growth in liquid MM-N or MM-C medium in order to identify genes expressed exclusively *in planta*. Figure 4 contains a Venn diagram showing the distribution of genes expressed exclusively in one host, within all combinations of two hosts or collectively among all three hosts – wheat, rice, and barley.

Genes expressed in all plants

This study identified 406 genes expressed in wheat, rice or barley that were not expressed during growth in various liquid media (Figure 4; Supplemental table A). Of these genes, 100 are expressed in all three hosts at some time during the course of infection. Annotation of infection-specific genes indicates significant enrichment for several functional categories during colonization of wheat, rice, and barley. Particularly enriched (P = 1.15E-16) are genes for polysaccharide metabolism (MIPS category 01.05.03) that largely encode proteins that degrade plant cell wall components. Among these infection-specific genes are those that encode enzymes predicted to degrade cellulose, as well as arabinose, galactose, xylose, and pectic polysaccharides.

F. graminearum transcripts for genes that influence secondary metabolite biosynthesis were detected among all three hosts. Nine genes implicated in trichothecene biosynthesis

(*Tri1*, *Tri3*, *Tri4*, *Tri*5, *Tri6*, *Tri*9, *Tri11*, *Tri12*, and *Tri14*) are specifically expressed *in planta* (Figure 5). Transcripts for all nine genes are detected in wheat and barley. Only four of these *Tri* genes (*Tri1*, *Tri4*, *Tri9*, and *Tri14*) are detected in rice. Considering that trichothecene accumulation in rice is much less than in wheat and barley, it is reasonable to suggest that reduced levels may be due to transcriptional control of those *Tri* genes not detected in rice. These genes include those for the enzyme catalyzing the first step in trichothecene biosynthesis (*Tri*5) and for the major transcriptional regulator of trichothecene biosynthesis (*Tri6*).

Two *Tri* genes that encode cytochrome P-450 oxygenases have defined roles in secondary metabolism biosynthesis. *Tri1* and *Tri4* are instrumental in the biosynthesis of Type B trichothecenes. Two other *Tri* genes, *Tri9* and *Tri14*, encode proteins that influence trichothecene biosynthesis and virulence in wheat, but have no described function. In the current study, *Tri9* influences trichothecene biosynthesis *in vivo* and *in planta*.

Elements of the secondary metabolite gene cluster for biosynthesis of butenolide are differentially regulated *in planta* (Figure 6). FGSG_08079 is required for the synthesis of butenolide (Harris et al., 2007) and encodes a probable cytochrome P450 monoxygenase that is expressed in all stages of infection in wheat and barley, but only during the early and intermediate stages of infection in rice. Three other members of the cluster (FGSG_08081, FSGS_08082, and FSGS_08083) are expressed exclusively and constitutively *in planta*. FGSG_08084 encodes a putative MFS transporter and is

expressed in the early and intermediate stages in rice and the intermediate and late stages in wheat. As reported by Harris et al. (2007), two other predicted members of the cluster, FGSG_08077 and FGSG_08078, are expressed *in planta*, but not exclusively. Expression of FGSG_08077 is constitutive in all situations. A similar situation is observed with FGSG_08078, which is also expressed during macroconidium germination. Curiously, FGSG_08078 is up-regulated (> 5-fold) in MM-N medium relative to MM-C cultures. Gardiner et al. (2009a) reported considerable up-regulation of both FGSG_08077 and FGSG_08078 when the polyamine agmatine is used as a nitrogen source in culture; this medium also induces trichothecene biosynthesis. Relative expression values for these genes were >10-fold greater in agmatine cultures that in glutamine cultures. Interestingly, FGSG_08080, a predicted Zn_2Cys_6 transcription factor, is expressed during the intermediate and late stages of infection in wheat and barley, but not at all in rice. It is also the only other gene in the predicted butenolide cluster that is induced by agmatine in culture.

Expression of the secondary metabolite genes *Tox1, Tox3,* and *Nps9* was observed in all plants.

Genes for several predicted proteases are expressed solely in plants (Figure 7). FGSG_00028 encodes a metalloprotease that has no established function in *F. graminearum*, though well-conserved (> 89% predicted amino acid identity) orthologous genes are present in *F. verticillioides* and *F. oxysporum*. FGSG_01818, FGSG_03315, FGSG_10595, and FGSG_10712 encode, respectively, predicted aminopeptidase,

peptidase K, and oryzin-like enzymes. FGSG_11164 encodes a putative trypsin precursor with high-level expression exclusively *in planta*.

F. graminearum genes exclusively expressed in two of the three plant hosts

While fungal transcript profiles from infected rice and barley or rice and wheat share few exclusive transcripts (two and eight, respectively – Figure 4), transcript profiles from wheat and barley express 142 exclusive transcripts. Several genes involved in secondary metabolite biosynthesis are exclusively expressed in wheat and barley, including the previously mentioned trichothecene biosynthetic genes *Tri3*, *Tri5*, *Tri6*, *Tri11*, and *Tri12*. FGSG_04588, which encodes a polyketide synthase of unknown function, and genes encoding cell wall degrading enzymes including pectinase and xylanases are also expressed in these plants. Multiple transcripts encoding predicted MFS transporters, permeases, multi-drug resistance proteins, and ABC transporters that are predicted to transport sugars, zinc, and other unidentified compounds are also specifically expressed in wheat and barley. Four genes with predicted involvement in phenylpropanoid metabolism (FGSG_00231, FGSG_02266, FGSG_03531, and FGSG_09169) and quinate transport (FGSG_04636 and FGSG_08177) are also expressed during the infection of these plants.

Genes expressed exclusively in a single host plant

Twelve genes are expressed exclusively in rice. Of these, only three have predicted functions. FGSG_02426 likely encodes a Na+/phosphate co-transporter, while FGSG_04748 and FGSG_06610 are predicted to encode an isoflavone reductase homolog and an alkaline phosphotase precursor, respectively.

A total of 115 genes are exclusively expressed in wheat. Annotation and functional categorization of these genes revealed that many likely play a role in the metabolism of lipids and polysaccharides. The genes FGSG_07640 and FGSG_13737 are likely involved in phenylpropanoid metabolism. FGSG_03257 is related to the nonribosomal peptide synthetase MxcG, though its role in secondary metabolite biosynthesis in *F. graminearum* is unclear. *Tox2* is also expressed exclusively in wheat. A survey of genes without identified functions nevertheless revealed FGSG_04581 encodes a protein predicted to possess a Zn_2Cys_6 transcription factor DNA binding motif. FGSG_07824 is the only other genes detected exclusively in wheat that encode a known or suspected transcription factor.

Twenty-seven genes were exclusively expressed in barley. Functional classification of these genes revealed enrichment for those implicated in nitrogen metabolism, while others are involved in secondary metabolism. FGSG_11106 encodes a monophenol monooxygenase with suspected involvement in phenylpropanoid metabolism.

Functional analysis of genes expressed exclusively *in planta*

Of the genes that are exclusively expressed in plants, four were chosen for reverse genetic analysis to determine their potential role in pathogenesis (Figure 8). FGSG_03539 is a small open reading frame found in the main trichothecene gene cluster with an unknown function with respect to trichothecene biosynthesis and pathogenicity toward plants. FGSG_04581 encodes an uncharacterized protein thought to be a potential transcription factor due to its Zn_2Cys_6 fungal-type DNA-binding domain. FGSG_08080 was chosen because it encodes a predicted transcription factor associated with the butenolide biosynthetic gene cluster. FGSG_11164 encodes a predicted trypsin protease. Mutants deleted for each gene were generated individually in the wild-type strain PH-1 by split-marker recombination mutagenesis (Catlett et al., 2003) with previously described modifications (Goswami et al., 2006) (Figure 9).

All deletion mutants were assayed by point inoculation of wheat spikelets at anthesis. No difference in the mean number of infected spikelets was observed between wild-type PH-1 and mutants deleted for FGSG_04581 or FGSG_08080. These mutant strains were not further examined. The two remaining mutant strains, deleted for *Tri9* (FGSG_03539) or FGSG_11164, exhibited reduced virulence on wheat in initial pathogenicity tests and were further characterized to determine the extent of influence they have on virulence or trichothecene biosynthesis *in vitro* or *in vivo*.

The mutation in the strain (PH-1*tri9*) containing the *Tri9* deletion was complemented by reintroducing a full-length copy of the *Tri9* gene via genetic transformation, resulting in the strain PH-1*tri9/Tri9*. Southern blotting was used to demonstrate the presence of single copies of the selectable marker *hph* and *Tri9* in PH-1*tri9/Tri9* and to confirm the presence of a single copy of *hph* and the absence of *Tri9* coding sequence in PH-1*tri9* (Figure 10).

Levels of *Tri9* transcript expression *in planta* increased during the course of *F. graminearum* infection of wheat and barley. *Tri9* transcripts were not detected in rice until 192 hai and transcript levels observed in wheat were more than17-fold greater than those observed in rice (Figure 8). Reverse genetic analysis revealed *Tri9* is a virulence factor that significantly influences fungal pathogenicity. Trichothecene biosynthetic capability is retained by the PH-1*tri9* strain *in vitro* and *in vivo*, but trichothecene accumulation is significantly reduced in both cases.

The pathogenicity of PH-1*tri9* was reduced compared to the wild-type strain or the PH-1 *tri9/Tri9* complement controls (Table 5, Figure 11). PH-1, PH-1*tri9*, and PH-1*tri9/Tri9* were assayed by point inoculation of wheat spikelets at anthesis. All strains were able to infect tissue and cause necrosis at the point of inoculation and were able to spread via the rachis, causing disease symptoms beyond the inoculated spikelet. However, the mean number of symptomatic spikelets was reduced by 64% for plants inoculated with PH-1*tri9* compared to plants inoculated with PH-1. Likewise, the mean mass of spikes inoculated with PH-1*tri9* was 35% greater than those inoculated with PH-1. No

significant difference in the mean number of symptomatic spikelets or mass of infected spikes was observed for plants inoculated with PH-1*tri9/Tri9* or PH-1.

Infection of wheat with PH-1, PH-1*tri9* or PH-1*tri9/Tri9* resulted in the accumulation of more DON than 15ADON (Table 5). The PH-1 *tri9* deletion mutant accumulated significantly lower trichothecene concentrations than wild-type PH-1. The mean DON concentration was 57% lower in spikelets inoculated with PH-1*tri9* compared to those inoculated with PH-1, while the mean 15ADON concentration was reduced by 76%. The *Tri9* complement PH-1*tri9/Tri9* did not fully restore the wild-type trichothecene levels. Nevertheless, the mean DON and 15ADON concentrations measured in spikelets inoculated with PH-1*tri9/Tri9* were still significantly greater than those measured in plants inoculated with PH-1*tri9*.

PH-1, PH-1*tri9*, and PH-1*tri9/Tri9* grown in liquid toxin biosynthesis induction (TBI) medium resulted in higher levels of 15ADON than DON (Table 6). Mean 15ADON concentration observed in cultures inoculated with PH-1*tri9* was significantly (67%) lower than in cultures inoculated with PH-1. Genetic complementation of the mutant increased the level of trichothecenes in culture to a level significantly higher than that of the wild type. The mean 15ADON concentration present in liquid TBI medium inoculated with PH-1*tri9/Tri9* was 127% of that observed in cultures inoculated with PH-1.

FGSG_11164 (called *Tpp1* for **T**rypsin **p**recursor **p**rotein 1) is expressed exclusively *in planta* continuously over all time points in rice and wheat, and during the intermediate and late time points in barley. A *Tpp1* deletion mutant in PH-1 (PH-1*tpp1*) was created by split marker mutagenesis. Southern blotting was used to demonstrate the presence of single copies of the selectable marker *hph* in PH-1*tpp1* (Figure 12). PH-1 and PH-1*tpp1* were assayed by point inoculation of wheat spikelets at anthesis. Both strains were able to infect tissue and cause necrosis at the point of inoculation and were able to spread, causing disease symptoms beyond the inoculated spikelet. However, the mean number of symptomatic spikelets was significantly reduced (6%) for plants inoculated with PH-1*tpp1* compared to plants inoculated with PH-1 (Table 7). Likewise, the mean mass of spikes inoculated with PH-1*tpp1* was 10% greater than those inoculated with PH-1.

Discussion

Symptom development, fungal biomass, transcript accumulation, and trichothecene accumulation in wheat, rice, and barley

Strong differences in disease phenotype are noted when *F. graminearum* is inoculated on wheat, rice or barley. On wheat and rice, discrete brown necrotic lesions are clearly visible 48 hai. In wheat, disease symptoms progressively increase such that, by 96 and 192 hours, lesions expand and coalesce while spreading to the rachis, followed by chlorosis and bleaching of the remaining tissue of the spike (Figure 2). However, in rice, discrete lesions present at 48 hours darken in color but do not appreciably expand or

coalesce (Figure 1). When levels of the fungal sterol ergosterol in plant tissue were used to estimate the amount of fungal biomass associated with *Fusarium* infection, ergosterol concentrations were nearly unchanged in rice, while levels increased in wheat (Table 4). At every time point, ergosterol levels were higher in wheat relative to rice. The congruence between disease symptoms and fungal biomass likely reflects the different infection strategies employed by the fungus on the two hosts. *F. graminearum* is likely growing as a delimited colony in infected rice tissue, while in wheat it is able to further spread and colonize more tissue over time.

Global distribution patterns of probe set signal intensities highlight the temporal similarities and differences in overall *F. graminearum* gene expression in rice, wheat, and barley (Figure 3). The highest levels of probe set signal intensity were consistently observed in wheat. Also, the distribution patterns of signal intensity in wheat changed with time; a greater number of probe sets with higher signal intensity were observed at each successive time point. In rice, signal intensity distribution patterns were uniform over time and probe sets with lower signal levels had the highest frequency. The skewed distribution for probe sets with lower intensity suggests that many fungal genes may be expressed at a level that cannot be resolved from background signal. Distribution patterns of probe set signal intensity in barley closely resemble those of wheat, though overall signal intensity levels were considerably lower in barley.

Collectively, these observations indicate that among the plants and fungal strains used in this study, the initial infection process likely occurs more slowly in rice and barley than

in wheat. This conclusion is supported by observations made by other research groups. Pritsch et al. (2000) reported that conidia germination on wheat often occurred within six hai, while Boddu et al. (2006) did not observe germination on barley until 24 hai. Moreover, Boddu et al. (2006) proposed the development of fungal infection structures and other morphological changes occur between 12 and 24 hours earlier in wheat than in barley.

Trichothecene mycotoxins are detectable in both wheat and rice four and eight days after inoculation with *F. graminearum* PH-1. Initial analysis of the *F. graminearum*-rice interaction by Goswami et al. (2005) did not detect trichothecenes in rice 14 days after infection with PH-1. In this study's experiments, trichothecenes are also undetectable in rice two days after inoculation but traces of 15ADON and an average concentration of 1ppm DON appear at four days after inoculation. Trichothecene levels peak in rice at 3 ppm, eight days after inoculation, while 15ADON remained present at trace levels. In wheat, DON was present at 1.5 ppm two days after inoculation. DON concentration was almost 40-fold greater in wheat than rice after four days and 55-fold greater after eight days. Trichothecene data for the *F. graminearum*-barley interaction published by Boddu et al. (2006) demonstrated that a considerable quantity of DON was present during the intermediate stage of infection and levels increased in the late infection.

F. graminearum gene expression *in planta*

Cell wall and protein degrading enzymes

Cell wall degrading enzymes (CWDE) produced by plant pathogenic fungi play important roles in the penetration and colonization of host tissues. Several studies have implicated these proteins as virulence factors (Kikot et al., 2009). Research on the interaction between *F. graminearum* and wheat has demonstrated the fungus secretes CWDE directed toward diverse components of plant cell walls. Commelinoid monocots of the order Poales possess type II cell walls that are distinctly different than the Type I cell walls of dicots. Type II cell walls contain smaller amounts of pectic polysaccharides and larger amounts of phenylpropanoids. In contrast to Type I cell walls, cellulose is more abundant in Type II walls than xyloglucans (Yokoyama and Nishitani, 2004). Enzyme-gold and immuno-gold labeling analysis of wheat spikes demonstrated tissue specific distribution of cellulose, xylan, and pectin (Kang and Buchenauer, 2000). Transcripts encoding xylanase, pectate lyase, cutinase, and cellulose binding proteins were among those identified as being expressed exclusively *in planta.* Interestingly, the expression of multiple pectate lyases in wheat and barley was observed during the intermediate and late stages of infection. Only one gene encoding a suspected pectate lyase, *OrfE* (FGSG_03526), is expressed in rice. These results suggest *F. graminearum* can tailor its arsenal of nutrient acquisition enzymes depending on the prevalence of nutrients available in a particular host. Two pectate lysases of *Nectria haematococca*, *pelA* and *pelD*, are induced by pectin and fungal growth on pea plants, respectively.

Deletion of these two genes results in a drastic reduction of virulence on infected plants (Rogers et al., 2000). The hulls and stamens of the developing rice inflorescence contain relatively high levels of pectic polysaccharides (Wang et al., 2010). Though these compounds are present in rice, *F. graminearum* does not appear to express its full complement of genes encoding known enzymes that degrade these compounds. The inability of the fungus to readily degrade these compounds could partially explain the lower virulence of the fungus in rice compared to wheat and barley.

Protein degrading enzymes also play an important role in plant-fungal interactions. *F. graminearum* can secrete a considerable arsenal of enzymes that break down plant proteins. Paper et al. (2007) used mass spectrometry to conduct a comparative proteomic study of extracellular proteins produced by *F. graminearum in vitro* and *in planta* in wheat. They detected several proteins predicted to encode peptide degrading enzymes. Several transcripts expressed exclusively *in planta* in the current study are predicted to encode similar enzymes with roles in peptide degradation. These include metalloproteases, aminopeptidases, peptidase K, and trypsin. One of the secreted trypsin-like proteins identified by Paper et al. (2007) was highly similar to the predicted protein encoded by FGSG_11164. Pekkarinen et al. (2002) also identified a trypsin-like protease secreted by *F. culmorum* in gluten-containing culture medium, and later confirmed the presence of this protein in *F. culmorum* infected barley (Pekkarinen et al, 2003).

The role of plant encoded trypsin inhibitors in protecting plants from fungal invasion has been a subject of considerable study. Grasses possess proteins that inhibit the activity of

fungal serine proteases. Qu et al. (2003) identified a cluster of seven genes that encode Bowman-Birk Type trypsin inhibitors (BBTI) in rice whose expression was tissue-specific and wound-inducible. *RBBI2-3*, a gene that encoded a BBTI that was expressed in rice leaves, was used to transform Taipei 309, a rice cultivar known to be susceptible to rice blast. Over-expression of *RBBI2-3* in this genetic background resulted in these plants being highly resistant to infection by the rice blast pathogen, *Magnaporthe grisea*. Jia et al. (2009) identified a wheat gene transcript encoding a BBTI that exhibited accumulation differences between the resistant and susceptible wheat lines infected with *F. graminearum*. Another BBTI purified from barley has demonstrated anti-fungal activity against *F. graminearum* growth *in vitro* (Chilosi et al., 2009).

Role of the FGSG_11164 encoded protease in disease

Because of the potential for interaction between pathogen proteases and host protease inhibitors, a gene encoding a protease that was highly up-regulated during infection was deleted to determine its potential effect on disease phenotype. FGSG_11164 likely encodes a trypsin like protease with no high identity paralogs in *F. graminearum*; the closest homolog has less than 10% sequence identity. Orthologous trypsin–like proteins are present in several plant pathogenic fungi including *F. oxysporum* (FOXG_13248), *F. verticillioides* (FVEG_12280), and *F. solani* (neha_12680) that share greater that 73% predicted amino acid sequence identity with FGSG_11164. Similar proteins in the plant pathogenic fungi *Cochliobolus heterostrophus*, *Phaeosphaeria nodorum*, *Verticillium dahliae*, and *Verticillium albo-atrum* share greater than 54% predicted amino acid

sequence identity (SIMAP). FGSG_11164 was targeted for deletion analysis because it is exclusively expressed at high levels *in planta*. A strain with a deletion of FGSG_11164 has a small but significant reduction in virulence on wheat. The trypsin precursor encoded by FGSG_11164 is the second secreted fungal protein with a demonstrated influence on the virulence of *F. graminearum* on wheat. Voigt et al., (2005) showed *Fgl1*, which encodes a secreted lipase, significantly influences *F. graminearum* pathogenicity on wheat; symptoms on wheat inoculated with *fgl1* did not spread beyond the spikelets adjacent to inoculated spikelets.

Secondary metabolism

The role of fungal secondary metabolism in plant disease is well documented (Proctor et al., 1995; Yu and Keller, 2005; Howlett, 2006). The results of this study suggest secondary metabolic processes play a broad role in interaction of *F. graminearum* with wheat and rice. Many genes that underlie processes related to secondary metabolism are expressed during host infection. Genome-wide, 442 genes have been assigned this classification by the MIPS FGDB. Seven percent (29) of theses genes are expressed exclusively *in planta* and six encode cytochrome P450-like enzymes. Of these six, *Tri1*, *Tri4*, and *Tri11* encode enzymes that are involved in trichothecene biosynthesis. The remaining three—FGSG_01661 (related to *E. coli* dioxygenase), FGSG_03700 (related to O-methylsterigmatocystin oxidoreductase), and FGSG_07765 (related to *Tri11*) — have no established function.

Exclusive *in planta* expression of genes in multiple known secondary metabolite biosynthetic clusters occurred in all hosts. Exclusive and robust expression of genes within the butenolide cluster was observed *in planta* (Figure 6). Five members of the putative butenolide cluster are expressed in all plants at all stages of infection. Similar to the observations made by Harris et al. (2007), three of these genes (FGSG_08081, FSGS_08082, and FSGS_08083) are expressed exclusively *in planta*, while the other two (FGSG_08077 and FGSG_08078) also are expressed in CM, MM-C, and MM-N cultures. To explain the differential regulation of the expression of genes within the putative cluster, the authors suggested that FGSG_08077 and FGSG_08078 play alternate roles under different growth conditions. Gardiner et al. (2009a) reported considerable up-regulation of FGSG_08077 and FGSG_08078 in agamatine cultures relative to glutamate cultures. Up-regulation in the expression of these genes occurred during growth in MM-N and CM, but not in MM-C cultures. Curiously, FGSG_08080 is the only other member of the predicted cluster that is induced by agmatine in culture. Harris et al. (2007) demonstrated the induction of expression of all members of the biosynthetic cluster in modified MYRO toxin induction medium. Detection of butenolide in cultures with agmatine as a nitrogen source would support a functional association between the genes in the cluster that are expressed exclusively *in planta* and those that are also expressed in culture. Based on the observation that *Tri6*, a regulator of trichothecene biosynthesis, exerts regulatory control over genes outside of the trichothecene biosynthetic cluster (Seong et al., 2009), FGSG_08080 was hypothesized to exhibit similar behavior. Targeted disruption of FGSG_08080, however, did not influence toxin production in culture or virulence in wheat.

Interestingly, several genes implicated in biosynthesis of secondary metabolites and not currently known to influence pathogenicity are exclusively expressed *in planta*. For example, all four genes of a cluster containing NPS9, a non-ribosomal peptide synthase without established function, are expressed in barley in the late stage of infection. The polyketide synthase gene *PKS15* also is expressed in wheat, rice, and barley during the late stage of infection, though its utility and function are both in question (Gaffoor et al., 2005). *Tox1*, *Tox2*, and *Tox3* – three genes predicted to be involved in the biosynthesis of toxins that specifically inhibit voltage-gated calcium channels – are expressed exclusively *in planta* (Gage et al., 2001). No published report has examined the functional significance of these toxins regarding fungal virulence in wheat, rice or barley.

There is a temporal and spatial correlation between morphological differentiation associated with plant infection and induction of secondary metabolism. Several studies indicate the cell morphology of *F. graminearum* noticeably changes *in planta* during the early and intermediate stages of infection. Pritsch et al. (2000) observed temporal patterns of fungal development in *F. graminearum*-inoculated wheat spikes within the first 48 to 76 hai. Thickened and ramified hyphae with coralloid branching were observed in Sumai 3 wheat glumes 48 hai and became more abundant after 72 hours. Jansen et al. (2005) observed the growth of a constitutively GFP-expressing strain of *F. graminearum* in isolated caryopses of wheat. Hyphae possessing appressorium-like structures were observed in epicarp cells of wheat 48 hai. Boddu et al. (2006) reported distinct hyphal structures with differences in hyphal thickness, length or both on the lemma of infected

barley florets. Coralloid bulges at the end of secondary peg-like structures were evident during subcutaneous growth. Illgen et al. (2009) also provided evidence of thickened and ramified hyphae with coralloid branching in wheat. Rittenour and Harris (2010) described bulbous coral-like infection hyphae in their investigation of *F. graminearum* on detached wheat glumes. Brown et al. (2010) also reported distinct morphological features of *F. graminearum* during infection of wheat spikes. In Chapter 2, the polyamine putrescine was used to induce trichothecene biosynthesis in culture. Notable changes in cell morphology under trichothecene induction conditions were observed *in vitro*. The structures formed by *F. graminearum* under these conditions are very similar to those reported by Rittenour and Harris (2010), Boddu et al. (2006), and Pritsch et al. (2000) during the early and intermediate stage of infection. The polyamine putrescine thus must be capable of inducing *in vitro* morphological changes in the fungus as well as the biosynthesis of trichothecenes.

Secondary metabolism is closely associated with morphological differentiation (Calvo et al., 2002) and it is known that polyamines can influence both secondary metabolite production and cell differentiation. A recent study by Gardiner et al. (2009b) demonstrated the ability of polyamines to induce trichothecene biosynthesis by *F. graminearum* in culture. To attempt to establish whether polyamines produced by the host may be inducing trichothecene accumulation during fungal infection, Gardiner et al. (2010) demonstrated that wheat genes implicated in polyamine biosynthesis were induced in the 24 hours following inoculation of wheat with *F. graminearum* and that putrescine accumulates in the plant prior to toxin production by the pathogen. In the present study,

only one gene implicated in fungal polyamine metabolism was among those expressed exclusively *in planta*. FGSG_04673 encodes a protein similar to ornithine amino-transferase. However, this gene is only expressed at low levels in barley and is not present in rice or wheat.

Cell differentiation and secondary metabolic processes likely influence each other, though how cell differentiation is regulated and implemented during infection is still not well understood. Since *F. graminearum* undergoes significant morphological changes *in planta* during the establishment of infection, differential expression of genes implicated in cellular differentiation over time was anticipated. Surprisingly, none of the 106 genes expressed during infection of wheat, rice, and barley and associated with cellular differentiation (MIPS category 43.0) are expressed exclusively *in planta*. Perhaps cellular components that influence differentiation are constitutively expressed and further regulated by secondary metabolites or unknown regulatory infection processes. It is also plausible that genes expressed exclusively *in planta* that have unknown function might be influential in differentiation associated with infection.

The considerable differences in trichothecene levels found in wheat and rice can be explained by host-specific expression patterns of genes associated with trichothecene biosynthesis. As expected, many genes associated with trichothecene biosynthesis are expressed in wheat. In contrast, less than half of the genes known to be involved in this process are detected as being expressed in rice. Of the genes expressed in rice, *Tri1* and *Tri*4 encode cytochrome P450 monooxygenases, while the functions of *Tri*9 and *Tri14*

are unknown. *Tri*5 — a gene that encodes a key enzyme in trichothecene biosynthesis — and *Tri*6 — a master regulator of this process — are not detected in rice. Though several enzymes that are instrumental in trichothecene biosynthesis are likely present in rice, these enzymes could be starved of substrates necessary for trichothecene synthesis. This also suggests the expression of some *Tri* genes is not substrate dependent. Seong et al. (2009) observed a similar phenomenon. In their study, three *Tri* genes (*Tri9*, *Tri10*, and *Tri14*) were modestly up-regulated when *tri5* mutants were fed trichodiene, but expression levels of other Tri genes were unaffected. It is also plausible the enzymes that are present in rice may not be involved exclusively in trichothecene biosynthesis, but may play roles in other processes. Collectively, these results suggest transcriptional regulation of trichothecene biosynthesis is a complex process that involves differential regulation of *Tri* genes. *Tri9* was selected for reverse genetic analysis based on its exclusive and high-level expression in wheat and barley and its suspected, but unconfirmed, role in trichothecene biosynthesis.

The role of *Tri9* in pathogenicity and trichothecene production

Levels of *Tri9* transcript expression *in planta* increased during the course of *F. graminearum* infection of wheat and barley. In contrast, *Tri9* transcripts were not detectable in the early stage of infection in rice and transcript levels observed in the intermediate and late stages of infection did not differ significantly. *Tri9* transcripts were more than 17-fold more abundant in wheat than in rice in the late stage of infection. Levels of *Tri9* transcript expression are at least 40-fold greater in trichothecene induction

cultures containing agmatine relative to cultures containing glutamine (Gardiner et al., 2009a). *Tri9* expression in wheat is regulated by *FgTri6* and, to a greater degree, *FgTri10*. *Tri9* expression is reduced at least two-fold in plants inoculated with *fgtri6* strains compared with the wild type, while expression is completely absent in plants inoculated with *fgtri10* strains. The minimum Tri6p binding motif is present at three different locations within the 100 bp region beginning 300 bp upstream and ending 200 bp upstream of the predicted start codon of *Tri9* (Seong et al., 2009).

Tri9 lies between *Tri10* and *Tri11* in the trichothecene biosynthetic cluster of *F. graminearum*. The two most commonly used sources of annotation for the *F. graminearum* genome (MIPS and the Broad Institute) present different predictions for the transcript structure of *Tri9*, but agree on the predicted coding region of the gene. This intron-less 132 nucleotide coding region is predicted to encode 43 amino acids (Wong et al., 2011; Cuomo et al., 2007). Orthologs of *Tri9* could not be identified in species outside of the genus *Fusarium* via BlastP (Altschul et al., 1997, 2005). The predicted amino acid sequences of *Tri9* are highly conserved between *F. graminearum* and the other trichothecene producing fungi *F. sporotrichioides* and *F. cerealis*; the latter two species possessing single exclusive amino acid substitutions relative to *F. graminearum*. Predicted amino acid sequences of *Tri9* in *F. incarnatum* and *F. camptoceras* are also highly conserved.

Reverse genetic analysis revealed that *Tri9* significantly influences fungal pathogenicity toward wheat. Although trichothecene biosynthetic capability is retained by the *tri9* strain

both *in vitro* and *in vivo*, trichothecene accumulation is significantly reduced in both cases. These results suggest the gene plays an important role in maximum trichothecene accumulation, but is not essential for trichothecene biosynthesis itself. Deletion of *Tri9* did not affect radial growth assays on TBI agar, suggesting it does not play a role in self-protection against trichothecenes. Kimura et al. (2003) suggested the diminutive nature of this hypothetical protein would preclude it from being a functional enzyme in the trichothecene biosynthetic pathway. Attempts to tag the predicted C-terminus of Tri9p with eGFP were unsuccessful. The unique nature of *Tri9* and the inability to link this gene to a physically identified protein leaves open the possibility that the sequence predicted to encode *Tri9* could instead have a regulatory role that influences the expression of genes involved in trichothecene biosynthesis.

Proposed roles of import and export mechanisms *in planta*

Over the course of infection, *F. graminearum* likely needs to transport a myriad of compounds in and out of cells. Genes encoding several predicted MFS transporters, permeases, multi-drug resistance proteins, and ABC transporters are expressed in wheat and barley, but not rice. This suggests trans-membrane transporters could play important roles in pathogenesis, making them attractive targets for functional analysis. The current study of trichothecene efflux in *F. graminearum* demonstrated the MFS transporter FgTri12p is a virulence factor. This plasma membrane bound protein influences the efflux of trichothecene from *F. graminearum in vitro* and *in vivo*, and appears to reach the plasma membrane via a process reminiscent of exocytosis. Recently, exocytosis has

been proposed as playing a role in the efflux of aflatoxin from *A. paraciticus* (Chanda et al., 2010). It is possible that exocytosis is active in the export of other secondary metabolites from fungal cells, though comprehensive study of this possible association has not been undertaken.

Fungal response to induced defense responses

Phenylpropanoids are well-studied compounds instrumental in plant response to fungal invasion. This pathogen induced response may present physical barriers to infection due to lignification of host walls, a process dependent on plant phenylpropanoid biosynthesis. These compounds may also function as an inhibitory chemical defense against pathogens (Naoumkina et al., 2010). During the course of infection, the fungus must negotiate the plant defenses supported by phenylpropanoid biosynthesis. Several genes that encode mechanisms *F. graminearum* uses to deal with phenylpropanoids were expressed exclusively *in planta*. Phenylpropanoids are produced from chorismate derived from the shikimic acid pathway (Parker et al., 2009). Dehydroquinate and dehydroshikimate metabolites from within this pathway can be used by plants to produce quinate, which in turn can be used to produce chlorogenic acids (Singh and Christendat, 2006). Eight genes encoding proteins implicated in phenylpropanoid metabolism and three genes that encode MFS transporters of quinate were expressed among wheat, rice or barley. Additionally, two genes encoding chloroperoxidase were expressed exclusively in wheat and barley. Collectively, the exclusive expression of these genes *in planta* suggests *F. graminearum*

not only recognizes and metabolizes plant defense related compounds, but also may take steps to metabolize upstream precursors of these defenses.

Conclusion

The comparative analysis of genes expressed by *F. graminearum* in wheat and rice, along with previous work in barley, expanded the knowledge of genes expressed by the fungus *in planta* and led to the identification of target genes for functional analysis. Two of the genes selected for analysis based on their exclusive expression *in planta* were demonstrated to influence virulence in wheat. *Tri9*, one of two genes in the trichothecene biosynthetic cluster with unknown function, has a considerable influence on trichothecene production. Moreover, this study provides evidence that a trypsin protein secreted by *F. graminearum* influences virulence. Collectively, genes involved in diverse biological or biochemical functions, conserved signaling pathways, and primary metabolism have been identified as virulence or pathogenicity factors (Wang et al., 2011). However, none of the genes are expressed exclusively *in planta.* With the exception of *FGSG_11164*, the only other virulence factors expressed exclusively in plants are genes involved in trichothecene production. With the recent completion of genomic sequencing of *F. oxysporum*, *F. verticillioides*, and *Nectria haematococca,* additional genomic resources are now available to develop tools for the comparative analysis of genes expressed by plant pathogenic *Fusarium* species during infection of their respective hosts. These resources will likely shed light on the biological significance of *F. graminearum* genes that are without defined function and lead to the identification

of additional pathogenicity and virulence factors that directly control the outcome of plant-fungal interactions. Recently, the induction of trichothecene biosynthesis by specific polyamines has linked morphological differentiation and trichothecene biosynthesis in culture (Chapter 2; Gardiner et al., 2009b). How polyamines induce toxin synthesis and cellular differentiation and the mechanisms by which these processes are coordinately regulated are still a mystery. Genes encoding these mechanisms are likely pathogenicity factors, making their identification and characterization imperative.

Methods

Strains and culture conditions

F. graminearum wild-type strain PH-1 (NRRL 31084) and all mutants were cultured at 25°C in liquid carboxymethylcellulose (CMC) medium (Per liter: low viscosity carboxmethylcellulose (Sigma), 15.0 g; NH_4NO_3 1.0 g; KH_2PO_4, 1.0 g; $MgSO_4$-$7H_2O$, 0.5 g; yeast extract (Difco)) for five days. Spores were harvested from cultures by centrifugation at 3000 rpm for 10 min. Conidia were washed twice with sterile distilled H_2O. Spore concentrations were determined using a hemacytometer.

Liquid trichothecene biosynthesis induction (TBI) cultures contained medium adapted from Gardiner et al., (2009b). Per liter, 1X TBI medium contained: sucrose, 30 g; 2 g $NaNO_3$, 2 g; 1 g KH_2PO_4, 1 g; $MgSO_4 \cdot 7H_2O$, 0.5 g; KCl, 0.5 g; $FeSO_4 \cdot 7H_2O$, 10 mg; putrescine 800 mg, and 200 µL of trace element solution (per 100 mL; citric acid, 5 g;

$ZnSO_4 \cdot 7H_2O$, 5 g; $CuSO_4 5H_2O$, 0.25 g; $MnSO_4 \cdot H_2O$, 50 mg; H_3BO_3, 50 mg; $NaMoO_4 \cdot 2H_2O$, 50 mg). In all cases, TBI stock medium was sterilized by passing it through a 0.45 μM bottle top filter (Corning). Tissue for DNA extraction was cultured in complete medium (CM) (Corell et al., 1987) for seven days at 25°C.

Plant growth, inoculation, and mycotoxin and ergosterol analysis

Wheat plants (*Triticum aestivum*) – cultivar Bobwhite – and rice plants (*Oryza sativa* spp. Japonica M210) were grown in temperature and light controlled growth chambers. Six seeds of wheat were planted in 6-in. pots filled with Sunshine LG3 soil mixture (Sun Gro Horticulture, Bellevue, WA). Plants were exposed to 16 hours of continuous light per day. Temperatures were maintained at 18˚C during the daytime and 16˚C at night. Six seeds of rice were planted in 6-in. pots filled with autoclaved topsoil. Rice plants were exposed to 14 hours of continuous light per day. Temperatures were maintained at 30˚C during the daytime and 23˚C at night. Rice plants were provided with an excess of H_2O throughout the growing and experimental period. In order to minimize variation due to environmental conditions, five days prior to inoculation, rice and wheat plants approaching anthesis were placed in the same chamber using a randomized block design. Temperature and light cycles were adjusted to 12 hours dark and 12 hours light with daytime temperatures of 20˚C and night temperatures of 18˚C.

Rice panicles and wheat heads were inoculated at early- to mid-anthesis. Both inflorescence types were sprayed to run-off with a hand-held sprayer containing a spore

suspension (1.2×10^5 spores per ml in 0.01% Triton X100). Spores were freshly prepared from CMC cultures on the day of inoculation. Following inoculation, heads and panicles were placed in plastic bags and returned to the growth chamber. Plastic bags were removed after 48 hours. Heads and panicles harvested 48, 96, and 192 hai were flash frozen in liquid nitrogen and stored at -80˚C. Samples of infected wheat and rice tissue ground in liquid nitrogen for RNA extraction also were weighed, freeze-dried, and analyzed for the presence of DON, 15ADON, and ergosterol as previously described (Goswami and Kistler, 2005, Dong et al., 2006).

Nucleic acid extraction, RNA labeling, and hybridization

Total RNA was isolated from infected wheat heads and rice panicles with TRIzol™ reagent (Invitrogen, Carlsbad, CA) using the manufacturer's protocol with the following modifications. Four rice panicles or wheat heads per time point were used for RNA extraction. Approximately eight volumes of TRIzol™ per one volume of fungus-infected plant tissue were used for RNA extraction. Tissues were finely ground in liquid nitrogen prior to extraction. After treatment with TRIzol™, each sample was washed three times with chloroform before isopropanol precipitation and a final 75% EtOH wash. RNA pellets were re-suspended in RNase free ddH_2O. Ten micrograms of total RNA were treated according to the Affymetrix eukaryotic RNA labeling protocols (Affymetrix, Santa Clara, CA). One GeneChip each was used for the three biological replicates of each time point in each experiment. Hybridizations, washes, and chip reading followed

standard Affymetrix procedures (http://www.affymetrix.com/support/index.affx) in use at the Biomedical Image Processing Facility at the University of Minnesota.

Analysis of microarray data

GeneChip hybridization signals were scanned with a GeneChip GCS 3000 scanner (Affymetrix, Santa Clara, CA) and the cell intensity (CEL) files were obtained from software GCOS 1.2 (Affymetrix, Santa Clara, CA). CEL files for *F. graminearum* isolate Butte86-AD transcript expression in barley at 48, 96, and 144 hai (experiment FG1); *F. graminearum* isolate PH-1 transcript expression in complete (CM), nitrogen starvation MM-N, and carbon starvation (MM-C) media after 12 hours (experiment FG2); *F. graminearum* isolate PH-1 transcript expression in newly formed conidia and conidia germination in complete medium for 2, 8, and 24 hours (experiment FG7); and *F. graminearum* isolate CS3005 transcript expression in defined media containing either glutamine or agmatine (experiment FG14) were obtained from the Plant Expression Database (www.plexdb.org; Wise et al., 2007) (Table 1). Methods used to generate these profiles can be found in Güldener et al., 2006, Seong et al., 2008, and Gardiner et al., 2009a. All files were loaded into the Expressionist Pro Refiner Array software version 5.2 (Genedata, San Francisco, CA). Refiner Array was used to provide a quality assessment of each hybridization scan based on chip statistics, control gene statistics, and the presence of chip defects. Data from experiments rated "good" were condensed using the Robust Multichip Analysis (RMA) algorithm (Irizarry et al., 2003) as implemented in the Refiner Array Software.

A series of steps was employed to identify transcripts that were present exclusively in a single plant species or combination of species but not present under any *in vitro* condition. In order for a transcript to be considered present, a probe set specific to that transcript had to be detected on all three GeneChips used to analyze tissue at a specific time point. Initially, expression profiles for all *in vitro* experiments were used to identify and assemble probe sets that were considered to be present at a detection P value ≤ 0.01. Probe sets called present at $P \leq 0.01$ at any time point during the infection of wheat, rice or barley then were assembled separately. Probe sets present *in vitro* were then subtracted from those called present *in planta*. This resulted in a refined group of probe sets present in a given plant type but not in any condition in culture. Refined probe sets from each plant species were compared to determine an exclusive or common presence of transcripts expressed within each plant species.

Probe set-gene association and gene categorization

The association between oligonucleotide probe sets and predicted genes was determined using the MIPS *F. graminearum* Genome Database FGDB (http://mips.helmholtz-muenchen.de/genre/proj/FGDB/) (Wong et al., 2011). Categorization of gene functions were assigned by the MIPS Functional Catalogue (FunCat; Ruepp et al., 2004) as implemented in FGDB. Genes expressed exclusively during infection of a single plant species or combinations of species were categorized for predicted function. To determine enrichment for particular gene categories within derived gene lists, a hypergeometric

distribution was used to calculate the cumulative probability of each single category, drawing from the population of total genes in that category found in the genome as a whole.

Protoplasting and transformation

Conidia were harvested from a five-day old CMC medium. One ml of 10^8 ml^{-1} washed conidia was used to inoculate a 100 ml YEPD (yeast extract, 3.0 g; Bactopeptone (Difco), 10.0g; glucose, 20.0 g; and distilled water to 1 l) culture that was incubated for 16-18 hours at room temperature with shaking at 150 rpm. Tissue present after incubation was used to prepare protoplasts. Protoplast preparation and fungal transformation were performed as described previously (Hou et al., 2002).

Targeted gene deletion

F. graminearum genes FGSG 03539 (*Tri9*), FGSG 04581, FGSG_08080, and FGSG_11164 were deleted in the wild-type strain PH-1 by split-marker recombination mutagenesis (Catlett et al., 2003) with previously described modifications (Goswami et al., 2006). DNA oligonucleotides listed in Table 2 were used to PCR amplify regions 5' and 3' of the coding regions of these genes. The right and left flanks of the hygromycin B resistance gene *hph* were amplified using pCX62, which contains the *hph* gene as a template and oligonucleotides also listed in Table 2. Transformants were initially screened on V8 agar plates containing 250 mg ml^{-1} hygromycin B. DNA samples from

resistant colonies were screened via PCR for the presence of the *hph* gene and the absence of the region targeted for deletion. Strains fulfilling these requirements were used to inoculate wheat spikes to test for phenotypic differences *in planta*.

Gene complementation

The full genomic sequence of FGSG 03539 (*Tri9*) as well as the 488 bp 5' upstream and 500 bp 3' downstream regions of the flanking genomic sequence were PCR amplified using the phosphorylated DNA oligonucleotides listed in Table 2. Genomic DNA from PH-1 was used as a template. The resulting amplicon was purified through a Qiagen PCR purification column and blunt end cloned into pSM334, which contains a copy of the neomycin/geneticin resistance gene *neo* that was utilized for selection of transformed complementation strains. Prior to ligation, pSM334 was digested with *EcoRV*, treated with shrimp alkaline phosphotase (Fermentas, Glen Burnie, MD), and purified through a PCR purification column (Qiagen, Valencia, CA).

Geneticin resistant transformants were isolated and gene replacement mutations were confirmed by restriction enzyme digestion of PCR amplicons and Southern hybridization. V8 juice agar (200 ml V-8 juice (Campbell Soup Company, Camden NJ), 2 g $CaCO_3$, 15 g agar, water to 1 l) supplemented with 250 mg ml^{-1} geneticin (Invitrogen, Carlsbad, California) was used for selection of transformants.

Genomic DNA extraction and Southern blotting

Cultured tissues were washed twice with ddH_2O and freeze-dried. Genomic DNA was extracted from dried cultures using G Biosciences Omniprep DNA kits. Genomic DNA used for Southern blotting was treated with RNAse A at room temperature for 15 minutes before digestion. For Southern blotting analysis, 20 µg of genomic DNA were digested. To characterize PH-1*tri9*, PH-1*tri9/Tri9*, and PH-1 strains, DNA samples were digested with *SpeI*. To characterize the FGSG_11164 deletion mutant and PH-1, DNAs were digested with *XmnI*. Probes were used to detect the presence of *hph*, *neo*, *Tri9*, and FGSG_11164 in the appropriate fungal strains via hybridization. The DNA oligonucleotides listed in Table 2 were used to synthesize these probes. Southern hybridization was performed as described by Rosewich et al. (1998), except probe hybridization and primary wash temperatures were increased to 65˚ C. The Amersham AlkPhos Direct Labeling and Detection System with CDP-Star (GE Healthcare) was used to label and detect the DNA probes.

Pathogenicity and *in planta* mycotoxin assays

Wheat plants (*Triticum aestivum*), cultivar Norm, were grown as previously described (Goswami and Kistler, 2005). After its awns were removed, the fifth spikelet above the first fully developed basal spikelet was inoculated with 10µl of a conidia suspension of 1 x 10^5 conidia ml^{-1} + 0.1% Triton X100. After inoculation, wheat plants were placed in a humidity chamber for 48 hours. Plants were then transferred to a lighted growth chamber

and allowed to grow for an additional eight days. Plants were exposed to a repeating 16/8 hour day/night diurnal cycle with daytime and nighttime temperatures maintained at 18° and 16°C, respectively. For pathogenicity determination, mycotoxin measurement, and average mass of infected spike measurements, single-point inoculated spikes were scored for disease at 10 days after inoculation and then collected, weighed, and stored at -20°C. The five upper and four lower spikelets adjacent to the inoculated spikelet, as well as the inoculated spikelet itself, were scored for disease symptoms. Quantification of deoxynivalenol (DON) and 15-acetlydeoxynivalenol (15ADON) in inoculated spikelets was conducted as previously described (Goswami and Kistler, 2005). Pathogenicity values for all strains as well as *in planta* trichothecene levels for PH-1 and *tri9* and *tri9/Tri9* mutants were determined from three independent biological replicates.

Trichothecene biosynthesis in liquid culture

Stationary liquid TBI cultures (2 ml) inoculated with 2 x 10^4 conidia were used to assay trichothecene production *in vitro* in cell culture plates (Corning, Lowell, MA). Cultures were incubated at 25°C in total darkness for seven days. Culture medium was filtered through cheesecloth to remove fungal tissue and freeze-dried. Dried samples were analyzed for the presence of DON and 15ADON as previously described. Results for *in vitro* trichothecene production by PH-1, PH-1*tri9,* and PH-1*tri9/Tri9* strains are based on nine biological replicates

Tables

Table 1. Microarray-based transcript profiles for *F. graminearum* obtained from PLEXdb (www.plexdb.org).

PLEXdb Experiment (www.plexdb.org)	Study	Condition	Replicate	File Name
FG1: Fusarium transcript detection on Morex barley spikes using Fusarium Affy GeneChips	Güldener, U., et al. (2006) Development of a *Fusarium graminearum* Affymetrix GeneChip for profiling fungal gene expression *in vitro* and *in planta*. *Fungal Genetics and Biology* 43: 316-325.	*F. graminearum* on barley 48 hours after inculation	1	R3_F48_fusarium
			2	R4_F48_fusarium
			3	R5_F48_fusarium
		F. graminearum on barley 96 hours after inculation	1	R3_F96_fusarium
			2	R4_F96_fusarium
			3	R5_F96_fusarium
		F. graminearum on barley 144 hours after inculation	1	R3_F144_fusarium
			2	R4_F144_fusarium
			3	R5_F144_fusarium
FG2: Expression profiles in carbon and nitrogen starvation conditions		Mycelia incubated in CM media for 12 hours	1	000242_CM-1-2
			2	000234_CM-2
			3	000235_CM-3
		Mycelia incubated in MM-C media for 12 hours	1	000243_MM-C-1-2
			2	000237_MM-C-2
			3	000238_MM-C-3
		Mycelia incubated in MM-N media for 12 hours	1	000239_MM-N-1
			2	000240_MM-N-2
			3	000241_MM-N-3
FG7: Fusarium gene expression profiles during conidia germination stages	Seong, K. Y., X. Zhao, J. R. Xu, U. Güldener & H. C. Kistler, (2008) Conidial germination in the filamentous fungus *Fusarium graminearum*. *Fungal Genetics and Biology* 45: 389-399.	Conidia 0 hours	1	KYS_0_1_fusariam
			2	KYS_0_2_fusariam
			3	KYS_0_3_fusariam
		Conidia incubated in CM media for two hours	1	KYS_2_1_fusariam
			2	KYS_2_2_fusariam
			3	KYS_2_3_fusariam
		Conidia incubated in CM media for eight hours	1	KYS_8_1_fusariam
			2	KYS_8_2_fusariam
			3	KYS_8_3_fusariam
		Conidia incubated in CM media for 24 hours	1	KYS_24_1_fusariam
			2	KYS_24_2_fusariam
			3	KYS_24_3_fusariam
FG14: DON induction media	Gardiner, D. M., K. Kazan & J. M. Manners, (2009a) Novel genes of *Fusarium graminearum* that negatively regulate deoxynivalenol production and virulence. *Molecular Plant-Microbe Interactions* 22: 1588-1600.	Growth in agmatine as the sole nitrogen source for four days	1	Agmatine1
			2	Agmatine2
			3	Agmatine3
			4	Agmatine4
		Growth in glutamine as the sole nitrogen source for four days	1	Glutamine1
			2	Glutamine2
			3	Glutamine3
			4	Glutamine4

Table 2. Oligonucleotides used in this study.

Method	Name	Sequence (5' to 3')
Disruption of FGSG_03539 (*Tri9*)	FGSG_03539_LF1F	GGCCTGTCATGAAAGCTTAAAA
	FGSG_03539_LF2R	TTGACCTCCACTAGCTCCAGCGGCGCGCTTGGAGATTGGGGGTGAGT
	FGSG_03539_RF3F	ATAGAGTAGATGCCGACCGGGCCGGCGACTGCAGTGCCAGATCAGC
	FGSG_03539 _RF4R	ATGATGCATGCAGGGAAGTT
	FGSG_03539_South5P	CAGCCGCTAAACTGATCGAC
	FGSG_03539_South3P	GACCCATATGGTAGCGCATAA
Disruption of FGSG_04581	FGSG_04581_LF1F	TTTGCGCTGCAAGACAGATA
	FGSG_04581_ LF2R	TTGACCTCCACTAGCTCCAGCGGCGCGGCTGATCAGAAGCCATGG
	FGSG_04581_RF3F	ATAGAGTAGATGCCGACCGGGCCGGCGGAGGCATGATGGAAGTG
	FGSG_04581_RF4R	GCTTGATAGCCAGCCTTGAC
Disruption of FGSG_08080	FGSG_08080_LF1F	CAAGTGCTCCGTGTGGTTAC
	FGSG_08080_LF2R	TTGACCTCCACTAGCTCCAGCGGCGCGTCGCCAAGATGTTCTTATCAAA
	FGSG_08080_RF3F	ATAGAGTAGATGCCGACCGGGCCGGCTGACGTCTTTTGTCGCTGTC
	FGSG_08080_RF4R	GAATCTTGCCGAGATGGAAC
Disruption of FGSG_11164 (*Tpp1*)	FGSG_11164_LF1F	CAGTCACCATCTTTCTCATTGC
	FGSG_11164_LF2R	TTGACCTCCACTAGCTCCAGCGGCGCGTGTGACGAAGTAGGAGTTATCCA
	FGSG_11164_RF3F	ATAGAGTAGATGCCGACCGGGCCGGCCGTCGCAACATGACTATGGA
	FGSG_11164_RF4R	ACGCTTGTAGAATGCCCACT
	FGSG_11164_South5P	TCAAGATCACTTCCCTCGTTG
	FGSG_11164_South3P	CGTTGCTGTCGATCCAAGAT
HYG split marker	HYG/R	GCCGGCCCGGTCGGCATCTACTCTAT
	HY/R	GTATTGACCGATTCCTTGCGGTCCGAA
	YG/F	GATGTAGGAGGGCGTGGATATGTCCT
	HYG/F	CGCGCCGCTGGAGCTAGTGGAGGTCAA
Complementation of PH-1*tri9*	FGSG_03539_LF1FPhos	5Phos-GGCCTGTCATGAAAGCTTAAAA
	FGSG_03539_RF4RPhos	5Phos-ATGATGCATGCAGGGAAGTT
	Neo_South5P	GAAGGGACTGGCTGCTATTG
	Neo_South3P	AAGGCGATAGAAGGCGATG

Table 3. Trichothecene concentrations in samples of infected wheat and rice spikelets used for mRNA extraction.

	Trichothecenes[a]			
	[DON]		[15ADON]	
Time (hr)	Wheat	Rice	Wheat	Rice
48	1.5 ± 0.1	0	0.9 ± 0.1	0
96	39.3 ± 0.3	1.0 ± 0.1	14.6 ± 1.1	0.6 ± 0.1
192	172.4 ± 71.1	3.0 ± 0.3	40.4 ± 2.5	0.8 ± 0.1

a. Mean ± SEM parts per million (ppm) in plant tissue exhibiting necrotic symptoms

Table 4. Ergosterol concentration in samples of infected wheat spikelets and rice panicles used for mRNA extraction.

	[Ergosterol][a]	
Time (hr)	Wheat	Rice
48	47.1 ± 4.2	3.3 ± 2.4
96	36.9 ± 21.3	5.4 ± 5.6
192	123.2 ± 71.1	3.7 ± 3.2

a. Mean ± SEM parts per million (ppm) in plant tissue exhibiting necrotic symptoms

Table 5. Pathogenicity and trichothecene concentrations for PH-1, PH-1*tri9*, and PH-1*tri9/Tri9* on wheat.

	Pathogenicity[a,b]		Trichothecenes[c]	
Strain	Symptomatic Spikelets	Mass of Spike	DON	15ADON
PH-1	7.4 ± 0.31	1.53 ± 0.07	503.1 ± 19.3	65.5 ± 3.4
PH-1*tri9*	2.7 ± 0.33[d]	2.07 ± 0.05[e]	214.3 ± 17.0[f]	15.9 ± 2.0[f]
PH-1*tri9/Tri9*	7.1 ± 0.30[g]	1.64 ± 0.05[h]	431.8 ± 24.2[i]	54.8 ± 3.9[i]

a. Mean ± SEM number of wheat spikelets per inflorescence exhibiting necrotic symptoms 10 days after inoculation of a single central spikelet.

b. Mean ± SEM mass of symptomatic spikes 10 days after inoculation of a single central spikelet.

c. Mean ± SEM of the concentration (ppm) of deoxynivalenol (DON) and 15-acetyldeoxynivalenol (15ADON) in inoculated wheat spikelets 10 days after inoculation.

d. Mean significantly less than value for PH-1, Mann-Whitney U test ($P < 0.0001$).

e. Mean significantly greater than value for PH-1, Student's Unpaired t-test ($P < 0.0001$).

f. Mean significantly less than value for PH-1, Student's Unpaired t-test ($P < 0.0001$).

g. Mean significantly greater than value for PH-1*tri9*, Mann-Whitney U test ($P < 0.0001$).

h. Mean significantly less than value for PH-1*tri9*, Student's Unpaired t-test ($P < 0.0001$).

i. Mean significantly greater than less for PH-1*tri9*, Student's Unpaired t-test ($P < 0.0001$).

Table 6. Concentrations of trichothecenes in liquid TBI medium after inoculation with PH-1, PH-1*tri9* or PH-1*tri9/Tri9*.

	Trichothecene Concentration[a,b]	
Strain	15ADON	DON
PH-1	38.8 ± 1.4	1.8 ± 0.05
PH-1*tri9*	12.7 ± 0.7[c]	0.6 ± 0.02[c]
PH-1*tri9*/*Tri9*	49.4 ± 1.3[d]	3.4 ± 0.09[d]

a. Mean ± SEM concentration (ppm) of 15-acetyldeoxynivalenol (15ADON) in clarified culture medium 7 days after inoculation

b. Mean ± SEM concentration (ppm) of deoxynivalenol (DON) in clarified culture medium 7 days after inoculation

c. Mean significantly less than value for PH-1, Student's Unpaired t-test ($P < 0.0001$)

d. Mean significantly greater than value for PH-1*tri9*, Student's Unpaired t-test ($P < 0.0001$)

Table 7. Pathogenicity of the PH-1*tpp1* mutant on wheat.

	Pathogenicity[a,b]	
Strain	Symptomatic Spikelets	Mass of Spike
PH-1	7.7± 0.3	1.38 ± 0.06
PH-1*tpp1*	7.2 ± 0.2[c]	1.52 ± 0.06[d]

a. Mean ± SEM number of wheat spikelets per inflorescence exhibiting necrotic symptoms 10 days after inoculation of a single central spikelet.

b. Mean ± SEM mass of symptomatic spikes 10 days after inoculation of a single central spikelet.

c. Mean significantly less than value for PH-1, Mann-Whitney U test ($P < 0.04$).

d. Mean significantly greater than value for PH-1, Student's Unpaired t-test ($P < 0.03$).

Figures

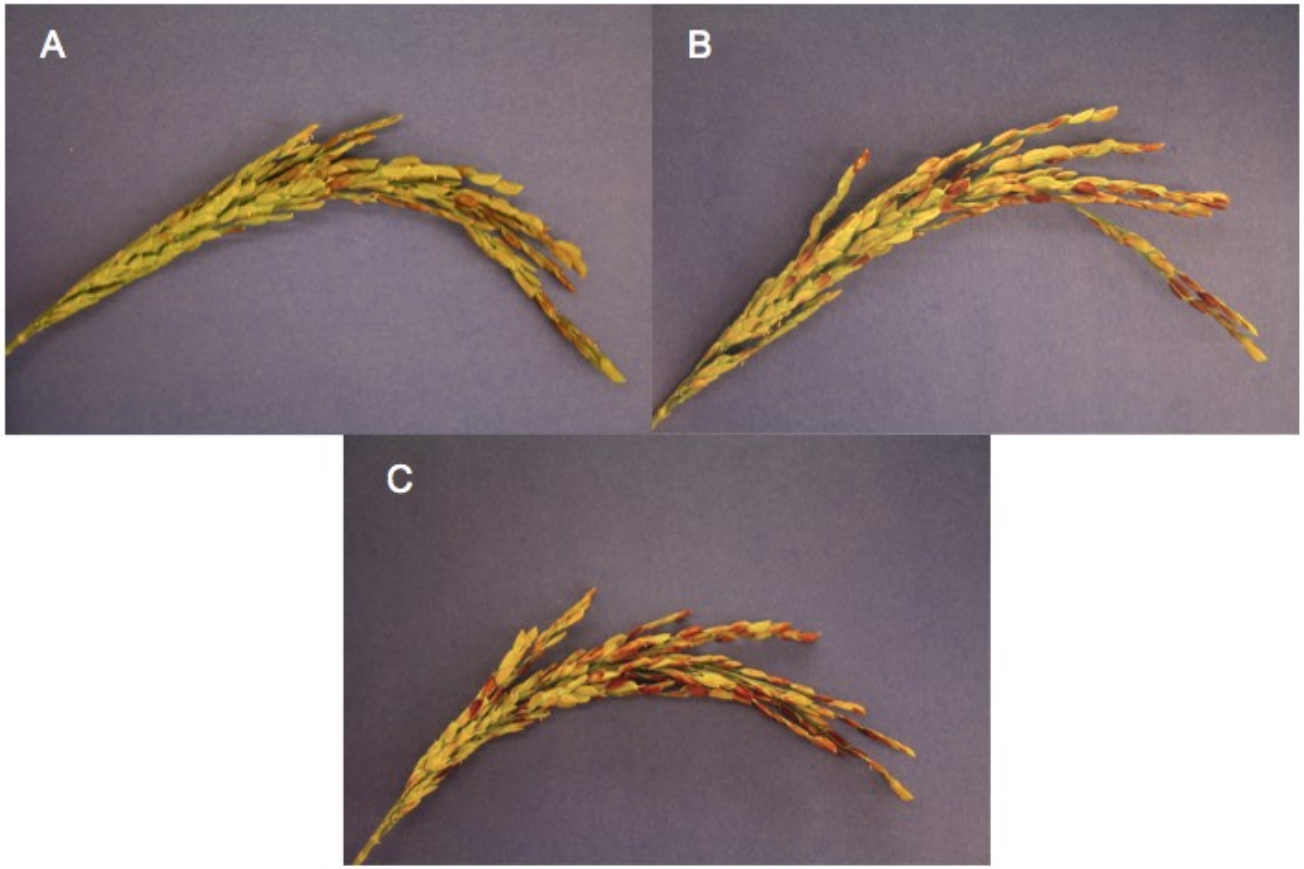

Figure 1. Disease symptoms on rice cultivar M201 inoculated with *F. graminearum* conidia A) 48 hai, B) 96 hai or C) 192 hai.

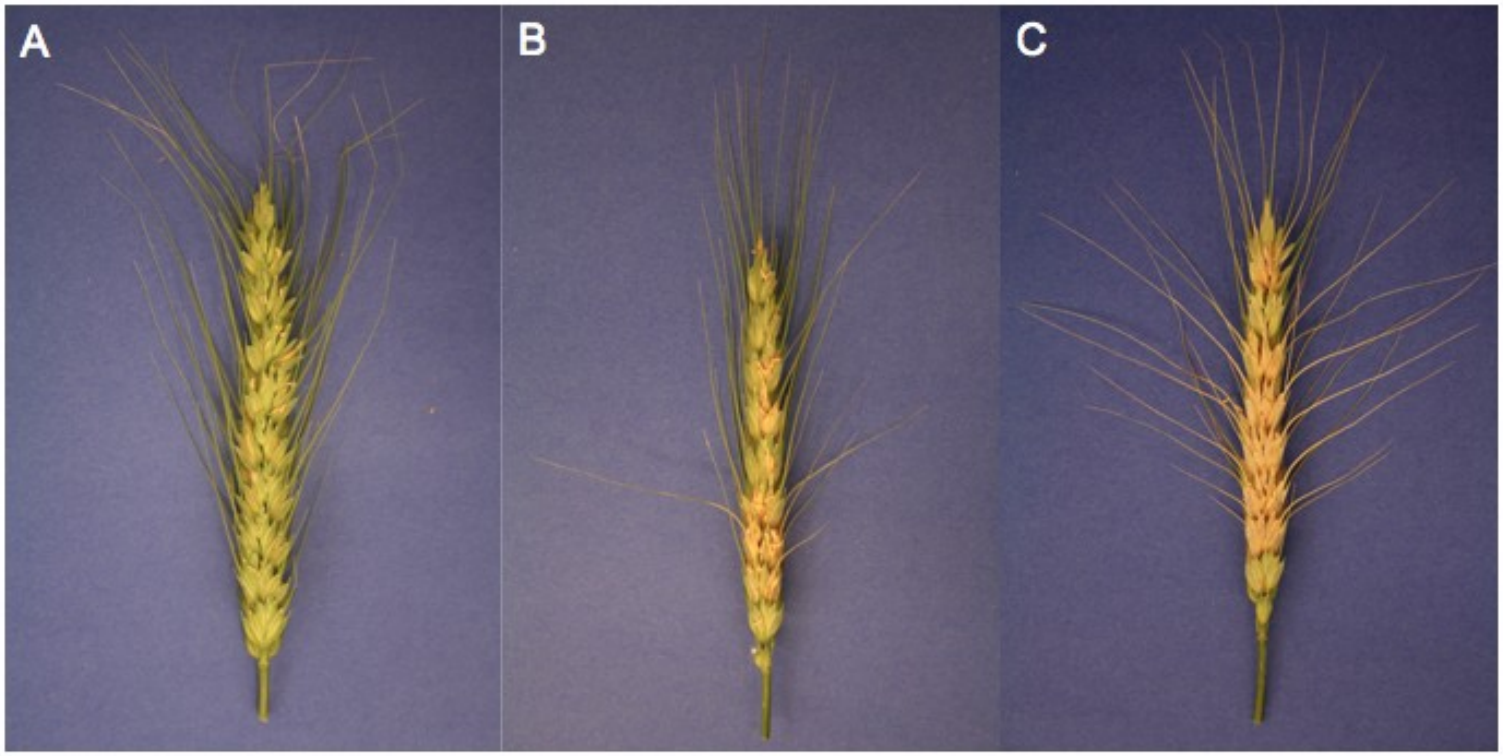

Figure 2. Disease symptoms on wheat cultivar Norm inoculated with *F. graminearum* conidia A) 48 hai, B) 96 hai or C) 192 hai.

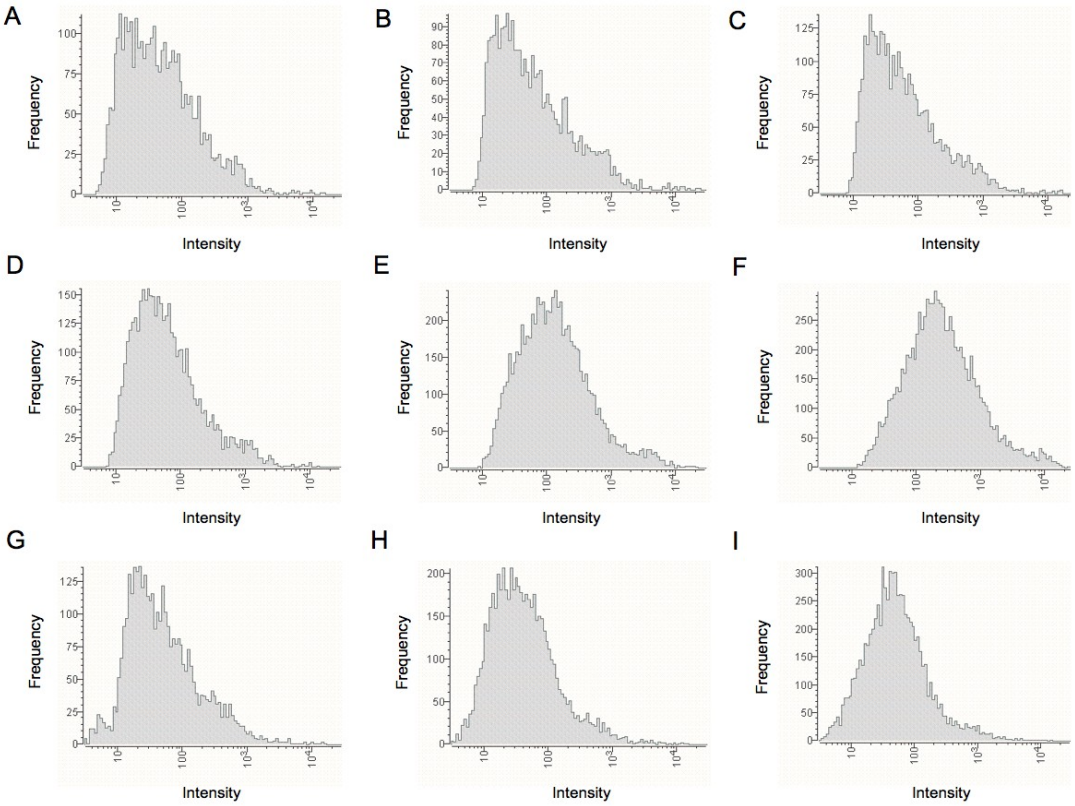

Figure 3. Global distribution of arithmetic means of probe set signal intensities. Each of the 100 bins displayed in each graph are derived from the average signal intensity of three microarray hybridizations for A) rice 48 hai, B) rice 96 hai, C) rice 192 hai, D) wheat 48 hai, E) wheat 96 hai, F) wheat 192 hai, G) barley 48 hai, H) barley 96 hai, and I) barley 144 hai with *F. graminearum* conidia.

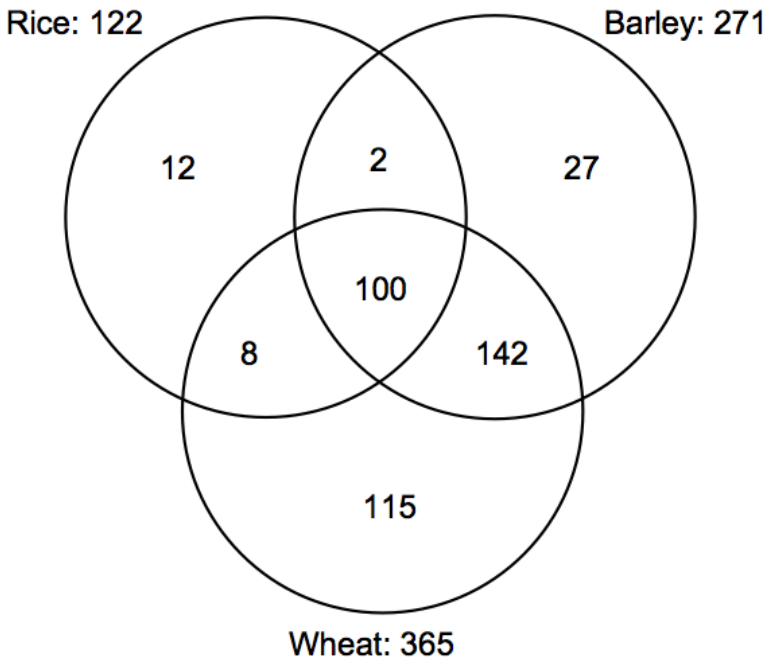

Figure 4. Venn diagram showing *F. graminearum* genes expressed exclusively *in planta*. These genes are expressed in wheat, rice, and barley but not in CM, MM-N, MM-C or in CM spore germination cultures. The identities of the genes in this diagram are listed in supplementary table A.

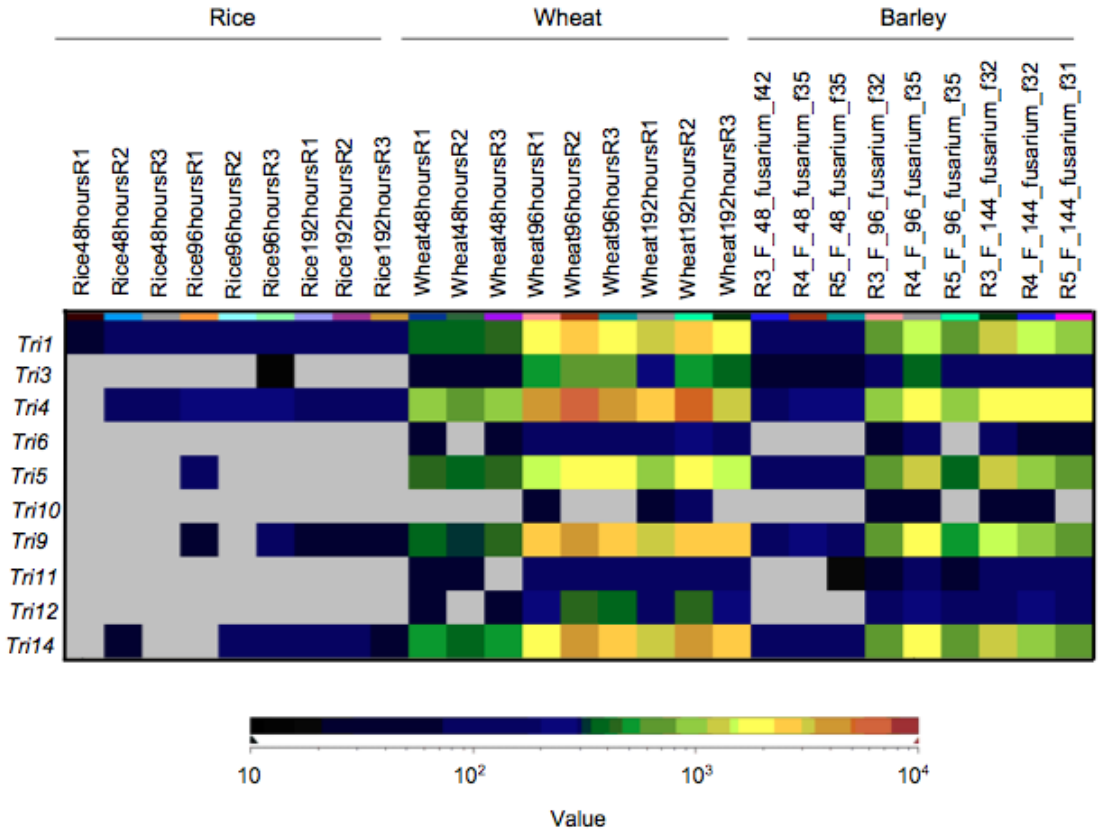

Figure 5. Expression profiles of *F. graminearum* genes involved in trichothecene biosynthesis and efflux in rice, wheat, and barley at early (48 hai), intermediate (96 hai), and late stages of infection (192 hai in rice and wheat; 144 hai in barley).

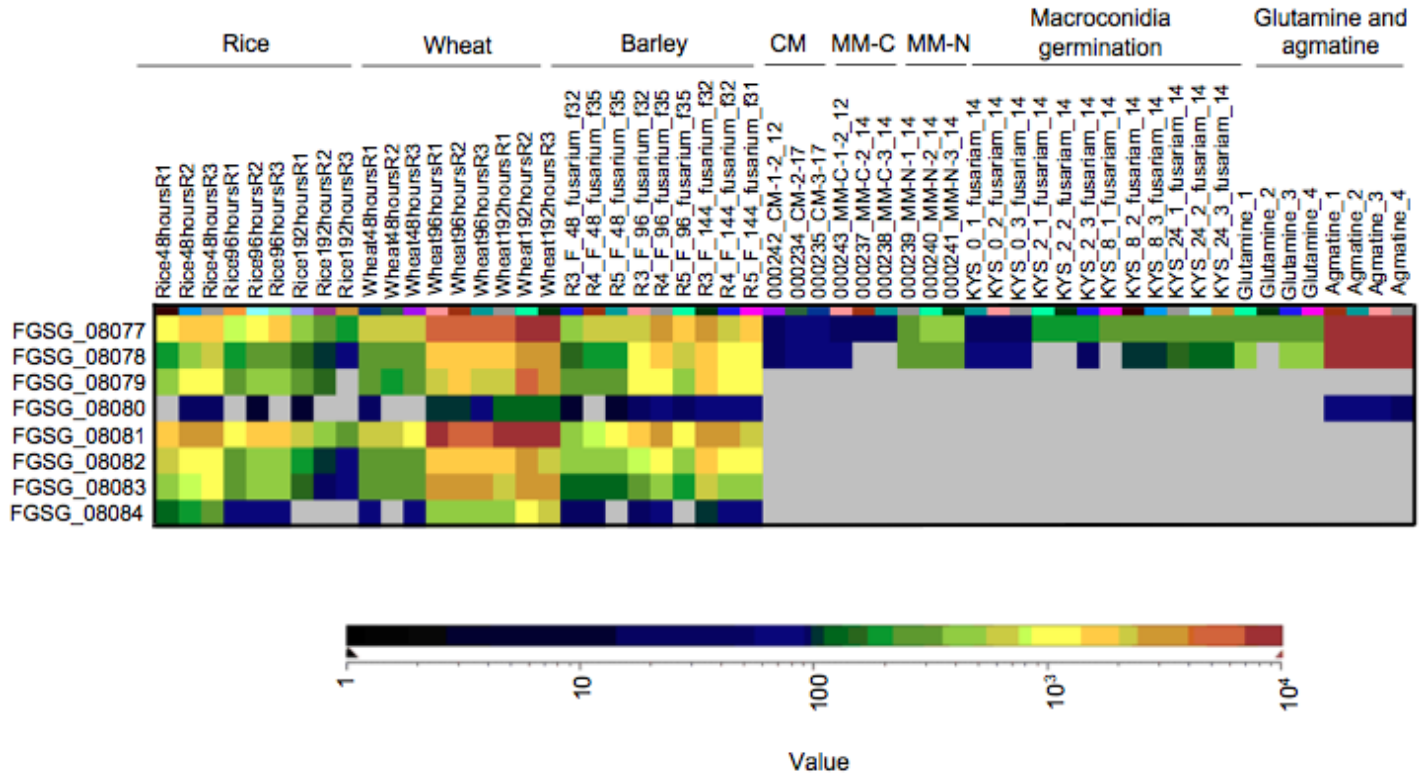

Figure 6. Expression of *F. graminearum* genes in the putative butenolide cluster during the infection of rice, wheat, and barley; growth in CM, MM-C or MM-N; spore germination in CM, and growth in medium containing glutamine or agmatine as a nitrogen source. In the current study, FGSG_08079 – FGSG_08084 are expressed exclusively *in planta*.

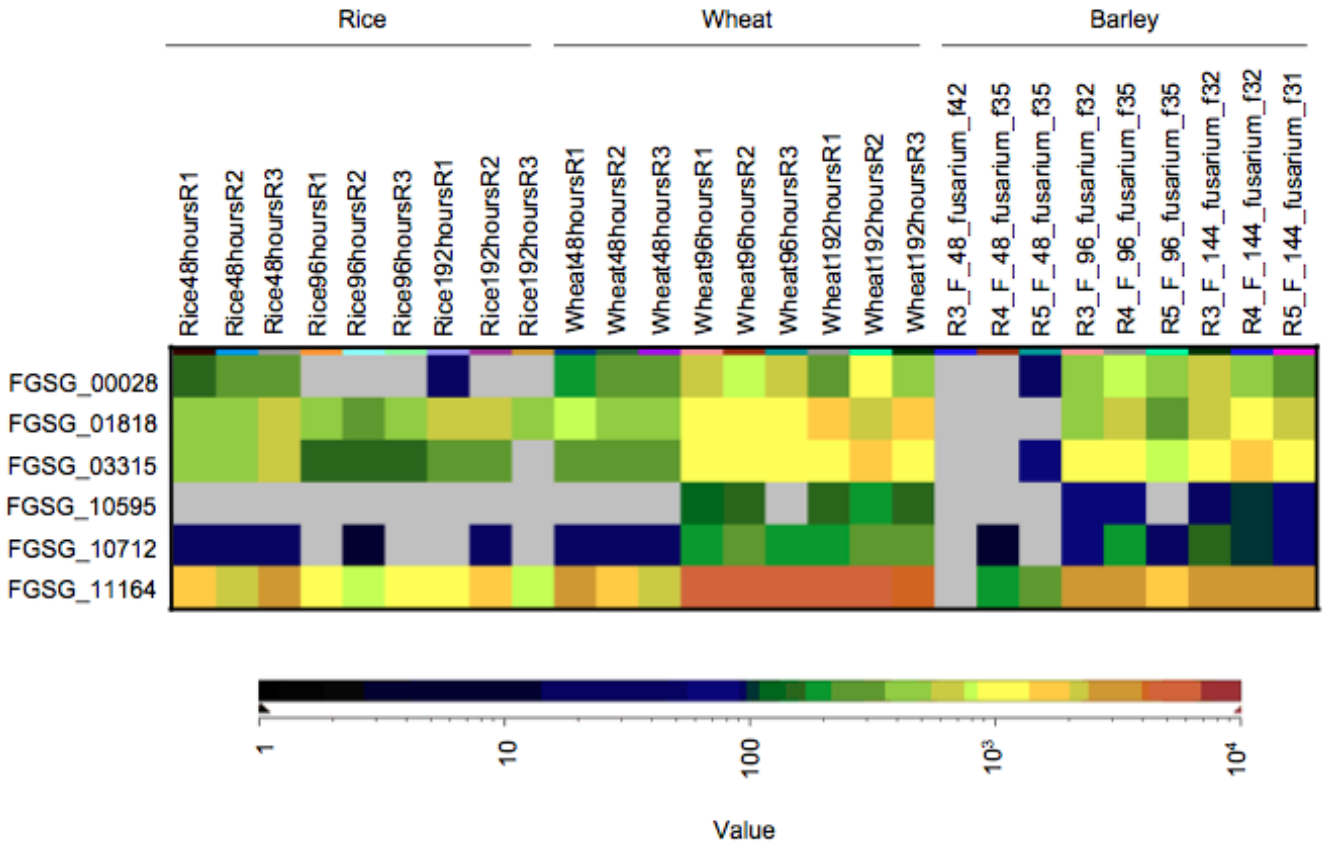

Figure 7. Expression profiles of genes that encode predicted proteases expressed exclusively *in planta*.

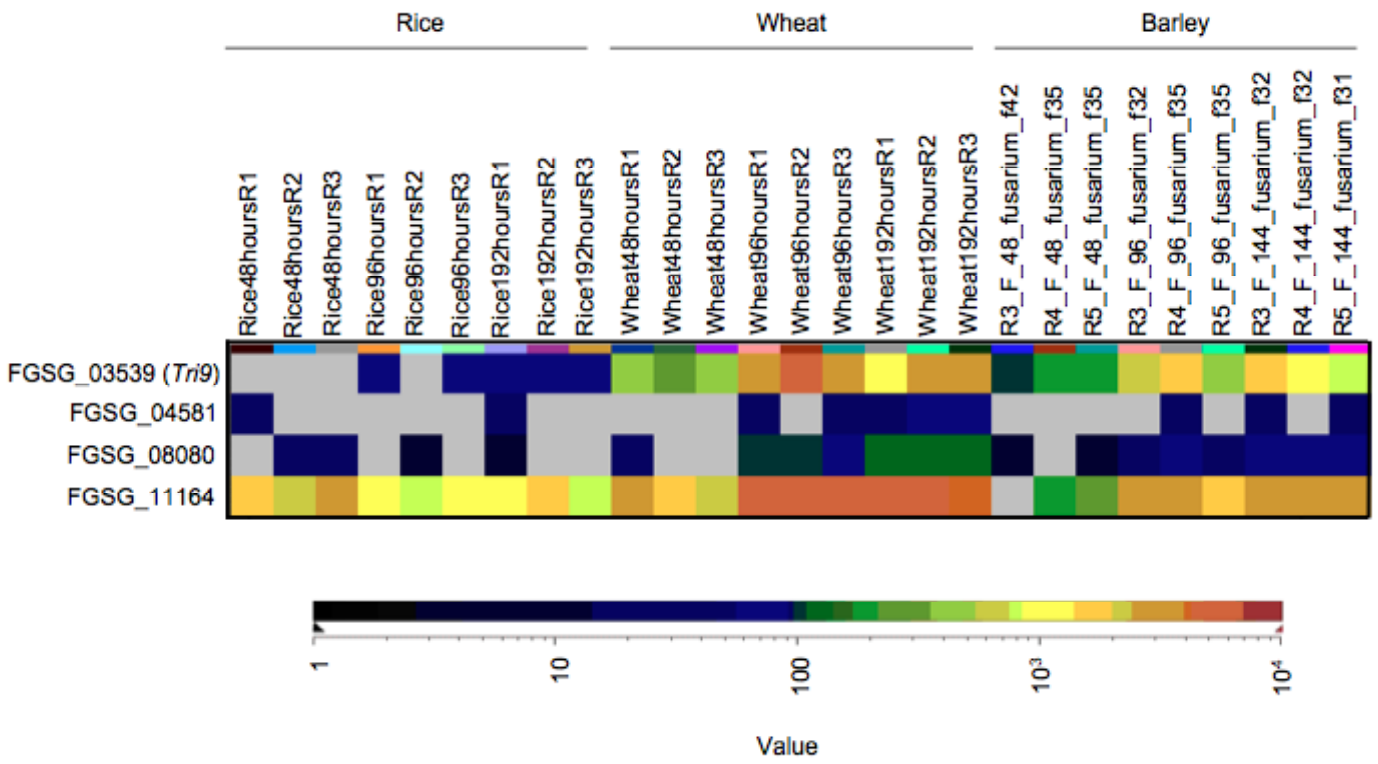

Figure 8. Expression profiles of four genes expressed exclusively *in planta* that were chosen for reverse genetic analysis.

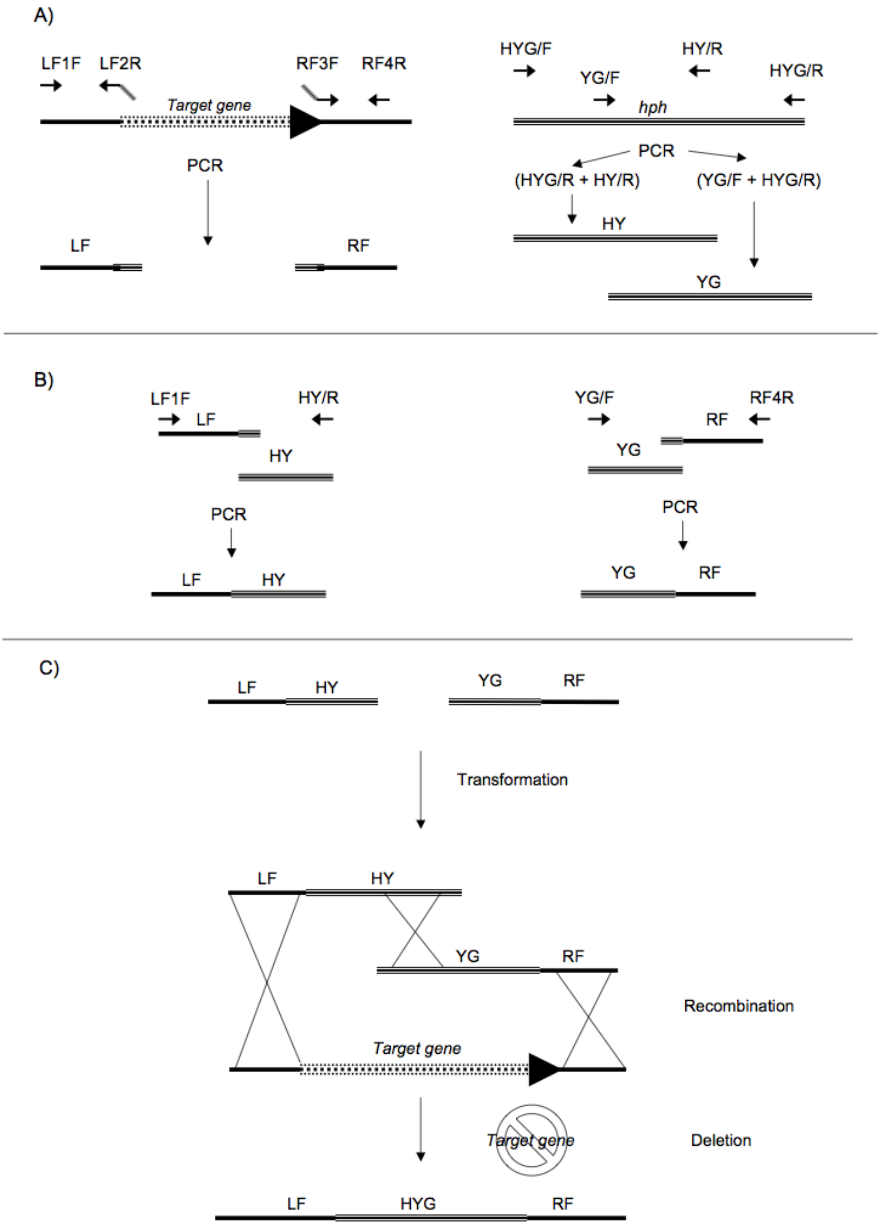

Figure 9. Split marker PCR method used for disruption of targeted genes. A) Left and right flanking (LF and RF) regions of target gene are amplified using LF1F + LF2R and RF3F + RF4R oligonucleotide combinations. Sequences specific to the 5' and 3' regions of *hph* have been added to the 5' ends of LF2R and RF3F. HY and YG regions of the *hph* are amplified using HYG/F + HY/R and HYG/R + YG/R oligonucleotide combinations. B) LF and HY amplicons and LF1F and HY/R oligonucleotides are used to produce LFHY fusion products via PCR. YG and RF amplicons and YG/F and RF4R oligo-nucleotides are used to produce YGRF fusion products via PCR. C) Transformation of protoplasts with LFHY and YGRF fusion products disrupt the target gene via a triple crossover event.

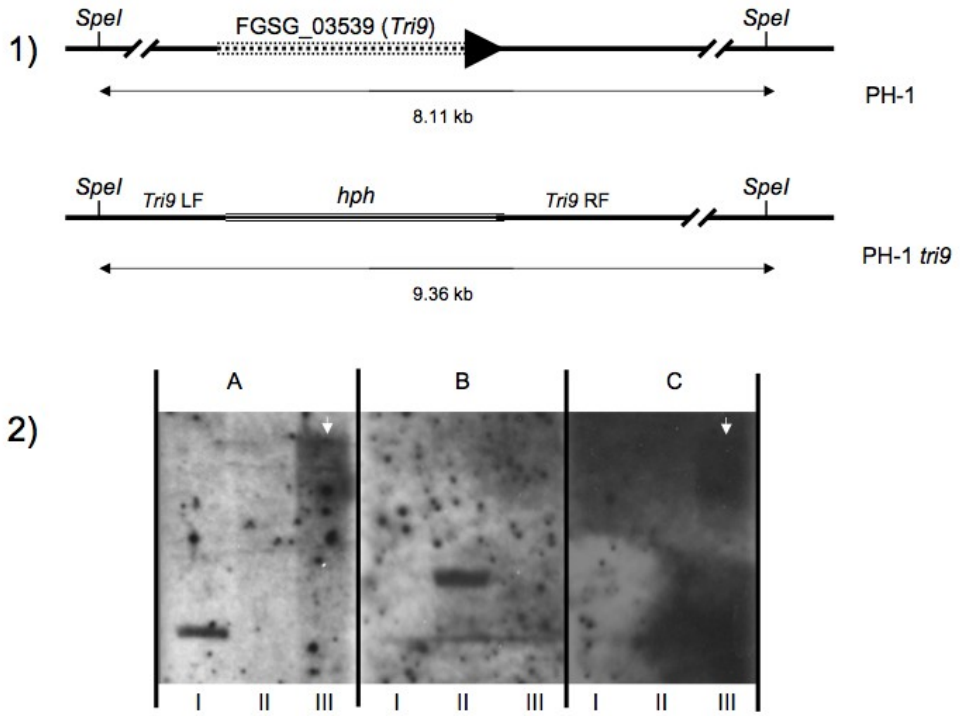

Figure 10. Southern blotting of PH-1*tri9*, PH-1*tri9/Tri9*, and PH-1 genomic DNA. 1) Location of *SpeI* restriction enzyme cut sites in the left and right flanking regions (LF and RF) of PH-1 and PH-1*tri9* and the expected sizes of fragments targeted by hybridization probes. 2) Hybridization of A) *Tri9* B) *hph* C) *neo* specific probes to digested genomic DNA from I) PH-1 II) PH-1*tri9* III) PH-1*tri9/Tri9.* These results demonstrate the presence of single copies of *Tri9* in PH-1 and PH-1*tri9/Tri9,* a single copy of *hph* in PH-1*tri9*, and a single copy of *neo* in PH-1*tri9/Tri9.* The relative sizes of the fragments labeled with the *Tri9* probe in PH-1 DNA and *hp*h probe in PH-1*tri9* DNA are consistent with expected digestion patterns. Integration of the *Tri9* complementation construct resulted in the deletion of the *hph* construct that was present in the PH-1*tri9* strain prior to transformation.

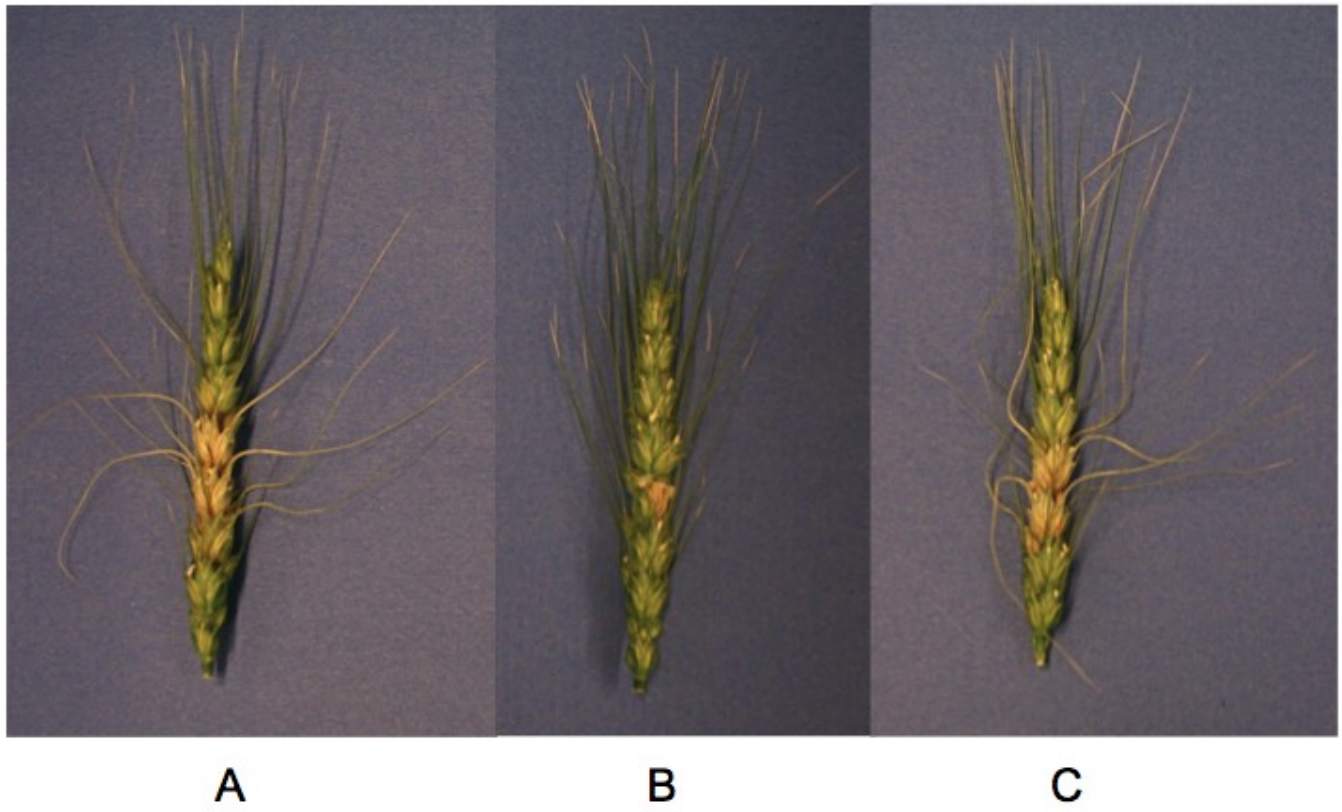

Figure 11. Disease symptoms on infected wheat spikes. A) PH-1, B) PH-1*tri9*, and C) PH-1*tri9/Tri9* strains were used to inoculate a central spikelet of the wheat cultivar Norm. Symptoms of disease are more widespread on spikelets infected with PH-1 and PH-1*tri9/Tri9*.

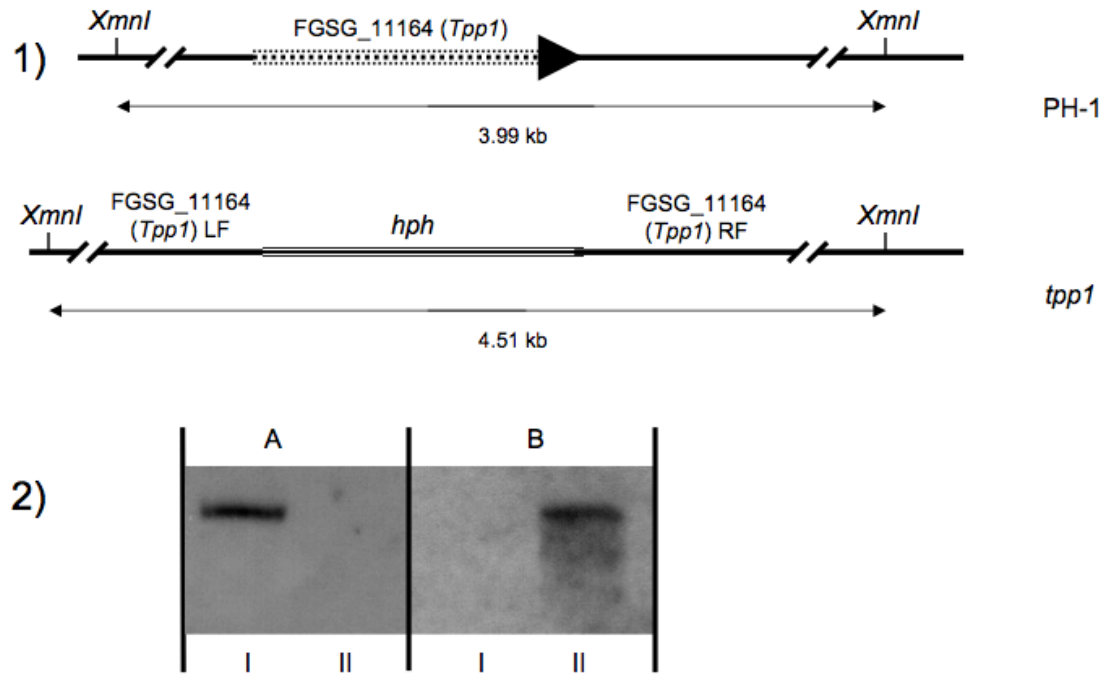

Figure 12. Southern blotting of PH-1*tpp1* and PH-1 genomic DNA. 1) Location of *XmnI* restriction enzyme cut sites in the right and left flanking regions (LF and RF) of PH-1 and PH-1*tpp1* and the expected sizes of the fragments targeted by hybridization probes. 2) Hybridization of A) *Tpp1* or B) *hph* specific probes to digested genomic DNA from I) PH-1 or II) PH-1 *tpp1*. These results demonstrate the presence of a single copy of *Tpp1* in PH-1 and a single copy of *hph* in *tpp1*. The relative sizes of the fragments labeled with the *Tpp1* probe in PH-1 DNA and *hph* probe in PH-1*tpp1* DNA are consistent with expected digestion patterns.

Supplemental Tables

Supplemental table A: Genes expressed exclusively *in planta.*

References

Altschul, S. F., T. L. Madden, A. A. Schaffer, J. H. Zhang, Z. Zhang, W. Miller & D. J. Lipman, (1997) Gapped BLAST and PSI-BLAST: a new generation of protein database search programs. *Nucleic Acids Research* **25**: 3389-3402.

Altschul, S. F., J. C. Wootton, E. M. Gertz, R. Agarwala, A. Morgulis, A. A. Schaffer & Y. K. Yu, (2005) Protein database searches using compositionally adjusted substitution matrices. *FEBS Journal* **272**: 5101-5109.

Boddu, J., S. Cho, W. M. Kruger & G. J. Muehlbauer, (2006) Transcriptome analysis of the barley-*Fusarium graminearum* interaction. *Molecular Plant-Microbe Interactions* **19**: 407-417.

Brown, N. A., M. Urban, A. M. L. Van De Meene & K. E. Hammond-Kosack, (2010) The infection biology of *Fusarium graminearum*: defining the pathways of spikelet to spikelet colonisation in wheat ears. *Fungal Biology* **114**: 555-571.

Bushnell, W.R., B. Hazen, and C Pritsch (2003) Histology and physiology of Fusarium head blight. In *Fusarium Head Blight of Wheat and Barley*. Leonard, K.J. and Bushnell, W.R. (eds). , St. Paul: American Phytopathology Society Press, pp. 44-83.

Calvo, A. M., R. A. Wilson, J. W. Bok & N. P. Keller, (2002) Relationship between secondary metabolism and fungal development. *Microbiology and Molecular Biology Reviews* **66**: 447-459.

Catlett N.I, Lee B.N, Yoder O.C, and Turgeon B.G, (2003) Split-marker recombination for efficient targeted deletion of fungal genes. *Fungal Genet News* **50**: 9–11.

Chanda, A., L. V. Roze & J. E. Linz, (2010) A possible role for exocytosis in aflatoxin export in *Aspergillus parasiticus*. *Eukaryotic Cell* **9**: 1724-1727.

Chilosi, G., C. Caruso, C. Caporale, L. Leonardi, L. Bertini, A. Buzi, M. *et al*. (2000) Antifungal activity of a Bowman-Birk-type trypsin inhibitor from wheat kernel. *Journal of Phytopathology-Phytopathologische Zeitschrift* **148**: 477-481.

Correll, J. C., C. J. R. Klittich & J. F. Leslie, (1987) Nitrate non-utilizing mutants of *Fusarium oxysporum* and their use in vegetative compatibility tests. P*hytopathology* **77**: 1640-1646.

Cuomo, C. A., U. Güldener, J. R. Xu, F. Trail, B. G. Turgeon, A. Di Pietro, *et al*. (2007) The *Fusarium graminearum* genome reveals a link between localized polymorphism and pathogen specialization. *Science* **317**: 1400-1402.

Desjardins, A. E., T. M. Hohn & S. P. McCormick, (1993) Trichothecene biosynthesis in fusarium species - chemistry, genetics, and significance. *Microbiological Reviews* **57**: 595-604.

Dong, Y. H., B. J. Steffenson & C. J. Mirocha, (2006) Analysis of ergosterol in single kernel and ground grain by gas chromatography-mass spectrometry. Journal of *Agricultural and Food Chemistry* **54**: 4121-4125.

Gaffoor, I., D. W. Brown, R. Plattner, R. H. Proctor, W. H. Qi & F. Trail, (2005) Functional analysis of the polyketide synthase genes in the filamentous fungus *Gibberella zeae* (Anamorph *Fusarium graminearum*). *Eukaryotic Cell* **4**: 1926-1933.

Gage, M. J., J. Bruenn, M. Fischer, D. Sanders & T. J. Smith, (2001) KP4 fungal toxin inhibits growth in *Ustilago maydis* by blocking calcium uptake. *Molecular Microbiology* **41**: 775-785.

Gardiner, D. M., K. Kazan & J. M. Manners, (2009a) Novel genes of *Fusarium graminearum* that negatively regulate deoxynivalenol production and virulence. *Molecular Plant-Microbe Interactions* **22**: 1588-1600.

Gardiner, D. M., K. Kazan & J. M. Manners, (2009b) Nutrient profiling reveals potent inducers of trichothecene biosynthesis in *Fusarium graminearum*. *Fungal Genetics and Biology* **46**: 604-613.

Gardiner, D. M., K. Kazan, S. Praud, F. J. Torney, A. Rusu & J. M. Manners, (2010) Early activation of wheat polyamine biosynthesis during Fusarium head blight implicates putrescine as an inducer of trichothecene mycotoxin production. *BMC Plant Biology* **10**: 13.

Goswami, R. S. & H. C. Kistler, (2004) Heading for disaster: *Fusarium graminearum* on cereal crops. *Molecular Plant Pathology* **5**: 515-525.

Goswami, R. S. & H. C. Kistler, (2005) Pathogenicity and *in planta* mycotoxin accumulation among members of the *Fusarium graminearum* species complex on wheat and rice. *Phytopathology* **95**: 1397-1404.

Güldener, U., K. Y. Seong, J. Boddu, S. H. Cho, F. Trail, J. R. Xu, *et al*. (2006) Development of a *Fusarium graminearum* Affymetrix GeneChip for profiling fungal gene expression *in vitro* and *in planta*. *Fungal Genetics and Biology* **43**: 316-325.

Harris, L. J., N. J. Alexander, A. Saparno, B. Blackwell, S. P. McCormick, A. E. Desjardins, *et al*. (2007) A novel gene cluster in *Fusarium graminearum* contains

a gene that contributes to butenolide synthesis. *Fungal Genetics and Biology* **44**: 293-306.

Hou, Z. M., C. Y. Xue, Y. L. Peng, T. Katan, H. C. Kistler & J. R. Xu, (2002) A mitogen-activated protein kinase gene (*MGV1*) in *Fusarium graminearum* is required for female fertility, heterokaryon formation, and plant infection. *Molecular Plant-Microbe Interactions* **15**: 1119-1127.

Howlett, B. J., (2006) Secondary metabolite toxins and nutrition of plant pathogenic fungi. *Current Opinion in Plant Biology* **9**: 371-375.

Ilgen, P., B. Hadeler, F. J. Maier & W. Schafer, (2009) Developing kernel and rachis node induce the trichothecene pathway of *Fusarium graminearum* during wheat head infection. *Molecular Plant-Microbe Interactions* **22**: 899-908.

Irizarry, R. A., B. M. Bolstad, F. Collin, L. M. Cope, B. Hobbs & T. P. Speed, (2003) Summaries of Affymetrix GeneChip probe level data. *Nucleic Acids Research* **31**: e15.

Jansen, C., D. von Wettstein, W. Schafer, K. H. Kogel, A. Felk & F. J. Maier, (2005) Infection patterns in barley and wheat spikes inoculated with wild-type and trichodiene synthase gene disrupted *Fusarium graminearum*. *Proceedings of the National Academy of Sciences of the United States of America* **102**: 16892-16897.

Jia, H. Y., S. H. Cho & G. J. Muehlbauer, (2009) Transcriptome analysis of a wheat near-isogenic line pair carrying fusarium head blight-resistant and -susceptible alleles. *Molecular Plant-Microbe Interactions* **22**: 1366-1378.

Kang, Z. & H. Buchenauer, (2000) Ultrastructural and cytochemical studies on cellulose, xylan and pectin degradation in wheat spikes infected by *Fusarium culmorum*. *Journal of Phytopathology-Phytopathologische Zeitschrift* **148**: 263-275.

Kikot, G. E., R. A. Hours & T. M. Alconada, (2009) Contribution of cell wall degrading enzymes to pathogenesis of *Fusarium graminearum*: a review. *Journal of Basic Microbiology* **49**: 231-241.

Kimura, M., T. Tokai, K. O'Donnell, T. J. Ward, M. Fujimura, H. Hamamoto, T. Shibata & I. Yamaguchi, (2003) The trichothecene biosynthesis gene cluster of *Fusarium graminearum* F15 contains a limited number of essential pathway genes and expressed non-essential genes. *FEBS Letters* **539**: 105-110.

McMullen, M., R. Jones & D. Gallenberg, (1997) Scab of wheat and barley: A re-emerging disease of devastating impact. *Plant Disease* **81**: 1340-1348.

Naoumkina, M. A., Q. A. Zhao, L. Gallego-Giraldo, X. B. Dai, P. X. Zhao & R. A.

Dixon, (2010) Genome-wide analysis of phenylpropanoid defence pathways. *Molecular Plant Pathology* **11**: 829-846.

Nielsen, H., and A Krogh, (1998) Prediction of signal peptides and signal anchors by a hidden Markov model. In *Proceedings of the Sixth International Conference on Intelligent Systems for Molecular Biology (ISMB 6)*. Menlo Park, CA: AAAI Press, pp. 122–130.

Nganje, W. E., D. A. Bangsund, F. L. Leistritz, W. W. Wilson & N. M. Tiapo, (2004) Regional economic impacts of Fusarium head blight in wheat and barley. *Review of Agricultural Economics* **26**: 332-347.

Paper, J. M., J. S. Scott-Craig, N. D. Adhikari, C. A. Cuom & J. D. Walton, (2007) Comparative proteomics of extracellular proteins *in vitro* and *in planta* from the pathogenic fungus *Fusarium graminearum*. *Proteomics* **7**: 3171-3183.

Parker, D., M. Beckmann, H. Zubair, D. P. Enot, Z. Caracuel-Rios, D. P. Overy, *et al*. (2009) Metabolomic analysis reveals a common pattern of metabolic re-programming during invasion of three host plant species by *Magnaporthe grisea*. *Plant Journal* **59**: 723-737.

Pekkarinen, A. I. & B. L. Jones, (2002) Trypsin-like proteinase produced by *Fusarium culmorum* grown on grain proteins. *Journal of Agricultural and Food Chemistry* **50**: 3849-3855.

Pekkarinen, A. I., T. H. Sarlin, A. T. Laitila, A. I. Haikara & B. L. Jones, (2003) Fusarium species synthesize alkaline proteinases in infested barley. *Journal of Cereal Science* **37**: 349-356.

Pestka, J. J. & A. T. Smolinski, (2005) Deoxynivalenol: toxicology and potential effects on humans. *Journal of Toxicology and Environmental Health-Part B-Critical Reviews* **8**: 39-69.

Pritsch, C., G. J. Muehlbauer, W. R. Bushnell, D. A. Somers & C. P. Vance, (2000) Fungal development and induction of defense response genes during early infection of wheat spikes by *Fusarium graminearum*. *Molecular Plant-Microbe Interactions* **13**: 159-169.

Qu, L. J., J. Chen, M. H. Liu, N. S. Pan, H. Okamoto, Z. Z. Lin, C. Y. *et al*. (2003) Molecular cloning and functional analysis of a novel type of Bowman-Birk inhibitor gene family in rice. *Plant Physiology* **133**: 560-570.

Rittenour, W. R. & S. D. Harris, (2010) An *in vitro* method for the analysis of infection-related morphogenesis in *Fusarium graminearum*. *Molecular Plant Pathology* **11**: 361-369.

Rogers, L. M., Y. K. Kim, W. J. Guo, L. Gonzalez-Candelas, D. X. Li & P. E. Kolattukudy, (2000) Requirement for either a host- or pectin-induced pectate lyase for infection of *Pisum sativum* by *Nectria hematococca*. *Proceedings of the National Academy of Sciences of the United States of America* **97**: 9813-9818.

Rosewich, U. L., R. E. Pettway, B. A. McDonald, R. R. Duncan & R. A. Frederiksen, (1998) Genetic structure and temporal dynamics of a *Colletotrichum graminicola* population in a sorghum disease nursery. *Phytopathology* **88**: 1087-1093.

Ruepp, A., A. Zollner, D. Maier, K. Albermann, J. Hani, M. Mokrejs, I. *et al.* (2004) The FunCat, a functional annotation scheme for systematic classification of proteins from whole genomes. *Nucleic Acids Research* **32**: 5539-5545.

Seong, K. Y., M. Pasquali, X. Y. Zhou, J. Song, K. Hilburn, S. McCormick, *et al*. (2009) Global gene regulation by Fusarium transcription factors Tri6 and Tri10 reveals adaptations for toxin biosynthesis. *Molecular Microbiology* **72**: 354-367.

Seong, K. Y., X. Zhao, J. R. Xu, U. Güldener & H. C. Kistler, (2008) Conidial germination in the filamentous fungus *Fusarium graminearum*. *Fungal Genetics and Biology* **45**: 389-399.

Singh, S. A. & D. Christendat, (2006) Structure of Arabidopsis dehydroquinate dehydratase-shikimate dehydrogenase and implications for metabolic channeling in the shikimate pathway. *Biochemistry* **45**: 7787-7796.

Voigt, C. A., W. Schafer & S. Salomon, (2005) A secreted lipase of *Fusarium graminearum* is a virulence factor required for infection of cereals. *Plant Journal* **42**: 364-375.

Wang, L. Q., K. Guo, Y. Li, Y. Y. Tu, H. Z. Hu, B. R. Wang, X. C. Cui & L. C. Peng, (2010) Expression profiling and integrative analysis of the CESA/CSL superfamily in rice. *BMC Plant Biology* **10**: 282.

Wang, Y., W. D. Liu, Z. M. Hou, C. F. Wang, X. Y. Zhou, W. Jonkers, *et al*. (2011) A novel transcriptional factor important for pathogenesis and ascosporogenesis in *Fusarium graminearum*. *Molecular Plant-Microbe Interactions* **24**: 118-128.

Wise, R.P., R.A. Caldo, L. Hong, L. Shen , E.K. Cannon, & J.A. Dickerson (2007) BarleyBase/PLEXdb: A unified expression profiling database for plants and plant pathogens. *In Plant Bioinformatics - Methods and Protocols*. Edwards D. (ed). Totowa, Humana Press, *Methods in Molecular Biology* **406**: 347-363.

Wong, P., M. Walter, W. Lee, G. Mannhaupt, M. Munsterkotter, H. W. Mewes, G. Adam & U. Güldener, (2011) FGDB: revisiting the genome annotation of the plant pathogen *Fusarium graminearum*. *Nucleic Acids Research* **39**: D637-D639.

Yokoyama, R. & K. Nishitani, (2004) Genomic basis for cell-wall diversity in plants. A comparative approach to gene families in rice and Arabidopsis. *Plant and Cell Physiology* **45**: 1111-1121.

Yu, J. H. & N. Keller, (2005) Regulation of secondary metabolism in filamentous fungi. *Annual Review of Phytopathology* **43**: 437-458.

Bibliography

Abenza, J. F., A. Pantazopoulou, J. M. Rodriguez, A. Galindo & M. A. Penalva, (2009) Long-distance movement of Aspergillus nidulans early endosomes on microtubule tracks. *Traffic* **10**: 57-75.

Alexander, N. J., S. P. McCormick & T. M. Hohn, (1999) Tri12, a trichothecene efflux pump from Fusarium sporotrichioides: gene isolation and expression in yeast. *Molecular and General Genetics* **261**: 977-984.

Altschul, S. F., T. L. Madden, A. A. Schaffer, J. H. Zhang, Z. Zhang, W. Miller & D. J. Lipman, (1997) Gapped BLAST and PSI-BLAST: a new generation of protein database search programs. *Nucleic Acids Research* **25**: 3389-3402.

Altschul, S. F., J. C. Wootton, E. M. Gertz, R. Agarwala, A. Morgulis, A. A. Schaffer & Y. K. Yu, (2005) Protein database searches using compositionally adjusted substitution matrices. *Febs Journal* **272**: 5101-5109.

Anand, A., T. Zhou, H. N. Trick, B. S. Gill, W. W. Bockus & S. Muthukrishnan, (2003) Greenhouse and field testing of transgenic wheat plants stably expressing genes for thaumatin-like protein, chitinase and glucanase against *Fusarium graminearum*. *Journal of Experimental Botany* **54**: 1101-1111.

Baba, M., M. Osumi, S. V. Scott, D. J. Klionsky & Y. Ohsumi, (1997) Two distinct pathways for targeting proteins from the cytoplasm to the vacuole/lysosome. *Journal of Cell Biology* **139**: 1687-1695.

Bai, G. H., A. E. Desjardins & R. D. Plattner, (2002) Deoxynivalenol-nonproducing *Fusarium graminearum* causes initial infection, but does not cause disease spread in wheat spikes. *Mycopathologia* **153**: 91-98.

Bai, G. H., F. L. Kolb, G. Shaner & L. L. Domier, (1999) Amplified fragment length polymorphism markers linked to a major quantitative trait locus controlling scab resistance in wheat. *Phytopathology* **89**: 343-348.

Bai, G. H. & G. Shaner, (2004) Management and resistance in wheat and barley to Fusarium head blight. *Annual Review of Phytopathology* **42**: 135-161.

Balconi, C., C. Lanzanova, E. Conti, T. Triulzi, F. Forlani, M. Cattaneo & E. Lupotto, (2007) Fusarium head blight evaluation in wheat transgenic plants expressing the maize b-32 antifungal gene. *European Journal of Plant Pathology* **117**: 129-140.

Baldwin, T. K., M. Urban, N. Brown & K. E. Hammond-Kosack, (2010) A role for Topoisomerase I in *Fusarium graminearum* and *F. culmorum* pathogenesis and

sporulation. *Molecular Plant-Microbe Interactions* **23**: 566-577.

Bernardo, A., G. H. Bai, P. G. Guo, K. Xiao, A. C. Guenzi & P. Ayoubi, (2007) *Fusarium graminearum*-induced changes in gene expression between Fusarium head blight-resistant and susceptible wheat cultivars. *Functional & Integrative Genomics* **7**: 69-77.

Bluhm, B. H. & C. P. Woloshuk, (2006) Fck1, a C-type cyclin-dependent kinase, interacts with Fcc1 to regulate development and secondary metabolism in *Fusarium verticillioides*. *Fungal Genetics and Biology* **43**: 146-154.

Bluhm, B. H., X. Zhao, J. E. Flaherty, J. R. Xu & L. D. Dunkle, (2007) *RAS2* regulates growth and pathogenesis in *Fusarium graminearum*. *Molecular Plant-Microbe Interactions* **20**: 627-636.

Boddu, J., S. Cho, W. M. Kruger & G. J. Muehlbauer, (2006) Transcriptome analysis of the barley-*Fusarium graminearum* interaction. *Molecular Plant-Microbe Interactions* **19**: 407-417.

Boddu, J., S. H. Cho & G. J. Muehlbauer, (2007) Transcriptome analysis of trichothecene-induced gene expression in barley. *Molecular Plant-Microbe Interactions* **20**: 1364-1375.

Breakspear, A., K. J. Langford, M. Momany & S. J. Assinder, (2007) CopA : GFP localizes to putative Golgi equivalents in *Aspergillus nidulans*. *FEMS Microbiology Letters* **277**: 90-97.

Brown, D. W., R. H. Proctor, R. B. Dyer & R. D. Plattner, (2003) Characterization of a Fusarium 2-gene cluster involved in trichothecene C-8 modification. *Journal of Agricultural and Food Chemistry* **51**: 7936-7944.

Brown, N. A., M. Urban, A. M. L. Van De Meene & K. E. Hammond-Kosack, (2010) The infection biology of *Fusarium graminearum*: Defining the pathways of spikelet to spikelet colonisation in wheat ears. *Fungal Biology* **114**: 555-571.

Buerstmayr, H., T. Ban & J. A. Anderson, (2009) QTL mapping and marker-assisted selection for Fusarium head blight resistance in wheat: a review. *Plant Breeding* **128**: 1-26.

Buerstmayr, H., M. Lemmens, L. Hartl, L. Doldi, B. Steiner, M. Stierschneider & P. Ruckenbauer, (2002) Molecular mapping of QTLs for Fusarium head blight resistance in spring wheat. I. Resistance to fungal spread (type II resistance). *Theoretical and Applied Genetics* **104**: 84-91.

Buerstmayr, H., B. Steiner, L. Hartl, M. Griesser, N. Angerer, D. Lengauer, *et al*. (2003)

Molecular mapping of QTLs for Fusarium head blight resistance in spring wheat. II. Resistance to fungal penetration and spread. *Theoretical and Applied Genetics* **107**: 503-508.

Bushnell, W.R., B. Hazen, and C Pritsch (2003) Histology and physiology of Fusarium head blight. In *Fusarium Head Blight of Wheat and Barley*. Leonard, K.J. and Bushnell, W.R. (eds). , St. Paul: American Phytopathology Society Press, pp. 44-83.

Callahan, T. M., M. S. Rose, M. J. Meade, M. Ehrenshaft & R. G. Upchurch, (1999) CFP, the putative cercosporin transporter of Cercospora kikuchii, is required for wild-type cercosporin production, resistance, and virulence on soybean. *Molecular Plant-Microbe Interactions* **12**: 901-910.

Calvo, A. M., R. A. Wilson, J. W. Bok & N. P. Keller, (2002) Relationship between secondary metabolism and fungal development. *Microbiology and Molecular Biology Reviews* **66**: 447-+.

Canci, P. C., L. M. Nduulu, R. Dill-Macky, G. J. Muehlbauer, D. C. Rasmusson & K. P. Smith, (2003) Genetic relationship between kernel discoloration and grain protein concentration in barley. *Crop Science* **43**: 1671-1679.

Catlett N.I, Lee B.N, Yoder O.C, and Turgeon B.G, (2003) Split-marker recombination for efficient targeted deletion of fungal genes. *Fungal Genet News* **50**: 9–11.

Chanda, A., L. V. Roze, S. Kang, K. A. Artymovich, G. R. Hicks, N. V. Raikhel, A. M. Calvo & J. E. Linz, (2009) A key role for vesicles in fungal secondary metabolism. *Proceedings of the National Academy of Sciences of the United States of America* **106**: 19533-19538.

Chanda, A., L. V. Roze & J. E. Linz, (2010) A possible role for exocytosis in aflatoxin export in *Aspergillus parasiticus*. *Eukaryotic Cell* **9**: 1724-1727.

Chang, P. K., J. J. Yu & J. H. Yu, (2004) *aflT*, a MFS transporter-encoding gene located in the aflatoxin gene cluster, does not have a significant role in aflatoxin secretion. *Fungal Genetics and Biology* **41**: 911-920.

Chen, W. P., P. D. Chen, D. J. Liu, R. Kynast, B. Friebe, R. Velazhahan, S. Muthukrishnan & B. S. Gill, (1999) Development of wheat scab symptoms is delayed in transgenic wheat plants that constitutively express a rice thaumatin-like protein gene. *Theoretical and Applied Genetics* **99**: 755-760.

Chilosi, G., C. Caruso, C. Caporale, L. Leonardi, L. Bertini, A. Buzi, *et al*. (2000) Antifungal activity of a Bowman-Birk-type trypsin inhibitor from wheat kernel.

Journal of Phytopathology-Phytopathologische Zeitschrift **148**: 477-481.

Correll, J. C., C. J. R. Klittich & J. F. Leslie, (1987) Nitrate non-utilizing mutants of *Fusarium oxysporum* and their use in vegetative compatibility tests. *Phytopathology* **77**: 1640-1646.

Cuomo, C. A., U. Gueldener, J. R. Xu, F. Trail, B. G. Turgeon, A. Di Pietro, et al. (2007) The *Fusarium graminearum* genome reveals a link between localized polymorphism and pathogen specialization. *Science* **317**: 1400-1402.

Cuthbert, P. A., D. J. Somers & A. Brule-Babel, (2007) Mapping of *Fhb2* on chromosome 6BS: a gene controlling Fusarium head blight field resistance in bread wheat (*Triticum aestivum* L.). *Theoretical and Applied Genetics* **114**: 429-437.

Dahleen, L. S., P. A. Okubara & A. E. Blechl, (2001) Transgenic approaches to combat Fusarium head blight in wheat and barley. *Crop Science* **41**: 628-637.

de la Pena, R. C., K. P. Smith, F. Capettini, G. J. Muehlbauer, M. Gallo-Meagher, R. Dill-Macky, D. A. Somers & D. C. Rasmusson, (1999) Quantitative trait loci associated with resistance to Fusarium head blight and kernel discoloration in barley. *Theoretical and Applied Genetics* **99**: 561-569.

Desjardins, A. E., (2009) From yellow rain to green wheat: 25 years of trichothecene biosynthesis research. *Journal of Agricultural and Food Chemistry* **57**: 4478-4484.

Desmond, O. J., J. M. Manners, A. E. Stephens, D. J. MaClean, P. M. Schenk, D. M. Gardiner, A. L. Munn & K. Kazan, (2008) The Fusarium mycotoxin deoxynivalenol elicits hydrogen peroxide production, programmed cell death and defence responses in wheat. *Molecular Plant Pathology* **9**: 435-445.

Di, R., A. Blechl, R. Dill-Macky, A. Tortora & N. E. Tumer, (2010) Expression of a truncated form of yeast ribosomal protein L3 in transgenic wheat improves resistance to Fusarium head blight. *Plant Science* **178**: 374-380.

Ding, S. L., R. Mehrabi, C. Koten, Z. S. Kang, Y. D. Wei, K. Y. Seong, H. C. Kistler & J. R. Xu, (2009) Transducin beta-like gene *FTL1* is essential for pathogenesis in Fusarium graminearum. *Eukaryotic Cell* **8**: 867-876.

Dong, Y. H., B. J. Steffenson & C. J. Mirocha, (2006) Analysis of ergosterol in single kernel and ground grain by gas chromatography-mass spectrometry. *Journal of Agricultural and Food Chemistry* **54**: 4121-4125.

Dufresne, M., T. van der Lee, S. Ben M'Barek, X. D. Xu, X. Zhang, T. G. Liu, *et al*.

(2008) Transposon-tagging identifies novel pathogenicity genes in Fusarium graminearum. *Fungal Genetics and Biology* **45**: 1552-1561.

Dyer, R. B., R. D. Plattner, D. F. Kendra & D. W. Brown, (2005) *Fusarium graminearum Tri14* is required for high virulence and DON production on wheat but not for DON synthesis *in vitro*. *Journal of Agricultural and Food Chemistry* **53**: 9281-9287.

Emanuelsson, O., S. Brunak, G. von Heijne & H. Nielsen, (2007) Locating proteins in the cell using TargetP, SignalP and related tools. *Nature Protocols* **2**: 953-971.

Eulgem, T. & I. E. Somssich, (2007) Networks of WRKY transcription factors in defense signaling. *Current Opinion in Plant Biology* **10**: 366-371.

Fleissner, A., C. Sopalla & K. M. Weltring, (2002) An ATP-binding cassette multidrug-resistance transporter is necessary for tolerance of *Gibberella pulicaris* to phytoalexins and virulence on potato tubers. *Molecular Plant-Microbe Interactions* **15**: 102-108.

Fried, H. M. & J. R. Warner, (1981) Cloning of yeast gene for trichodermin resistance and ribosomal protein-L3. *Proceedings of the National Academy of Sciences of the United States of America-Biological Sciences* **78**: 238-242.

Gaffoor, I., D. W. Brown, R. Plattner, R. H. Proctor, W. H. Qi & F. Trail, (2005) Functional analysis of the polyketide synthase genes in the filamentous fungus *Gibberella zeae* (Anamorph *Fusarium graminearum*). *Eukaryotic Cell* **4**: 1926-1933.

Gage, M. J., J. Bruenn, M. Fischer, D. Sanders & T. J. Smith, (2001) KP4 fungal toxin inhibits growth in *Ustilago maydis* by blocking calcium uptake. *Molecular Microbiology* **41**: 775-785.

Gardiner, D. M., K. Kazan & J. M. Manners, (2009) Novel genes of *Fusarium graminearum* that negatively regulate deoxynivalenol production and virulence. *Molecular Plant-Microbe Interactions* **22**: 1588-1600.

Gardiner, D. M., K. Kazan & J. M. Manners, (2009) Nutrient profiling reveals potent inducers of trichothecene biosynthesis in *Fusarium graminearum*. *Fungal Genetics and Biology* **46**: 604-613.

Gardiner, D. M., K. Kazan, S. Praud, F. J. Torney, A. Rusu & J. M. Manners, (2010) Early activation of wheat polyamine biosynthesis during Fusarium head blight implicates putrescine as an inducer of trichothecene mycotoxin production. *BMC Plant Biology* **10**: 13.

Gardiner, S. A., J. Boddu, F. Berthiller, C. Hametner, R. M. Stupar, G. Adam & G. J. Muehlbauer, (2010) Transcriptome analysis of the barley-deoxynivalenol interaction: evidence for a role of glutathione in deoxynivalenol detoxification. *Molecular Plant-Microbe Interactions* **23**: 962-976.

Garvey, G. S., S. P. McCormick, N. J. Alexander & I. Rayment, (2009) Structural and functional characterization of Tri3 trichothecene 15-O-acetyltransferase from *Fusarium sporotrichioides*. *Protein Science* **18**: 747-761.

Geddes, J., F. Eudes, A. Laroche & L. B. Selinger, (2008) Differential expression of proteins in response to the interaction between the pathogen Fusarium graminearum and its host, *Hordeum vulgare*. *Proteomics* **8**: 545-554.

Gilbert, J. & W. G. D. Fernando, (2004) Epidemiology and biological control of *Gibberella zeae Fusarium graminearum*. *Canadian Journal of Plant Pathology-Revue Canadienne De Phytopathologie* **26**: 464-472.

Glazebrook, J., (2005) Contrasting mechanisms of defense against biotrophic and necrotrophic pathogens. *Annual Review of Phytopathology* **43**: 205-227.

Golkari, S., J. Gilbert, S. Prashar & J. D. Procunier, (2007) Microarray analysis of *Fusarium graminearum*-induced wheat genes: identification of organ-specific and differentially expressed genes. *Plant Biotechnology Journal* **5**: 38-49.

Goswami, R. S. & H. C. Kistler, (2004) Heading for disaster: *Fusarium graminearum* on cereal crops. *Molecular Plant Pathology* **5**: 515-525.

Goswami, R. S. & H. C. Kistler, (2005) Pathogenicity and in planta mycotoxin accumulation among members of the *Fusarium graminearum* species complex on wheat and rice. *Phytopathology* **95**: 1397-1404.

Goswami, R. S., J. R. Xu, F. Trail, K. Hilburn & H. C. Kistler, (2006) Genomic analysis of host-pathogen interaction between *Fusarium graminearum* and wheat during early stages of disease development. *Microbiology-Sgm* **152**: 1877-1890.

Greenshields, D. L., G. S. Liu, J. Feng, G. Selvaraj & Y. D. Wei, (2007) The siderophore biosynthetic gene *SID1*, but not the ferroxidase gene *FET3*, is required for full *Fusarium graminearum* virulence. *Molecular Plant Pathology* **8**: 411-421.

Guldener, U., G. Mannhaupt, M. Munsterkotter, D. Haase, M. Oesterheld, V. Stumpflen, H. W. Mewes & G. Adam, (2006) FGDB: a comprehensive fungal genome resource on the plant pathogen *Fusarium graminearum*. *Nucleic Acids Research* **34**: D456-D458.

Guldener, U., K. Y. Seong, J. Boddu, S. H. Cho, F. Trail, J. R. Xu, et al. (2006)

Development of a *Fusarium graminearum* Affymetrix GeneChip for profiling fungal gene expression *in vitro* and *in planta*. *Fungal Genetics and Biology* **43**: 316-325.

Haas, H., (2003) Molecular genetics of fungal siderophore biosynthesis and uptake: the role of siderophores in iron uptake and storage. *Applied Microbiology and Biotechnology* **62**: 316-330.

Han, Y. K., M. D. Kim, S. H. Lee, S. H. Yun & Y. W. Lee, (2007) A novel F-box protein involved in sexual development and pathogenesis in *Gibberella zeae*. *Molecular Microbiology* **63**: 768-779.

Harris, L. J., N. J. Alexander, A. Saparno, B. Blackwell, S. P. McCormick, A. E. Desjardins, et al. (2007) A novel gene cluster in *Fusarium graminearum* contains a gene that contributes to butenolide synthesis. *Fungal Genetics and Biology* **44**: 293-306.

Hill-Ambroz, K., C. A. Webb, A. R. Matthews, W. L. Li, B. S. Gill & J. P. Fellers, (2006) Expression analysis and physical mapping of a cDNA library of Fusarium head blight infected wheat spikes. *Crop Science* **46**: S15-S26.

Hohn, T. M., R. Krishna & R. H. Proctor, (1999) Characterization of a transcriptional activator controlling trichothecene toxin biosynthesis. *Fungal Genetics and Biology* **26**: 224-235.

Hollingsworth, C. R., C. D. Motteberg, J. V. Wiersma & L. M. Atkinson, (2008) Agronomic and economic responses of spring wheat to management of Fusarium head blight. *Plant Disease* **92**: 1339-1348.

Honda, S. & E. U. Selker, (2009) Tools for fungal Proteomics: multifunctional neurospora vectors for gene replacement, protein expression and protein purification. *Genetics* **182**: 11-23.

Hong, S. Y. & J. E. Linz, (2008) Functional expression and subcellular localization of the aflatoxin pathway enzyme Ver-1 fused to enhanced green fluorescent protein. *Applied and Environmental Microbiology* **74**: 6385-6396.

Hong, S. Y. & J. E. Linz, (2009) Functional expression and sub-cellular localization of the early aflatoxin pathway enzyme Nor-1 in *Aspergillus parasiticus*. *Mycological Research* **113**: 591-601.

Hong, S. Y., J. So, J. Lee, K. Min, H. Son, C. Park, S. H. Yun & Y. W. Lee, (2010) Functional analyses of two syntaxin-like SNARE genes, *GzSYN1* and *GzSYN2*, in the ascomycete Gibberella zeae. *Fungal Genetics and Biology* **47**: 364-372.

Hong, W. J., (2005) SNAREs and traffic. *Biochimica et Biophysica Acta-Molecular Cell Research* **1744**: 493-517.

Hou, Z. M., C. Y. Xue, Y. L. Peng, T. Katan, H. C. Kistler & J. R. Xu, (2002) A mitogen-activated protein kinase gene (*MGV1*) in *Fusarium graminearum* is required for female fertility, heterokaryon formation, and plant infection. *Molecular Plant-Microbe Interactions* **15**: 1119-1127.

Howlett, B. J., (2006) Secondary metabolite toxins and nutrition of plant pathogenic fungi. *Current Opinion in Plant Biology* **9**: 371-375.

Hubbard, M. A. & S. G. W. Kaminskyj, (2008) Rapid tip-directed movement of Golgi equivalents in growing *Aspergillus nidulans* hyphae suggests a mechanism for delivery of growth-related materials. *Microbiology* **154**: 1544-1553.

Ilgen, P., B. Hadeler, F. J. Maier & W. Schafer, (2009) Developing kernel and rachis node induce the trichothecene pathway of *Fusarium graminearum* during wheat head infection. *Molecular Plant-Microbe Interactions* **22**: 899-908.

Irizarry, R. A., B. M. Bolstad, F. Collin, L. M. Cope, B. Hobbs & T. P. Speed, (2003) Summaries of affymetrix GeneChip probe level data. *Nucleic Acids Research* **31**.

Jansen, C., D. von Wettstein, W. Schafer, K. H. Kogel, A. Felk & F. J. Maier, (2005) Infection patterns in barley and wheat spikes inoculated with wild-type and trichodiene synthase gene disrupted *Fusarium graminearum*. *Proceedings of the National Academy of Sciences of the United States of America* **102**: 16892-16897.

Jenczmionka, N. J., F. J. Maier, A. P. Losch & W. Schafer, (2003) Mating, conidiation and pathogenicity of *Fusarium graminearum*, the main causal agent of the head-blight disease of wheat, are regulated by the MAP kinase Gpmk1. *Current Genetics* **43**: 87-95.

Jenczmionka, N. J. & W. Schafer, (2005) The Gpmk1 MAP kinase of *Fusarium graminearum* regulates the induction of specific secreted enzymes. *Current Genetics* **47**: 29-36.

Jeon, J., S. Y. Park, M. H. Chi, J. Choi, J. Park, H. S. Rho, S. et al. (2007) Genome-wide functional analysis of pathogenicity genes in the rice blast fungus. *Nature Genetics* **39**: 561-565.

Jiang, L. H., J. R. Yang, F. Y. Fan, D. J. Zhang & X. L. Wang, (2010) The Type 2C protein phosphatase FgPtc1p of the plant fungal pathogen *Fusarium graminearum* is involved in lithium toxicity and virulence. *Molecular Plant Pathology* **11**: 277-282.

Kang, Z. & H. Buchenauer, (2000) Ultrastructural and cytochemical studies on cellulose, xylan and pectin degradation in wheat spikes infected by *Fusarium culmorum*. *Journal of Phytopathology-Phytopathologische Zeitschrift* **148**: 263-275.

Kikot, G. E., R. A. Hours & T. M. Alconada, (2009) Contribution of cell wall degrading enzymes to pathogenesis of *Fusarium graminearum*: a review. *Journal of Basic Microbiology* **49**: 231-241.

Kim, J. E., H. J. Lee, J. Lee, K. W. Kim, S. H. Yun, W. B. Shim & Y. W. Lee, (2009) Gibberella zeae chitin synthase genes, *GzCHS5* and *GzCHS7*, are required for hyphal growth, perithecia formation, and pathogenicity. *Current Genetics* **55**: 449-459.

Kim, J. E., K. Myong, W. B. Shim, S. H. Yun & Y. W. Lee, (2007) Functional characterization of acetylglutamate synthase and phosphoribosylamine-glycine ligase genes in *Gibberella zeae*. *Current Genetics* **51**: 99-108.

Kimura, M., I. Kaneko, M. Komiyama, A. Takatsuki, H. Koshino, K. Yoneyama & I. Yamaguchi, (1998) Trichothecene 3-O-acetyltransferase protects both the producing organism and transformed yeast from related mycotoxins - Cloning and characterization of *Tri101*. *Journal of Biological Chemistry* **273**: 1654-1661.

Kimura, M., T. Tokai, K. O'Donnell, T. J. Ward, M. Fujimura, H. Hamamoto, T. Shibata & I. Yamaguchi, (2003) The trichothecene biosynthesis gene cluster of *Fusarium graminearum* F15 contains a limited number of essential pathway genes and expressed non-essential genes. *Febs Letters* **539**: 105-110.

Kimura, M., T. Tokai, N. Takahashi-Ando, S. Ohsato & M. Fujimura, (2007) Molecular and genetic studies of Fusarium trichothecene biosynthesis: Pathways, genes, and evolution. *Bioscience Biotechnology and Biochemistry* **71**: 2105-2123.

Kolb, F. L., G. H. Bai, G. J. Muehlbauer, J. A. Anderson, K. P. Smith & G. Fedak, (2001) Host plant resistance genes for fusarium head blight: Mapping and manipulation with molecular markers. *Crop Science* **41**: 611-619.

Kong, L., J. M. Anderson & H. W. Ohm, (2005) Induction of wheat defense and stress-related genes in response to *Fusarium graminearum*. *Genome* **48**: 29-40.

Kong, L., H. W. Ohm & J. M. Anderson, (2007) Expression analysis of defense-related genes in wheat in response to infection by *Fusarium graminearum*. *Genome* **50**: 1038-1048.

Kuratsu, M., A. Taura, J. Shoji, S. Kikuchi, M. Arioka & K. Kitamoto, (2007) Systematic analysis of SNARE localization in the filamentous fungus *Aspergillus oryzae*.

Fungal Genetics and Biology **44**: 1310-1323.

Kusano, T., T. Berberich, C. Tateda & Y. Takahashi, (2008) Polyamines: essential factors for growth and survival. *Planta* **228**: 367-381.

Langevin, F., F. Eudes & A. Comeau, (2004) Effect of trichothecenes produced by Fusarium graminearum during Fusarium head blight development in six cereal species. *European Journal of Plant Pathology* **110**: 735-746.

Langseth, W. & O. Elen, (1996) Differences between barley, oats and wheat in the occurrence of deoxynivalenol and other trichothecenes in Norwegian grain. *Journal of Phytopathology-Phytopathologische Zeitschrift* **144**: 113-118.

Lee, L. W., C. H. Chiou, K. L. Klomparens, J. W. Cary & J. E. Linz, (2004) Subcellular localization of aflatoxin biosynthetic enzymes Nor-1, Ver-1, and OmtA in time-dependent fractionated colonies of Aspergillus parasiticus. *Archives of Microbiology* **181**: 204-214.

Lee, S. C. & B. D. Shaw, (2008) Localization and function of ADP ribosylation factor A in *Aspergillus nidulans*. *FEMS Microbiology Letters* **283**: 216-222.

Lee, S. H., Y. K. Han, S. H. Yun & Y. W. Lee, (2009) Roles of the glyoxylate and methylcitrate cycles in sexual development and virulence in the cereal pathogen *Gibberella zeae*. *Eukaryotic Cell* **8**: 1155-1164.

Lee, S. H., J. Lee, S. Lee, E. H. Park, K. W. Kim, M. D. Kim, S. H. Yun & Y. W. Lee, (2009) *GzSNF1* is required for normal sexual and asexual development in the ascomycete *Gibberella zeae*. *Eukaryotic Cell* **8**: 116-127.

Lemmens, M., U. Scholz, F. Berthiller, C. Dall'Asta, A. Koutnik, R. Schuhmacher, G. et al. (2005) The ability to detoxify the mycotoxin deoxynivalenol colocalizes with a major quantitative trait locus for fusarium head blight resistance in wheat. *Molecular Plant-Microbe Interactions* **18**: 1318-1324.

Lendenfeld, T., D. Ghali, M. Wolschek, E. M. Kubicekpranz & C. P. Kubicek, (1993) Subcellular compartmentation of penicillin biosynthesis in *Penicillium chrysogenum* - the amino-acid precursors are derived from the vacuole. *Journal of Biological Chemistry* **268**: 665-671.

Li, W. L., J. D. Faris, S. Muthukrishnan, D. J. Liu, P. D. Chen & B. S. Gill, (2001) Isolation and characterization of novel cDNA clones of acidic chitinases and beta-1,3-glucanases from wheat spikes infected by *Fusarium graminearum*. *Theoretical and Applied Genetics* **102**: 353-362.

Lipschutz, J. H. & K. E. Mostov, (2002) Exocytosis: The many masters of the Exocyst.

Current Biology **12**: R212-R214.

Lu, S. W., S. Kroken, B. N. Lee, B. Robbertse, A. C. L. Churchill, O. C. Yoder & B. G. Turgeon, (2003) A novel class of gene controlling virulence in plant pathogenic ascomycete fungi. *Proceedings of the National Academy of Sciences of the United States of America* **100**: 5980-5985.

Ma, Z. P., B. J. Steffenson, L. K. Prom & N. L. V. Lapitan, (2000) Mapping of quantitative trait loci for Fusarium head blight resistance in barley. *Phytopathology* **90**: 1079-1088.

Mackintosh, C. A., J. Lewis, L. E. Radmer, S. Shin, S. J. Heinen, L. A. Smith, et al. (2007) Overexpression of defense response genes in transgenic wheat enhances resistance to Fusarium head blight. *Plant Cell Reports* **26**: 479-488.

Maggio-Hall, L. A., R. A. Wilson & N. P. Keller, (2005) Fundamental contribution of beta-oxidation to polyketide mycotoxin production in planta. *Molecular Plant-Microbe Interactions* **18**: 783-793.

Makandar, R., J. S. Essig, M. A. Schapaugh, H. N. Trick & J. Shah, (2006) Genetically engineered resistance to Fusarium head blight in wheat by expression of Arabidopsis NPR1. *Molecular Plant-Microbe Interactions* **19**: 123-129.

Manoharan, M., L. S. Dahleen, T. M. Hohn, S. M. Neate, X. H. Yu, N. J. Alexander, et al. (2006) Expression of 3-OH trichothecene acetyltransferase in barley (Hordeum vulgare L.) and effects on deoxynivalenol. *Plant Science* **171**: 699-706.

McCormick, S. P. & N. J. Alexander, (2002) Fusarium *Tri8* encodes a trichothecene C-3 esterase. *Applied and Environmental Microbiology* **68**: 2959-2964.

McCormick, S. P., N. J. Alexander, S. E. Trapp & T. M. Hohn, (1999) Disruption of *TRI101*, the gene encoding trichothecene 3-O-acetyltransferase, from *Fusarium sporotrichioides*. *Applied and Environmental Microbiology* **65**: 5252-5256.

McCormick, S. P., L. J. Harris, N. J. Alexander, T. Ouellet, A. Saparno, S. Allard & A. E. Desjardins, (2004) *Tri1* in *Fusarium graminearum* encodes a P450 oxygenase. *Applied and Environmental Microbiology* **70**: 2044-2051.

McMullen, M., R. Jones & D. Gallenberg, (1997) Scab of wheat and barley: A re-emerging disease of devastating impact. *Plant Disease* **81**: 1340-1348.

Meek, I. B., A. W. Peplow, C. Ake, T. D. Phillips & M. N. Beremand, (2003) *Tri1* encodes the cytochrome P450 monooxygenase for C-8 hydroxylation during trichothecene biosynthesis in *Fusarium sporotrichioides* and resides upstream of

another new Tri gene. *Applied and Environmental Microbiology* **69**: 1607-1613.

Meijer, W. H., L. Gidijala, S. Fekken, J. Kiel, M. A. van den Berg, R. Lascaris, R. A. L. Bovenberg & I. J. van der Klei, (2010) Peroxisomes are required for efficient penicillin biosynthesis in *Penicillium chrysogenum*. *Applied and Environmental Microbiology* **76**: 5702-5709.

Mesfin, A., K. P. Smith, R. Dill-Macky, C. K. Evans, R. Waugh, C. D. Gustus & G. J. Muehlbauer, (2003) Quantitative trait loci for Fusarium head blight resistance in barley detected in a two-rowed by six-rowed population. *Crop Science* **43**: 307-318.

Meyers, B. C., A. Kozik, A. Griego, H. H. Kuang & R. W. Michelmore, (2003) Genome-wide analysis of NBS-LRR-encoding genes in Arabidopsis. *Plant Cell* **15**: 809-834.

Muhitch, M. J., S. P. McCormick, N. J. Alexander & T. M. Hohn, (2000) Transgenic expression of the *Tri101* or *Pdr5* gene increases resistance of tobacco to the phytotoxic effects of the trichothecene 4,15-diacetoxyscirpenol. *Plant Science* **157**: 201-207.

Muller, W. H., R. A. L. Bovenberg, M. H. Groothuis, F. Kattevilder, E. B. Smaal, L. H. M. Vandervoort & A. J. Verkleij, (1992) Involvement of microbodies in penicillin biosynthesis. *Biochimica et Biophysica Acta* **1116**: 210-213.

Nakaune, R., H. Hamamoto, J. Imada, K. Akutsu & T. Hibi, (2002) A novel ABC transporter gene, *PMR5*, is involved in multidrug resistance in the phytopathogenic fungus *Penicillium digitatum*. *Molecular Genetics and Genomics* **267**: 179-185.

Naoumkina, M. A., Q. A. Zhao, L. Gallego-Giraldo, X. B. Dai, P. X. Zhao & R. A. Dixon, (2010) Genome-wide analysis of phenylpropanoid defence pathways. *Molecular Plant Pathology* **11**: 829-846.

Nduulu, L. M., A. Mesfin, G. J. Muehlbauer & K. P. Smith, (2007) Analysis of the chromosome 2(2H) region of barley associated with the correlated traits Fusarium head blight resistance and heading date. *Theoretical and Applied Genetics* **115**: 561-570.

Ochiai, N., T. Tokai, T. Nishiuchi, N. Takahashi-Ando, M. Fujimura & M. Kimura, (2007) Involvement of the osmosensor histidine kinase and osmotic stress-activated protein kinases in the regulation of secondary metabolism in *Fusarium graminearum*. *Biochemical and Biophysical Research Communications* **363**: 639-644.

Ohsato, S., T. Ochiai-Fukuda, T. Nishiuchi, N. Takahashi-Ando, S. Koizumi, H. Hamamoto, *et al*. (2007) Transgenic rice plants expressing trichothecene 3-O-acetyltransferase show resistance to the Fusarium phytotoxin deoxynivalenol. *Plant Cell Reports* **26**: 531-538.

Oide, S., W. Moeder, S. Krasnoff, D. Gibson, H. Haas, K. Yoshioka & B. G. Turgeon, (2006) *NPS6*, encoding a nonribosomal peptide synthetase involved in siderophore-mediated iron metabolism, is a conserved virulence determinant of plant pathogenic ascomycetes. *Plant Cell* **18**: 2836-2853.

Okubara, P. A., A. E. Blechl, S. P. McCormick, N. J. Alexander, R. Dill-Macky & T. M. Hohn, (2002) Engineering deoxynivalenol metabolism in wheat through the expression of a fungal trichothecene acetyltransferase gene. *Theoretical and Applied Genetics* **106**: 74-83.

Pantazopoulou, A. & M. A. Penalva, (2009) Organization and dynamics of the *Aspergillus nidulans* Golgi during apical extension and mitosis. *Molecular Biology of the Cell* **20**: 4335-4347.

Paper, J. M., J. S. Scott-Craig, N. D. Adhikari, C. A. Cuom & J. D. Walton, (2007) Comparative proteornics of extracellular proteins *in vitro* and *in planta* from the pathogenic fungus *Fusarium graminearum*. *Proteomics* **7**: 3171-3183.

Parker, D., M. Beckmann, H. Zubair, D. P. Enot, Z. Caracuel-Rios, D. P. Overy, *et al*. (2009) Metabolomic analysis reveals a common pattern of metabolic re-programming during invasion of three host plant species by *Magnaporthe grisea*. *Plant Journal* **59**: 723-737.

Pekkarinen, A. I. & B. L. Jones, (2002) Trypsin-like proteinase produced by *Fusarium culmorum* grown on grain proteins. *Journal of Agricultural and Food Chemistry* **50**: 3849-3855.

Pekkarinen, A. I., T. H. Sarlin, A. T. Laitila, A. I. Haikara & B. L. Jones, (2003) Fusarium species synthesize alkaline proteinases in infested barley. *Journal of Cereal Science* **37**: 349-356.

Pestka, J. J. & A. T. Smolinski, (2005) Deoxynivalenol: toxicology and potential effects on humans. *Journal of Toxicology and Environmental Health-Part B-Critical Reviews* **8**: 39-69.

Pitkin, J. W., D. G. Panaccione & J. D. Walton, (1996) A putative cyclic peptide efflux pump encoded by the *TOXA* gene of the plant-pathogenic fungus *Cochliobolus carbonum*. *Microbiology-Uk* **142**: 1557-1565.

Poppenberger, B., F. Berthiller, D. Lucyshyn, T. Sieberer, R. Schuhmacher, R. Krska, et

al. (2003) Detoxification of the Fusarium mycotoxin deoxynivalenol by a UDP-glucosyltransferase from *Arabidopsis thaliana*. *Journal of Biological Chemistry* **278**: 47905-47914.

Pritsch, C., G. J. Muehlbauer, W. R. Bushnell, D. A. Somers & C. P. Vance, (2000) Fungal development and induction of defense response genes during early infection of wheat spikes by *Fusarium graminearum*. *Molecular Plant-Microbe Interactions* **13**: 159-169.

Proctor, R. H., T. M. Hohn & S. P. McCormick, (1995a) Reduced virulence of *Gibberella zeae* caused by disruption of a trichothecene toxin biosynthetic gene. *Molecular Plant-Microbe Interactions* **8**: 593-601.

Proctor, R. H., T. M. Hohn, S. P. McCormick & A. E. Desjardins, (1995b) *Tri6* encodes an unusual zinc-finger protein involved in regulation of trichothecene biosynthesis in *Fusarium sporotrichioides*. *Applied and Environmental Microbiology* **61**: 1923-1930.

Qi, W. H., K. Chil & F. Trail, (2006) Microarray analysis of transcript accumulation during perithecium development in the filamentous fungus *Gibberella zeae* (anamorph *Fusarium graminearum*). *Molecular Genetics and Genomics* **276**: 87-100.

Qu, L. J., J. Chen, M. H. Liu, N. S. Pan, H. Okamoto, Z. Z. Lin, et al. (2003) Molecular cloning and functional analysis of a novel type of Bowman-Birk inhibitor gene family in rice. *Plant Physiology* **133**: 560-570.

Ramamoorthy, V., E. B. Cahoon, M. Thokala, J. Kaur, J. Li & D. M. Shah, (2009) Sphingolipid C-9 methyltransferases are important for growth and virulence but not for sensitivity to antifungal plant defensins in *Fusarium graminearum*. *Eukaryotic Cell* **8**: 217-229.

Rep, M. & H. C. Kistler, (2010) The genomic organization of plant pathogenicity in Fusarium species. *Current Opinion in Plant Biology* **13**: 420-426.

Rittenour, W. R. & S. D. Harris, (2008) Characterization of *Fusarium graminearum Mes1* reveals roles in cell-surface organization and virulence. *Fungal Genetics and Biology* **45**: 933-946.

Rittenour, W. R. & S. D. Harris, (2010) An *in vitro* method for the analysis of infection-related morphogenesis in *Fusarium graminearum*. *Molecular Plant Pathology* **11**: 361-369.

Rogers, L. M., Y. K. Kim, W. J. Guo, L. Gonzalez-Candelas, D. X. Li & P. E. Kolattukudy, (2000) Requirement for either a host- or pectin-induced pectate

lyase for infection of *Pisum sativum* by *Nectria hematococca*. *Proceedings of the National Academy of Sciences of the United States of America* **97**: 9813-9818.

Rosewich, U. L., R. E. Pettway, T. Katan & H. C. Kistler, (1999) Population genetic analysis corroborates dispersal of *Fusarium oxysporum* f. sp radicis-lycopersici from Florida to Europe. *Phytopathology* **89**: 623-630.

Rotter, B. A., D. B. Prelusky & J. J. Pestka, (1996) Toxicology of deoxynivalenol (vomitoxin). *Journal of Toxicology and Environmental Health* **48**: 1-34.

Roze, L., A. Chanda & J. Linz, (2011) Compartmentalization and molecular traffic in secondary metabolism: A new understanding of established cellular processes. *Fungal Genetics and Biology* **48**: 35-48.

Ruepp, A., A. Zollner, D. Maier, K. Albermann, J. Hani, M. Mokrejs, I. et al. (2004) The FunCat, a functional annotation scheme for systematic classification of proteins from whole genomes. *Nucleic Acids Research* **32**: 5539-5545.

Schoonbeek, H., G. Del Sorbo & M. A. De Waard, (2001) The ABC transporter BcatrB affects the sensitivity of *Botrytis cinerea* to the phytoalexin resveratrol and the fungicide fenpiclonil. *Molecular Plant-Microbe Interactions* **14**: 562-571.

Schoonbeek, H. J., J. G. M. van Nistelrooy & M. A. de Waard, (2003) Functional analysis of ABC transporter genes from *Botrytis cinerea* identifies BcatrB as a transporter of eugenol. *European Journal of Plant Pathology* **109**: 1003-1011.

Schweiger, W., J. Boddu, S. Shin, B. Poppenberger, F. Berthiller, M. Lemmens, G. J. Muehlbauer & G. Adam, (2010) Validation of a candidate deoxynivalenol-inactivating UDP-glucosyltransferase from barley by heterologous expression in yeast. *Molecular Plant-Microbe Interactions* **23**: 977-986.

Seabra, M. C. & E. Coudrier, (2004) Rab GTPases and myosin motors in organelle motility. *Traffic* **5**: 393-399.

Seiler, S., M. Plamann & M. Schliwa, (1999) Kinesin and dynein mutants provide novel insights into the roles of vesicle traffic during cell morphogenesis in Neurospora. *Current Biology* **9**: 779-785.

Seo, B. W., H. K. Kim, Y. W. Lee & S. H. Yun, (2007) Functional analysis of a histidine auxotrophic mutation in *Gibberella zeae*. *Plant Pathology Journal* **23**: 51-56.

Seong, K., Z. M. Hou, M. Tracy, H. C. Kistler & J. R. Xu, (2005) Random insertional mutagenesis identifies genes associated with virulence in the wheat scab fungus *Fusarium graminearum*. *Phytopathology* **95**: 744-750.

Seong, K., L. Li, Z. M. Hou, M. Tracy, H. C. Kistler & J. R. Xu, (2006) Cryptic promoter activity in the coding region of the HMG-CoA rediactase gene in *Fusarium graminearum*. *Fungal Genetics and Biology* **43**: 34-41.

Seong, K. Y., M. Pasquali, X. Y. Zhou, J. Song, K. Hilburn, S. McCormick, *et al*. (2009) Global gene regulation by Fusarium transcription factors *Tri6* and *Tri10* reveals adaptations for toxin biosynthesis. *Molecular Microbiology* **72**: 354-367.

Seong, K. Y., X. Zhao, J. R. Xu, U. Guldener & H. C. Kistler, (2008) Conidial germination in the filamentous fungus *Fusarium graminearum*. *Fungal Genetics and Biology* **45**: 389-399.

Shim, W. B., U. S. Sagaram, Y. E. Choi, J. So, H. H. Wilkinson & Y. W. Lee, (2006) *FSR1* is essential for virulence and female fertility in *Fusarium verticillioides* and *F. graminearum*. *Molecular Plant-Microbe Interactions* **19**: 725-733.

Shim, W. B. & C. P. Woloshuk, (2001) Regulation of fumonisin B-1 biosynthesis and conidiation in *Fusarium verticillioides* by a cyclin-like (C-type) gene, *FCC1*. *Applied and Environmental Microbiology* **67**: 1607-1612.

Shin, S. Y., C. A. Mackintosh, J. Lewis, S. J. Heinen, L. Radmer, R. Dill-Macky, *et al*. (2008) Transgenic wheat expressing a barley class II chitinase gene has enhanced resistance against *Fusarium graminearum*. *Journal of Experimental Botany* **59**: 2371-2378.

Singh, S. A. & D. Christendat, (2006) Structure of Arabidopsis dehydroquinate dehydratase-shikimate dehydrogenase and implications for metabolic channeling in the shikimate pathway. *Biochemistry* **45**: 7787-7796.

Skadsen, R. W. & T. A. Hohn, (2004) Use of *Fusarium graminearum* transformed with gfp to follow infection patterns in barley and Arabidopsis. *Physiological and Molecular Plant Pathology* **64**: 45-53.

Skov, J., M. Lemmens & H. Giese, (2004) Role of a Fusarium culmorum ABC transporter (FcABC1) during infection of wheat and barley. *Physiological and Molecular Plant Pathology* **64**: 245-254.

Smith, K. P., C. K. Evans, R. Dill-Macky, C. Gustus, W. Xie & Y. Dong, (2004) Host genetic effect on deoxynivalenol accumulation in Fusarium head blight of barley. *Phytopathology* **94**: 766-771.

Smith T. F. & M.S. Waterman, (1981) Identification of common molecular subsequences. J. *Molecular Biology* **147**: 195-197.

Somers, D. J., J. Thomas, R. DePauw, S. Fox, G. Humphreys & G. Fedak, (2005)

Assembling complex genotypes to resist Fusarium in wheat (*Triticum aestivum* L.). *Theoretical and Applied Genetics* **111**: 1623-1631.

Sprote, P., A. A. Brakhage & M. J. Hynes, (2009) Contribution of peroxisomes to penicillin biosynthesis in *Aspergillus nidulans*. *Eukaryotic Cell* **8**: 421-423.

Steinberg, G., (2007) On the move: endosomes in fungal growth and pathogenicity. *Nature Reviews Microbiology* **5**: 309-316.

Steiner, B., H. Kurz, M. Lemmens & H. Buerstmayr, (2009) Differential gene expression of related wheat lines with contrasting levels of head blight resistance after *Fusarium graminearum* inoculation. *Theoretical and Applied Genetics* **118**: 753-764.

Stephens, A. E., D. M. Gardiner, R. G. White, A. L. Munn & J. M. Manners, (2008) Phases of infection and gene expression of *Fusarium graminearum* during crown rot disease of wheat. *Molecular Plant-Microbe Interactions* **21**: 1571-1581.

Stergiopoulos, I., L. H. Zwiers & M. A. De Waard, (2002) Secretion of natural and synthetic toxic compounds from filamentous fungi by membrane transporters of the ATP-binding cassette and major facilitator superfamily. *European Journal of Plant Pathology* **108**: 719-734.

Suelmann, R. & R. Fischer, (2000) Mitochondrial movement and morphology depend on an intact actin cytoskeleton in *Aspergillus nidulans*. *Cell Motility and the Cytoskeleton* **45**: 42-50.

Szewczyk, E., T. Nayak, C. E. Oakley, H. Edgerton, Y. Xiong, N. Taheri-Talesh, S. A. Osmani & B. R. Oakley, (2006) Fusion PCR and gene targeting in *Aspergillus nidulans*. *Nature Protocols* **1**: 3111-3120.

Tag, A. G., G. F. Garifullina, A. W. Peplow, C. Ake, T. D. Phillips, T. M. Hohn & M. N. Beremand, (2001) A novel regulatory gene, *Tri10*, controls trichothecene toxin production and gene expression. *Applied and Environmental Microbiology* **67**: 5294-5302.

Teijeira, F., R. V. Ullan, S. M. Guerra, C. Garcia-Estrada, I. Vaca & J. F. Martin, (2009) The transporter CefM involved in translocation of biosynthetic intermediates is essential for cephalosporin production. *Biochemical Journal* **418**: 113-124.

TerBush, D. R., T. Maurice, D. Roth & P. Novick, (1996) The Exocyst is a multiprotein complex required for exocytosis in *Saccharomyces cerevisiae*. *Embo Journal* **15**: 6483-6494.

Trail, F., J. R. Xu, P. San Miguel, R. G. Halgren & H. C. Kistler, (2003) Analysis of

expressed sequence tags from *Gibberella zeae* (anamorph *Fusarium graminearum*). *Fungal Genetics and Biology* **38**: 187-197.

Ueno, Y., (1984) Toxicological features of T-2 toxin and related trichothecenes. *Fundamental and Applied Toxicology* **4**: S124-S132.

Upadhyay, S. & B. D. Shaw, (2008) The role of actin, fimbrin and endocytosis in growth of hyphae in *Aspergillus nidulans*. *Molecular Microbiology* **68**: 690-705.

Urano, K., T. Hobo & K. Shinozaki, (2005) Arabidopsis ADC genes involved in polyamine biosynthesis areb essential for seed development. *FEBS Letters* **579**: 1557-1564.

Urban, M., T. Bhargava & J. E. Hamer, (1999) An ATP-driven efflux pump is a novel pathogenicity factor in rice blast disease. *EMBO Journal* **18**: 512-521.

Urban, M., E. Mott, T. Farley & K. Hammond-Kosack, (2003) The *Fusarium graminearum MAP1* gene is essential for pathogenicity and development of perithecia. *Molecular Plant Pathology* **4**: 347-359.

van der Biezen, E.A. & D.G Jones, (1998) The NB-ARC domain: A novel signalling motif shared by plant resistance gene products and regulators of cell death in animals. *Current Biology* **8**: R226-R227.

Voigt, C. A., W. Schafer & S. Salomon, (2005) A secreted lipase of *Fusarium graminearum* is a virulence factor required for infection of cereals. *Plant Journal* **42**: 364-375.

Waldron, B. L., B. Moreno-Sevilla, J. A. Anderson, R. W. Stack & R. C. Frohberg, (1999) RFLP mapping of QTL for Fusarium head blight resistance in wheat. *Crop Science* **39**: 805-811.

Wang, L. Q., K. Guo, Y. Li, Y. Y. Tu, H. Z. Hu, B. R. Wang, X. C. Cui & L. C. Peng, (2010) Expression profiling and integrative analysis of the CESA/CSL superfamily in rice. *BMC Plant Biology* **10**.

Wang, Y., W. D. Liu, Z. M. Hou, C. F. Wang, X. Y. Zhou, W. Jonkers, *et al*. (2011) A novel transcriptional factor important for pathogenesis and ascosporogenesis in *Fusarium graminearum*. *Molecular Plant-Microbe Interactions* **24**: 118-128.

Ward, T. J., J. P. Bielawski, H. C. Kistler, E. Sullivan & K. O'Donnell, (2002) Ancestral polymorphism and adaptive evolution in the trichothecene mycotoxin gene cluster of phytopathogenic Fusarium. *Proceedings of the National Academy of Sciences of the United States of America* **99**: 9278-9283.

Watson, R. J., S. Burchat & J. Bosley, (2008) A model for integration of DNA into the genome during transformation of *Fusarium graminearum*. *Fungal Genetics and Biology* **45**: 1348-1363.

Wedlich-Soldner, R., I. Schulz, A. Straube & G. Steinberg, (2002) Dynein supports motility of endoplasmic reticulum in the fungus *Ustilago maydis*. *Molecular Biology of the Cell* **13**: 965-977.

Windels, C. E., (2000) Economic and social impacts of Fusarium head blight: Changing farms and rural communities in the Northern Great Plains. *Phytopathology* **90**: 17-21.

Wise, R.P., R.A. Caldo, L. Hong, L. Shen , E.K. Cannon, & J.A. Dickerson (2007) BarleyBase/PLEXdb: A unified expression profiling database for plants and plant pathogens. In *Plant Bioinformatics - Methods and Protocols*. Edwards D. (ed). Totowa, Humana Press, *Methods in Molecular Biology* **406**: 347-363.

Wise, R. P., M. J. Moscou, A. J. Bogdanove & S. A. Whitham, (2007) Transcript profiling in host-pathogen interactions. *Annual Review of Phytopathology* **45**: 329-369.

Wong, P., M. Walter, W. Lee, G. Mannhaupt, M. Munsterkotter, H. W. Mewes, G. Adam & U. Guldener, (2011) FGDB: revisiting the genome annotation of the plant pathogen *Fusarium graminearum*. *Nucleic Acids Research* **39**: D637-D639.

Wu, H., G. Rossi & P. Brennwald, (2008) The ghost in the machine: small GTPases as spatial regulators of exocytosis. *Trends in Cell Biology* **18**: 397-404.

Yang, Z. P., J. Gilbert, D. J. Somers, G. Fedak, J. D. Procunier & I. H. McKenzie, (2003) Marker assisted selection of Fusarium head blight resistance genes in two doubled haploid populations of wheat. *Molecular Breeding* **12**: 309-317.

Yokoyama, R. & K. Nishitani, (2004) Genomic basis for cell-wall diversity in plants. A comparative approach to gene families in rice and Arabidopsis. *Plant and Cell Physiology* **45**: 1111-1121.

Yu, H. Y., J. A. Seo, J. E. Kim, K. H. Han, W. B. Shim, S. H. Yun & Y. W. Lee, (2008) Functional analyses of heterotrimeric G protein G alpha and G beta subunits in *Gibberella zeae*. *Microbiology-Sgm* **154**: 392-401.

Yu, J. H., (2006) Heterotrimeric G protein signaling and RGSs in *Aspergillus nidulans*. *Journal of Microbiology* **44**: 145-154.

Yu, J. H. & N. Keller, (2005) Regulation of secondary metabolism in filamentous fungi.

Annual Review of Phytopathology **43**: 437-458.

Zhang, D. J., F. Y. Fan, J. R. Yang, X. L. Wang, D. W. Qiu & L. H. Jiang, (2010) FgTep1p is linked to the phosphatidylinositol-3 kinase signalling pathway and plays a role in the virulence of *Fusarium graminearum* on wheat. *Molecular Plant Pathology* **11**: 495-502.

Zhou, W. C., F. L. Kolb & D. E. Riechers, (2005) Identification of proteins induced or upregulated by Fusarium head blight infection in the spikes of hexaploid wheat (*Triticum aestivum*). *Genome* **48**: 770-780.

Zhou, X. Y., C. Heyer, Y. E. Choi, R. Mehrabi & J. R. Xu, (2010) The *CID1* cyclin C-like gene is important for plant infection in *Fusarium graminearum*. *Fungal Genetics and Biology* **47**: 143-151.

Zhu, H., L. Gilchrist, P. Hayes, A. Kleinhofs, D. Kudrna, Z. Liu, L. et al. (1999) Does function follow form? Principal QTLs for Fusarium head blight (FHB) resistance are coincident with QTLs for inflorescence traits and plant height in a doubled-haploid population of barley. *Theoretical and Applied Genetics* **99**: 1221-1232.

Zwiers, L. H. & M. A. De Waard, (2000) Characterization of the ABC transporter genes *MgAtr1* and *MgAtr2* from the wheat pathogen *Mycosphaerella graminicola*. *Fungal Genetics and Biology* **30**: 115-125.